AD NUMBER
ADC070512
CLASSIFICATION CHANGES
TO: unclassified
FROM: confidential
LIMITATION CHANGES
TO: Approved for public release, distribution unlimited
FROM: Distribution authorized to DoD only; Administrative/Operational Use; SEP 1975. Other requests shall be referred to Office of Naval Research, Code 102-OSC, Arlington, VA 22217.
AUTHORITY
ONR ltr, 31 Jan 2006; ONR ltr, 31 Jan 2006

CONFIDENTIAL

(C) CHURCH ANCHOR
AMBIENT NOISE FINAL REPORT (U)
SEPTEMBER 1975

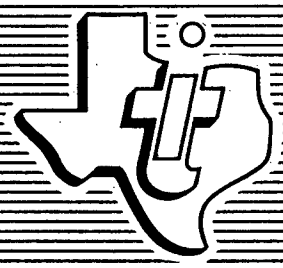

TEXAS INSTRUMENTS
INCORPORATED

CONFIDENTIAL

Copy 42

CONFIDENTIAL

NATIONAL SECURITY INFORMATION
Unauthorized Disclosure
Subject to Criminal Sanctions

Classified by ONR: Code 102
~~Exempt from GDS of E.O. 11652~~
~~Exempt Category: 3~~
Declassify on: (~~Undetermined~~) OADR

NRL

(C) CHURCH ANCHOR
AMBIENT NOISE FINAL REPORT (U)
SEPTEMBER 1975

Prepared for

Office of Naval Research
Code 102-OSC
Contract N00014-74-C-0100

Prepared by

J. Hoffmann and A. Kirst, Jr.
Texas Instruments Incorporated

With Contributions From

The University of Texas
Applied Research Laboratory

Marine Physical Laboratory
Scripps Institution of Oceanography

Defence Research Establishment Pacific

B-K Dynamics, Inc.

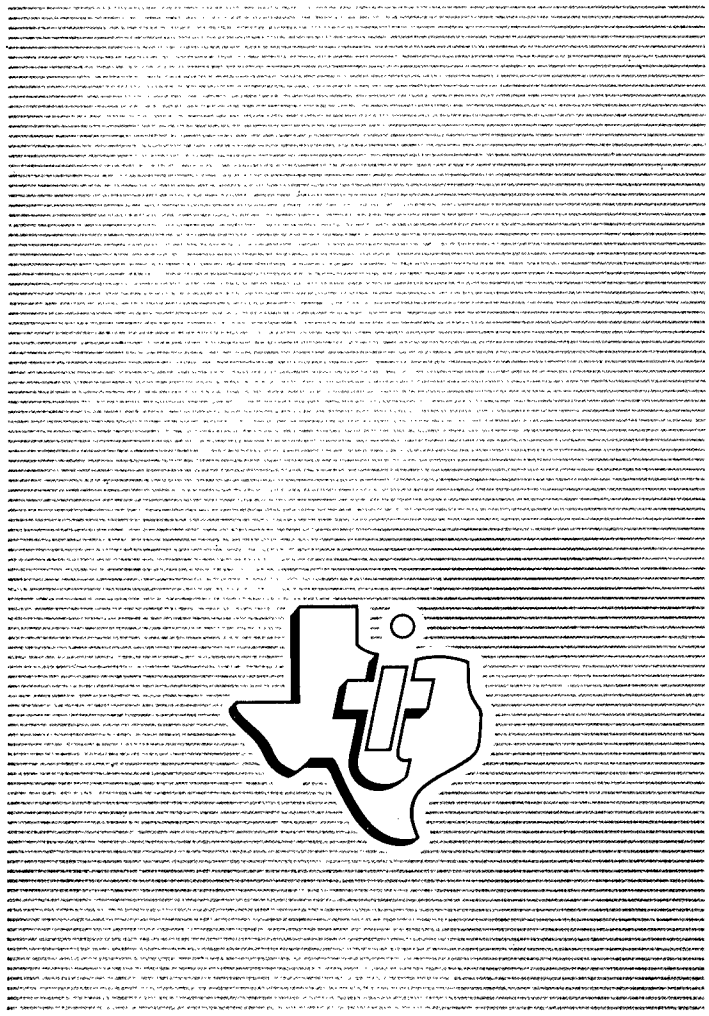

Texas Instruments Report
No. C1-871976-F

TEXAS INSTRUMENTS
INCORPORATED

CONFIDENTIAL

CONFIDENTIAL

SECURITY CLASSIFICATION OF THIS PAGE *(When Data Entered)*

REPORT DOCUMENTATION PAGE

READ INSTRUCTIONS BEFORE COMPLETING FORM

1. REPORT NUMBER	2. GOVT ACCESSION NO. / 3. RECIPIENT'S CATALOG NUMBER
4. TITLE *(and Subtitle)* CHURCH ANCHOR AMBIENT NOISE REPORT (U)	5. TYPE OF REPORT & PERIOD COVERED Final Report–September 1975
	6. PERFORMING ORG. REPORT NUMBER C1-871976-F
7. AUTHOR(s) J. Hoffmann, A. Kirst of Texas Instruments, with contributions from The University of Texas, Marine Physical Laboratory, Scripps, Defence Research Establishment Pacific, B-K Dynamics, Inc.	8. CONTRACT OR GRANT NUMBER(s) N00014-74-C-0100
9. PERFORMING ORGANIZATION NAME AND ADDRESS Texas Instruments Incorporated Equipment Group–P.O. Box 6015, MS 400 Dallas, Texas 75222	10. PROGRAM ELEMENT, PROJECT, TASK AREA & WORK UNIT NUMBERS
11. CONTROLLING OFFICE NAME AND ADDRESS Long Range Acoustic Propagation Project (LRAPP) ONR–Department of the Navy–Code 102-OSC Arlington, Virginia 22217	12. REPORT DATE September 1975 13. NUMBER OF PAGES 152
14. MONITORING AGENCY NAME & ADDRESS *(if different from Controlling Office)* Defense Contract Administration Service Office Texas Instruments Incorporated P.O. Box 6015, MS 256 Dallas, Texas 75222	15. SECURITY CLASS. *(of this report)* Confidential 15a. DECLASSIFICATION/DOWNGRADING SCHEDULE ~~XGDS Category 3~~ OADR

16. DISTRIBUTION STATEMENT *(of this Report)*

In addition to security requirements which apply to this document and must be met, each transmittal outside the Department of Defense must have prior approval of Office of Naval Research (Code 102-OSC).

520509

17. DISTRIBUTION STATEMENT *(of the abstract entered in Block 20, if different from Report)*

DISTRIBUTION STATEMENT E:
Distribution authorized to DoD Components only.
Other requests shall be referred to:
OFFICE OF NAVAL RESEARCH, CODE 102-OSC, ARLINGTON, VA 22217

Administrative or Operational Use
SEP 1975

18.

19. KEY WORDS *(Continue on reverse side if necessary and identify by block number)*

Northeast Pacific	MESA
Ambient Noise	LRAPP
ACODAC	CHURCH ANCHOR Exercise
FLIP	

20. ABSTRACT *(Continue on reverse side if necessary and identify by block number)*

(C) Omnidirectional ambient noise intensity measurements obtained in the CHURCH ANCHOR Exercise area, the eastern quarter of the Pacific north of 20°N, during September 1973, are discussed as a function of time, depth, frequency, and location. The measurement platforms used were: (1) three ACODAC systems, each with six vertically distributed omnidirectional hydrophones; (2) the MPL vertical array consisting of 20 hydrophones distributed in six depth groups; and (3) the six-element horizontal MESA array. In the mean, the ambient noise intensity indicated a trend of decreasing level with increasing depth. The rate of change of ambient noise intensity with depth appeared to be significantly greater at the lower frequencies (50 Hz) than at the higher frequencies (250 Hz), and the rate of change for all frequencies was steeper between the critical depth and the bottom than between the axis and critical depth.

DD FORM 1 JAN 73 1473 EDITION OF 1 NOV 65 IS OBSOLETE

CONFIDENTIAL

SECURITY CLASSIFICATION OF THIS PAGE *(When Data Entered)*

(U) ACKNOWLEDGMENTS

The contributions of the many Navy and contractor personnel who made completion of this report possible are gratefully acknowledged. Dr. R.D. Gaul, Mr. R.N. Lane, and Dr. R.E. Morrison of the Long Range Acoustic Propagation Project (LRAPP) funded and encouraged the work.

Technical direction of the CHURCH ANCHOR program, under COMTHIRDFLT operation control, was assigned by the LRAPP manager to Mr. A.E. Fadness of B-K Dynamics, Inc. His review of this report and technical guidance is greatly appreciated. This report is based on technical contributions from the following individuals and organizations: Dr. T.D. Plemmons and Messrs. G.E. Ellis, J.A. Shooter, and S.L. Watkins of Applied Research Laboratories, The University of Texas at Austin; Dr. G. Morris of Marine Physical Laboratory, Scripps Institution of Oceanography; Messrs. J.S. Bird and J.M. Thorleifson of the Defence Research Establishment Pacific, Canada; Messrs. C.I. Black and R. Carvell of Texas Instruments Incorporated.

(U) TABLE OF CONTENTS

LIST OF ILLUSTRATIONS

LIST OF TABLES

SECTION I

(C) INTRODUCTION (U)

A. (C) CHURCH ANCHOR AMBIENT NOISE EXPERIMENT (U)

(C) This report presents the omnidirectional ambient noise intensity measurements obtained in the CHURCH ANCHOR exercise area, the eastern quarter of the Pacific north of 20°N. The data were collected in September 1973 during the CHURCH ANCHOR exercise sponsored by the Long Range Acoustic Propagation Project (LRAPP). The data are also discussed in the CHURCH ANCHOR Synopsis Report[1] and the CHURCH ANCHOR Environmental Acoustic Summary Report.[2]

(U) The purpose of this technical report is to present CHURCH ANCHOR ambient noise data reduced by the data processing laboratories of The University of Texas at Austin (UT), Marine Physical Laboratory (MPL), the Defence Research Establishment Pacific (DREP), and Texas Instruments and to discuss a preliminary analysis of that data. In Section II, the omnidirectional ambient noise data from the four laboratories are discussed as a function of time, depth, frequency, and location. Appendixes A through D are inputs from each of the four individual processing laboratories. These appendixes contain descriptions of each facility's hardware and software systems, in addition to a compilation of each facility's reduced data.

(C) Omnidirectional noise intensity measurements were made with Acoustic Data Capsule (ACODAC) systems, the MPL array, and the MESA array of DREP. The site locations of the measurement platforms are shown in Figure 1-1.

(C) ACODAC systems were moored at sites A, C, and D and were aligned on the exercise baseline (143°30'W). Each ACODAC system consisted of six vertically distributed hydrophones. At sites A and C, hydrophones were positioned near axis (670 m at site A and 655 m at site C), critical depths (4,515 m at site A and 3,860 m at site C), and, at site C, near the sea floor (5,555 m). At site D, all hydrophones were distributed between the bottom of the sound channel and the sea floor (4,646 m). In Table 1-1, the location of each ACODAC and the hydrophone depths at each site are compiled.

(C) The MPL acoustic receiving system consisted of a 20-element vertical array suspended from the Floating Instrument Platform (R/P FLIP) at site B. The location of site B is given in Table 1-1.

(C) DREP collected acoustic measurements with the six-element horizontal MESA array from the CFAV *Endeavour.* Omnidirectional ambient noise intensity measurements were made at two moored stations, site E (46°N) and site F (57°N), located on the exercise baseline.

B. (C) SUMMARY OF RESULTS (U)

(U) The significant results of the ambient noise study, based on measurements taken by the ACODACs, MPL array and the MESA array, are as follows.

TABLE 1-1. (C) SUMMARY OF CHURCH ANCHOR AMBIENT NOISE DATA (U)

ACODAC: Site A

Location: 30°31.9'N, 143°30.0'W
Axis Depth = 670 m
Critical Depth = 4,515 m
Sea Floor Depth = 5,091 m

HYD	SER. NO.	DEPTH	DATA
1	11	749	Yes
2	7	1,330	No
3	2	2,612	No
4	13	4,046	Yes
5	14	4,353	Yes
6	3	4,659	Yes

Recording Time: "ON" 130600Z Sep 73
"OFF" 2401400Z Sep 73

FLIP: Site B

Location: 32°11.8'N, 143°35.4'W
Hydrophone Depths = 200, 790, 2,492, 4,222, 4,474, 5,180 m

Recording Times: 162000Z–171000Z Sep 73
201500Z–210325Z Sep 73

ACODAC: Site C

Location: 39°13.3'N, 143°28.1'W
Axis Depth = 655 m
Critical Depth = 3,860 m
Sea Floor Depth = 5,555 m

HYD	SER. NO.	DEPTH	DATA
1	101	696	Yes
2	102	2,497	No
3	103	3,748	No
4	104	4,055	Yes
5	105	4,361	Yes
6	106	5,521	Yes

Recording Time: "ON" 160022Z Sep 73
"OFF' 270313Z Sep 73

ACODAC: Site D

Location: 45°05.1'N, 143°30.5'W
Axis Depth = 478 m
Critical Depth = 2,840 m
Sea Floor Depth = 4,646 m

HYD	SER. NO.	DEPTH	DATA
1	5	3,325	Yes
2	12	3,625	Yes
3	1	3,925	Yes
4	9	4,225	Yes
5	4	4,520	Yes
6	6	4,612	Yes

Recording Time: "ON" 180732Z Sep 73
"OFF" 281730Z Sep 73

Endeavour: Site E — 46°N, 143°30'W

Endeavour: Site F — 57°N, 143°30'W

6-element planar array at depth of 460 m

Recording Time: 222253Z–240302Z Sep 73

CONFIDENTIAL

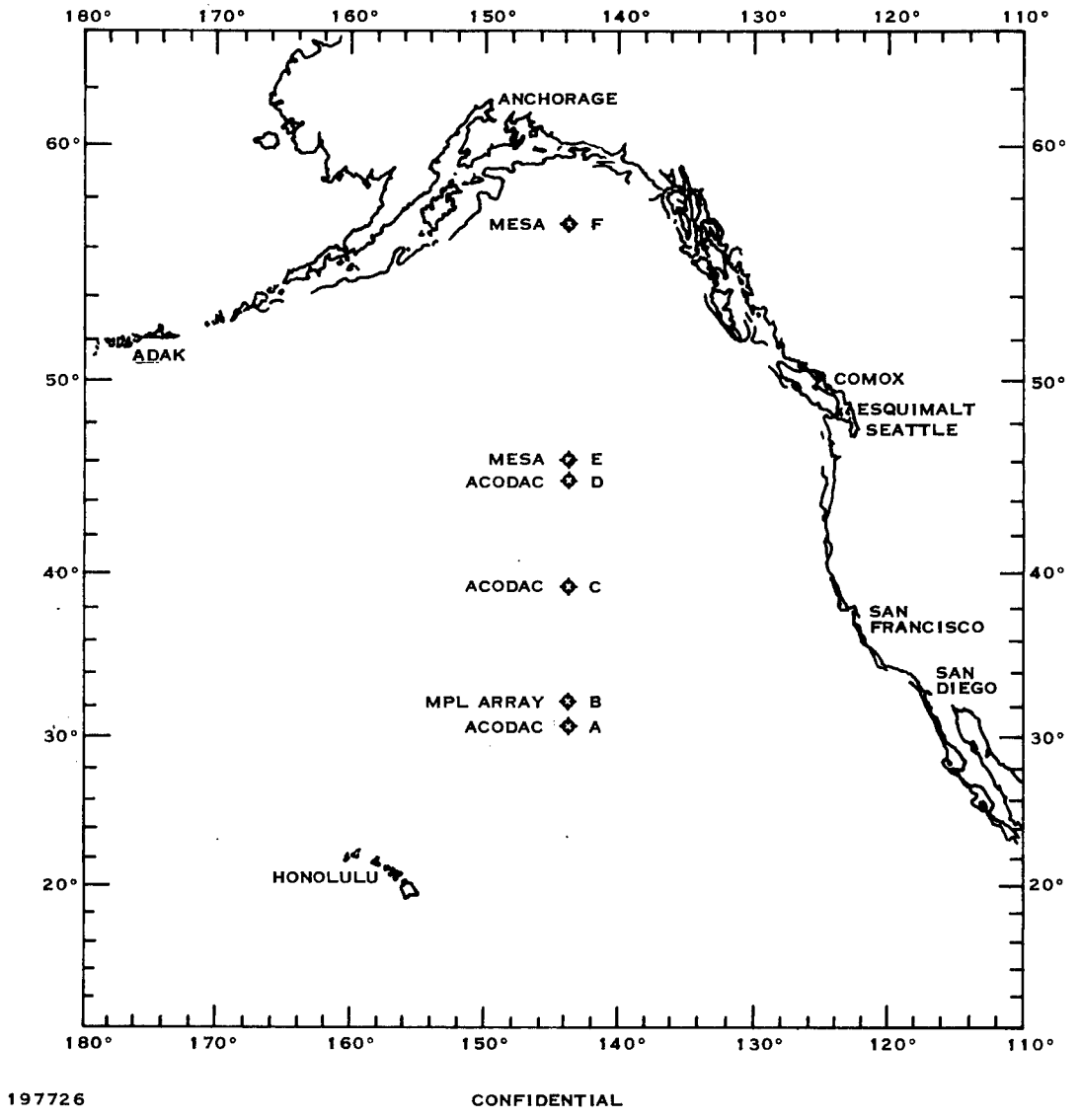

Figure 1-1. (C) Exercise Area Showing Primary Acoustic Measurement Sites (U)

1. (C) Depth Effects (U)

(C) Ambient noise intensity levels below the sound channel exhibit strong correlation to local noise sources.

(C) In the mean, the measured intensities at all sites indicate a trend of decreasing noise intensity with increasing depth in the water column.

(C) At sites B and C, the change in ambient noise intensity with depth was greater between the critical depth and bottom than between the axis and the critical depth for nearly all frequencies.

2. (C) Frequency Effects (U)

(C) The 1/3-octave ambient noise intensity levels were relatively constant over the 10- to 70-Hz band.

(C) In the 70- to 250-Hz band, the noise intensity decreased with increasing frequency at approximately 10 dB per octave.

(C) In the 200- to 800-Hz band, the noise intensity decreased at approximately 5 dB per octave.

3. (C) Environmental Effects (U)

(C) Twenty-hertz pulses attributed to a biological source occasionally raised the noise level in the 25-Hz band by as much as 5 dB at all depths.

(C) At sites C and D, good correlation between intensity level and wind force was observed, particularly in the 160- and 250-Hz bands.

(C) Energy from nearby surface ships increased the intensity level in all bands by as much as 30 dB below the sound channel and 20 dB in the sound channel.

4. (C) Geographic Effects (U)

(C) Near the sound channel axis, the noise intensity level in the 50- to 160-Hz bands at sites B, C, and E was generally 2 to 4 dB greater than at site A.

(C) Intensity levels in the 12.5- to 250-Hz band at site A were 8 to 9 dB lower than at sites C and D, at depths below critical depth.

5. (C) System Effects (U)

(C) Cable strumming energy occasionally raised the noise intensity level in the 12.5-Hz band, for some depths at sites A and C, by as much as 20 dB.

(C) Self-noise, generated by FLIP, necessitated some adjustments or deletion of selected 1/3-octave measurements obtained at site B.

(U) REFERENCES

1. CHURCH ANCHOR Synopsis Report, December 1973. SECRET

2. CHURCH ANCHOR Environmental Acoustic Summary Report, June 1974. SECRET

SECTION II
(C) ANALYSIS OF RESULTS (U)

A. (C) DESCRIPTION OF DISCRETE NOISE SOURCES (U)

(C) The acoustic data observed at sites A, B, C, D, E, and F were composed of signals from many sources, several of which are identifiable. Lofargrams and 10-day ambient-noise-intensity time-series plots of the data from sites A, C, and D were made for selected hydrophones. The lofargrams and 10-day plots were used in the identification of discrete noise sources. The 10-day plots are presented in Subsection II.B and a selected set of lofargrams are shown in Appendixes E and F. For this discussion, the discrete noise sources are separated into three categories as follows:

Biological

ACODAC cable strumming

Nearby surface ships.

Other types of signals were observed in the data but were not categorized because they were of short duration, infrequent, or did not appreciably affect the ambient noise levels. After estimating the contribution of each known discrete source to the composite ambient level, uncontaminated ambient levels can be determined.

1. (U) Biological

(U) A distinctive noise source was observed in the data from sites A and C. These signals were of a repetitive nature and occurred in the vicinity of 20 Hz.

(U) The 20-Hz pulses are believed to be of biological origin,[1,2,3,4] probably the finback whale, species Balaenoptera Physalus, that may have been in the vicinity during the CHURCH ANCHOR tests. The 20-Hz pulses are discussed in Appendix E.

2. (U) ACODAC Cable Strumming

(U) ACODAC systems at sites A and C were deployed in taut-line (high cable tension) vertical moorings. The ACODAC system at site D was deployed in a compliant (low cable tension) vertical mooring. Low-frequency signals caused by strumming of the taut cables are present in the data from sites A and C. The compliant array at site D gives no evidence of the strumming. Figure 2-1 shows the extent of strumming as a function of time for each of the hydrophones at sites A and C.

(U) Analysis of the data from site A indicates that the strumming was strongest and more frequent at the deep phones and weakest and more infrequent at the shallow phones. However, this trend is reversed on site C where the strumming is more severe at the shallow depth phone and is only occasionally observed at the deeper phones.

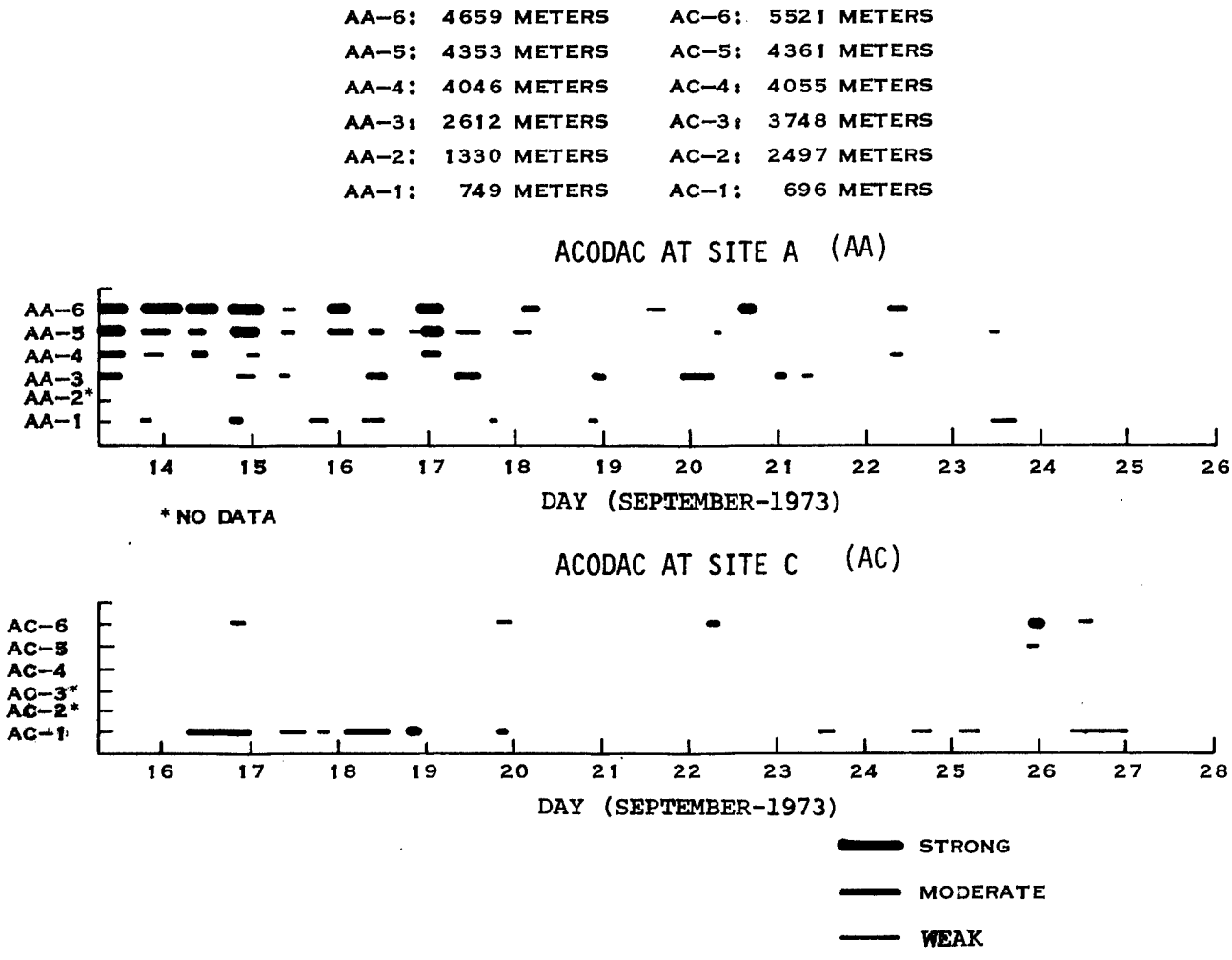

Figure 2-1. (U) Occurrence of Cable Strumming

3. (U) Shipping

(U) The level of ship-generated ambient noise that exists at any point in the ocean depends on the ship population and distribution about that point and the number and quality of acoustic paths to each ship. In general, the overall level of shipping noise is due to a large aggregate of ships. But, if an individual ship passes within a few miles (25 miles or less), the broadband radiated noise may dominate the broadband ambient noise level. In addition, multipath interference patterns may occur in the spectrum. The largest amount of surface traffic was observed at site C, much of it being caused by ships involved in the CHURCH ANCHOR exercise. The deeper phones were consistently affected by nearby shipping to a greater degree and for longer periods of time than were the shallow phones. A summary of typical ship signatures identified from the lofargrams is presented in Appendix F.

B. (C) 10-DAY ACODAC INTENSITY TIME SERIES PLOTS (U)

(C) One of the main features of ambient noise is that it can be divided into three distinct frequency domains. Ambient noise in the region from 10 Hz to a few hundred hertz is dominated by energy radiated from surface ships, while above a few hundred hertz it is most heavily influenced by wind or weather-related phenomena.[5,6,7,8] Below about 10 Hz, shipping noise diminishes and seismic activity becomes the dominant source of energy. Other sources, such as biological sources, can sometimes dominate in either or both regions. As previously mentioned, strong biological activity in the 20-Hz region is observed in much of the data from sites A and C.

(U) To obtain the 10-day plots, data from selected hydrophones were analyzed in six 1/3-octave bands centered at 12.5, 25, 50, 100, 160, and 250 Hz. Ten-minute power averages were computed and plotted over a 10-day period. The spectral levels were plotted in units of $dB/\mu Pa/Hz^{1/2}$. The calibration signals, which occurred for a duration of 5 minutes every 6 hours, are intermixed with the data. The 50- and 200-Hz calibration signals appear as spikes in the 50-, 160-, and 250-Hz bands. In the generation of the 10-day plots, the only calibration signals processed were the header calibration signals. Therefore, the levels of the 6-hour calibration signals shown in the 10-day plots are not accurate and should be ignored.

1. (C) Site A (U)

(C) Figures 2-2, 2-3, and 2-4 show 10-day intensity time-series plots for the 749 m, 4,353 m, and 4,659 m hydrophones at site A for the period 130600Z to 240800Z (September 1973). The average sound channel axis depth occurs at 670 m and the critical depth at 4,515 m. Most of the large-level increases noted on the plots were caused by ships passing nearby. One exception is that of cable strumming, which at times raised the level in the 12.5-Hz band for some phones by as much as 20 dB. The prominent periods of cable strumming are identified on the plots.

(C) An observation of the 10-day plot indicates that at least six ships passed close enough to site A to raise the noise level in one or more 1/3-octave bands for the three phones analyzed. From the track charts, at least two of these are believed to be CHURCH ANCHOR exercise ships. Less variation in average levels was observed at the 749 m depth, and the noise level (below about 160 Hz) received from distant traffic was higher.

(C) No wind force data were available for site A to correlate with the data. However, observation of the 10-day plots at this site shows no prominent change in ambient noise levels that might be attributed to local weather conditions.

2. (C) Site C (U)

(C) Figures 2-5, 2-6, and 2-7 show 10-day time-series plots for the 696 m, 4,055 m, and 5,521 m depths at site C for the period 160000Z to 262200Z (September 1973). For this site, the average sound channel axis depth occurred at approximately 655 m and the critical depth at 3,860 m.

(C) The ambient noise intensity level at site C was dominated a large percent of the time by nearby ships. This was expecially true at depths below the sound channel which contained less long-range components and exhibited a stronger correlation to level changes in local noise sources. The noise at these depths seldom reached a mean level characteristic of distant traffic.

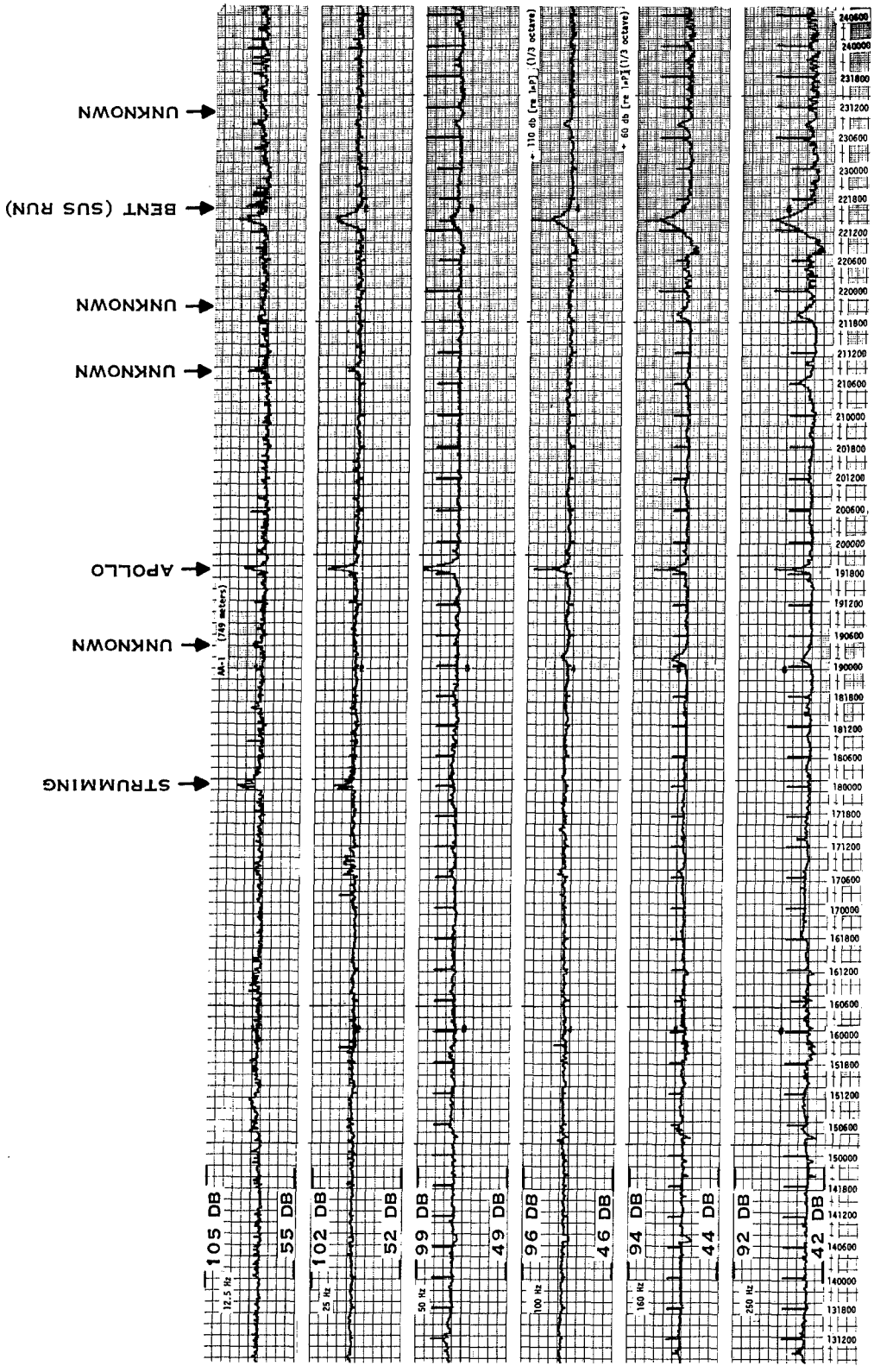

CONFIDENTIAL

197727

Figure 2-2. (C) Ten-Day Ambient Noise Intensity Time-Series Hydrophone Depth: 749 m (79 m Below Axis Depth) Site A Day 130600Z–240800Z (September 1973) (U)

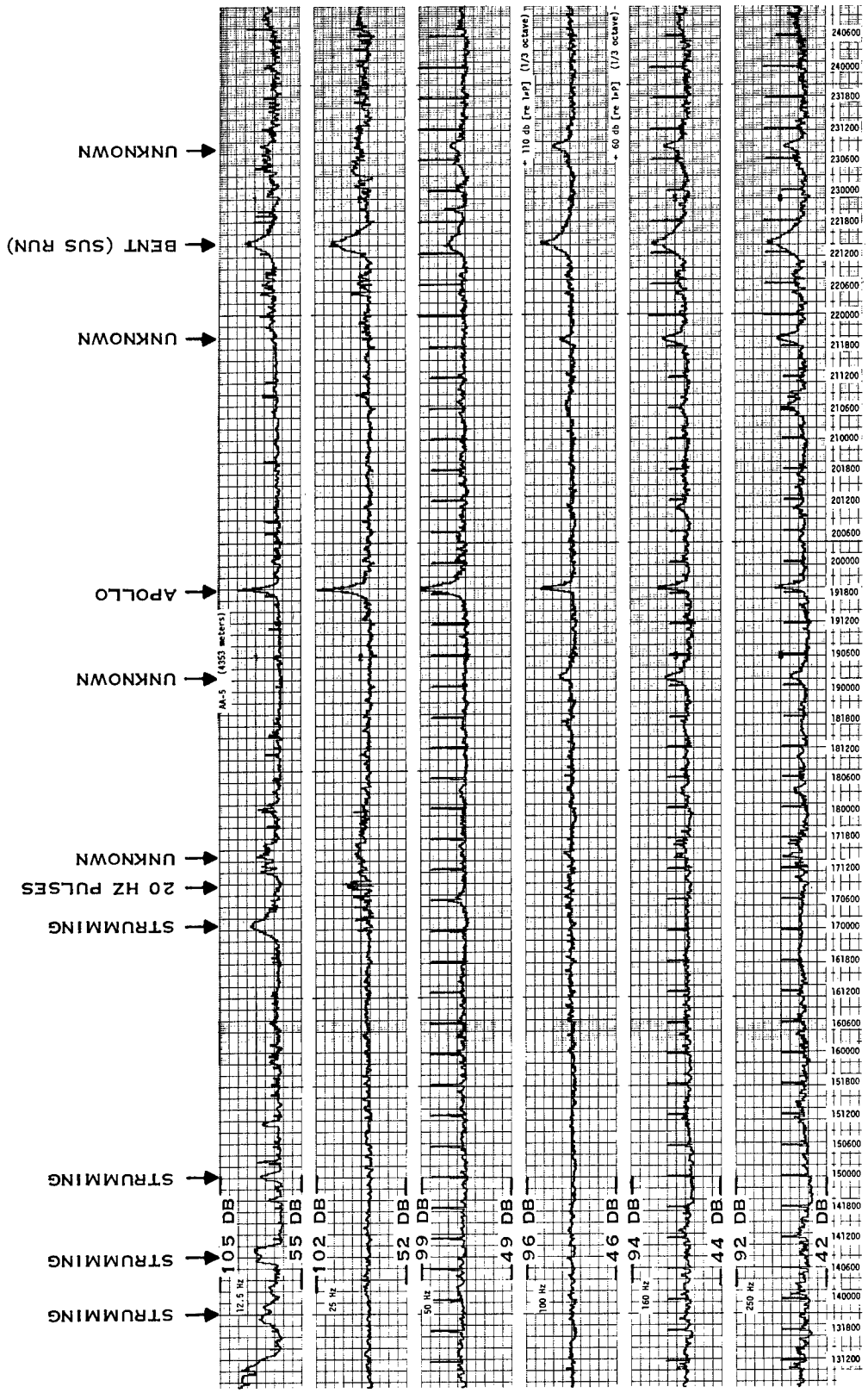

CONFIDENTIAL

Figure 2-3. (C) Ten-Day Ambient Noise Intensity Time-Series Hydrophone Depth: 4,353 m (162 m Above Critical Depth) Site A Day 130600Z–240800Z (September 1973) (U)

197728

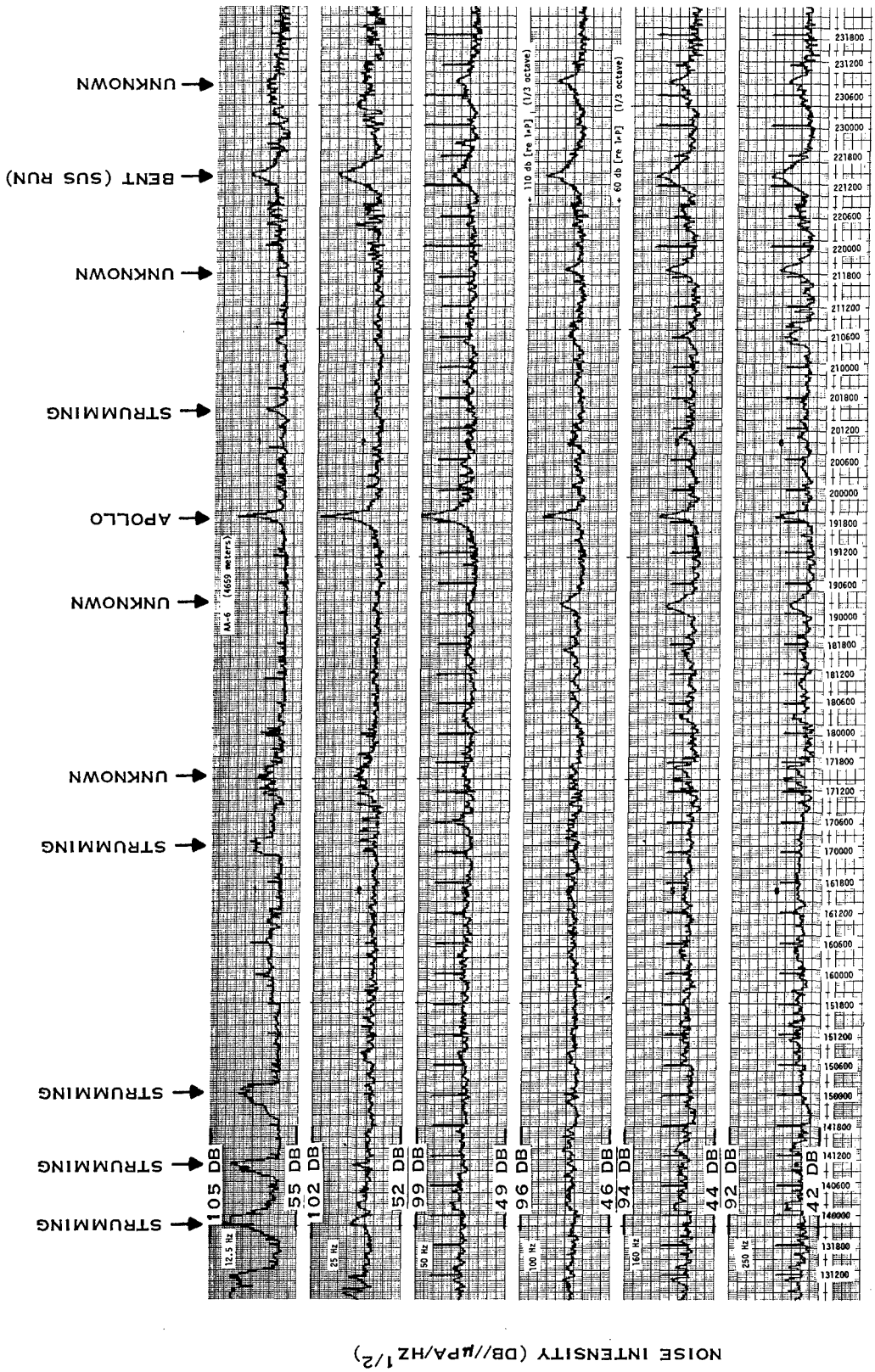

CONFIDENTIAL

Figure 2-4. (C) Ten-Day Ambient Noise Intensity Time-Series Hydrophone Depth: 4,650 m (144 m Below Critical Depth) Site A Day 130600Z–240800Z (September 1973) (U)

197729

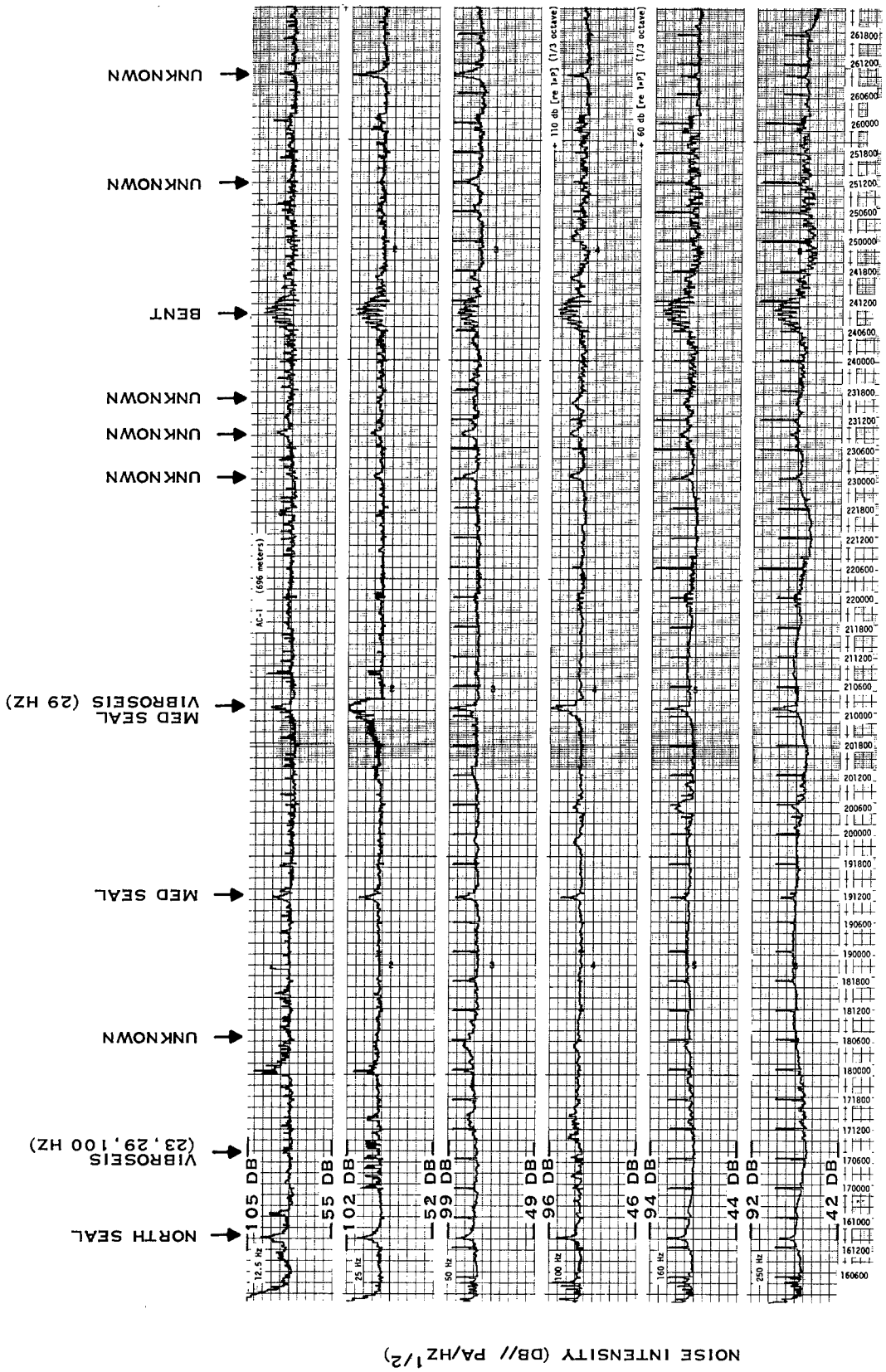

CONFIDENTIAL

Figure 2-5. (C) Ten-Day Ambient Noise Intensity Time-Series Hydrophone Depth: 696 m (41 m Below Sound Channel Axis) Site C Day 160000Z–262200Z (September 1973) (U)

197730

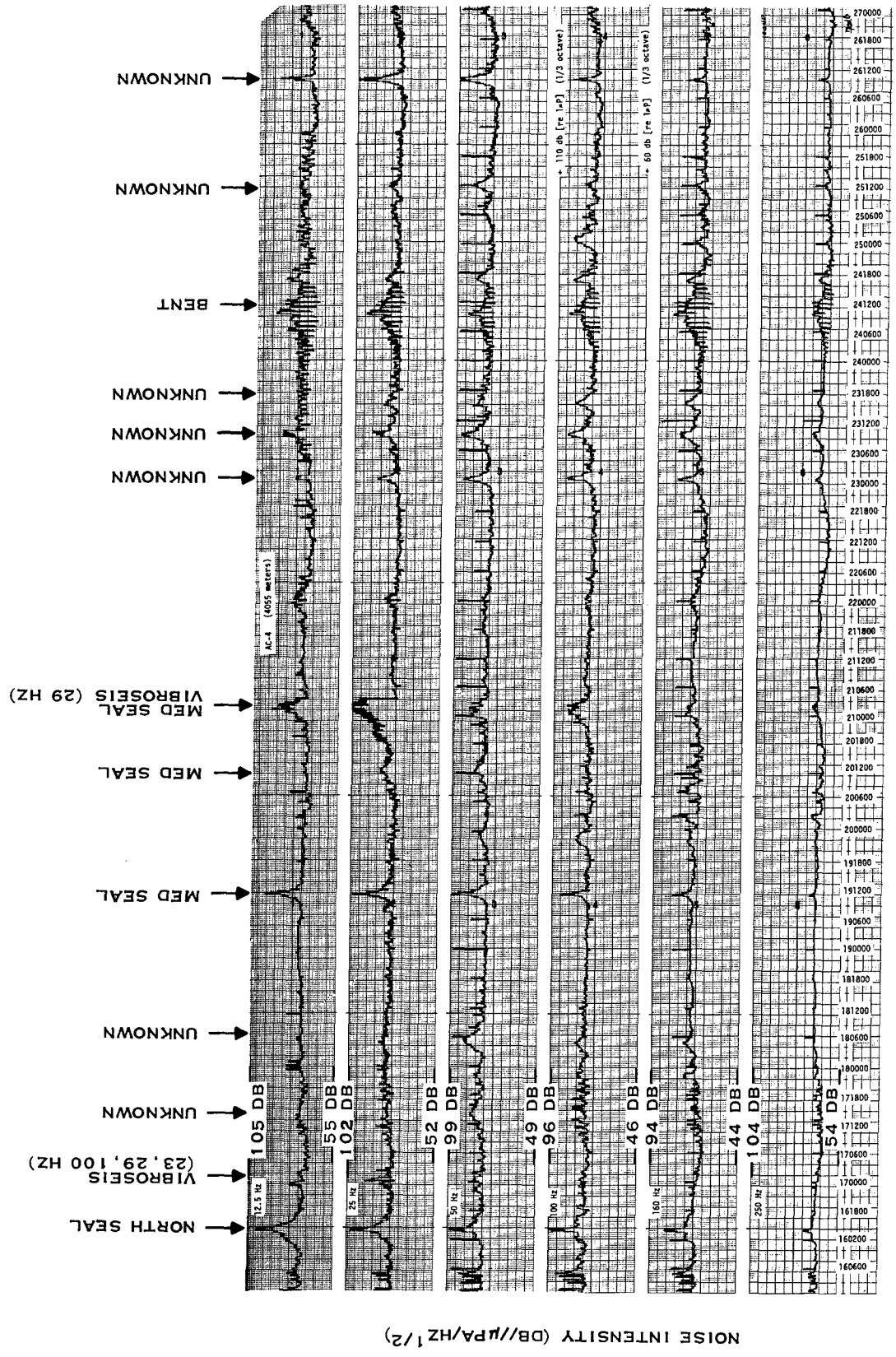

CONFIDENTIAL

Figure 2-6. (C) Ten-Day Ambient Noise Intensity Time-Series Hydrophone Depth: 4,055 m (195 m Below Critical Depth) Site C Day 160000Z–262200Z (September 1973) (U)

197731

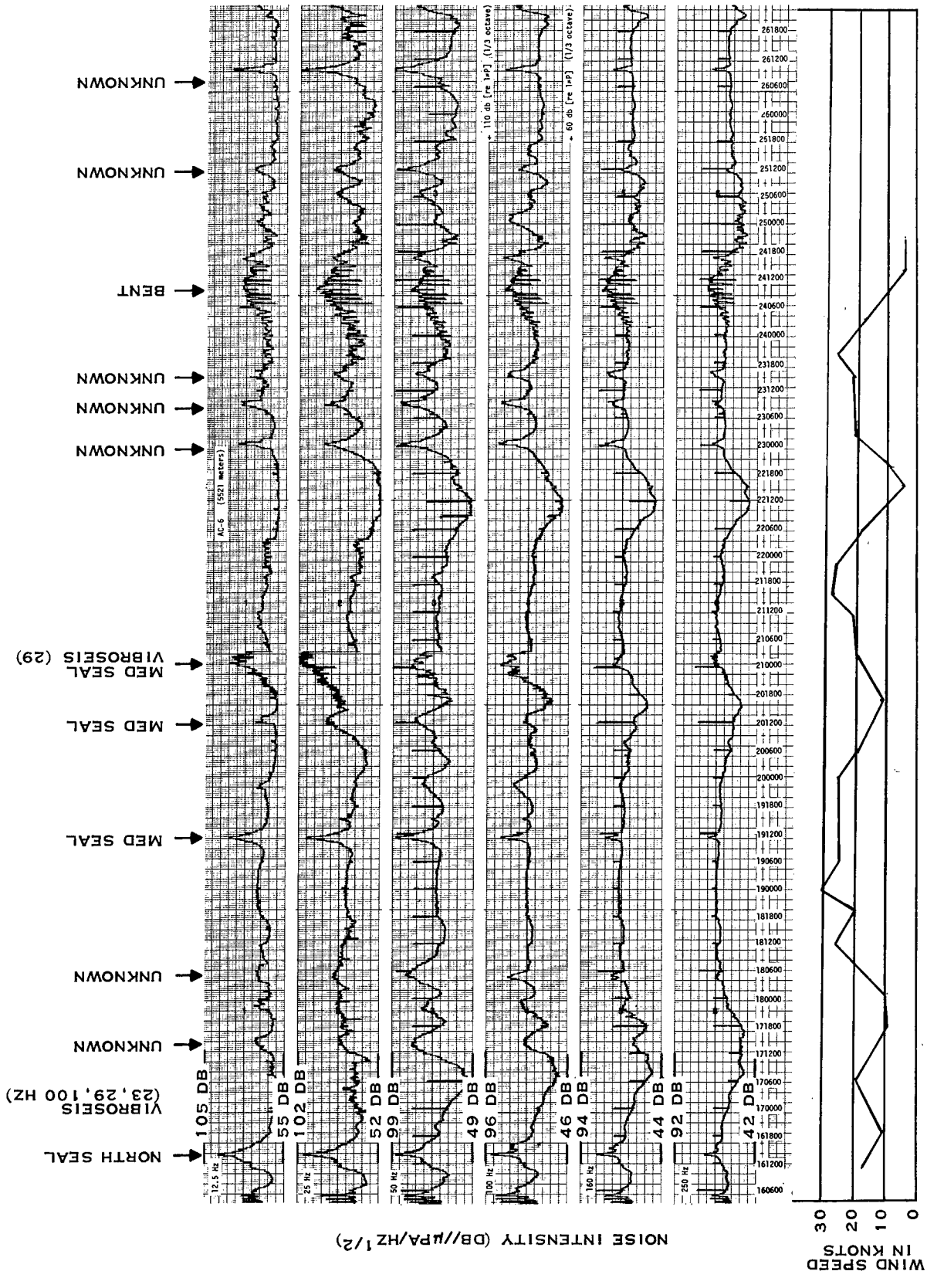

Figure 2-7. (C) Ten-Day Ambient Noise Intensity Time-Series Hydrophone Depth: 5,521 m (34 m Above Seafloor) Site C Day 160000Z–262200Z (September 1973) (U)

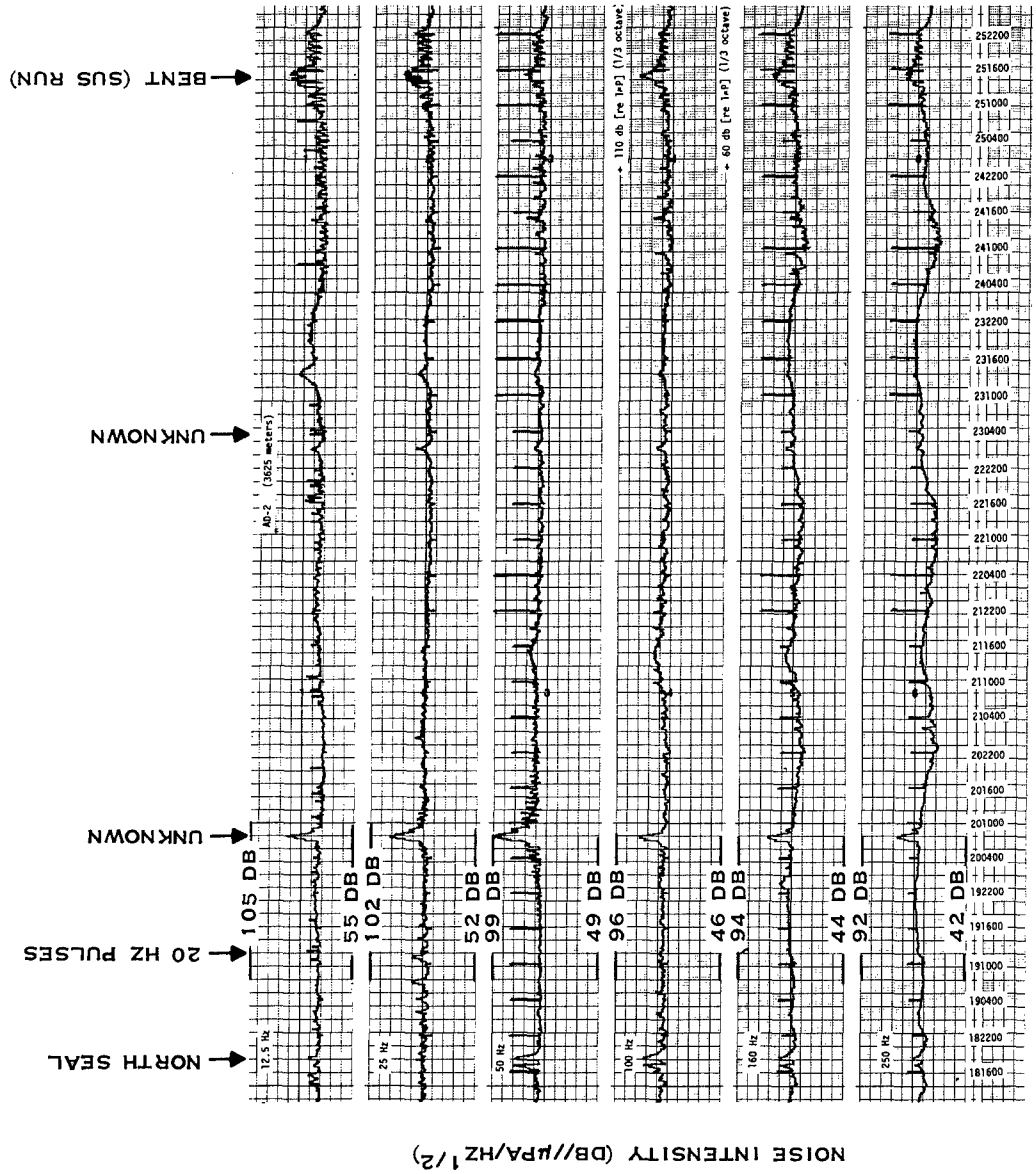

CONFIDENTIAL

Figure 2-8. (C) Ten-Day Ambient Noise Intensity Time-Series Hydrophone Depth: 3,625 m (785 m Below Critical Depth) Site D Day 181000Z–271000Z (September 1973) (U)

197733

(C) Some 12 ships, of which at least three were CHURCH ANCHOR exercise vessels, passed close enough to site C to significantly increase the noise levels in one or more 1/3-octave bands. Strong ship signature lines were observed in the lofargrams most of the time, even when no appreciable changes in the spectrum levels were noted in the 10-day plots.

(C) Twenty-hertz pulses that are attributed to a biological source noticeably raised (5 dB) the level in the 25-Hz band at times. Occurrences of 20 Hz pulses are identified on the plots.

(C) Wind force data obtained from Fleet Weather Central, Pearl Harbor, is shown plotted at the bottom of Figure 2-7. Observation of the weather data indicates good correlation between ambient level and wind force, especially in the 160- and 250-Hz bands. The periods of low ambient levels which occurred at approximately 171200Z, 201200Z, and 221200Z at all three depths also correspond to periods of low wind force. These level changes, moreover, were more pronounced for the deepest phone at 5,521 m than for the other phones at 4,055 m and 696 m. The data from the 5,521 m phone at site C were suspect in absolute level terms since a postcalibration at the Underwater Sound Reference Division, Naval Research Laboratory (Orlando, Florida), indicated a 6-dB drift in sensitivity caused by temperature changes from 23° to 3°C. But, since the data from the 4,612 m phone at site D exhibited the same characteristics, the validity of the data from the 5,521 m phone at site C is supported. The peak-to-peak swings in the noise levels for the 160- and 250-Hz bands correspond to approximately 15 to 20 dB for the 5,521 m phone, as opposed to 5 to 7 dB for the 4,055 m and 696 m phones. The average noise level was observed to decrease with depth by 10 to 15 dB between the 696 m phone and the 5,521 m phone at low frequencies (50 Hz and below). The 5,521 m phone (34 m above sea floor) was well below critical depth and consequently did not receive the long-distance ship-generated energy from refracted paths. It should, therefore, be quieter than those phones above critical depth except when local traffic raised the level, which did not occur an appreciable percent of the time at this site.

3. (C) Site D (U)

(C) Figures 2-8, 2-9, and 2-10 show the 10-day time-series plots for the 3,625 m, 3,925 m, and 4,612 m phones at site D for the period 181000Z to 271000Z (September 1973). For this site, all hydrophones were distributed between the bottom of the sound channel and the sea floor. The average sound axis depth occurred at 478 m and the critical depth at 2,840 m. Two and possibly three ships that passed close enough to this site to raise the noise level in one or more bands have been identified as CHURCH ANCHOR exercise ships.

(C) Wind force data recorded on the *Endeavour*, which was in the area of site D from 18 September through 28 September, are shown plotted at the bottom of Figure 2-10. As can be seen, site D exhibits a correlation between noise level and wind force in the 160- and 250-Hz bands for all three hydrophones. The periods of low noise levels and wind force occurred at approximately 210000Z, 221000Z, and 241000Z. These phones, being below the sound channel, normally exhibited a strong correlation between level changes and local noise sources. The noise level below 100 Hz showed very little wind dependence and can be explained by Wenz curves,[9] which indicate that ocean traffic noise peaks in the frequency band from 40 to 100 Hz. Above this frequency, ambient noise level is strongly dependent on wind force. The variations in level (15 to 20 dB) for the 4,612 m phone compare in magnitude to the variations in level for the 5,521 m phone at site C, both of which are 34 m above the sea floor.

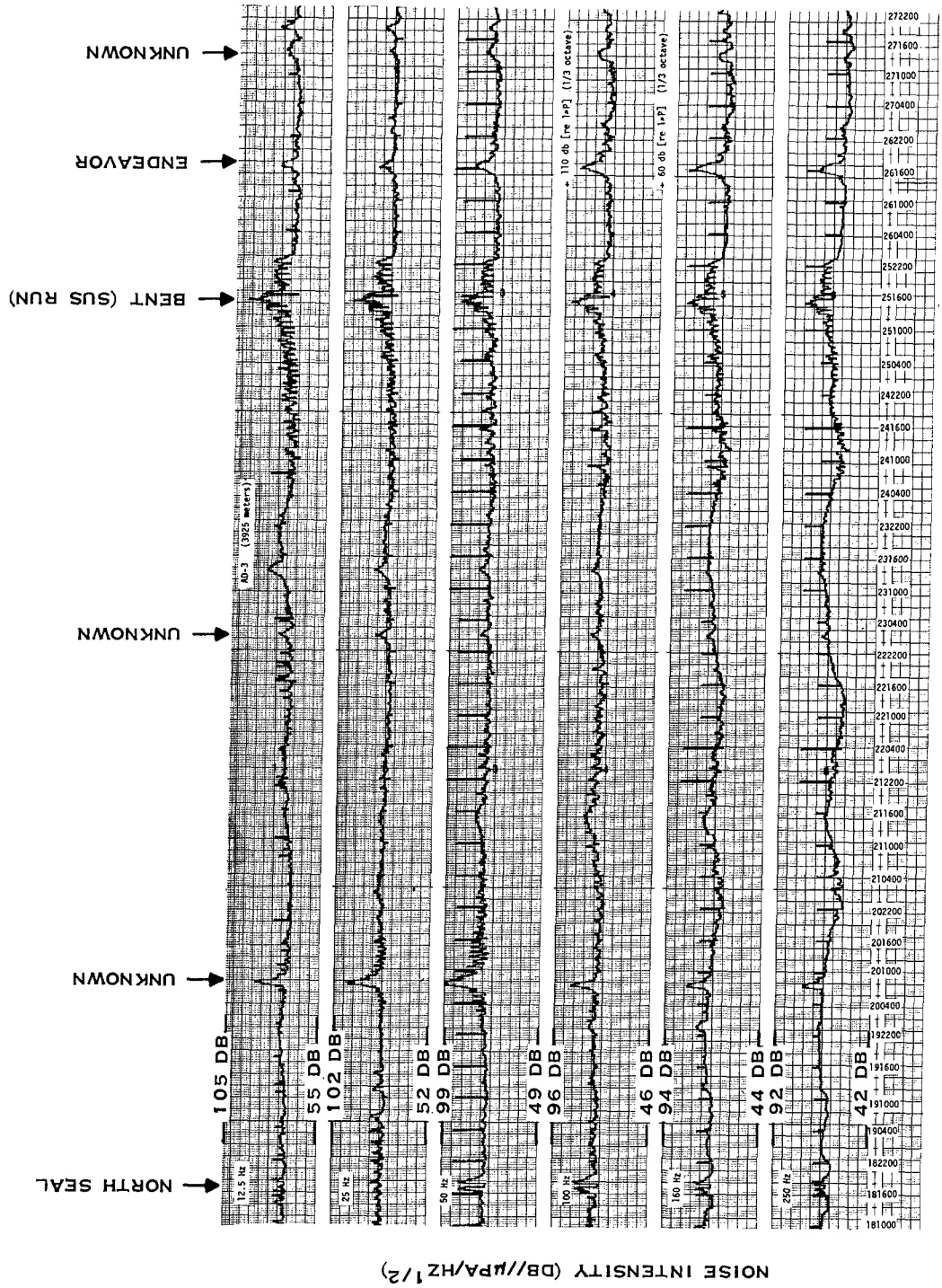

CONFIDENTIAL

Figure 2-9. (C) Ten-Day Ambient Noise Intensity Time-Series Hydrophone Depth: 3,925 m (1,085 m Below Critical Depth) Site D Day 181000Z–271000Z (September 1973) (U)

197734

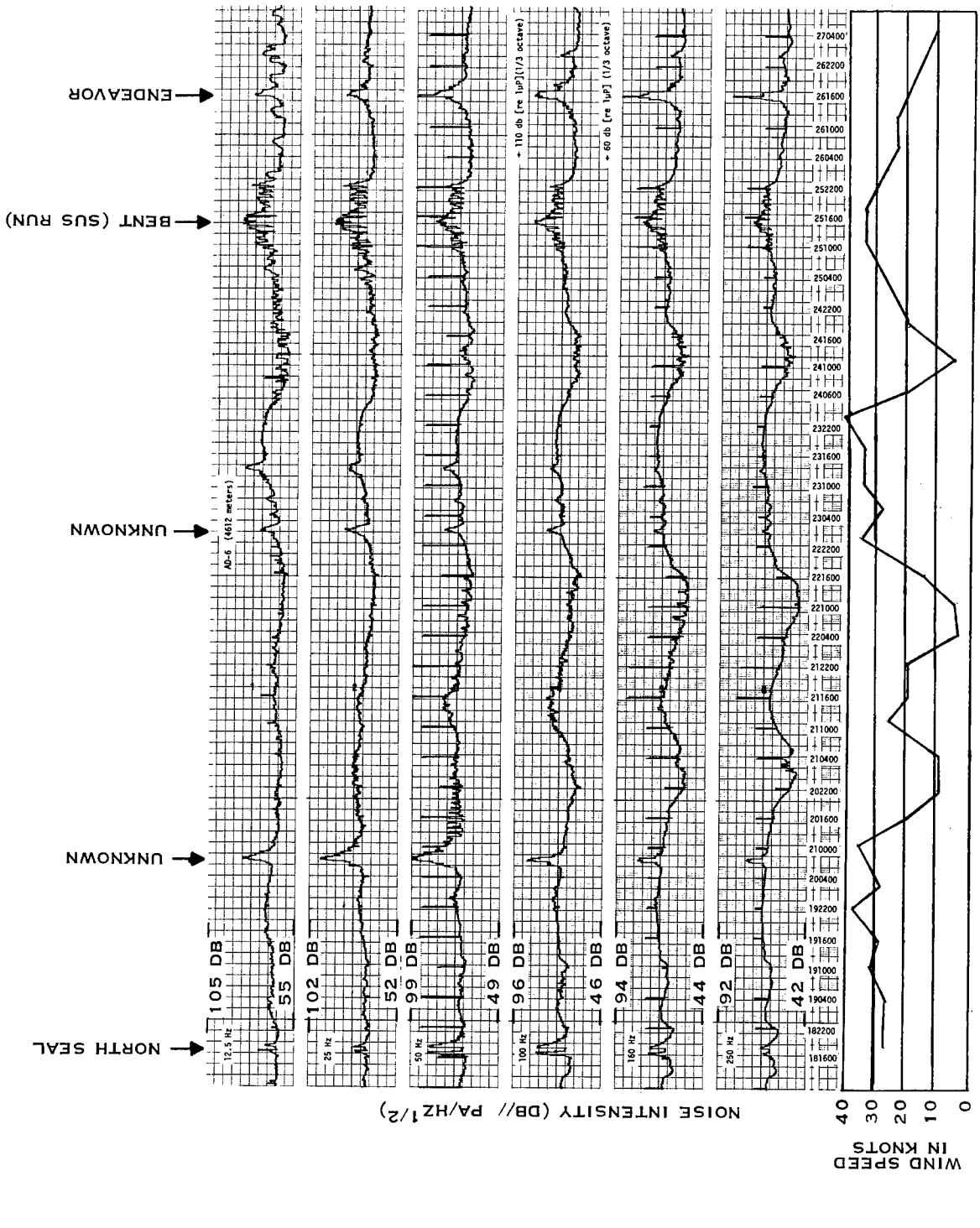

CONFIDENTIAL

Figure 2-10. (C) Ten-Day Ambient Noise Intensity Time-Series Hydrophone Depth: 4,612 m (34 m Above Seafloor) Site D Day 181000Z–271000Z (September 1973) (U)

197735

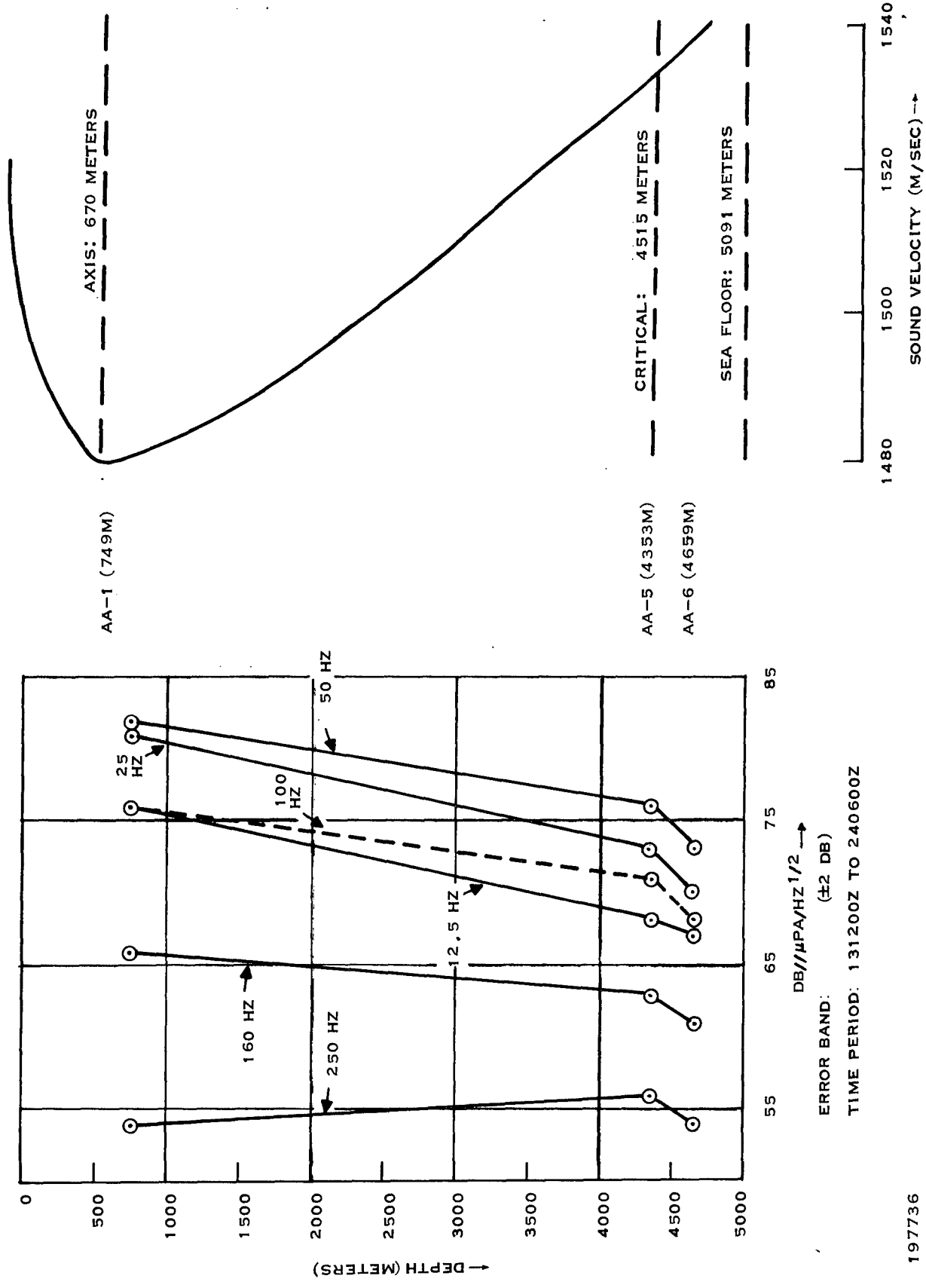

Figure 2-11. (C) Depth Dependence of Uncontaminated Ambient Noise Intensity at Site A (10-Day Averages) (U)

C. (C) ANALYSIS OF UNCONTAMINATED AMBIENT NOISE DATA (U)

1. (C) Definition of Uncontaminated Noise Intensity (U)

(C) Uncontaminated noise levels were determined by visually estimating what the level would be in the absence of local surface traffic. This was accomplished by positioning a see-through ruler so that half the noise intensity levels were above and half below the straight edge. Finally, the ambient noise data base was enlarged by combining the processing results from Texas Instruments, The University of Texas, the Marine Physical Laboratory, and the Defence Research Establishment Pacific.

2. (C) Depth Profiles (U)

(C) The ship-generated energy that follows refracted paths for long distances would be expected to be strongest in those depth regions occupied by refracted paths.[6] In general, very shallow or very deep hydrophones will not intercept these paths.

(U) To illustrate the variation of the ambient noise intensity with depth, depth profiles for two 24-hour and one 10-day observation periods were constructed for sites A and C and two 24-hour periods for site B. In addition, a depth profile for one 10-day average was made for site D. Thus, a total of nine depth profiles, Figures 2-11 through 2-19, were made available for analysis. The data presented in this manner indicate that the spread in the noise levels across the frequency band was greater at the shallower depths (near the sound channel axis) than it was near the critical level and below. These spreads are summarized in Table 2-1. This phenomenon was caused by the noise in the lower frequency bands decreasing at greater rate with respect to depth than the higher frequencies. Thus, the noise in the 250-Hz band decreased very slightly, whereas the level in the lower frequency bands consistently decreased several decibels when the transition to greater depths occurred. The energy in the lower frequency bands originated at long ranges and propagated mainly in the sound channel axis. This propagation mode would explain the rapid decrease in low-frequency energy for depths below critical depth. The higher frequencies, however, were generated more locally than the lower frequencies and, consequently, were not dependent on the sound channel for their relatively short propagation paths. Thus, the effect of the transition from the sound channel axis to critical depth and deeper for high frequencies was not as severe as for the lower frequencies.

3. (C) Depth Dependence of the Nonstationarity of the Ambient Noise Field (U)

(C) One of the most significant features of the ambient noise data is the nonstationarity as reflected in the rapid change in noise intensity that can occur over a period of only a few hours. This behavior is easily observed in Figures 2-2 through 2-10, which were constructed with 10-minute averages. Generally, as the depth increased, the relative nonstationarity likewise increased, an effect that occurred at all frequencies. This phenomenon can be attributed to the fact that the stationary component of the total ambient noise field was generated by a large number of sources at long distances. Thus, the stationary component of the noise relied on the sound channel for propagation and, as a result, a decrease in depth below the critical depth can cause a significant decrease in the intensity of the stationary component of the noise. Local sources of noise, on the other hand, were relatively few in number and their appearance and disappearance with time generated the rapid fluctuations observed in the total noise intensity plots.

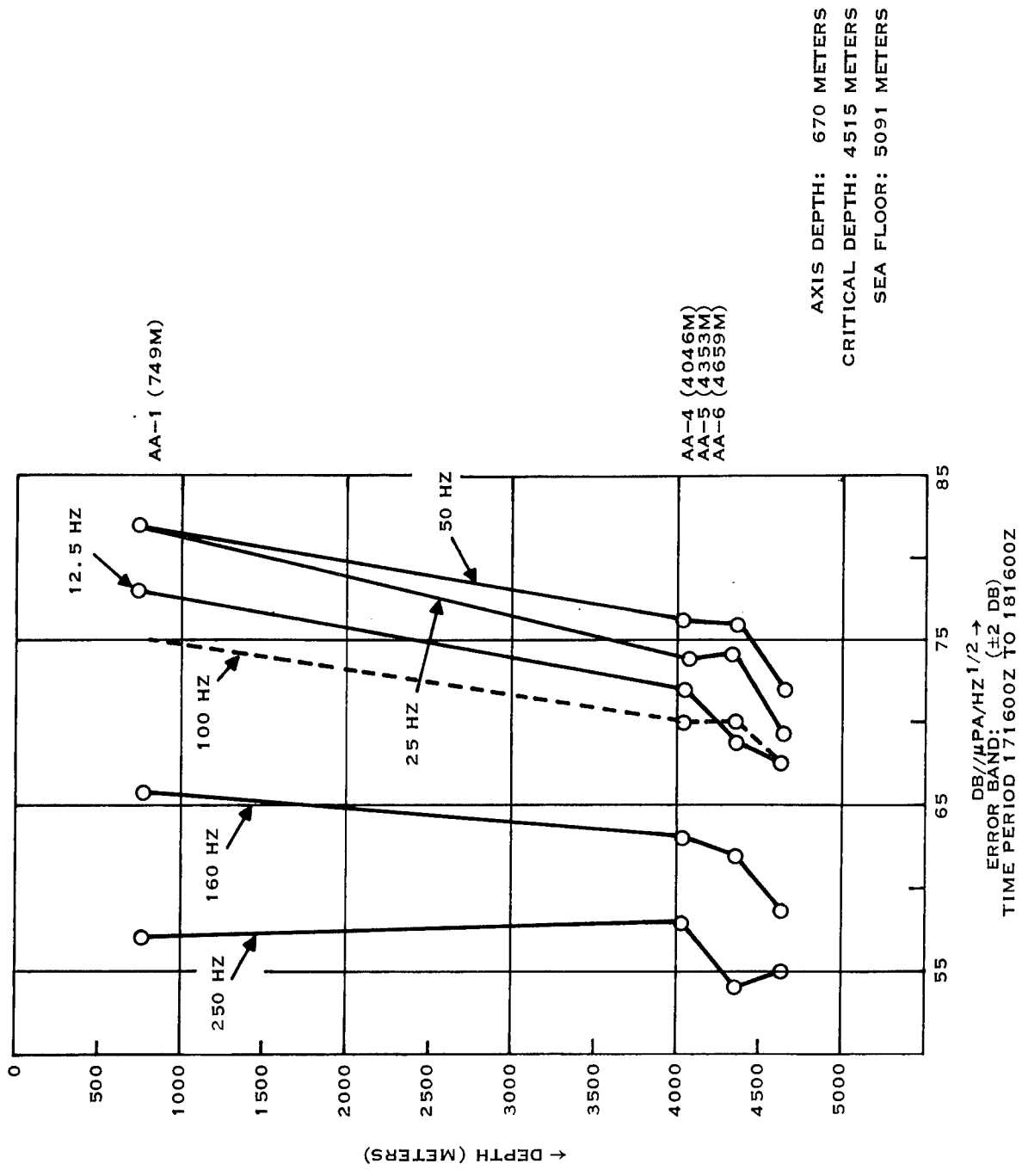

Figure 2-12. (C) Depth Dependence of Uncontaminated Ambient Noise Intensity at Site A (24-Hour Averages) (U)

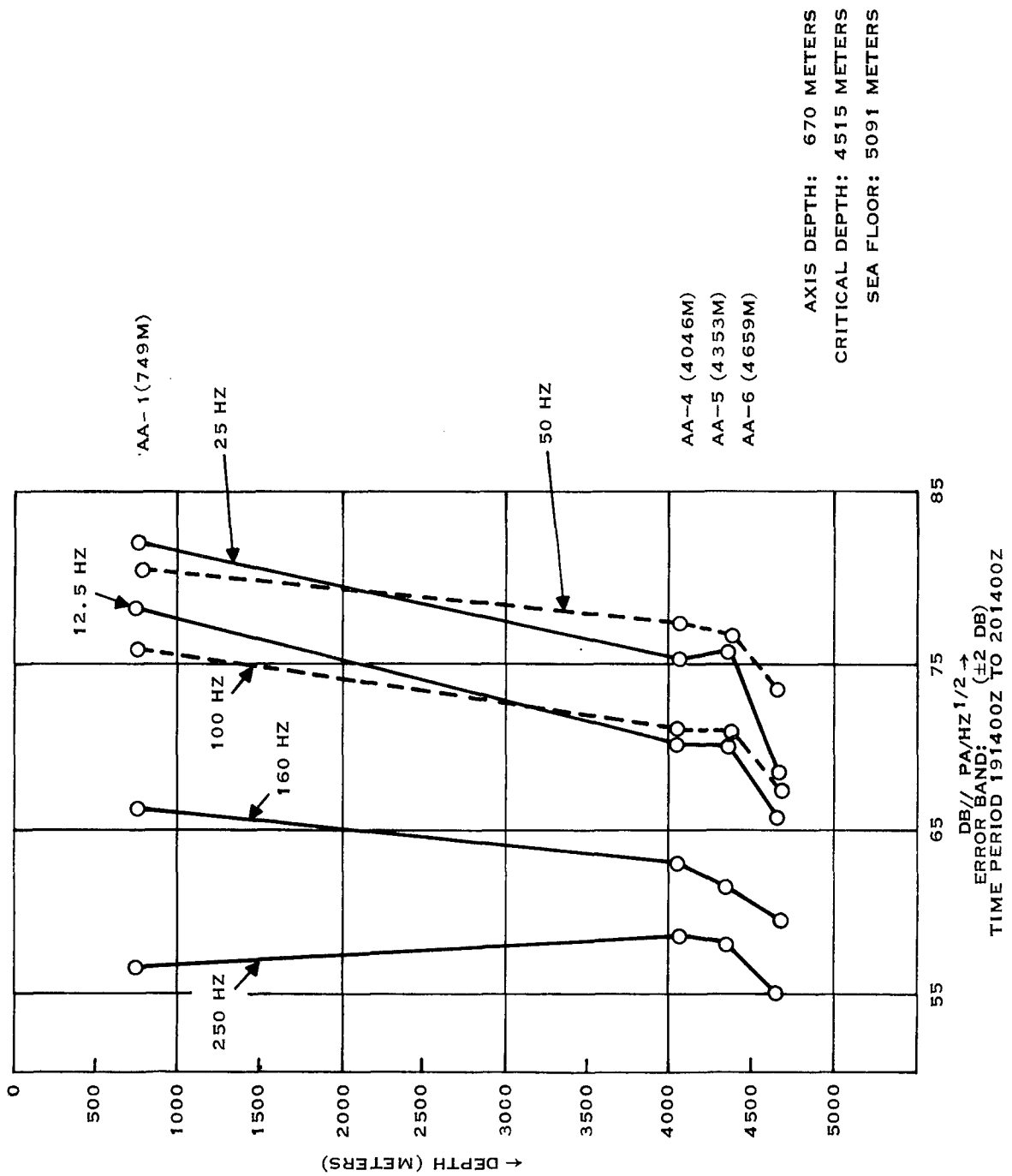

Figure 2-13. (C) Depth Dependence of Uncontaminated Ambient Noise Intensity at Site A (24-Hour Averages) (U)

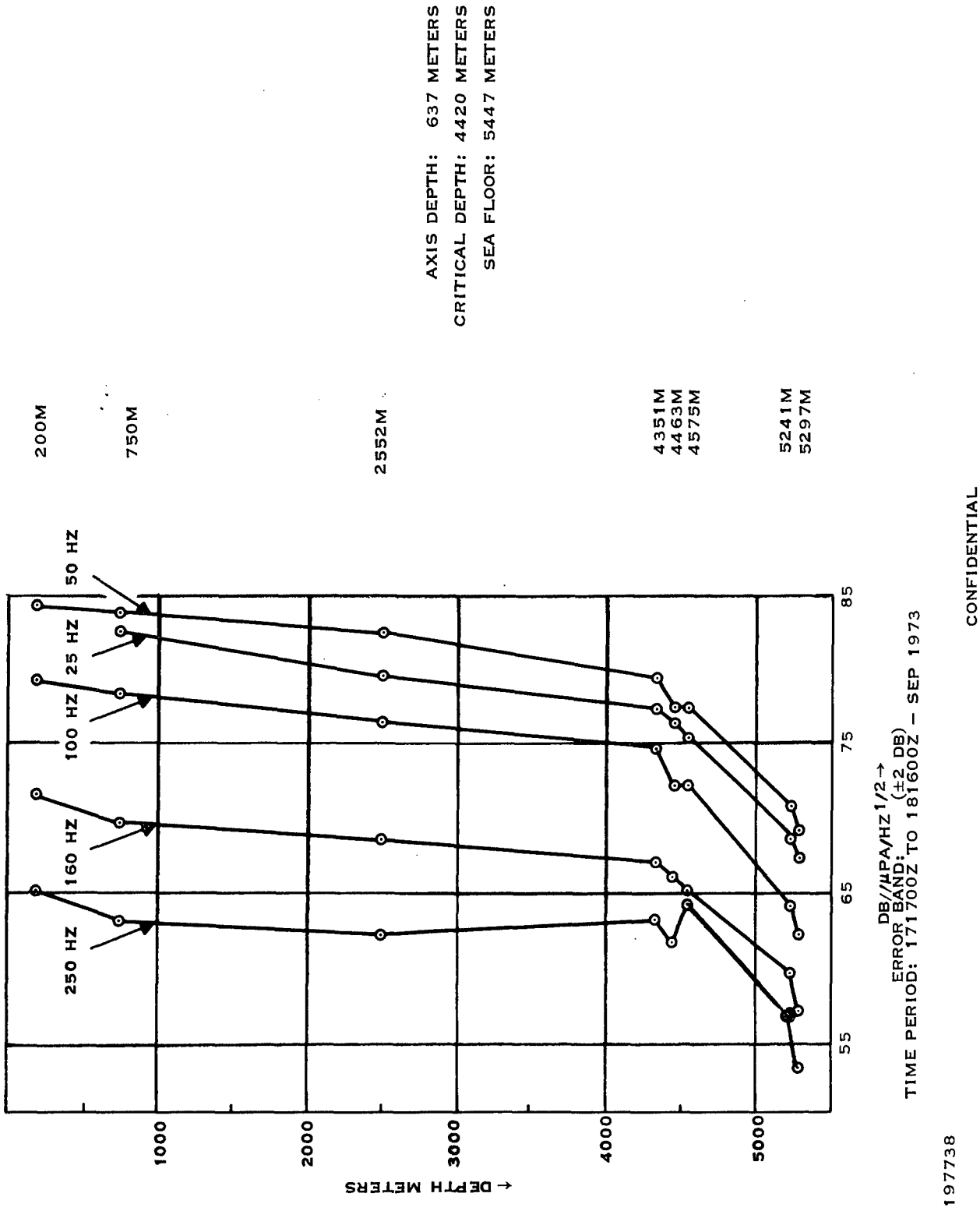

Figure 2-14. (C) Depth Dependence of Uncontaminated Ambient Noise Intensity at Site B (24-Hour Averages) (U)

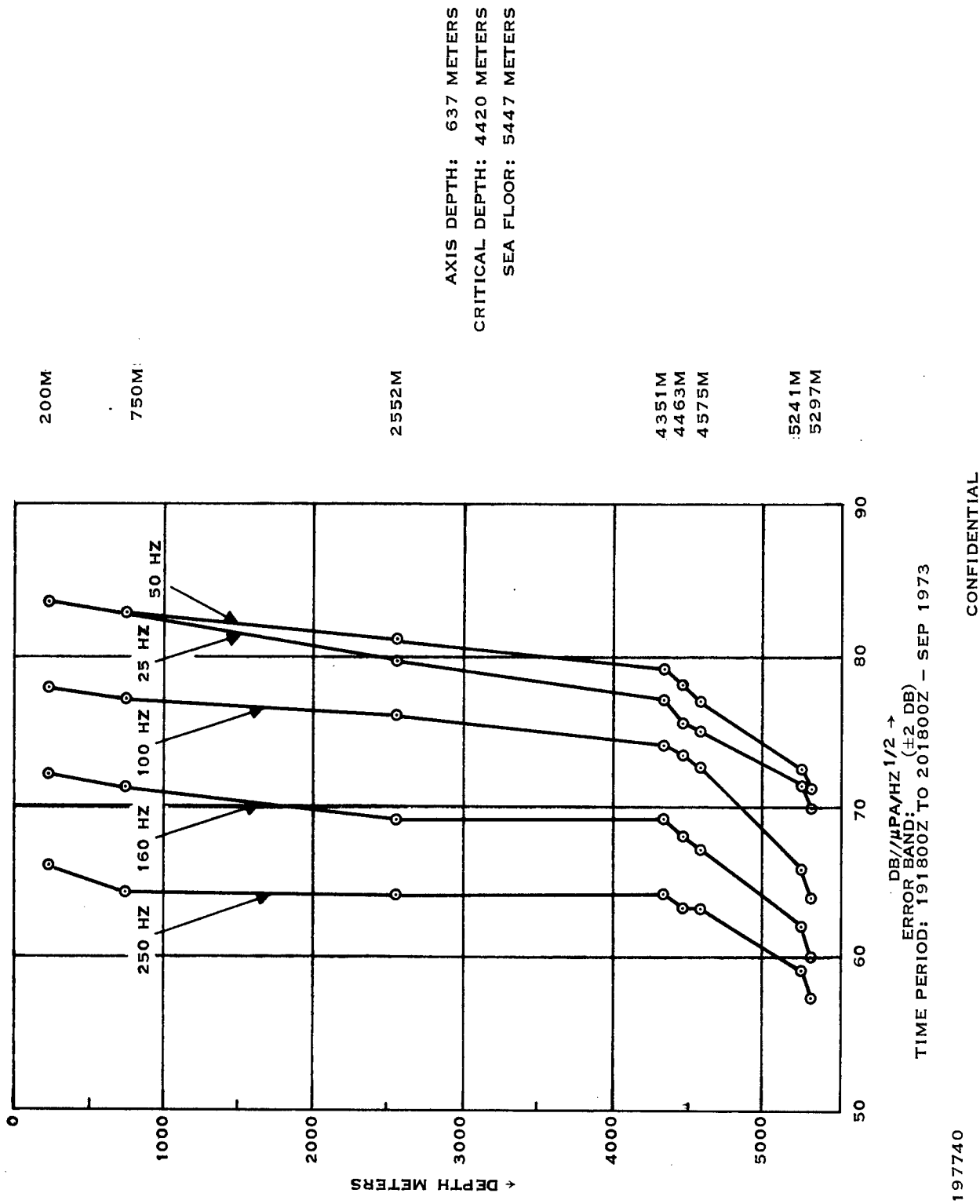

Figure 2-15. (C) Depth Dependence of Uncontaminated Ambient Noise Intensity at Site B (24-Hour Averages) (U)

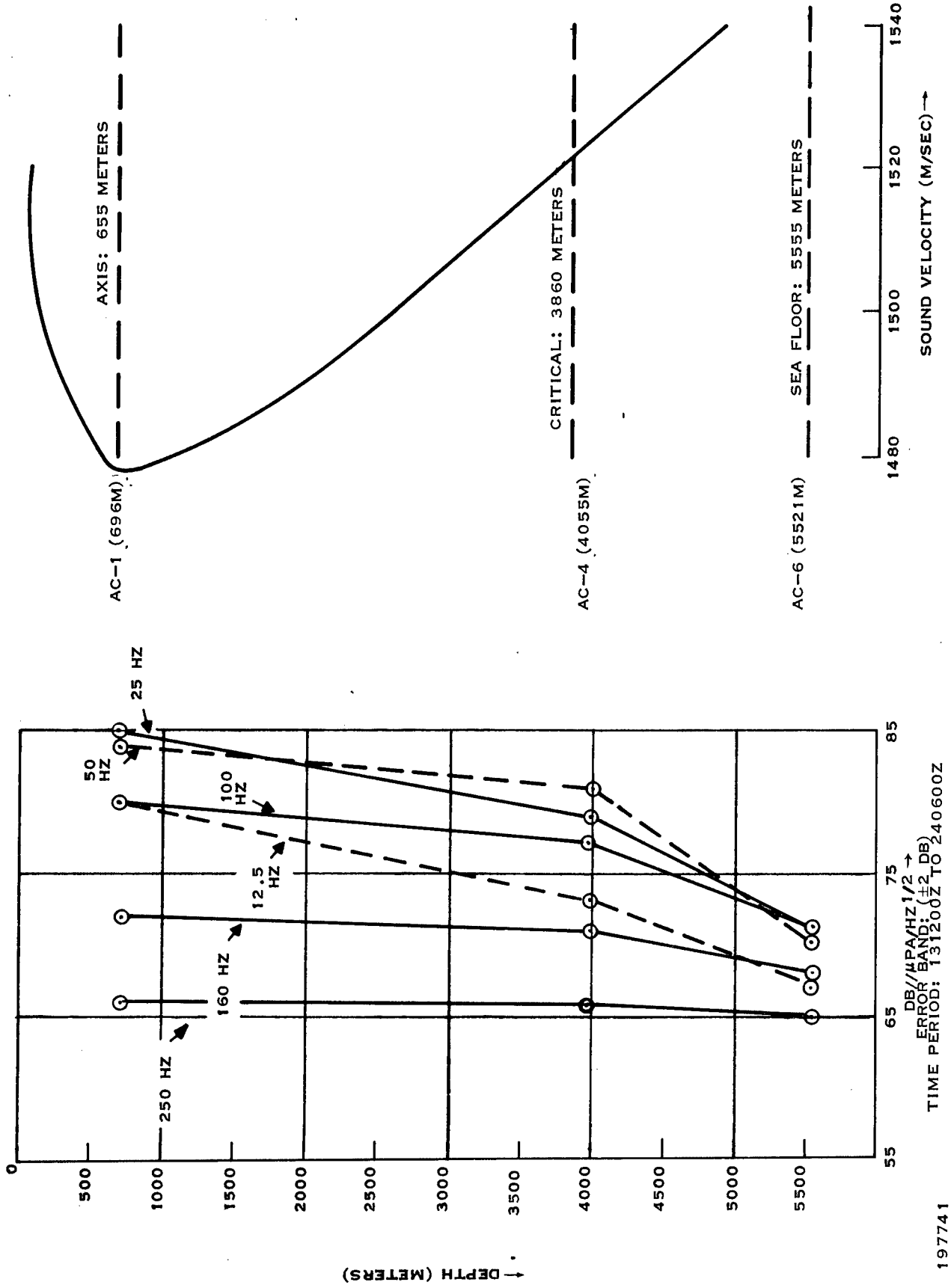

Figure 2-16. (C) Depth Dependence of Uncontaminated Ambient Noise Intensity at Site C (10-Day Averages) (U)

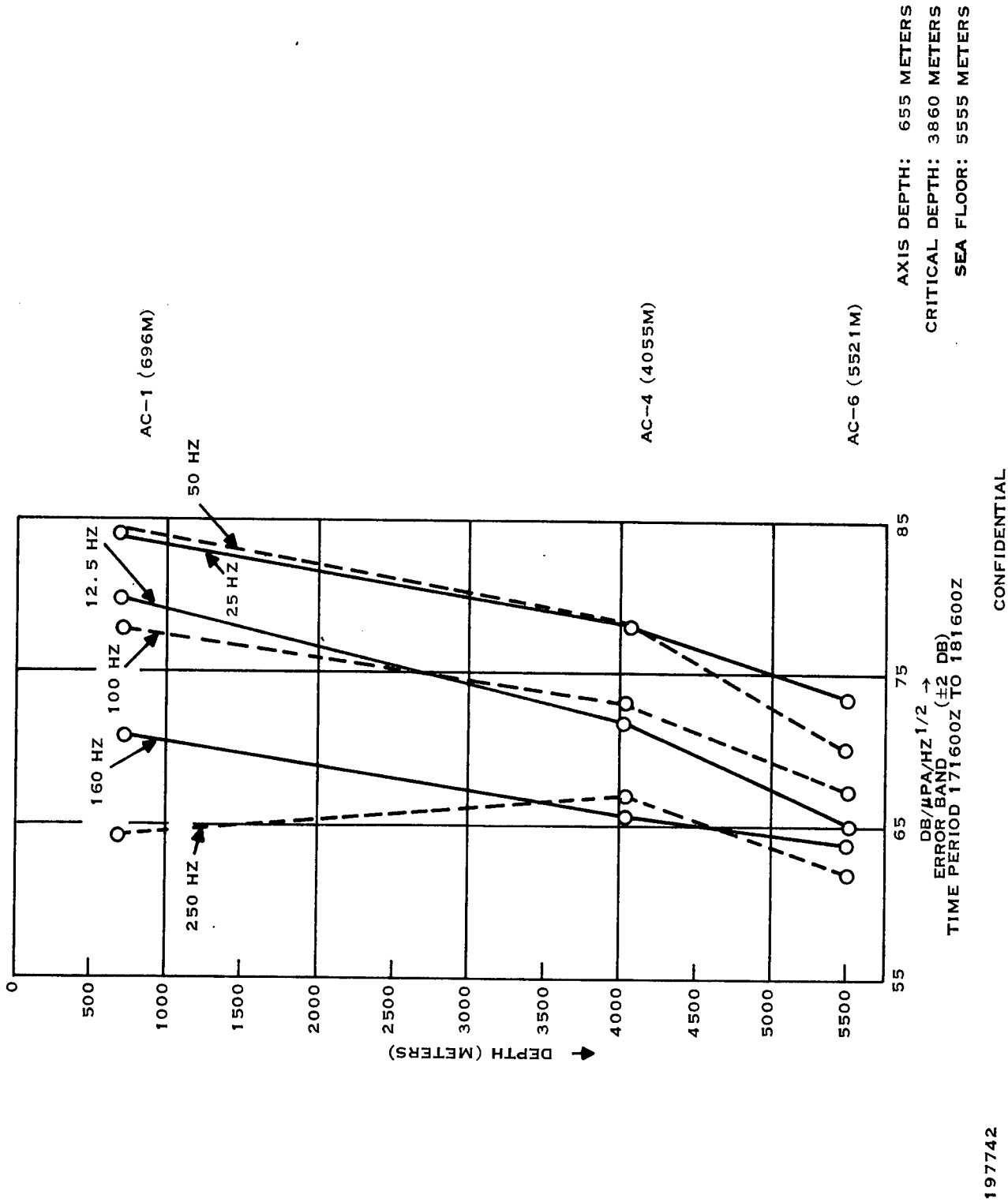

Figure 2-17. (C) Depth Dependence of Uncontaminated Ambient Noise Intensity at Site C (24-Hour Averages) (U)

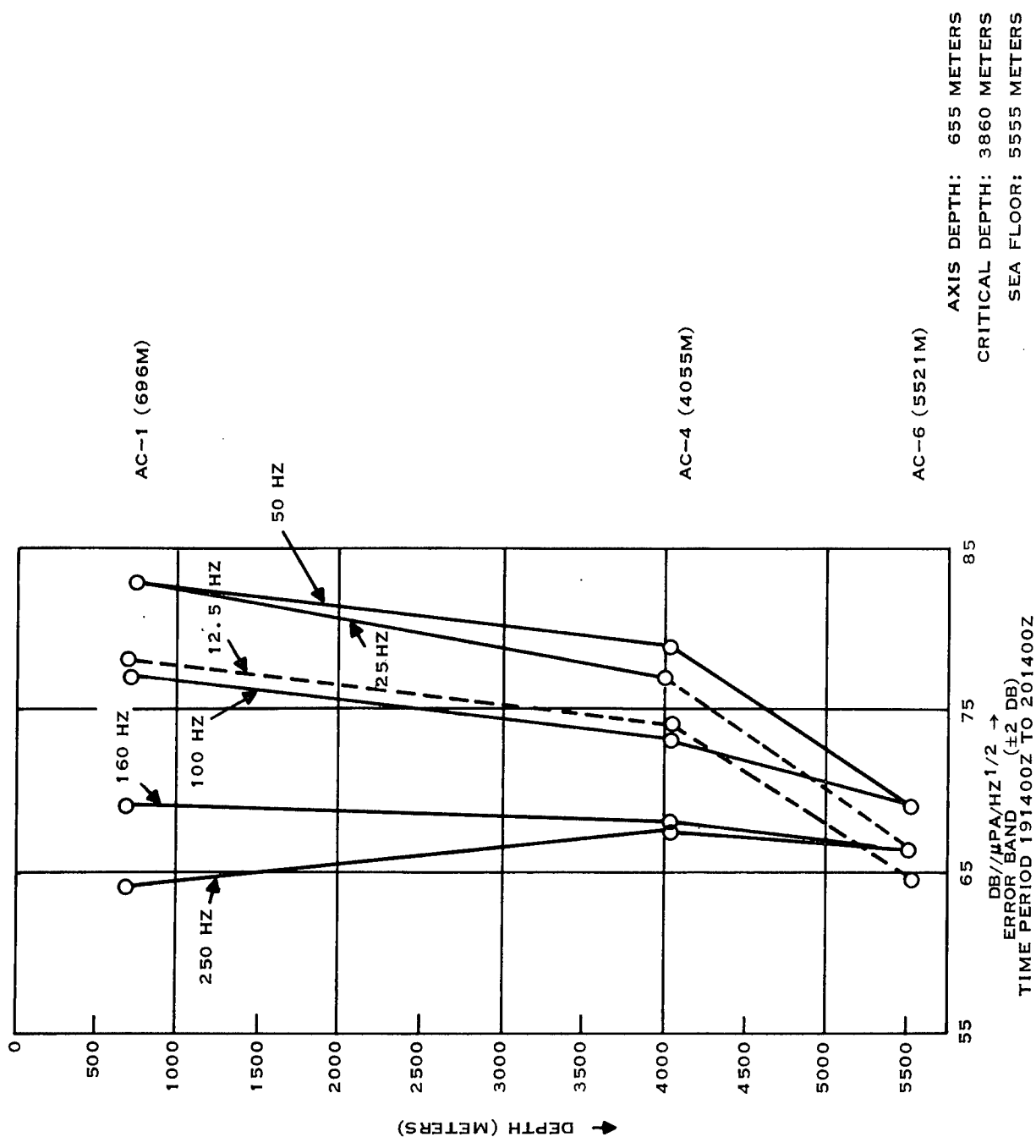

Figure 2-18. (C) Depth Dependence of Uncontaminated Ambient Noise Intensity at Site C (24-Hour Averages) (U)

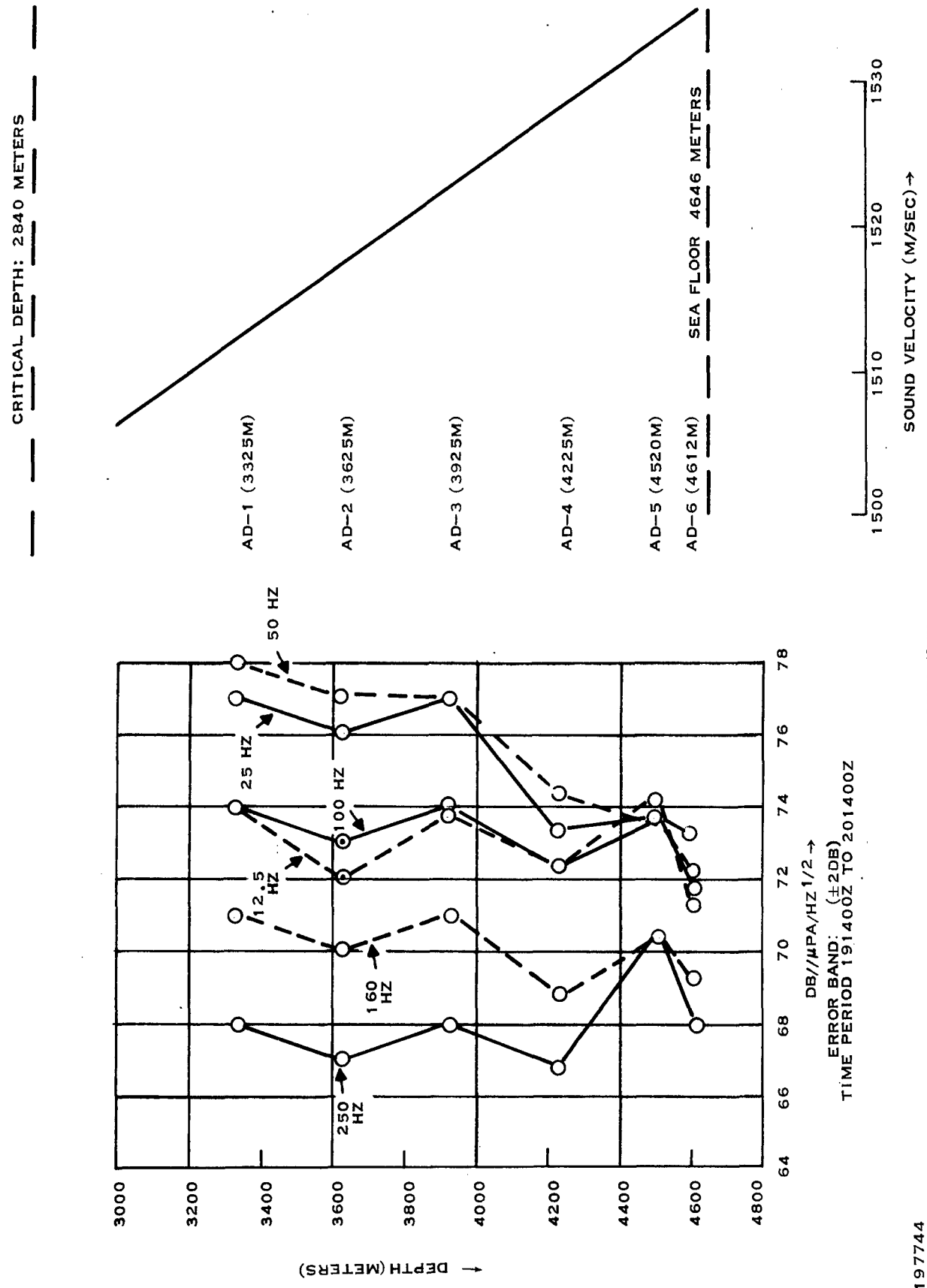

Figure 2-19. (C) Depth Dependence of Uncontaminated Ambient Noise Intensity at Site D (24-Hour Averages) (U)

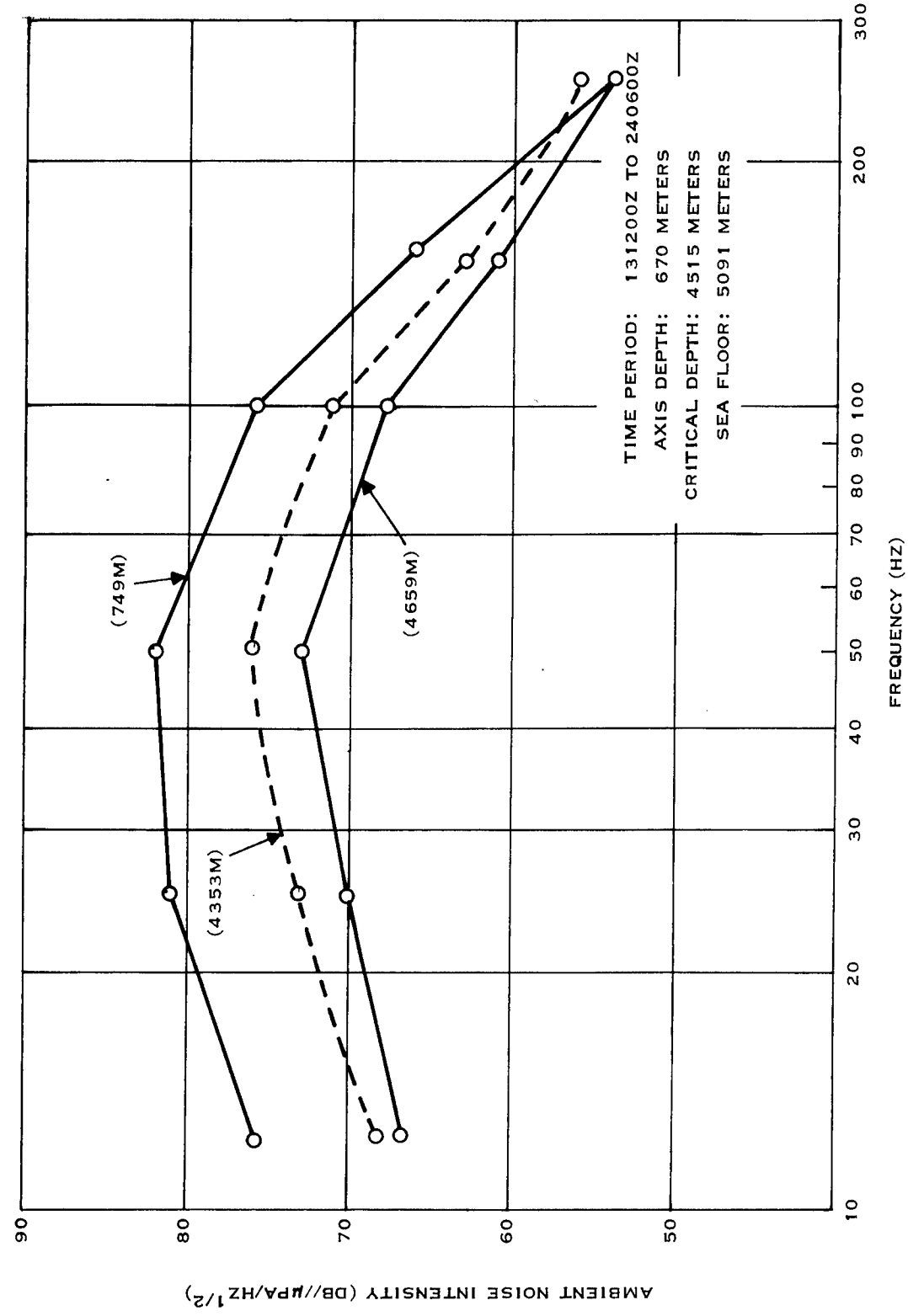

Figure 2-20. (C) Frequency Dependence of Uncontaminated Ambient Noise Intensity at Site A (10-Day Averages) (U)

Owing to the closeness of these sources to the hydrophone, the sound channel was not a critical factor in the propagation of their noise fields. Therefore, the nonstationary components become a larger percentage of the total ambient noise field at greater depths; the net effect is that nonstationarity increases with depth.

4. (C) Noise Intensity Spectra (U)

(U) An alternative presentation of the variation of the noise intensity with frequency and depth is possible with the construction of noise-intensity spectra. Noise-intensity spectra were generated by plotting 10-day and 24-hour averages of the noise intensity, measured at a given depth and site, as functions of frequency. Figures 2-20 through 2-28 are noise-intensity spectra corresponding to site A (one 10-day and two 24-hour averages), site B (two 24-hour averages), site C (one 10-day and two 24-hour averages), and site D (one 24-hour average).

(C) As with the depth profiles, these noise intensity spectra indicate a general decrease in noise intensity (for a given frequency) with depth. In addition, the rate of decrease with depth is frequency-dependent. Thus, the transition in depth from the sound channel axis to near the critical depth has a more marked effect on the lower frequencies than on the higher frequencies.

TABLE 2-1. (C) SPREAD IN AMBIENT NOISE INTENSITY AT VARIOUS DEPTHS ACROSS FREQUENCY BAND 12.5 TO 250 HZ, FOR SITES A, C, AND D, AND 25 to 250 HZ, FOR SITE B (SEPTEMBER 1973) (U)

Site	Depth	24-Hour Average 171600Z–181600Z	24-Hour Average 191400Z–201400Z	10-Day Average
A	749 m	25 dB	25 dB	28 dB
Axis Depth–670 m	4,046 m	18 dB	19 dB	
Critical Depth–4,515 m	4,353 m	19 dB	19 dB	20 dB
Sea Floor–5,091 m	4,659 m	17 dB	18 dB	19 dB
	200 m	19 dB	18 dB	
B	750 m	21 dB	19 dB	
Axis Depth–637 m	2,552 m	20 dB	17 dB	
	4,351 m	17 dB	15 dB	
Critical Depth–4,420 m	4,463 m	16 dB	15 dB	
	4,575 m	13 dB	14 dB	
Sea Floor–5,447 m	5,241 m	12 dB	14 dB	
	5,297 m	16 dB	14 dB	
C				
Axis Depth–655 m	696 m	20 dB	19 dB	19 dB
Critical Depth–3,860 m	4,055 m	12 dB	12 dB	15 dB
Sea Floor–5,555 m	5,521 m	11 dB	5 dB	6 dB
D	3,325 m		10 dB	
Axis Depth–478 m	3,625 m		10 dB	15 dB
Critical Depth–2,840 m	3,925 m		9 dB	13 dB
Sea Floor–4,646 m	4,225 m		8 dB	
	4,520 m		4 dB	
	4,612 m		5 dB	11 dB

CONFIDENTIAL

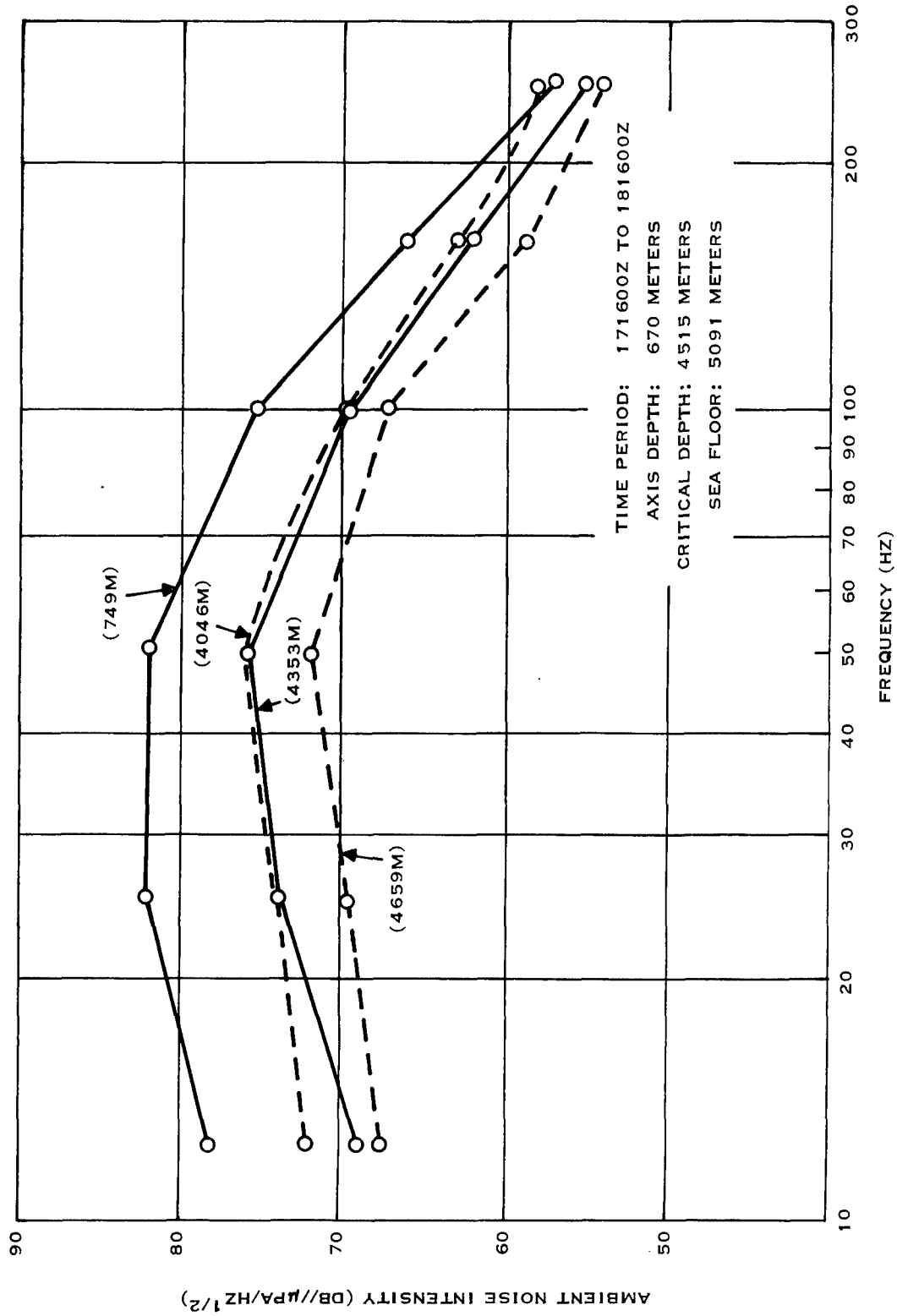

Figure 2-21. (C) Frequency Dependence of Uncontaminated Ambient Noise Intensity at Site A (24-Hour Averages) (U)

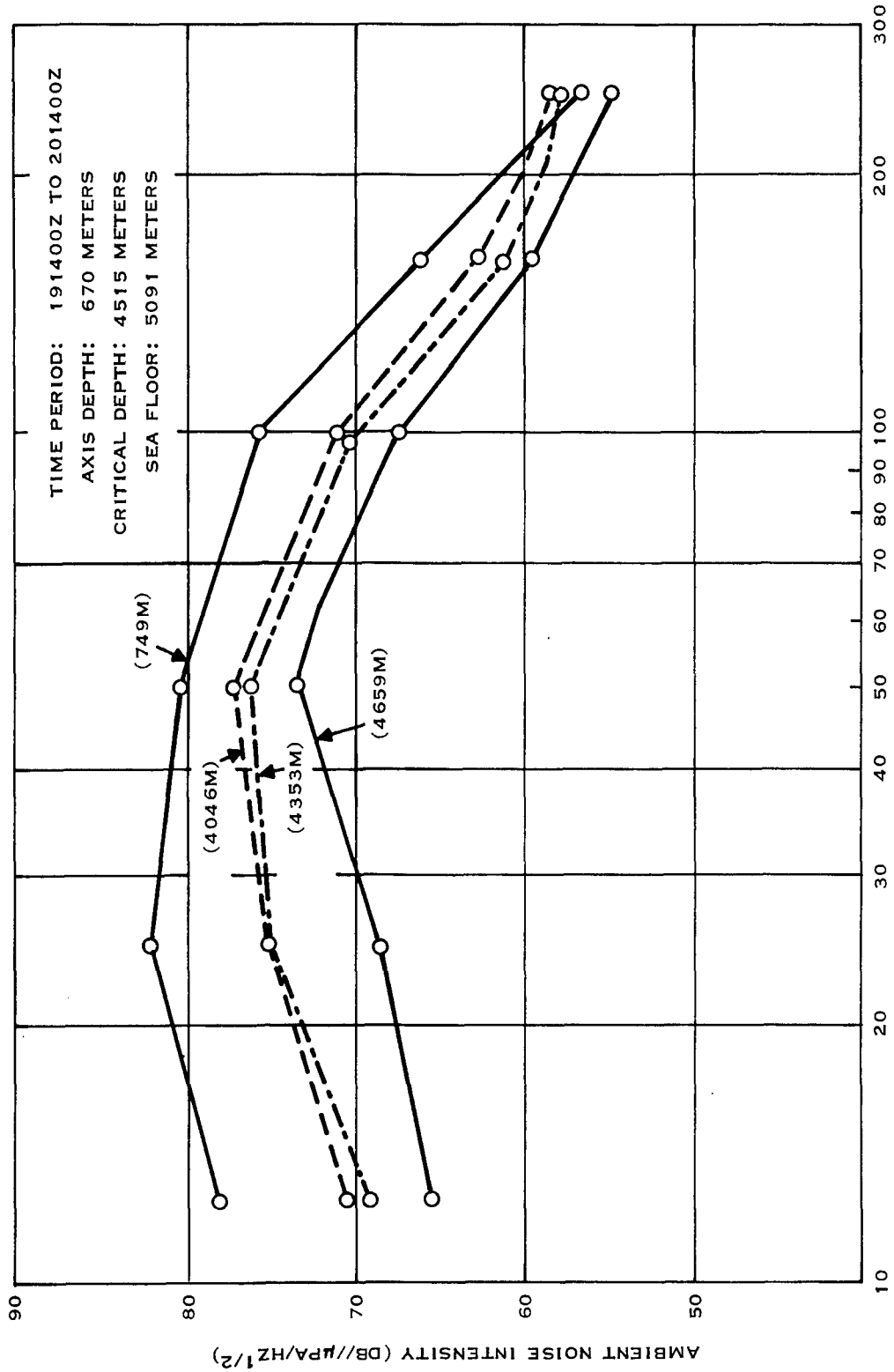

Figure 2-22. (C) Frequency Dependence of Uncontaminated Ambient Noise Intensity at Site A (24-Hour Averages) (U)

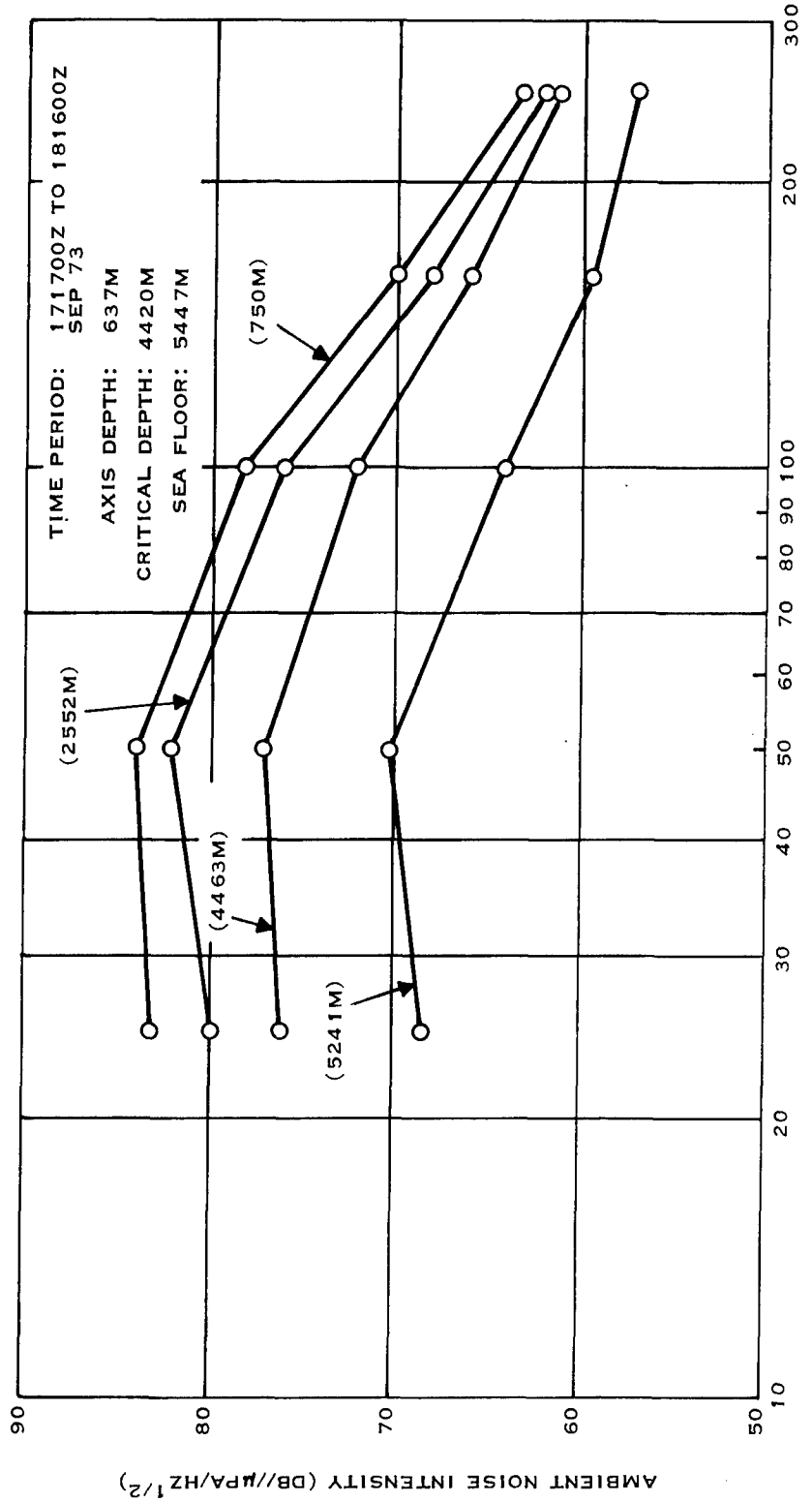

CONFIDENTIAL

197748

Figure 2-23. (C) Frequency Dependence of Uncontaminated Ambient Noise Intensity at Site B (24-Hour Averages) (U)

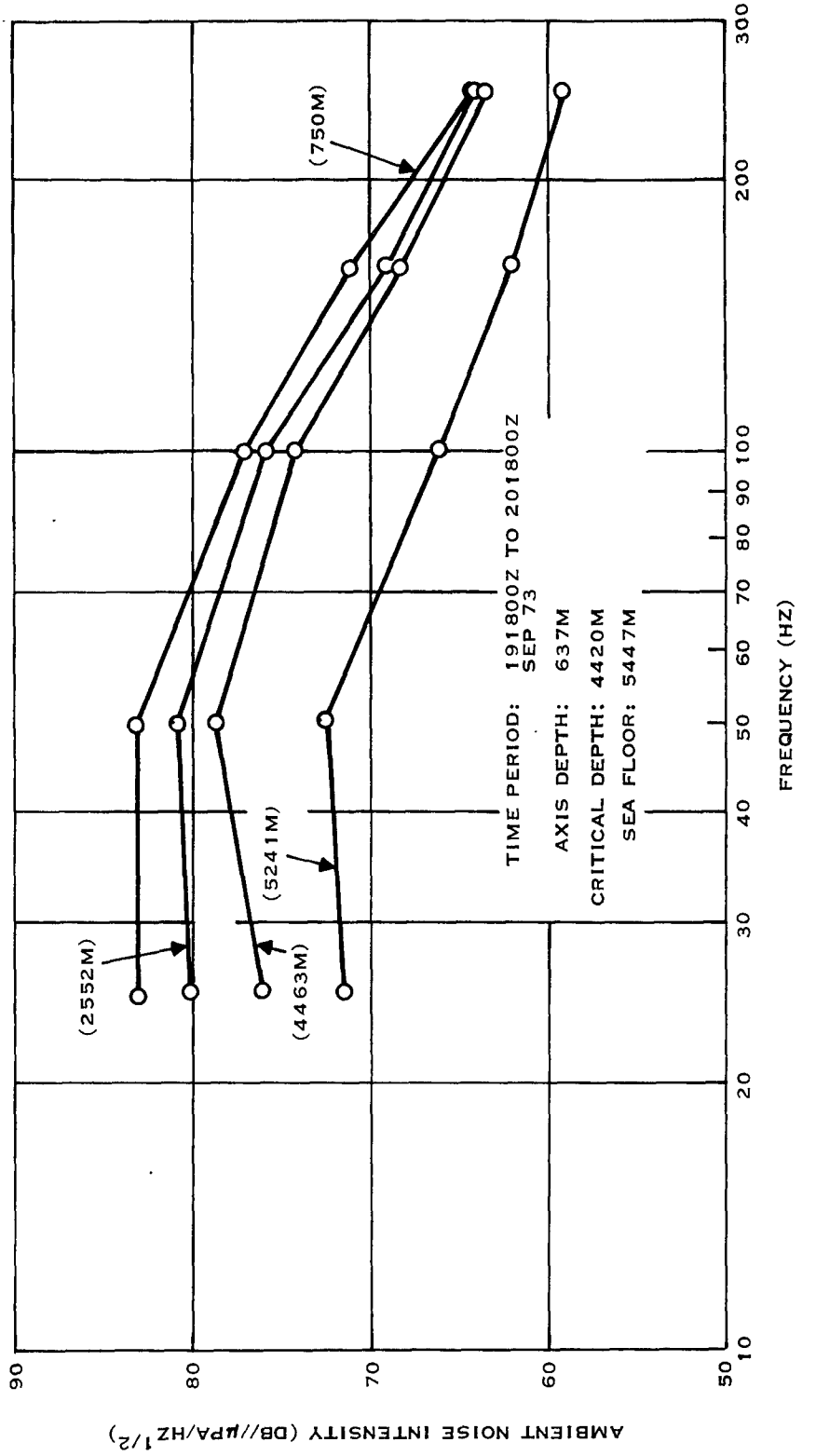

FREQUENCY (HZ)

197749

Figure 2-24. (C) Frequency Dependence of Uncontaminated Ambient Noise Intensity at Site B (24-Hour Averages) (U)

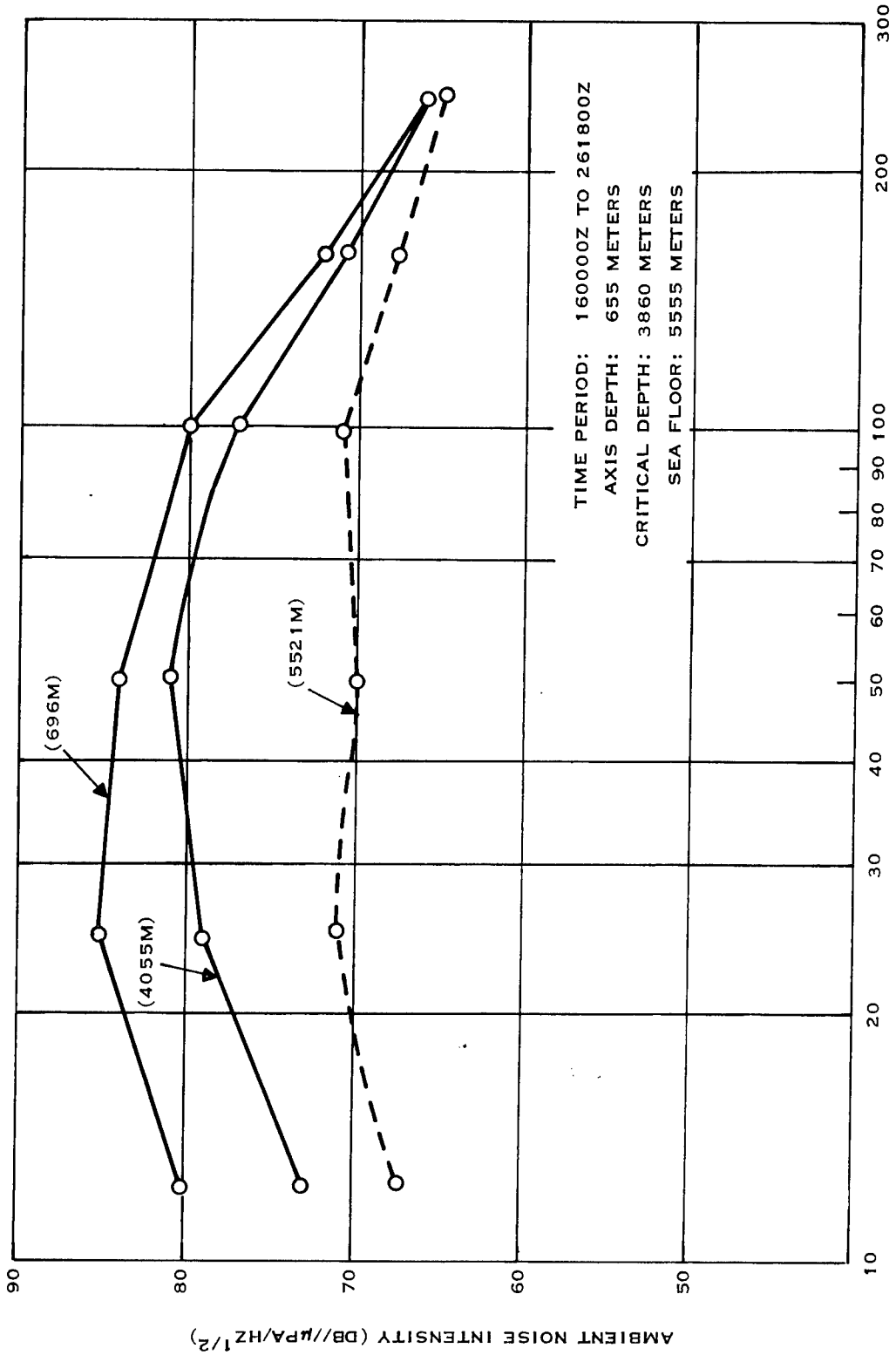

Figure 2-25. (C) Frequency Dependence of Uncontaminated Ambient Noise Intensity at Site C (10-Day Averages) (U)

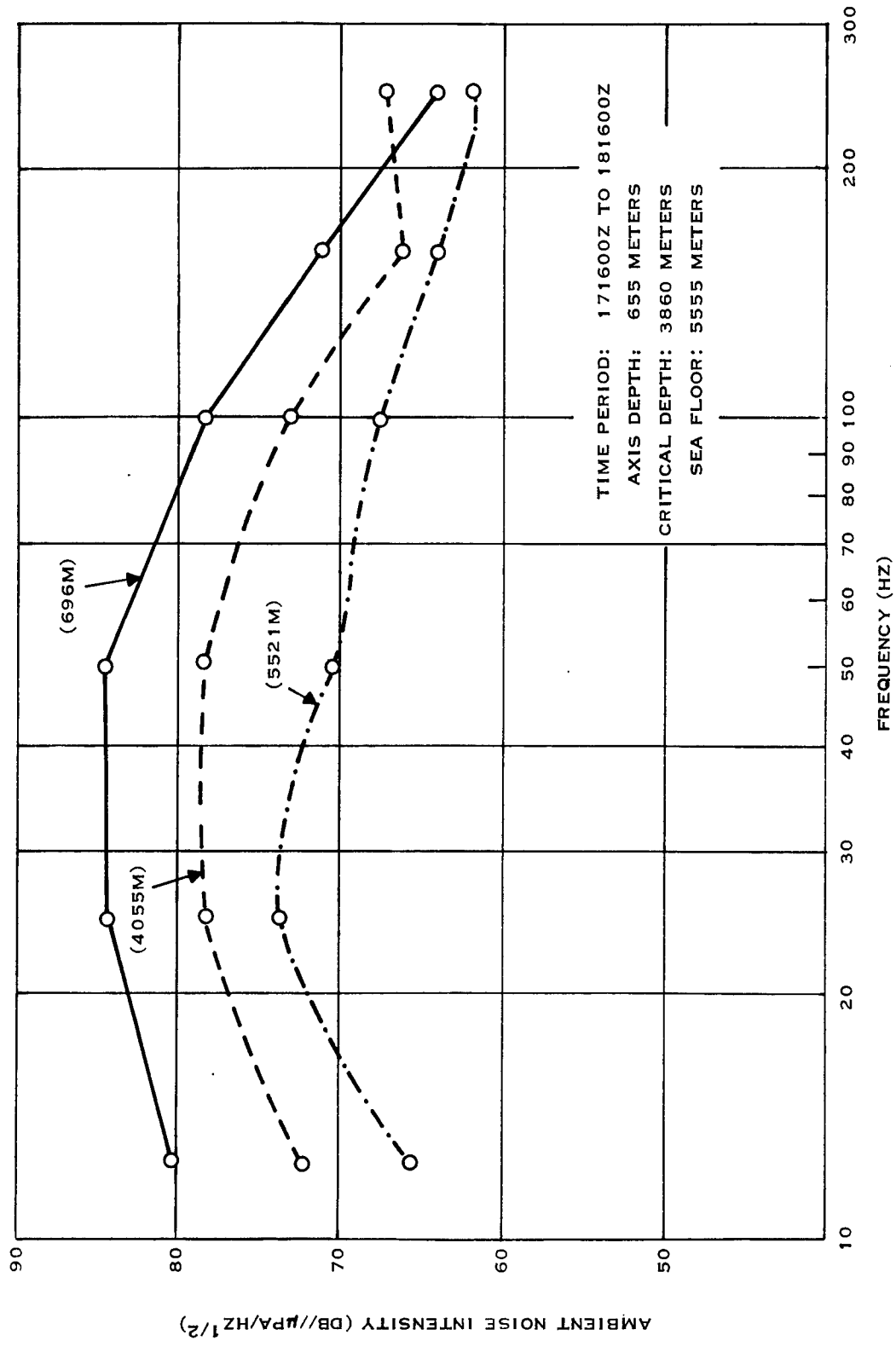

Figure 2-26. (C) Frequency Dependence of Uncontaminated Ambient Noise Intensity at Site C (24-Hour Averages) (U)

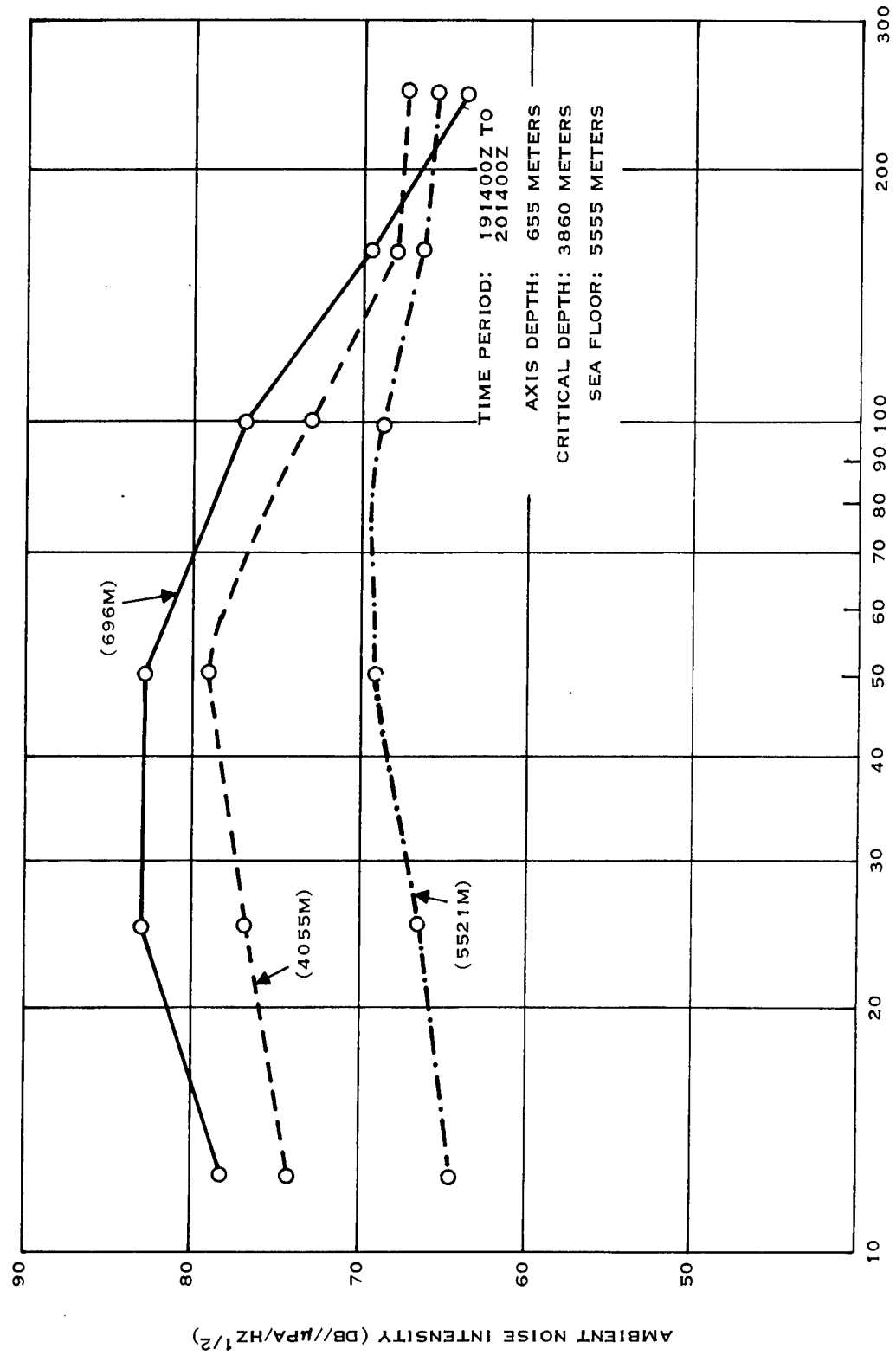

CONFIDENTIAL

Figure 2-27. (C) Frequency Dependence of Uncontaminated Ambient Noise Intensity at Site C (24-Hour Averages) (U)

197752

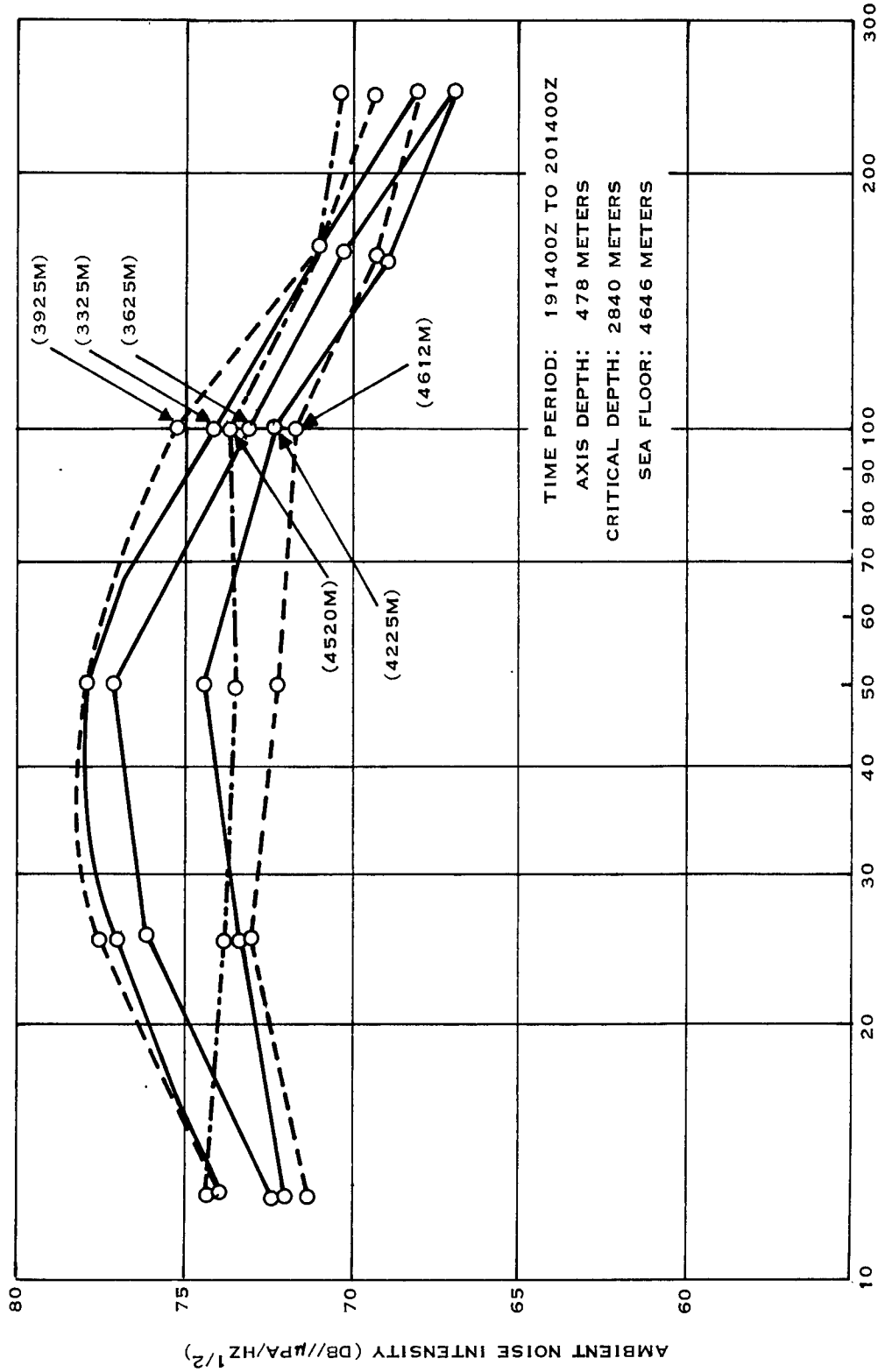

Figure 2-28. (C) Frequency Dependence of Uncontaminated Ambient Noise Intensity at Site D (24-Hour Averages) (U)

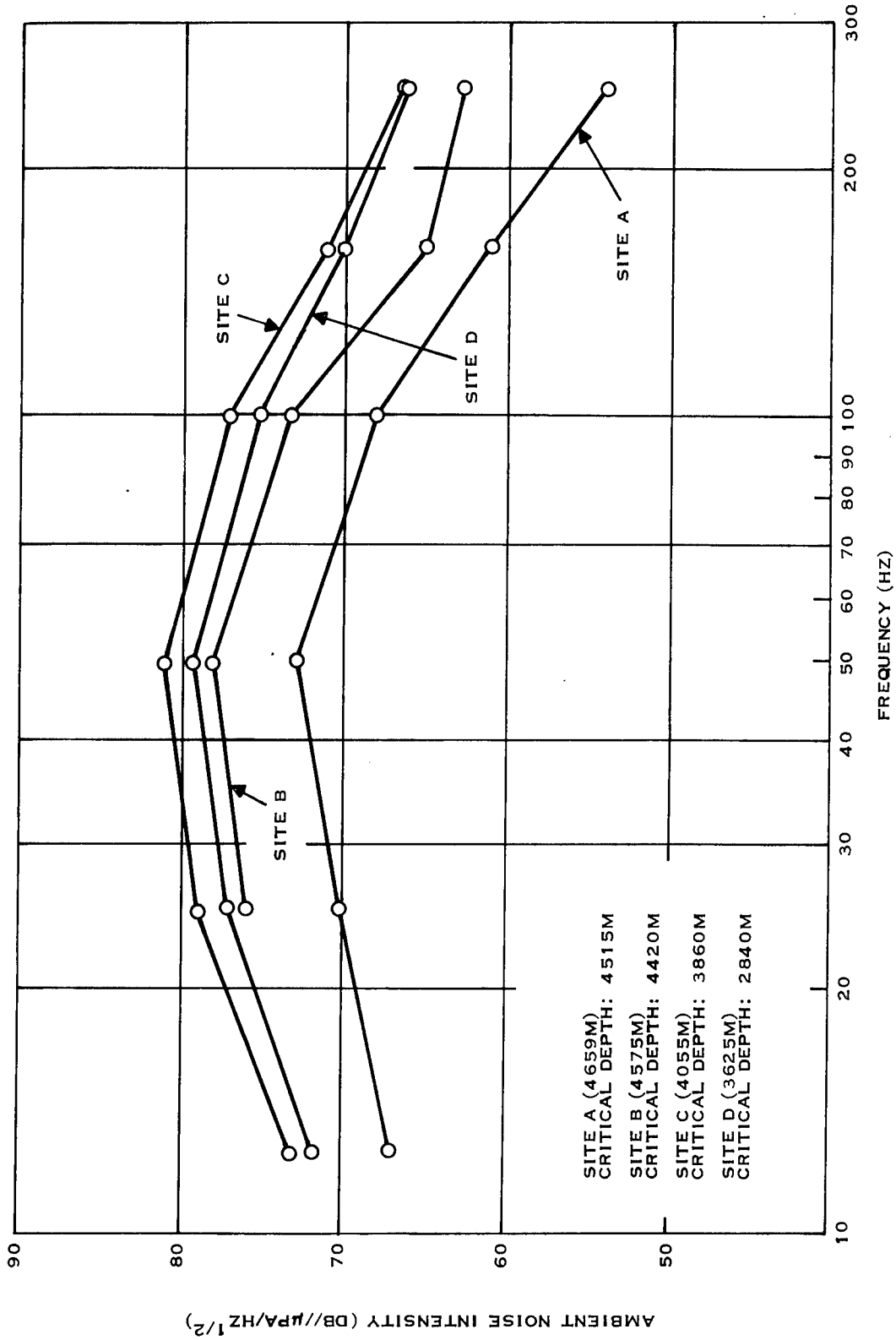

CONFIDENTIAL

Figure 2-29. (C) Frequency Dependence of Uncontaminated Ambient Noise Intensity at Sites A, B, C, and D (10-Day Averages, Below Critical Depth) (U)

197754

This appears to be the case for both 24-hour and 10-day averages. This same phenomenon is also observed when the depth is increased to below the critical depth. These statements are quantified in Table 2-2, which gives the decrease in ambient noise intensity with depth at a given frequency as estimated over specified depths at a given site. For example, one can see from Table 2-2 that, at site A on day 171600Z to 181600Z, the 12.5-Hz noise level decreased by 11 dB when the depth increased from 749 to 4,659 m. The corresponding decrease in the noise intensity at 160 Hz was only 7 dB. Similar observations can be made at other sites and days.

(C) Consistently, the ambient noise level reached a maximum in the frequency range from 25 to 50 Hz at all sites and depths. Between 50 Hz and 100 Hz, there was a general decrease of about 5 dB per octave. Beyond 100 Hz, however, the ambient level decreased at approximately 10 to 15 dB per octave.

5. (C) Intersite Comparison (U)

(C) Figure 2-29 shows 10-day uncontaminated ambient noise intensity averages for the first hydrophone below critical depth at each of the measurement sites. (No hydrophone was located near critical depth for site E.) Figure 2-30 shows the same data for the hydrophone located

TABLE 2-2. (C) DECREASE IN AMBIENT NOISE INTENSITY AT A GIVEN FREQUENCY FOR SITES A, B, C, AND D (U)

Site	Frequency	24-Hour Average 171600Z–181600Z	24-Hour Average 191400Z–201400Z	10-Day Average
	12.5 Hz	11 dB	12 dB	9 dB
A	25.0 Hz	12 dB	13 dB	11 dB
Axis Depth–670 m	50.0 Hz	10 dB	8 dB	9 dB
Critical Depth–4,515 m	100.0 Hz	8 dB	8 dB	8 dB
Sea Floor–5,091 m	160.0 Hz	7 dB	7 dB	7 dB
	25.0 Hz	15 dB	12 dB	
B	50.0 Hz	14 dB	10 dB	
Axis Depth–637 m	100.0 Hz	14 dB	11 dB	
Critical Depth–4,420 m	160.0 Hz	10 dB	9 dB	
Sea Floor–5,447 m	250.0 Hz	6 dB	5 dB	
	12.5 Hz	15 dB	14 dB	13 dB
C	25.0 Hz	10 dB	17 dB	14 dB
Axis Depth–655 m	50.0 Hz	13 dB	14 dB	14 dB
Critical Depth–3,860 m	100.0 Hz	10 dB	8 dB	9 dB
Sea Floor–5,555 m	160.0 Hz	7 dB	4 dB	4 dB
D	25.0 Hz		9 dB	
Axis Depth–478 m	50.0 Hz		12 dB	
Critical Depth–2,840 m	100.0 Hz		8 dB	
Sea Floor–4,646 m				

NOTES: Depths 749 m to 4,659 m for Site A
Depths 750 m to 5,241 m for Site B
Depths 696 m to 5,521 m for Site C
Depths 3,925 m to 4,612 m for Site D

CONFIDENTIAL

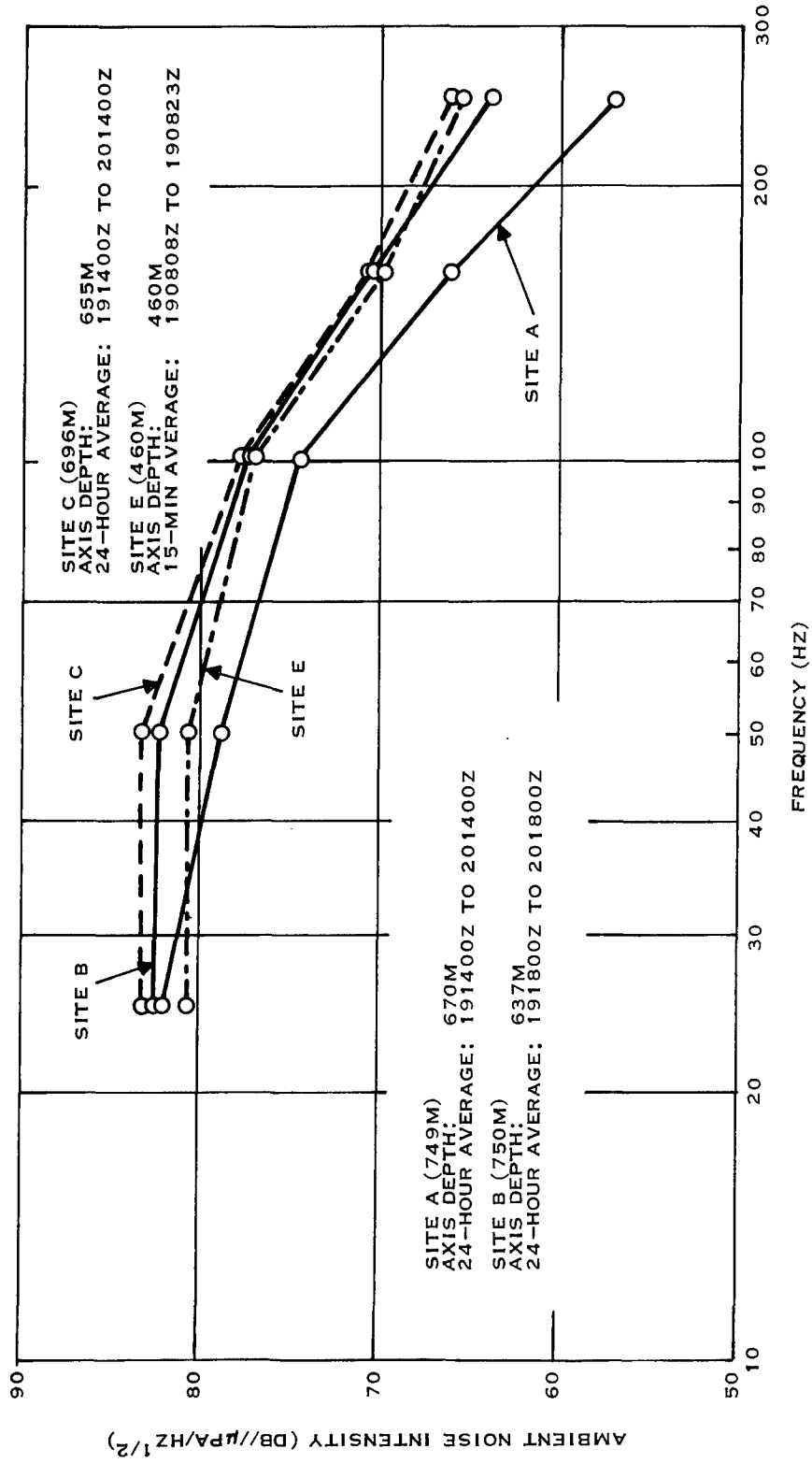

CONFIDENTIAL

197755

Figure 2-30. (C) Frequency Dependence of Uncontaminated Ambient Noise Intensity at Sites A, B, C, and E (Axis Depth) (U)

nearest the sound axis for each site. (No hydrophone was located near the axis for site D.) The data in these figures show that site A has considerably lower ambient level than do the other sites. Although data are plotted for only two depths, visual inspection of Figures 2-11 through 2-19 shows that the lower level holds at other depths. There are no known sound-velocity-profile nor bathymetric characteristics at site A that would account for this difference; one possible reason for the difference at the higher frequencies is wind speed.

(C) Although no wind data are available for site A, wind data were collected for sites C, D, and E. Figures 2-6 through 2-9 show how well the ambient level at 160 and 250 Hz on the deeper hydrophones correlates with the rising and falling of the wind speed. Furthermore, Appendix C shows correlation of the higher ambient noise levels at 160 and 250 Hz with wind speed at site E. Since the ambient levels of site A shown in Figures 2-3 and 2-4 do not show the gradual changes seen at sites C and D (Figures 2-6 through 2-9), one possible reason for the lower ambient level in the higher frequency region is lower wind speed.

6. (C) Observations of the DREP Data (U)

(C) The data received from Defence Research Establishment Pacific (DREP) of Canada allow additional interpretation of the noise intensity in that the frequency range of the intensity estimates extends to 800 Hz (see Appendix C). The general shapes of the noise spectra in the band 20 to 250 Hz were similar to those spectra reported from other sources (UT, Texas Instruments, and MPL). Thus, the spectra reached their maxima in the regions 25 to 50 Hz and monotonically decreased with decreasing and increasing frequencies, respectively, outside this band. In the frequency region between 70 and 200 Hz, the decrease was most rapid: about 10 dB per octave. Beyond 200 Hz, the rate of decrease with frequency was only about 5 dB per octave.

(U) REFERENCES

1. Northrop and Berman, "Location and Classification of Some Unusual Noises in the North Atlantic (U)," *Journal of Underwater Acoustics* (2 January 1969). CONFIDENTIAL
2. Patterson and Hamilton, "Low Frequency Pulsed Signals Received on Bermuda Hydrophones (U)," *Journal of Underwater Acoustics* (2 January 1961). CONFIDENTIAL
3. Walker, "Twenty-Cycle Pulses at Nantucket (U)," *Journal of Underwater Acoustics* (11 July 1961). CONFIDENTIAL
4. Stutt, Kinloch, Kincaid, and Wood, *Pulsed Signals From Balaenoptera Physalus* (U), Office of Naval Research Report (22 February 1971). SECRET
5. Robert J. Urick, *Principles of Underwater Sound for Engineers* McGraw-Hill (New York, 1967).
6. *Undersea Acoustic Propagation, Reverberation and Noise Data, A Summary* (U) (March 1969), Naval Research Laboratory, Washington, D.C. (2 September 1969). CONFIDENTIAL
7. R.D. Gaul, A.E. White, and A.E. Fadness, *An Environmental Acoustic Exercise in the Ionian Basin of the Mediterranean Sea* (U), Office of Naval Research (April 1972). CONFIDENTIAL
8. Samuel W. Marshall, *Ambient Noise and Signal-to-Noise Profiles in IOMEDEX* (U), Naval Research Laboratory, Washington, D.C. (June 1973). CONFIDENTIAL
9. G.M. Wenz, "Low-Frequency Deep-Water Ambient Noise Along the Pacific Coast of The United States," *Journal of Underwater Acoustics* (19 October 1969).

APPENDIX A
(C) AMBIENT NOISE INTENSITY MEASUREMENTS (U)

I. (U) PROCESSING SYSTEM AND METHOD

(U) The block diagram in Figure A-1 presents the hybrid facility at Texas Instruments that was used for the reduction of ACODAC ambient noise data into 1/3-octave bands. At 80-to-1 playback speed, the analog tape recorder was speed-compensated to correct for wow and flutter by locking onto a higher harmonic of the time code carrier. To prevent aliasing and to remove low strumming frequencies, the data were filtered through the passband of 10 to 300 Hz. The gains of the variable amplifiers located in front of and behind the 1/3-octave filter were set to allow the processing system to accommodate the full dynamic range of the data. The center frequencies of the fourteen 1/3-octave filters ranged from 12.5 to 250 Hz. The output of each filter was squared and then integrated for a 10-second period which was synchronized to the time code signal. After A-to-D conversion, 10-second samples of the integrators were transmitted to the EAI 640 digital computer and stored on digital magnetic tape. The time code and data amplifier gain state were decoded and transmitted to the digital computer and also stored on digital magnetic tape.

(U) From the 10-second samples, first- and second-order statistics (μ and σ) were computed for each 10-minute period. After 24 hours of ambient data had been processed, the quantities, 10 log (μ), 10 log ($\mu + \sigma$) and 10 log ($\mu - \sigma$), were plotted as a function of time for each of the six frequencies: 12.5, 25, 50, 100, 160, and 250 Hz. A flow diagram describing the computation of the first-order statistic is shown in Figure A-2. In addition to the 24-hour plots, Texas Instruments plotted 10 log μ as a function of time for the above six 1/3-octave bands for a 10-day period. These 10-day plots were presented in Subsection II.B. Figure A-3 shows the information plotted on a strip chart recorder during the real-time computation of the ambient statistics.

(U) Figure A-4 contains a flow diagram describing the various steps required to process the front-end calibration signals. The input voltage for each front-end calibration signal was known to within ±0.1 dB. From knowledge of the amplitude of the input and processed calibration signals, a frequency response at each gain state and at each calibration frequency for the composite system, namely, the data amplifier, record and reproduce amplifier, bandpass filter, and 1/3-octave filter, was computed. A corrective scale factor was then applied to the levels of the processed ambient data. Included in the scale factor was a compensation for changes in the data and record amplifier response caused by differences in environmental temperature (25° to 0°C).

II. (U) ERROR ANALYSIS

(U) Several studies have been made involving an error analysis on ACODAC data. Two reports are referenced; namely, a report by B.K. Dynamics,[1] and a report by Texas Instruments.[2] The two reports are in close agreement concerning an estimate of the total error for the composite system which includes the ACODACs, the processing hardware, and processing software. The total error spread on the ambient data is estimated as ±1.8 dB. Individual error estimates for the 1/3-octave filters, the squarers, and integrators are shown in Figure A-5.

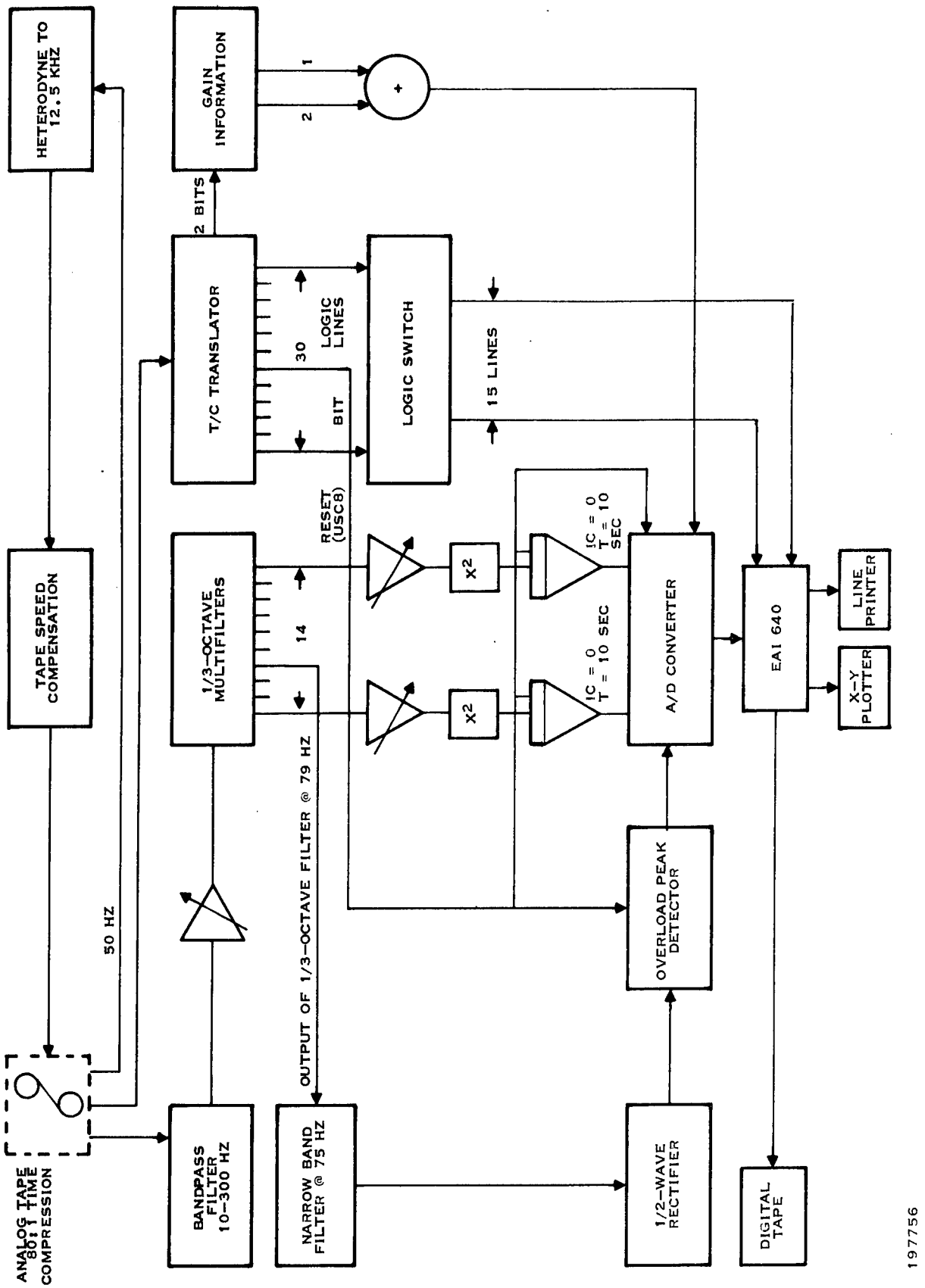

Figure A-1. (U) Diagram of Texas Instruments Hybrid Facility for Ambient Noise Reduction

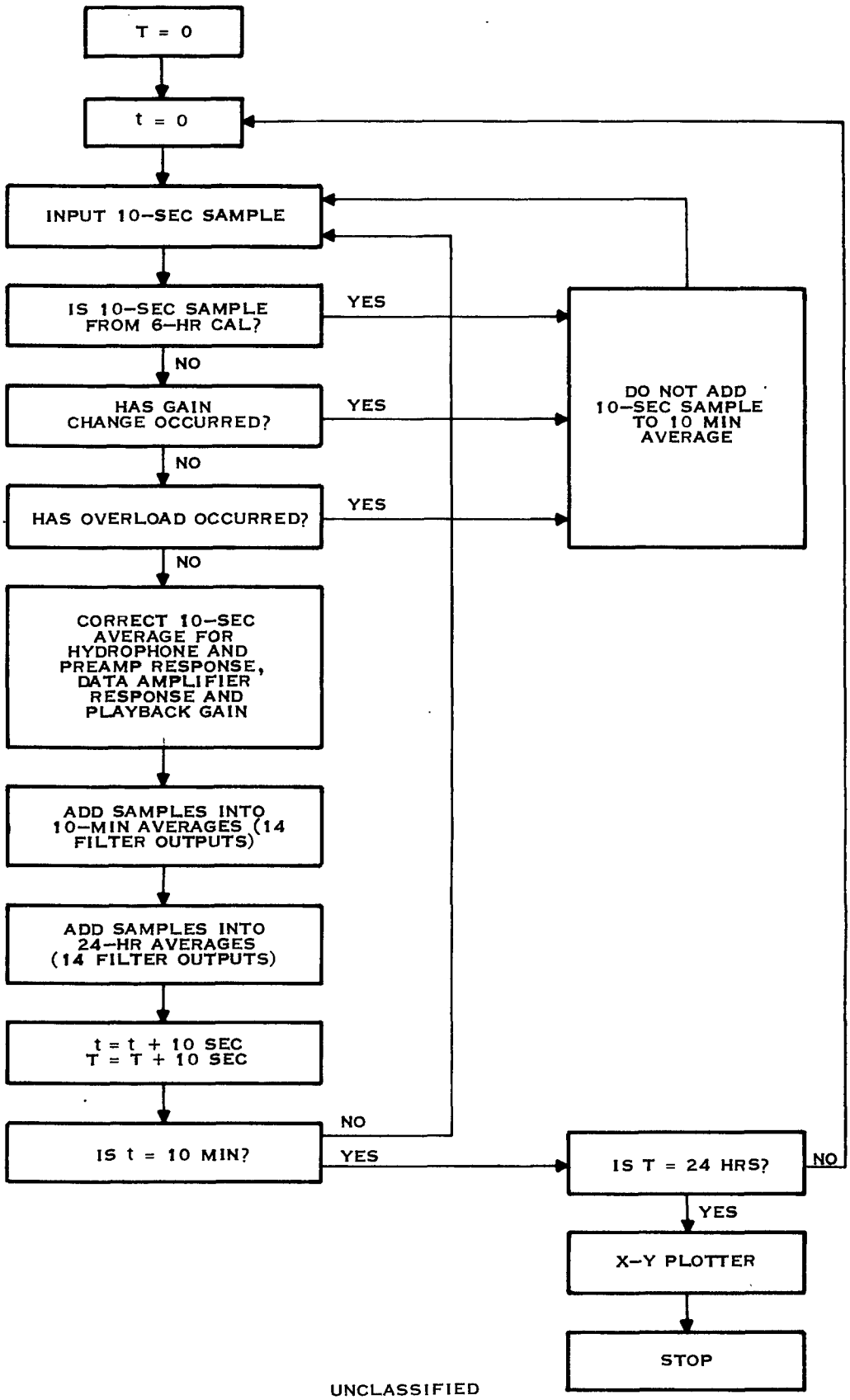

Figure A-2. (U) Flow Diagram for Computation of First Order Statistic

LEFT MARGIN	–	DIGITIZATION INDICATION
CHANNEL 1	–	12.5 HZ (1/3 OCTAVE FILTER OUTPUT)
2	–	25
3	–	50
4	–	100
5	–	160
6	–	200 (CAL) OR 250 (DATA)
7	–	OVERLOAD OUTPUT
8	–	ACODAC GAIN STATE
RIGHT MARGIN	–	1 MIN TICKS (ACODAC TIME CODE)

UNCLASSIFIED

Figure A-3. (U) Strip Chart Recorder Output

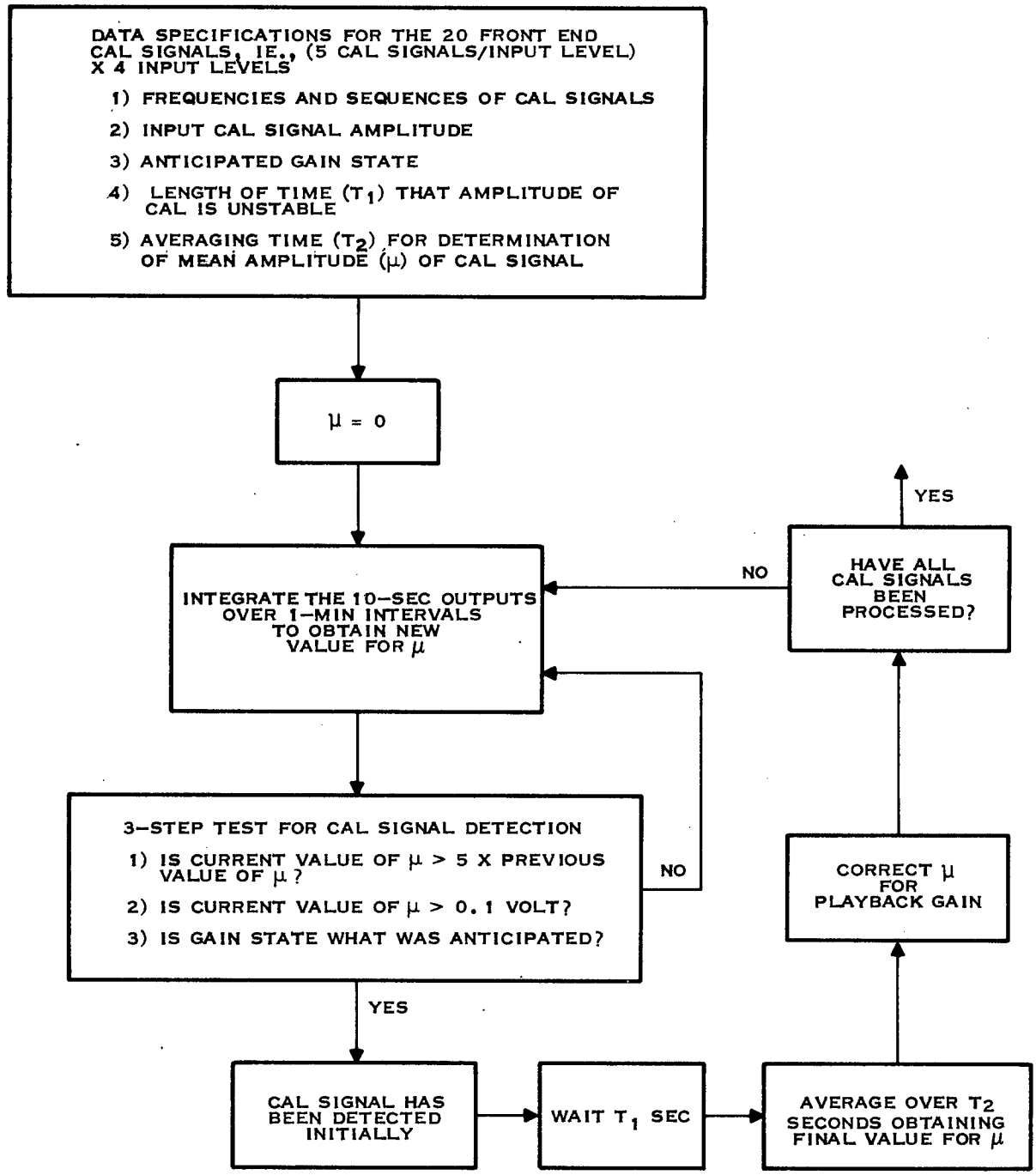

Figure A-4. (U) Flow Diagram for Processing Front End Calibration Signals

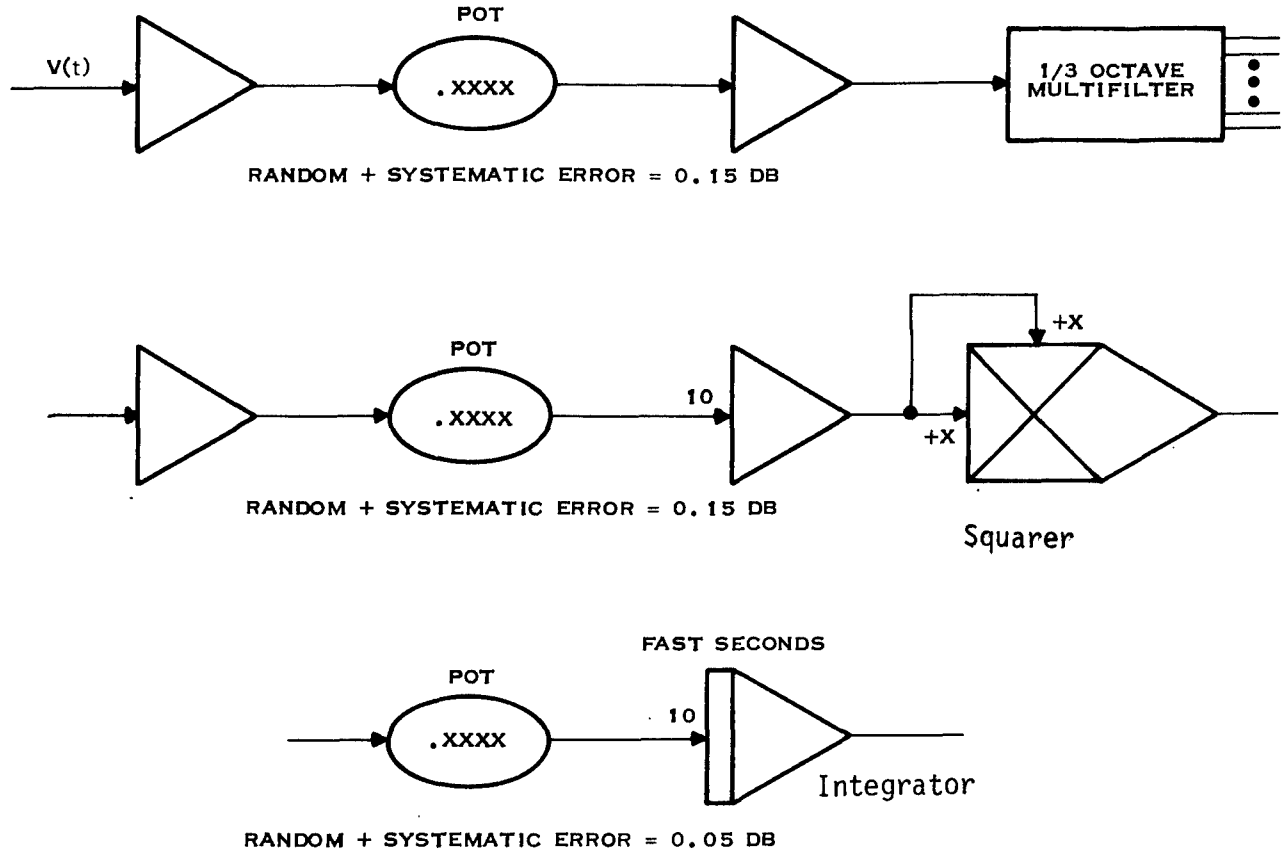

197760

UNCLASSIFIED

Figure A-5. (U) Random and Systematic Errors for Each Major Processing Component 1/3-Octave Filter, Squarer and Integrator

TABLE A-1. (U) SUMMARY OF AMBIENT NOISE INTENSITY TIME-SERIES PLOTS SHOWN IN FIGURES A-6 THROUGH A-26

Figure	Site	Time Period	Hydrophone
A-6	A	171600Z to 181600Z	749 m, 4,353 m, 4,659 m
A-7	A	171600Z to 181600Z	749 m, 4,353 m, 4,659 m
A-8	A	171600Z to 181600Z	749 m, 4,353 m, 4,659 m
A-9	C	171600Z to 181600Z	4,055 m, 5,521 m
A-10	C	171600Z to 181600Z	4,055 m, 5,521 m
A-11	C	171600Z to 181600Z	4,055 m, 5,521 m
A-12	A	191400Z to 201400Z	749 m, 4,046 m, 4,353 m, 4,659 m
A-13	A	191400Z to 201400Z	749 m, 4,046 m, 4,353 m, 4,659 m
A-14	A	191400Z to 201400Z	749 m, 4,046 m, 4,353 m, 4,659 m
A-15	A	191400Z to 201400Z	749 m, 4,046 m, 4,353 m, 4,659 m
A-16	A	191400Z to 201400Z	749 m, 4,046 m, 4,353 m, 4,659 m
A-17	A	191400Z to 201400Z	740 m, 4,046 m, 4,353 m, 4,659 m
A-18	C	191400Z to 201400Z	696 m, 5,521 m
A-19	C	191400Z to 201400Z	696 m, 5,521 m
A-20	C	191400Z to 201400Z	696 m, 5,521 m
A-21	D	191400Z to 201400Z	3,925 m, 4,225 m, 4,520 m, 4,612 m
A-22	D	191400Z to 201400Z	3,925 m, 4,225 m, 4,520 m, 4,612 m
A-23	D	191400Z to 201400Z	3,925 m, 4,225 m. 4,520 m, 4,612 m
A-24	D	191400Z to 201400Z	3,925 m, 4,225 m, 4,520 m, 4,612 m
A-25	D	191400Z to 201400Z	3,925 m, 4,225 m, 4,520 m, 4,612 m
A-26	D	191400Z to 201400Z	3,925 m, 4,225 m, 4,520 m, 4,612 m

UNCLASSIFIED

III. (C) PRESENTATION OF REDUCED DATA (U)

(C) Table A-1 summarizes the ambient-noise-intensity time-series plots presented in Figures A-6 through A-26. A 24-hour time-series plot for each of the six 1/3-octave bands, 12.5, 25, 50, 100, 160, and 250 Hz, at each depth is shown. The noise intensity is expressed in units of $dB/\mu Pa/Hz^{1/2}$. For each time-series plot, a histogram of the noise intensity points was drawn along the ordinate. In addition, a dashed line representing a 60-dB noise level is drawn parallel to each abscissa to facilitate an analysis of depth dependence.

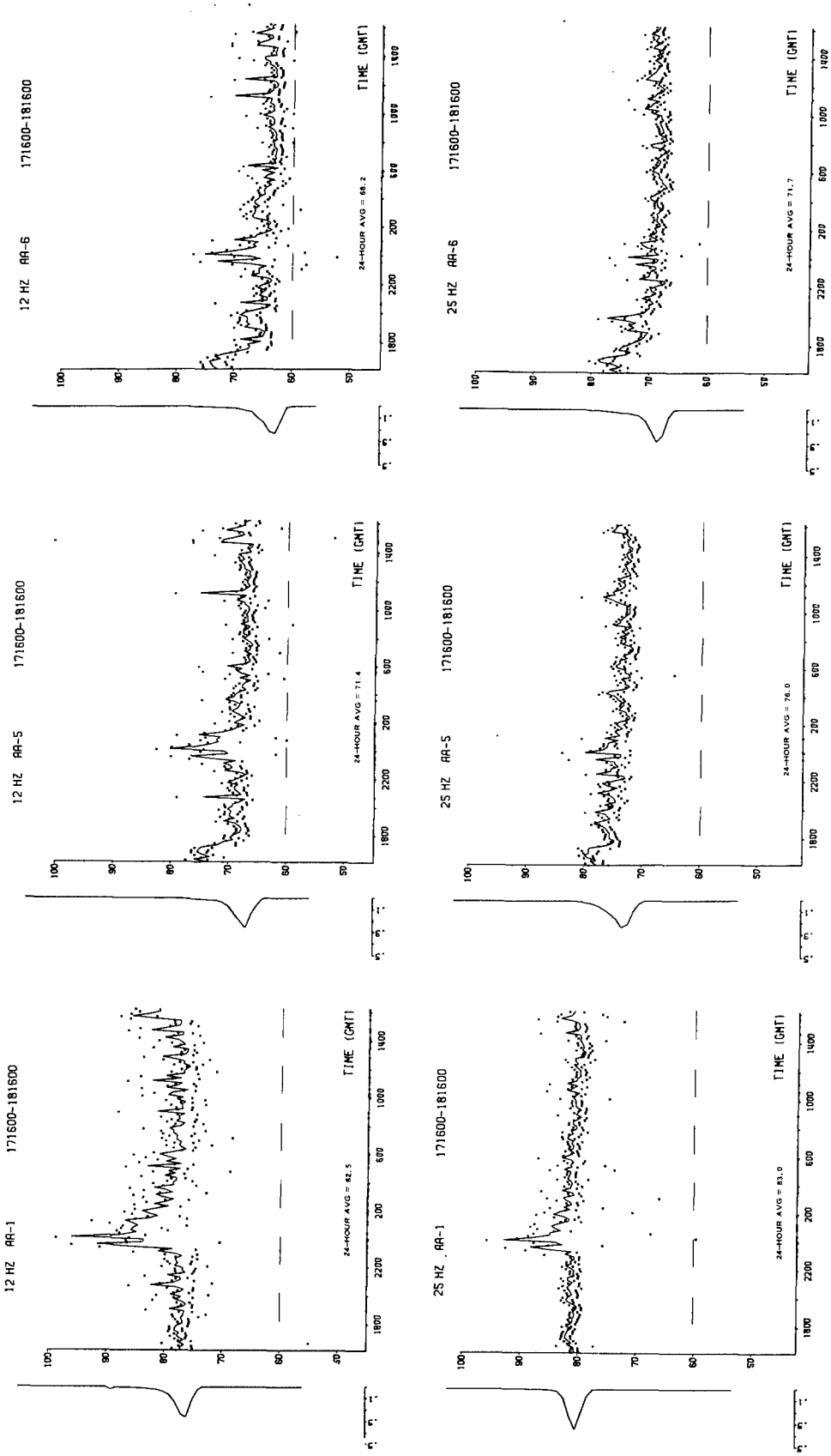

CONFIDENTIAL

197761

Figure A-6. (C) Twenty-Four-Hour Intensity Time-Series at Site A, 749 m, 4,353 m, and 4,659 m Depths 171600Z to 181600Z (September 1973) (U)

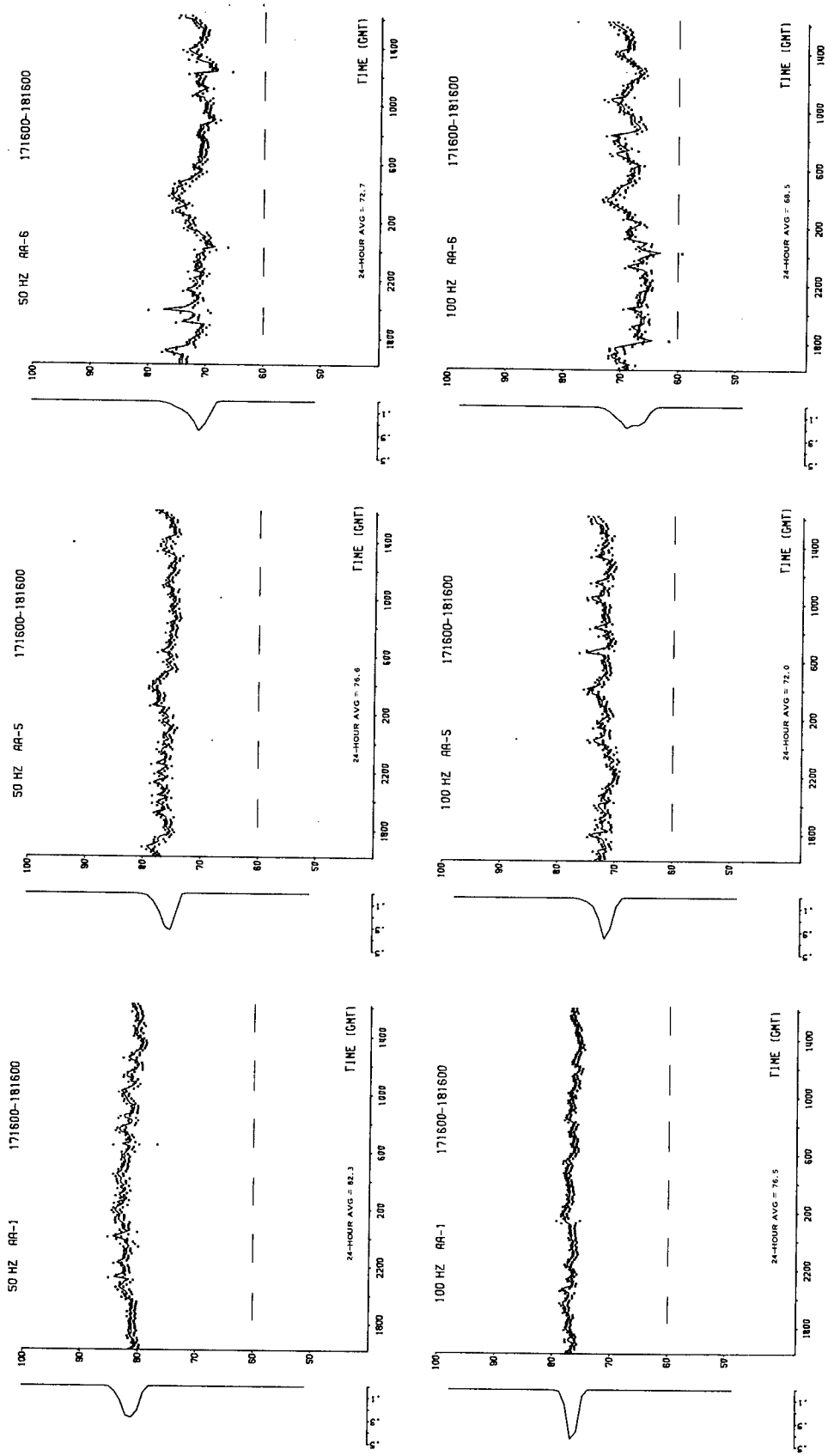

CONFIDENTIAL

Figure A-7. (C) Twenty-Four-Hour Intensity Time-Series at Site A, 749 m, 4,353 m, and 4,659 m Depths 171600Z to 181600Z (September 1973) (U)

197762

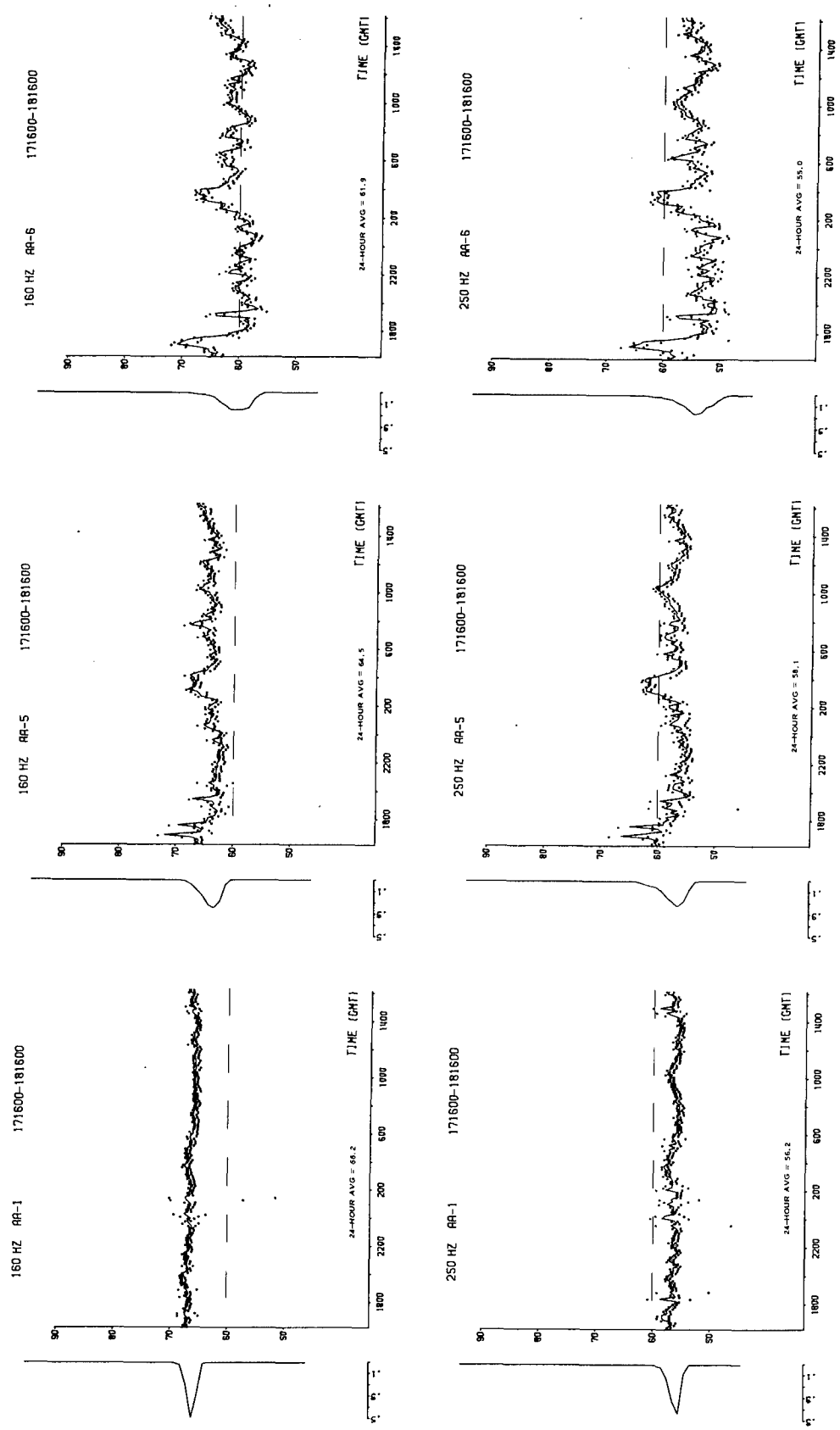

CONFIDENTIAL

197763

Figure A-8. (C) Twenty-Four-Hour Intensity Time-Series at Site A, 749 m, 4,353 m, and 4,659 m Depths 171600Z to 181600Z (September 1973) (U)

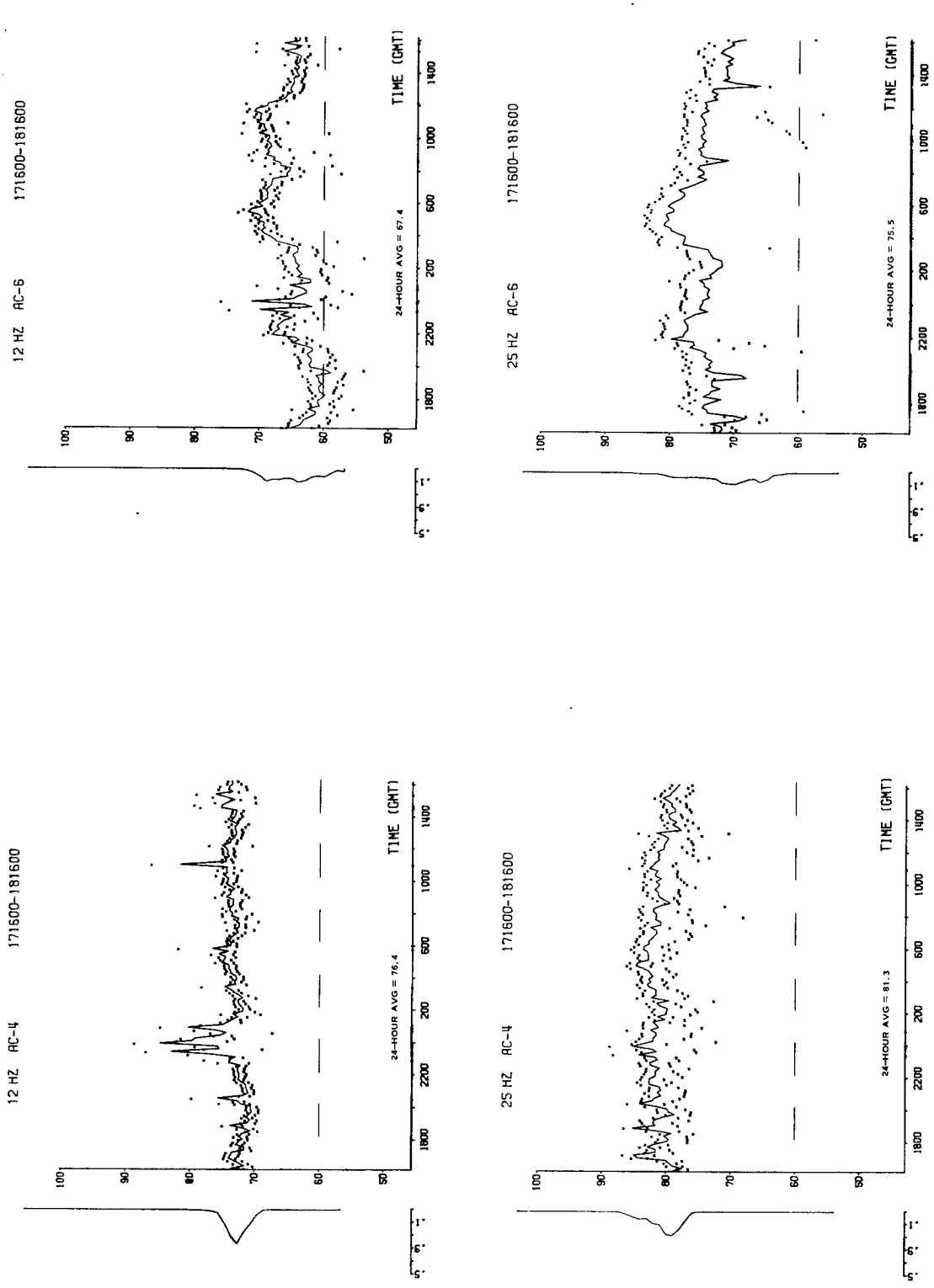

CONFIDENTIAL

Figure A-9. (C) Twenty-Four-Hour Intensity Time-Series at Site C, 4,055 m and 5,521 m Depths 171600Z to 181600Z (September 1973) (U)

197764

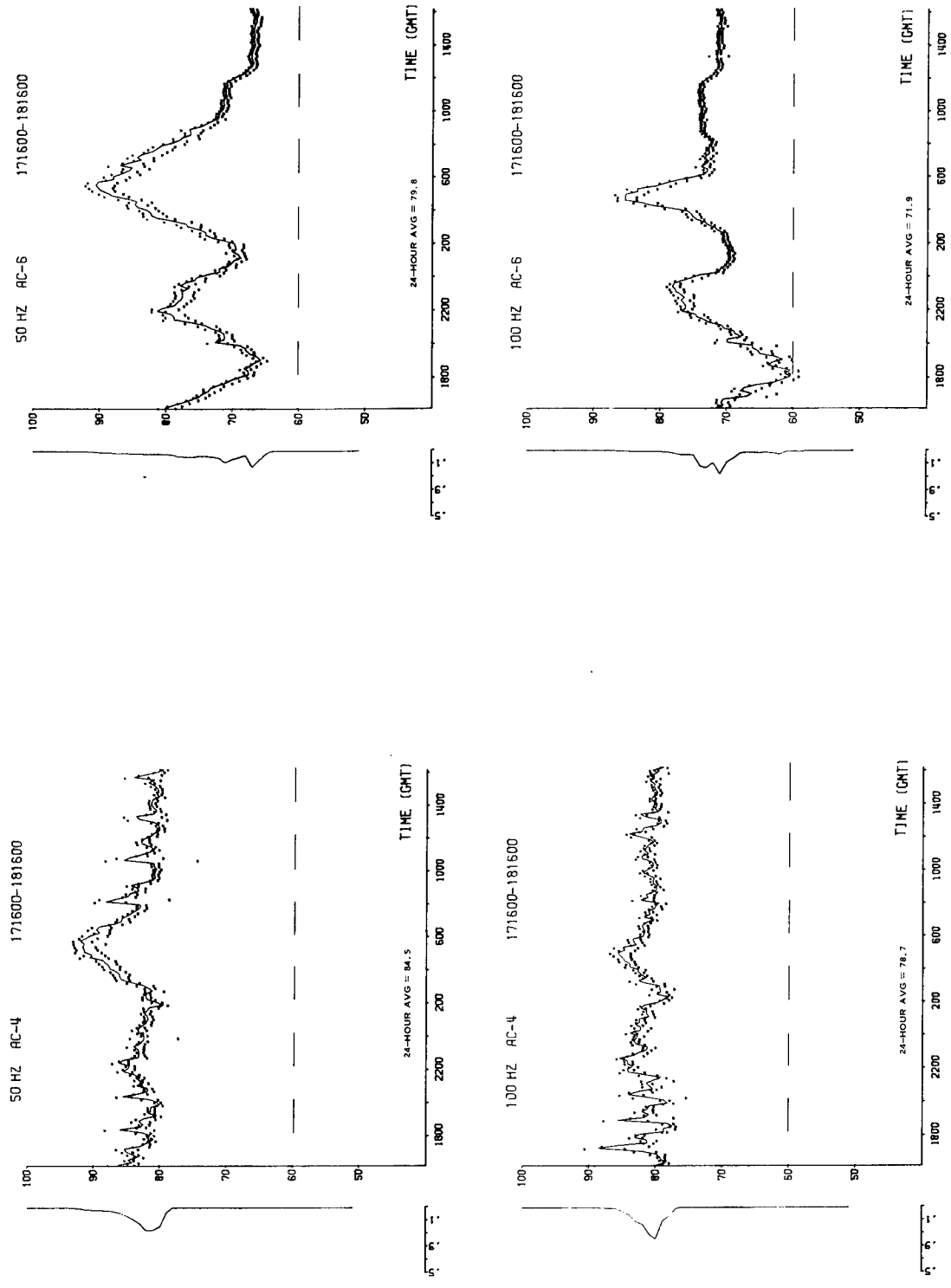

CONFIDENTIAL

Figure A-10. (C) Twenty-Four-Hour Intensity Time-Series at Site C, 4,055 m and 5,521 m Depths 171600Z to 181600Z (September 1973) (U)

197765

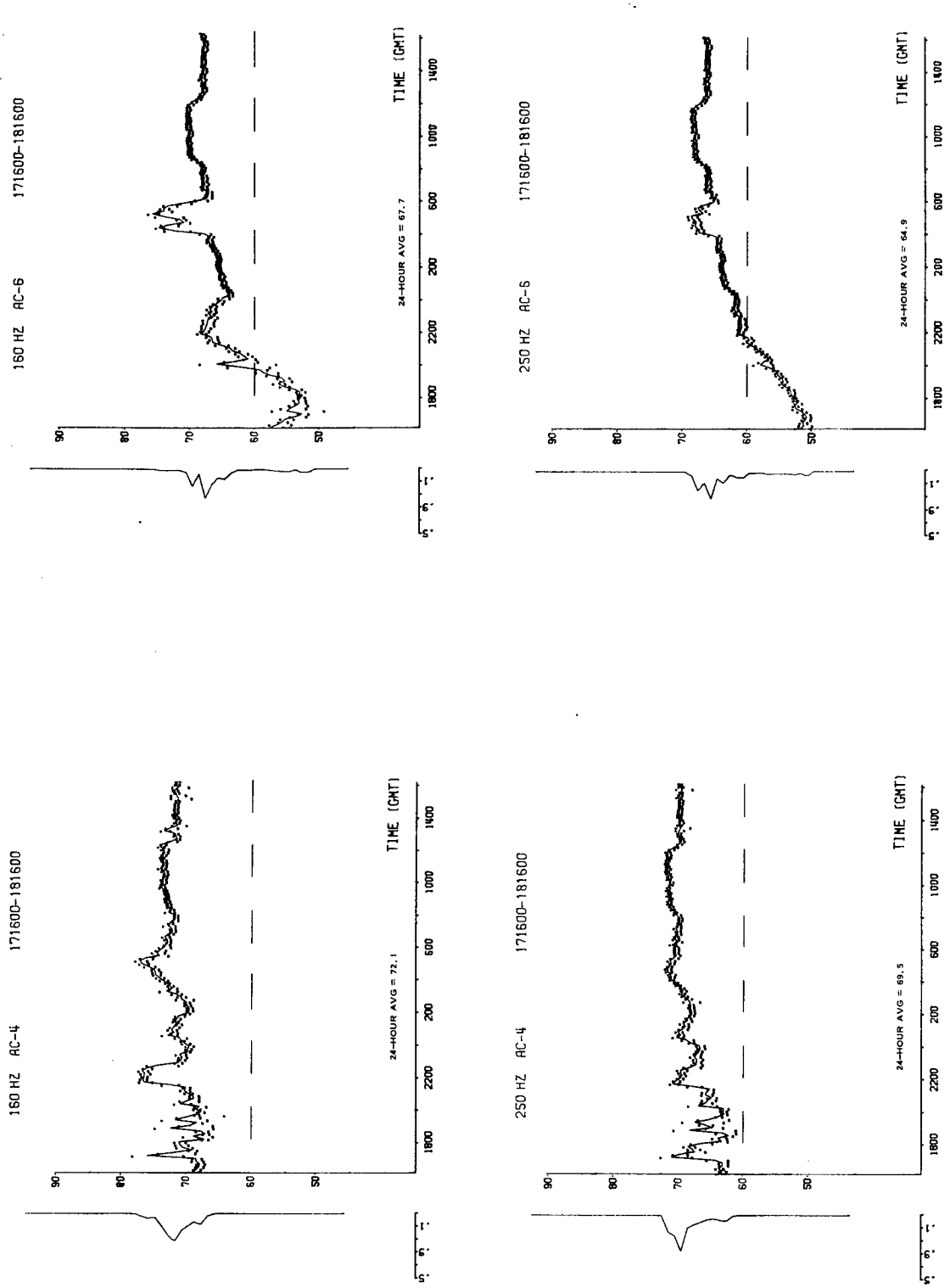

CONFIDENTIAL

Figure A-11. (C) Twenty-Four-Hour Intensity Time-Series at Site C, 4,055 m and 5,521 m Depths 171600Z to 181600Z (September 1973) (U)

197766

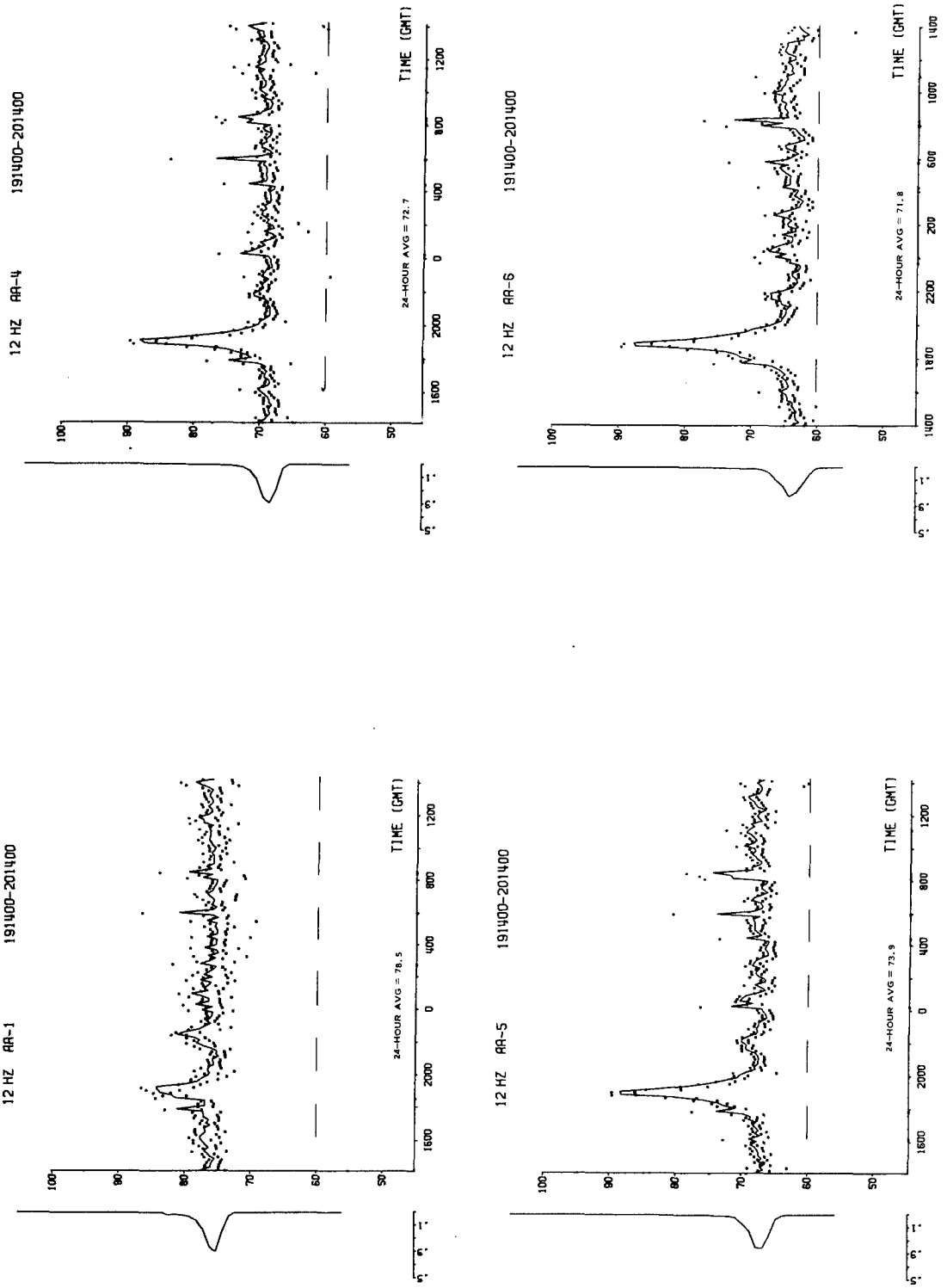

CONFIDENTIAL

Figure A-12. (C) Twenty-Four-Hour Intensity Time-Series at Site A, 749 m, 4,353 m, and 4,659 m Depths 191400Z to 201400Z (September 1973) (U)

197767

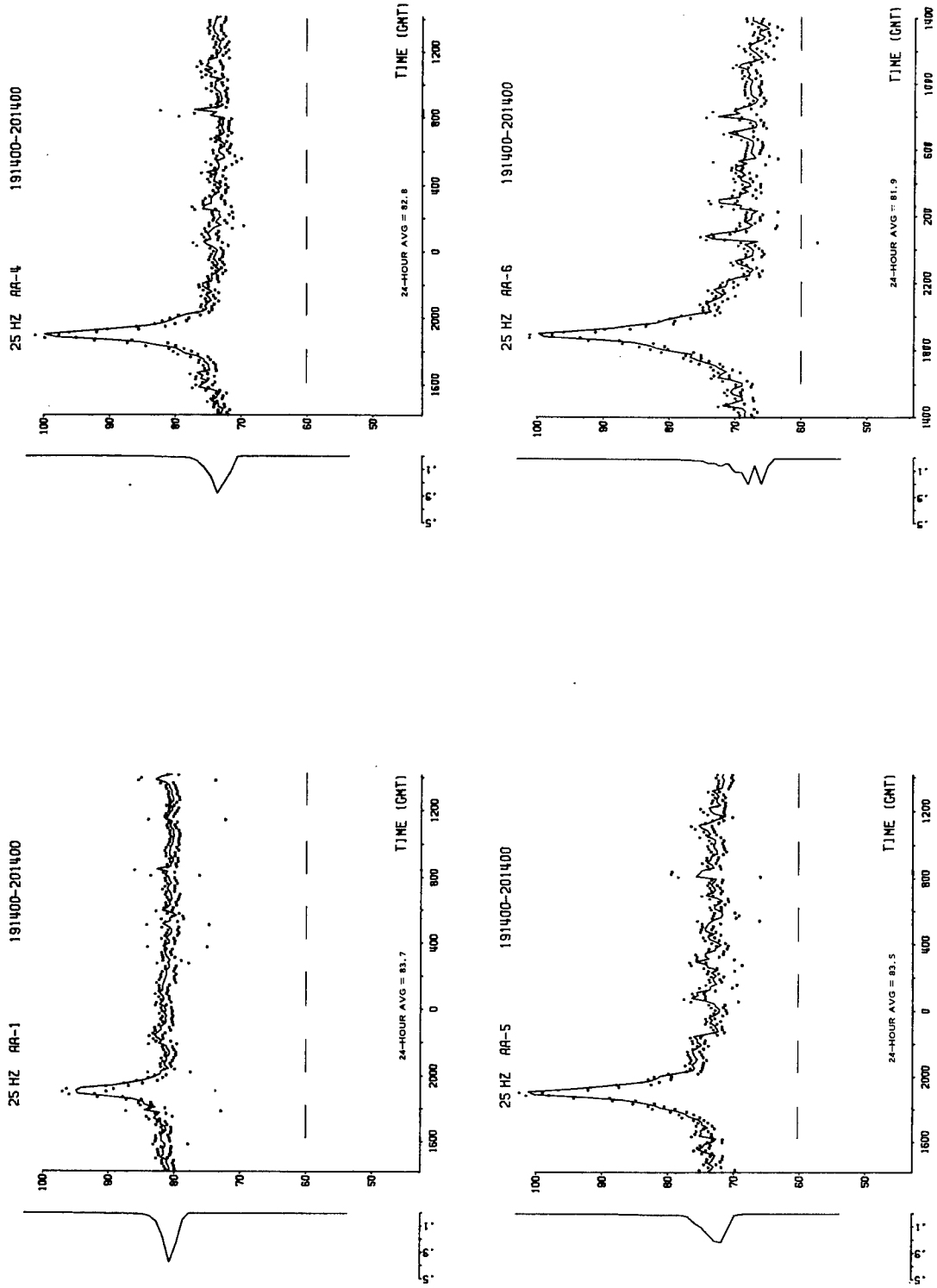

CONFIDENTIAL

Figure A-13. (C) Twenty-Four-Hour Intensity Time-Series at Site A, 749 m, 4,353 m, and 4,659 m Depths 191400Z to 201400Z (September 1973) (U)

197768

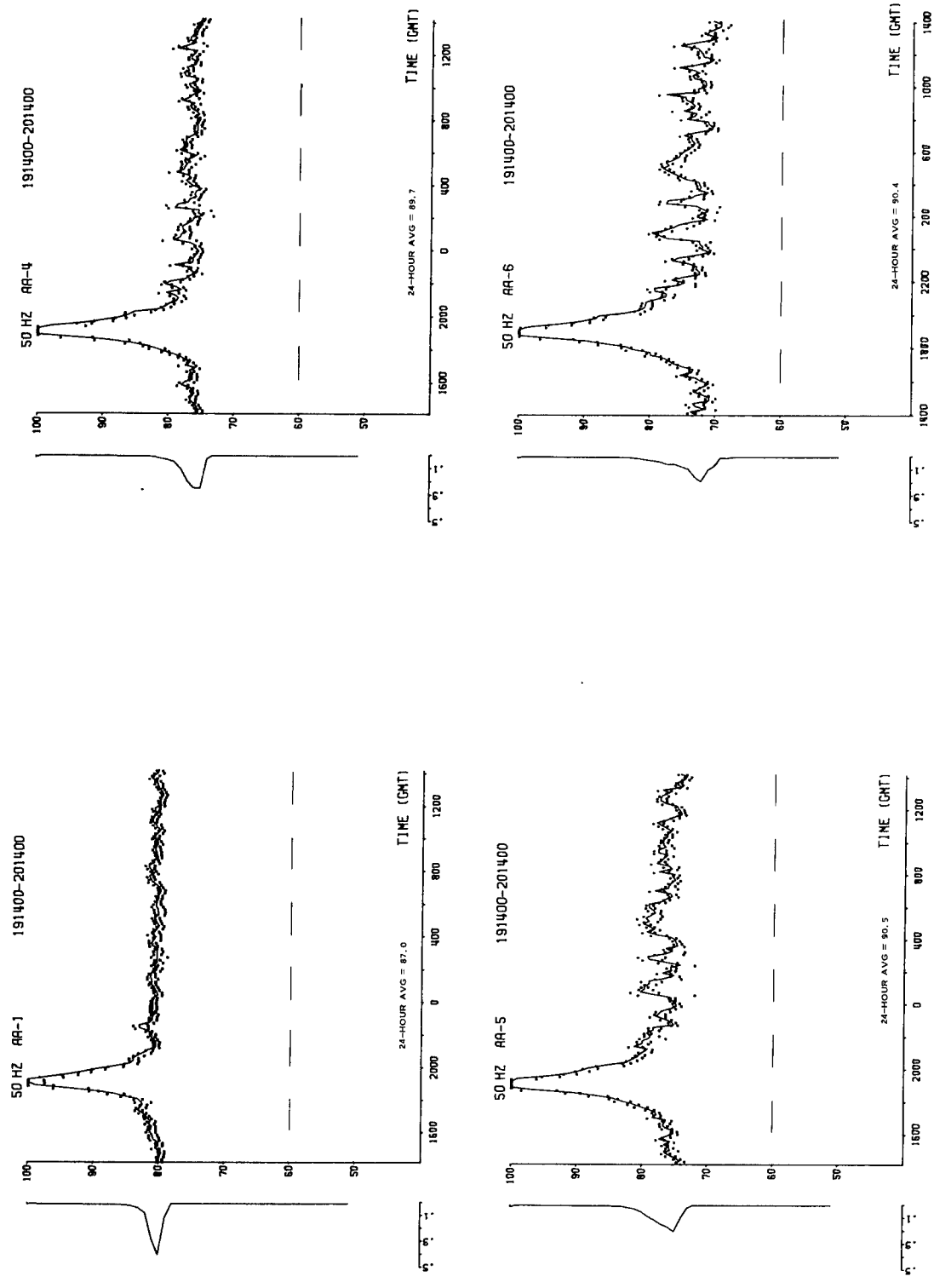

CONFIDENTIAL

197769

Figure A-14. (C) Twenty-Four-Hour Intensity Time-Series at Site A, 749 m, 4,046 m, 4,353 m, and 4,659 m Depths 191400Z to 201400Z (September 1973) (U)

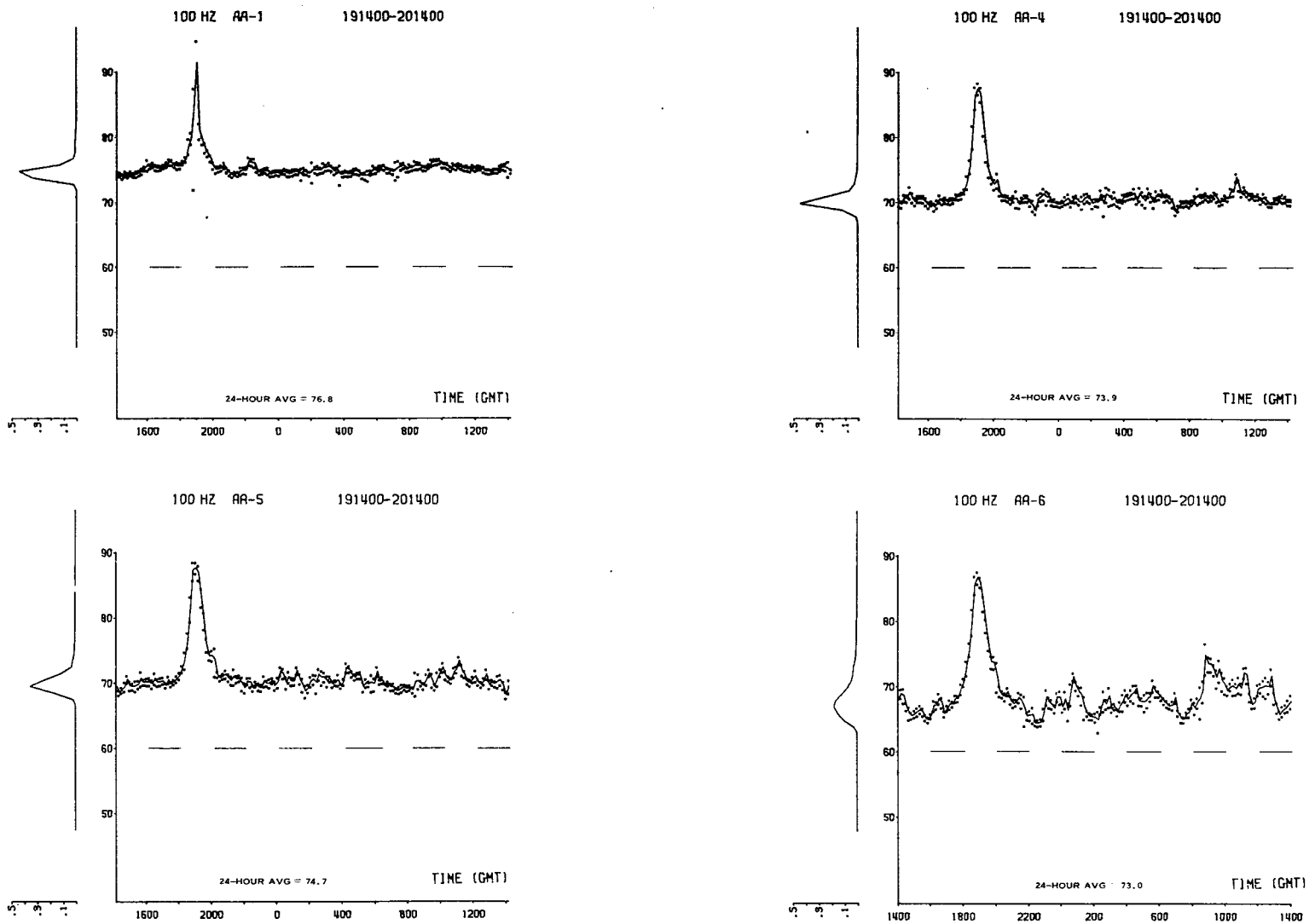

197770

CONFIDENTIAL

Figure A-15. (C) Twenty-Four-Hour Intensity Time-Series at Site A, 749 m, 4,046 m, 4,353 m, and 4,659 m Depths 191400Z to 201400Z (September 1973) (U)

CONFIDENTIAL

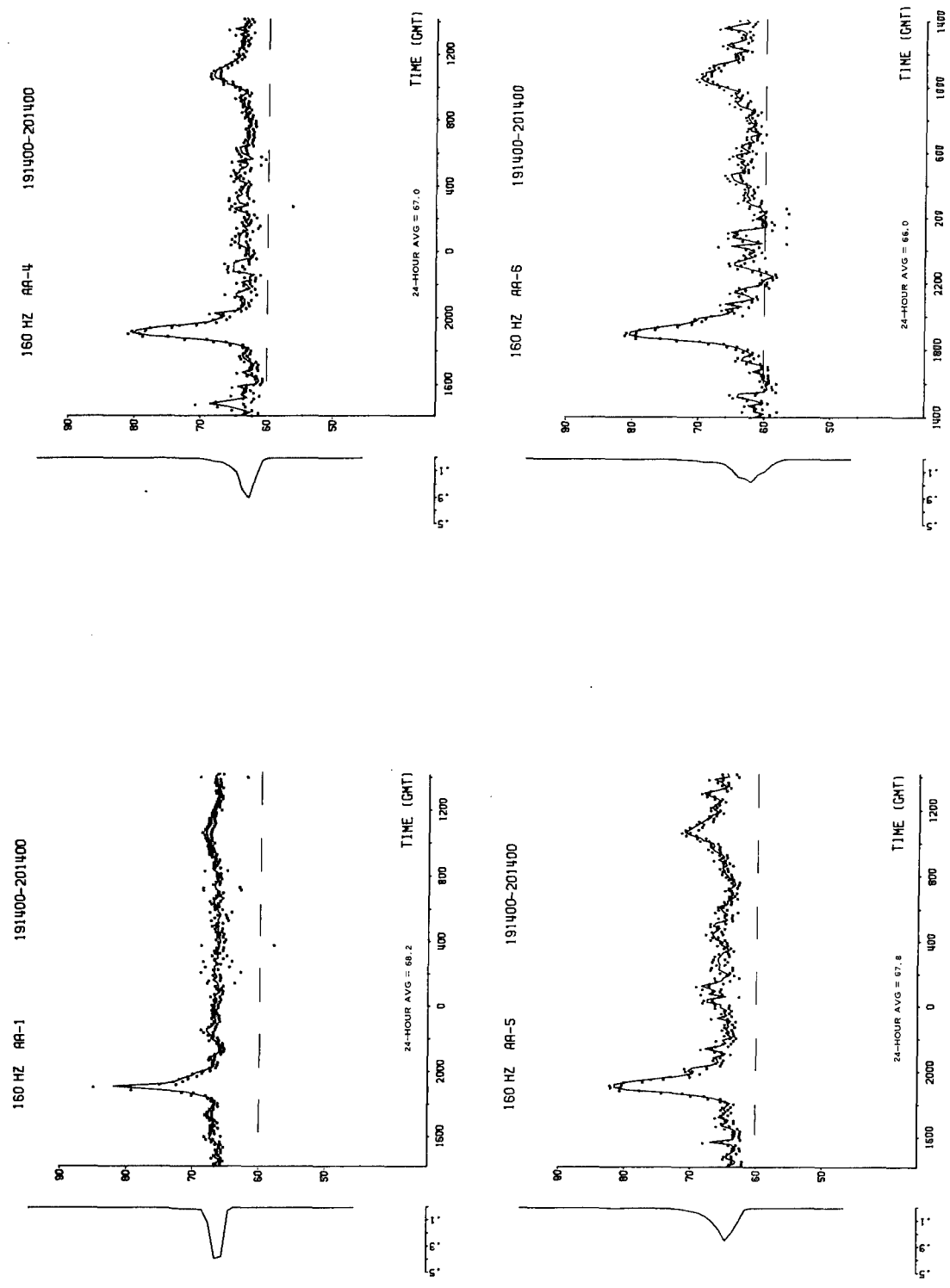

CONFIDENTIAL

Figure A-16. (C) Twenty-Four-Hour Intensity Time-Series at Site A, 749 m, 4,046 m, 4,353 m, and 4,659 m Depths 191400Z to 201400Z (September 1973) (U)

197771

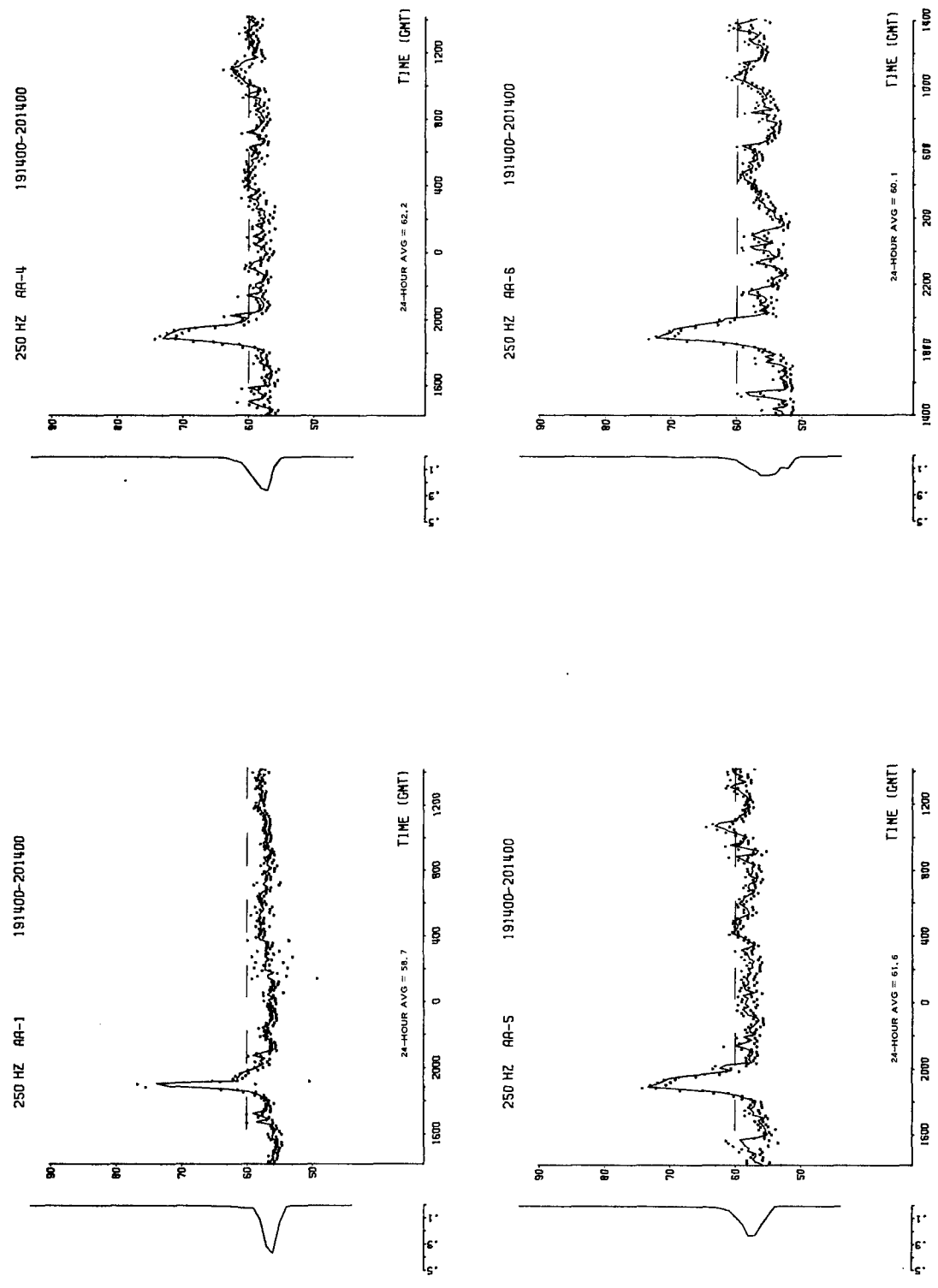

CONFIDENTIAL

Figure A-17. (C) Twenty-Four-Hour Intensity Time-Series at Site A, 749 m, 4,046 m, 4,353 m, and 4,659 m Depths 191400Z to 201400Z (September 1973) (U)

197772

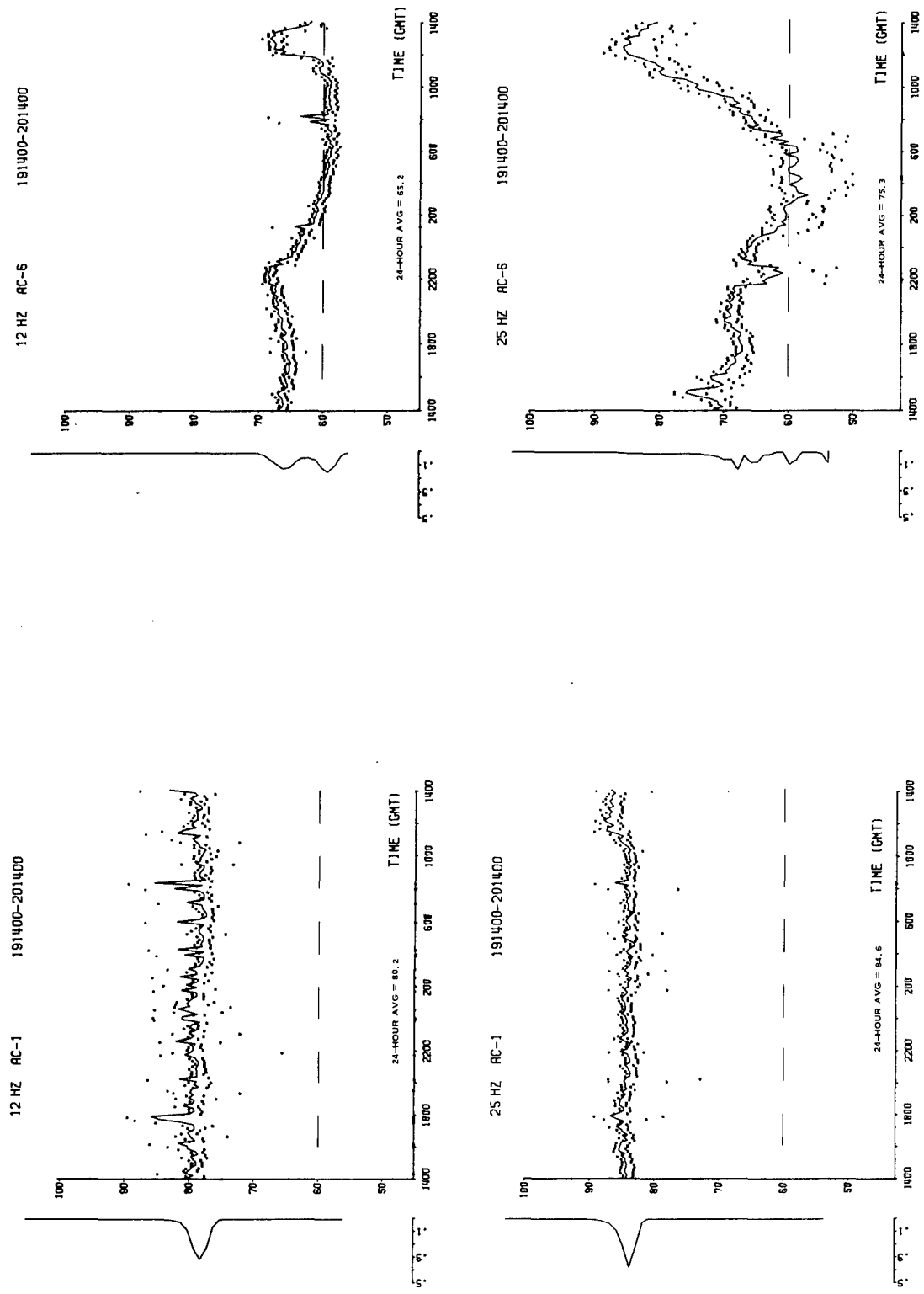

CONFIDENTIAL

Figure A-18. (C) Twenty-Four-Hour Intensity Time-Series at Site C, 696 m and 5,521 m Depths 191400Z to 201400Z (September 1973) (U)

197773

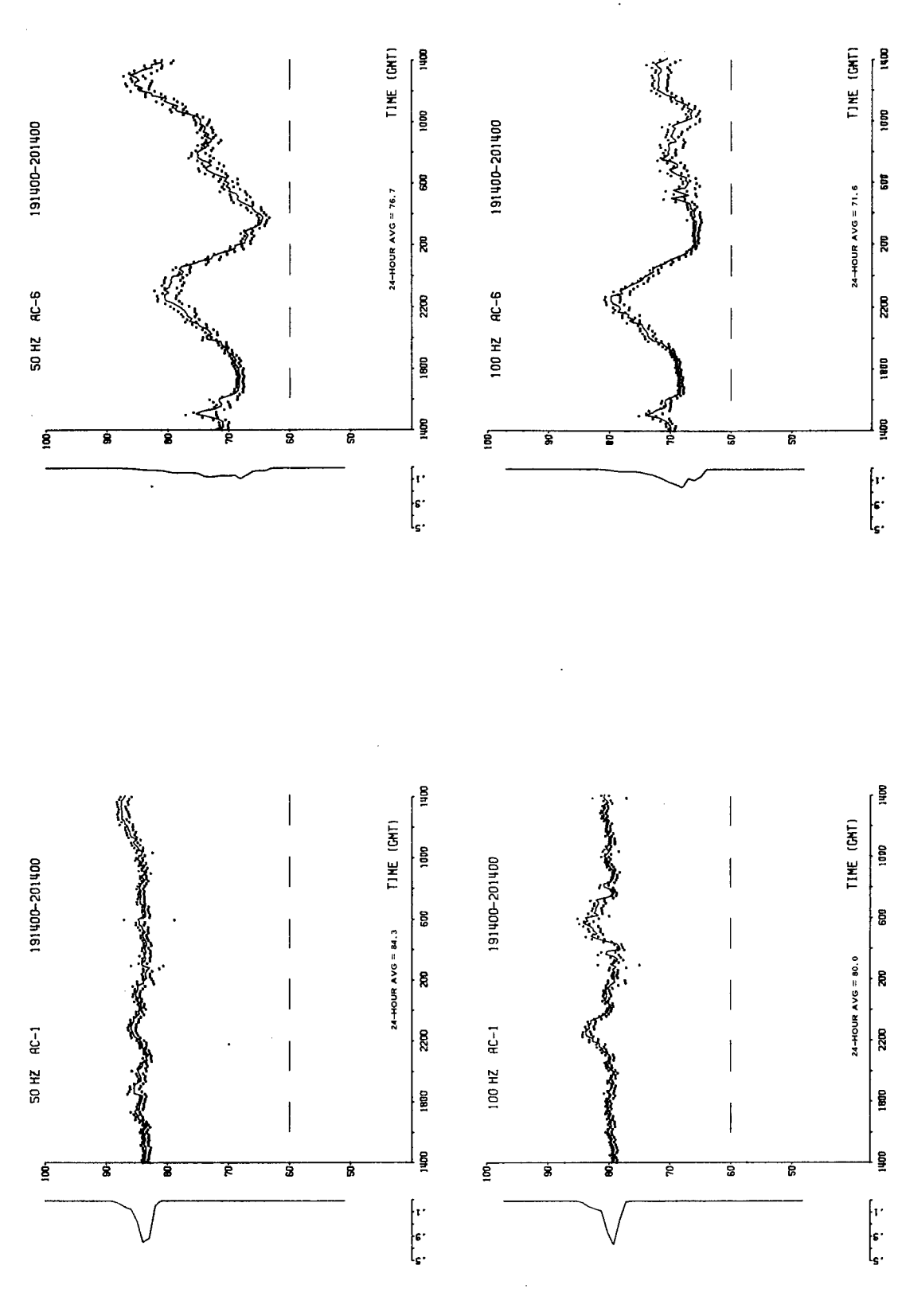

CONFIDENTIAL

Figure A-19. (C) Twenty-Four-Hour Intensity Time-Series at Site C, 696 m and 5,521 m Depths 191400Z to 201400Z (September 1973) (U)

197774

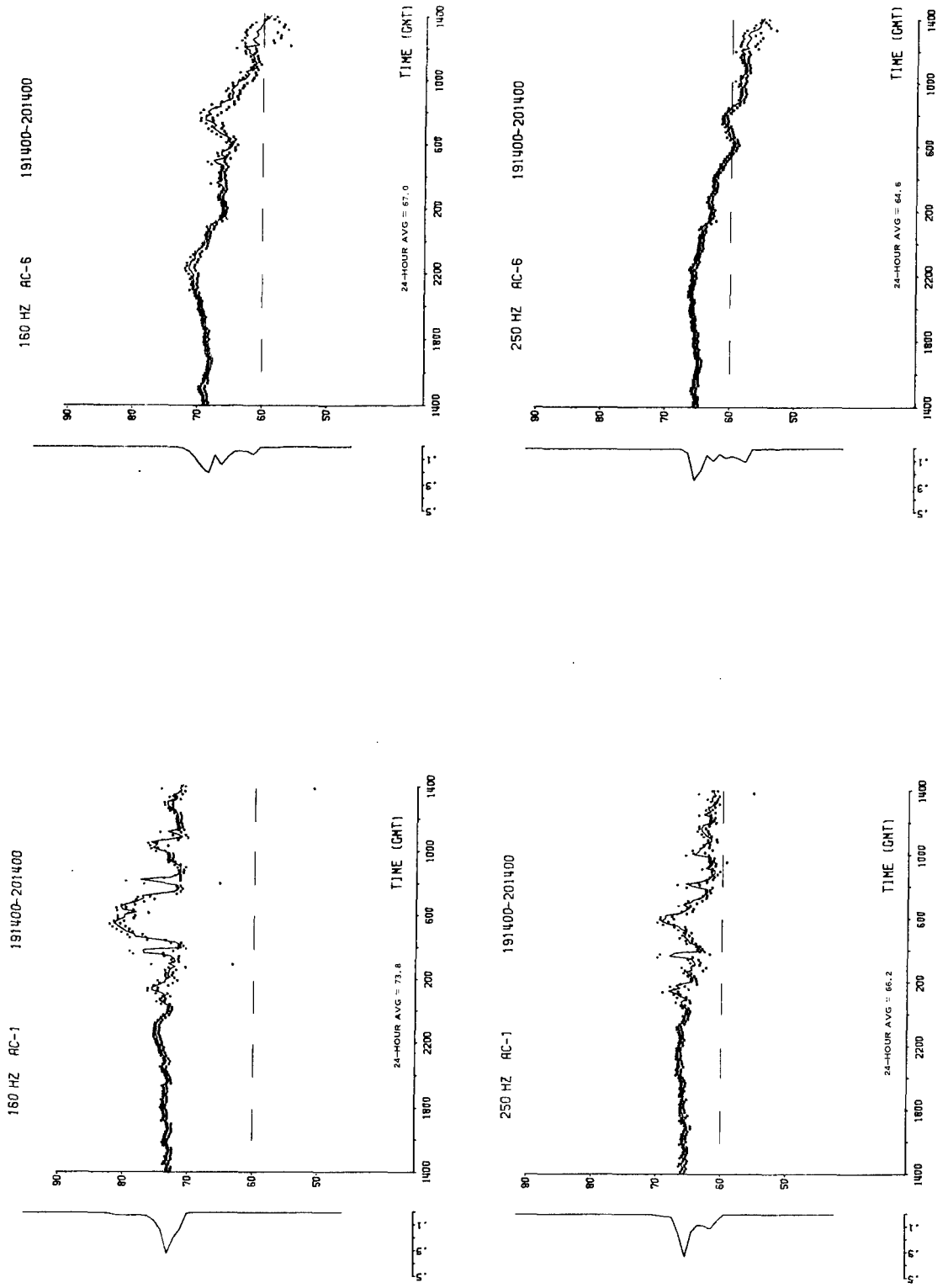

CONFIDENTIAL

Figure A-20. (C) Twenty-Four-Hour Intensity Time-Series at Site C, 696 m and 5,521 m Depths 191400Z to 201400Z (September 1973) (U)

197775

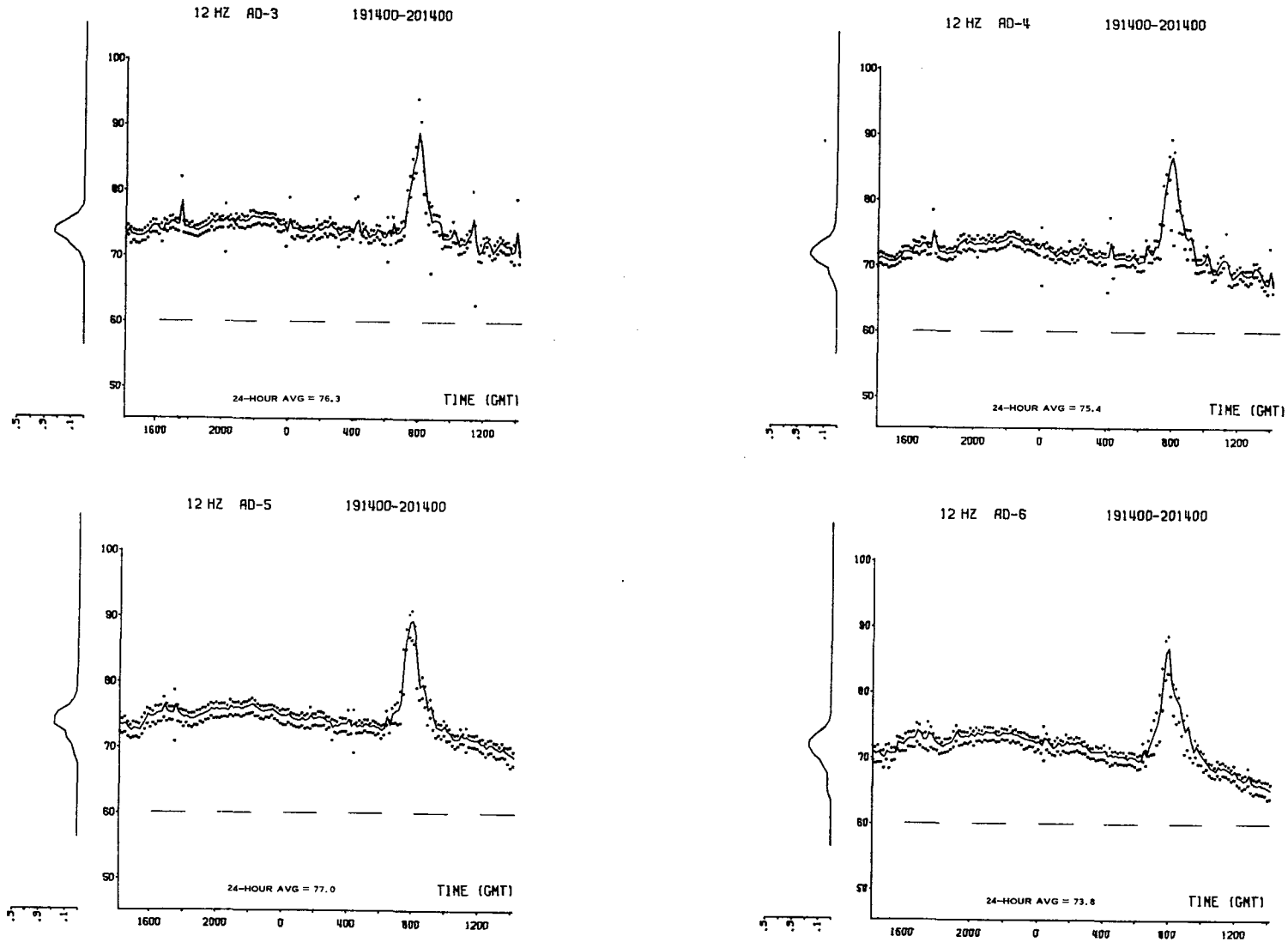

197776

CONFIDENTIAL

Figure A-21. (C) Twenty-Four-Hour Intensity Time-Series at Site D, 3,925 m, 4,225 m, 4,520 m, and 4,612 m Depths 191400Z to 201400Z (September 1973) (U)

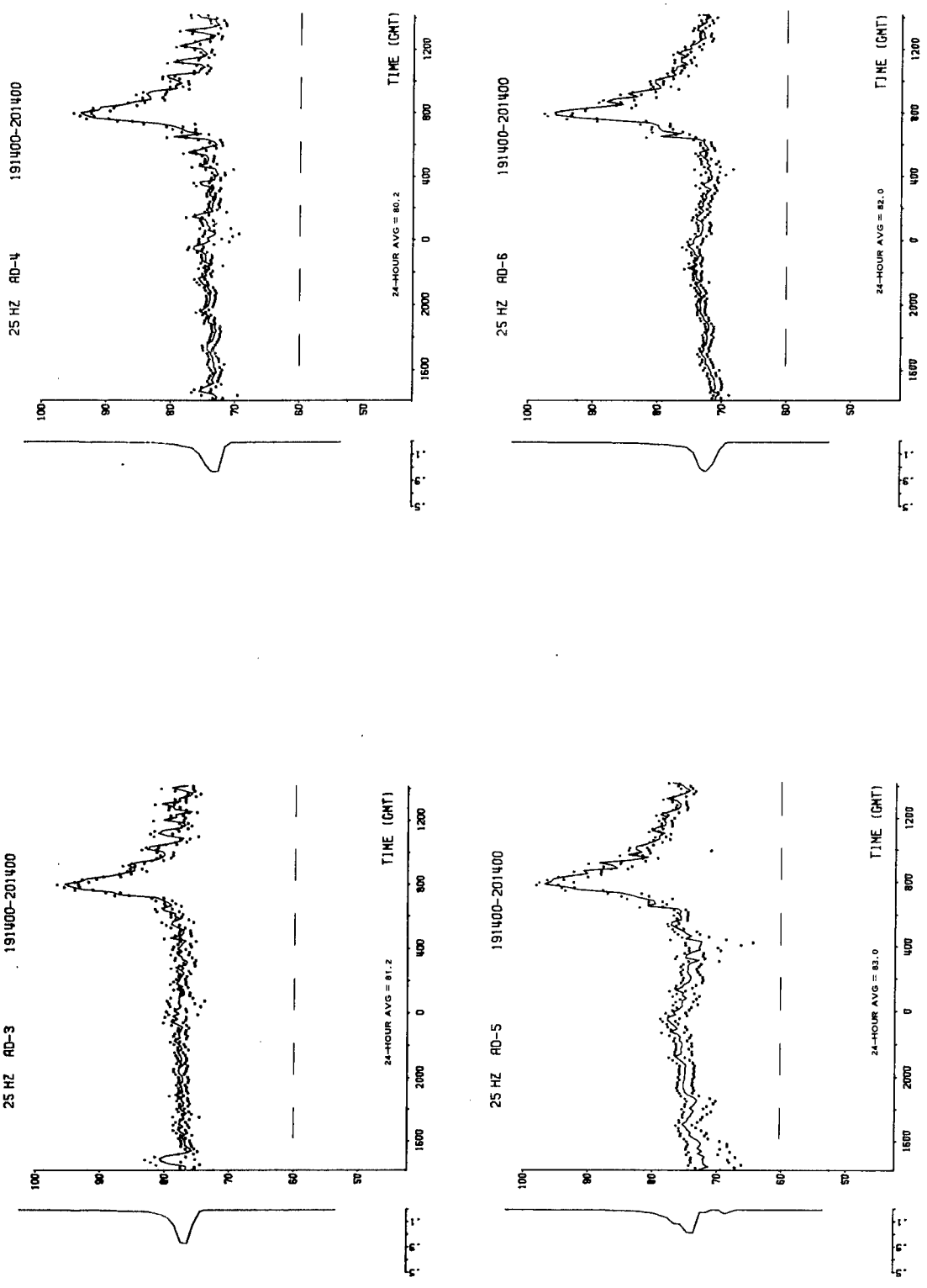

CONFIDENTIAL

Figure A-22. (C) Twenty-Four-Hour Intensity Time-Series at Site D, 3,925 m, 4,225 m, 4,520 m, and 4,612 m Depths 191400Z to 201400Z (September 1973) (U)

197777

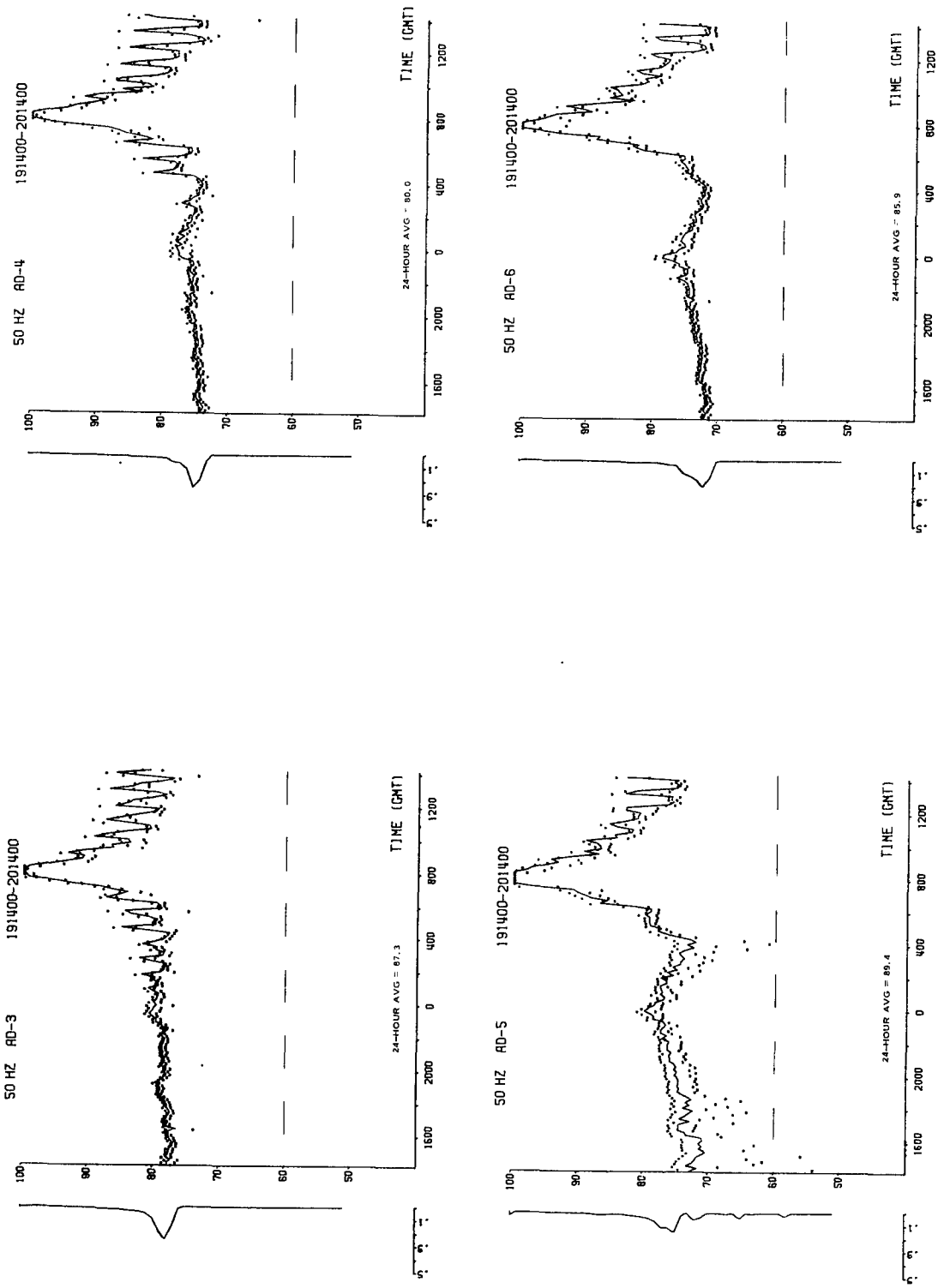

CONFIDENTIAL

Figure A-23. (C) Twenty-Four-Hour Intensity Time-Series at Site D, 3,925 m, 4,225 m, 4,520 m, and 4,612 m Depths 191400Z to 201400Z (September 1973) (U)

197778

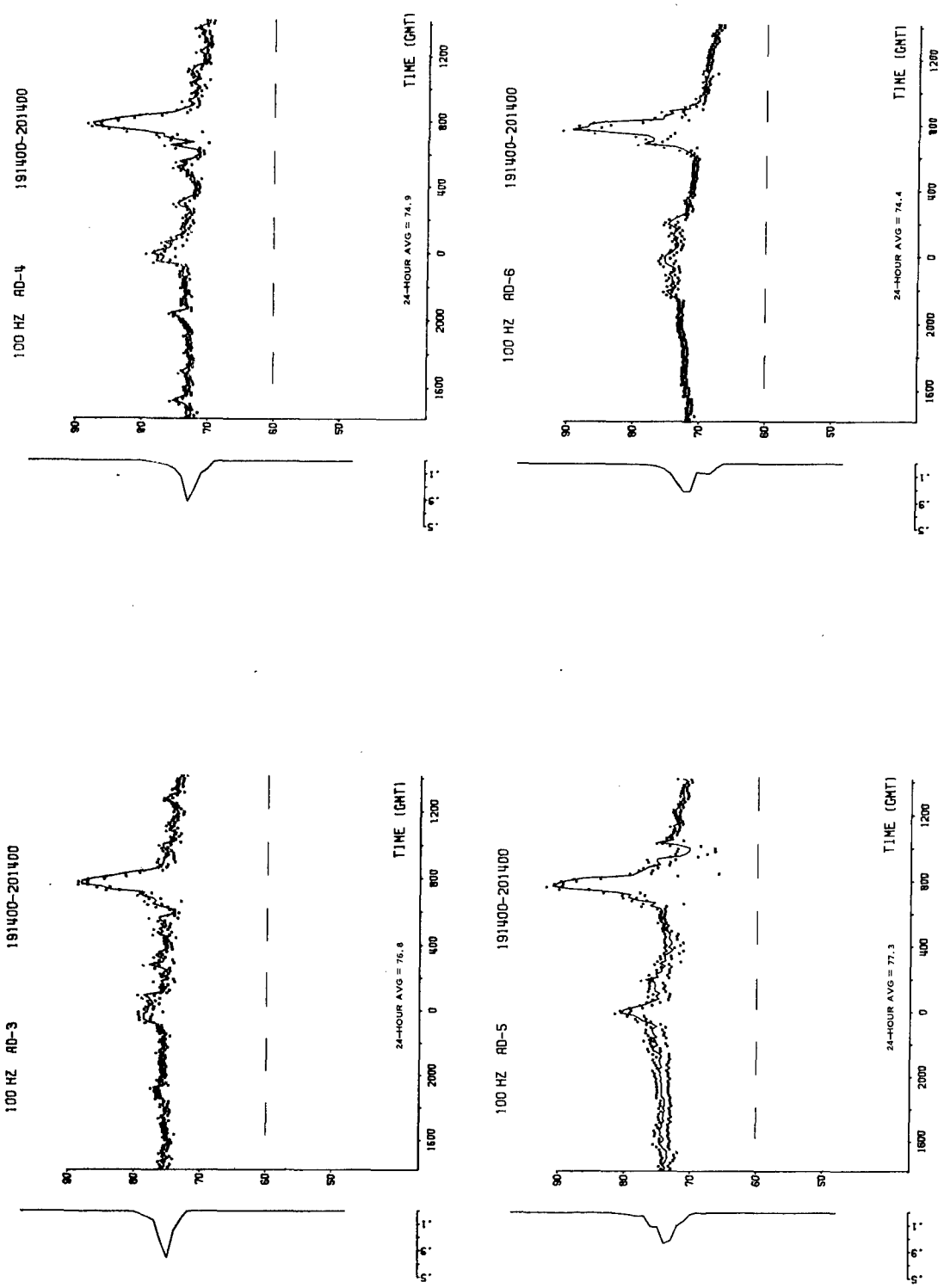

CONFIDENTIAL

Figure A-24. (C) Twenty-Four-Hour Intensity Time-Series at Site D, 3,925 m, 4,225 m, 4,520 m, and 4,512 m Depths 191400Z to 201400Z (September 1973) (U)

197779

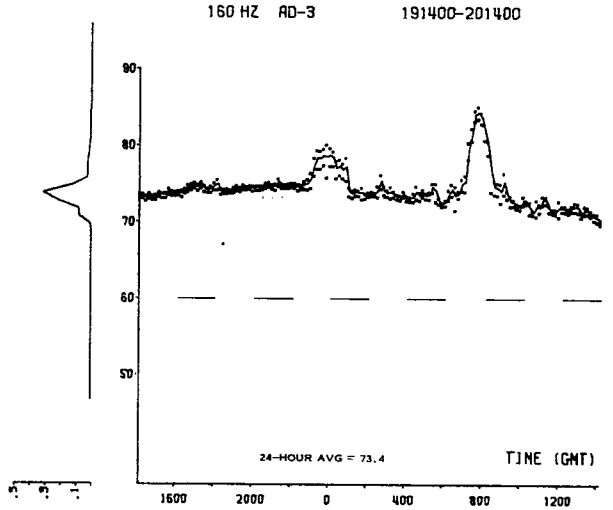

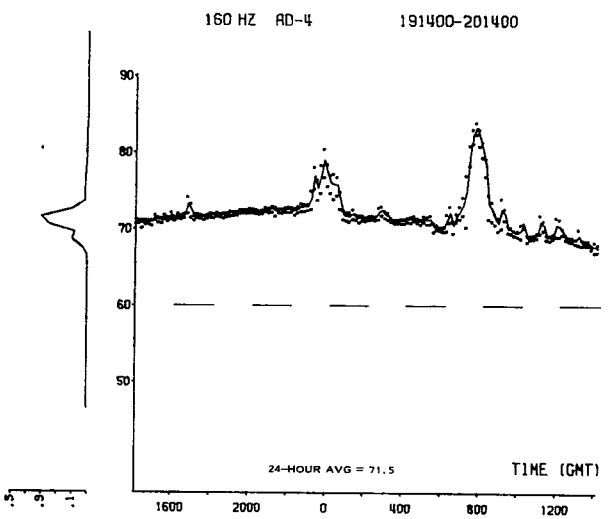

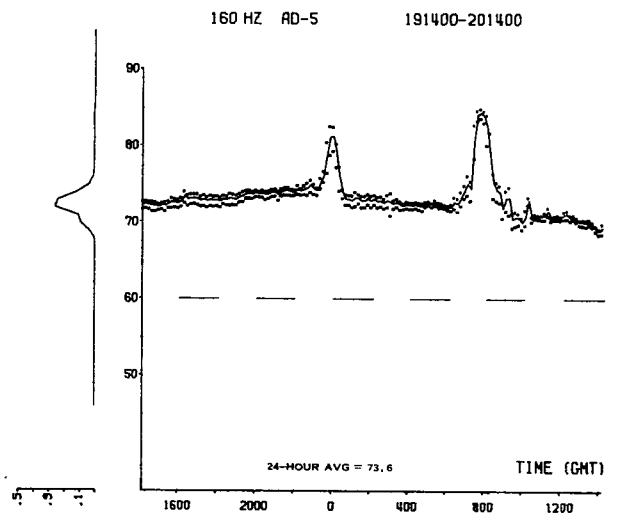

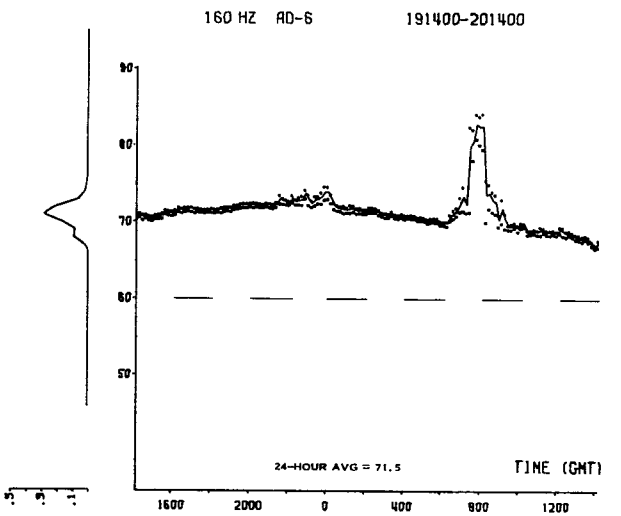

197780

CONFIDENTIAL

Figure A-25. (C) Twenty-Four-Hour Intensity Time-Series at Site D, 3,925 m, 4,225 m, 4,520 m, and 4,612 m Depths 191400Z to 201400Z (September 1973) (U)

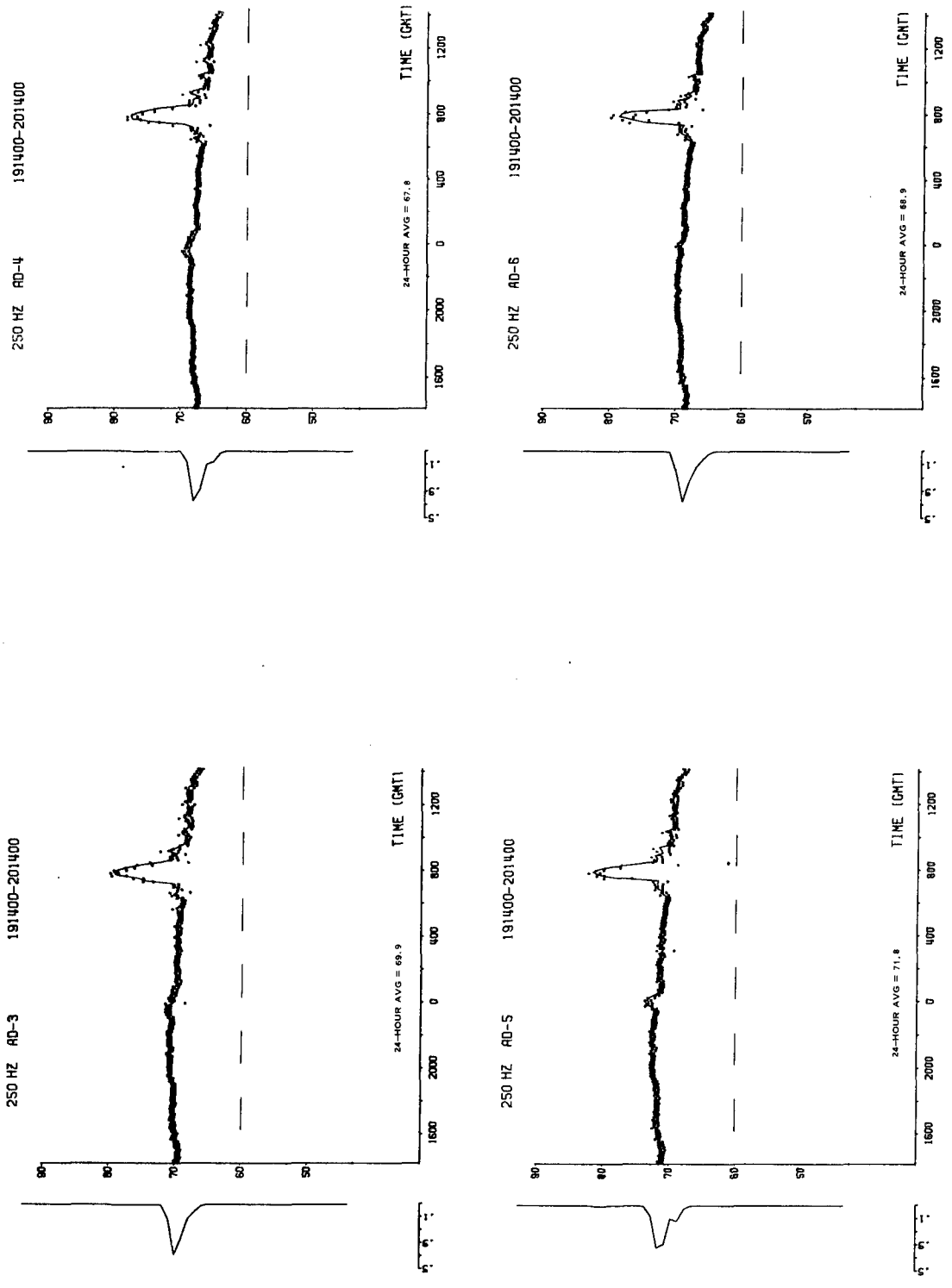

CONFIDENTIAL

Figure A-26. (C) Twenty-Four-Hour Intensity Time-Series at Site D, 3,925 m, 4,225 m, 4,520 m, and 4,612 m Depths 191400Z to 201400Z (September 1973) (U)

197781

(U) REFERENCES

1. B.K. Dynamics, *ACODAC Processing Error Budget Analysis*, TR-3186 (March 1974).

2. *ACODAC Error Analysis for CHURCH ANCHOR*, Texas Instruments (15 March 1974).

APPENDIX B

(C) AMBIENT NOISE INTENSITIES AT ACODAC SITES A, C, AND D (U)

(U) This appendix provides in some detail the analysis of a portion of the ambient noise data recorded by ACODAC receivers located at sites A, C, and D. Two 24-hour periods were investigated: day 171600Z to 181600Z and day 191400Z to 201400Z. Table B-1 summarizes the data analyzed.

TABLE B-1. (U) SUMMARY OF ACODAC AMBIENT NOISE ANALYZED

Site	Day	Depth (m)
A	171600Z to 181600Z	749, 4,046, 4,353
A	191400Z to 201400Z	749, 4,046, 4,658
C	171600Z to 181600Z	696, 4,055
C	191400Z to 201400Z	696, 4,055, 4,361
D	191400Z to 201400Z	3,325, 3,625, 3,925

UNCLASSIFIED

(U) The data processing, designed to obtain the noise levels in selected 1/3-octave filter bands, is described in Section I. The main product of the processing (Section II) was a set of 24-hour plots that show the structure of the ambient noise intensity with depth, frequency, and location as the fundamental parameters. Although general conclusions about the data can be made by a cursory inspection of these 24-hour records, a set of more quantitative statements about the data is presented with the analysis given in Sections III, IV, and V. This appendix concludes with Section VI, which presents comments on these data and their analyses.

I. (U) DATA PROCESSING SYSTEM DESCRIPTION

(U) The ARL/UT ambient noise measurement system (ANMS) is a hardware/software configuration designed to perform 1/3-octave band analysis over the frequency range of 10 to 300 Hz. The primary source of data collection for the current analyses is the ACODAC receiving array. The processing system is divided into three tasks: data conversion, calibration, and display.

A. (U) Data Conversion

(U) The first task performed by the analysis system is the conversion of time-series data to the frequency domain using a real-time analyzer (RTA) as the front end to a digital computer (Figure B-1). Figure B-2 shows the configuration and data paths of the CDC 3200 digital computer system.

(U) The ACODAC analog tape is played back at a 20:1 time compression. The analysis is performed on one data channel on each pass of the analog tape. The analog data are filtered (5 to 300 Hz), amplified, and input to the RTA, making use of the full dynamic range of the analyzer. Simultaneously, the ACODAC time code, gain state, and overload information are input to the digital computer (Figure B-1). The sample synchronization (900 Hz) for the RTA is derived from the 50-Hz time code carrier by multiplication with a phase-lock frequency multiplier. Synchronization of the RTA to the analog tape allows compensation for the speed variations in tape recorder speed that can occur during recording, duplication, and playback. This

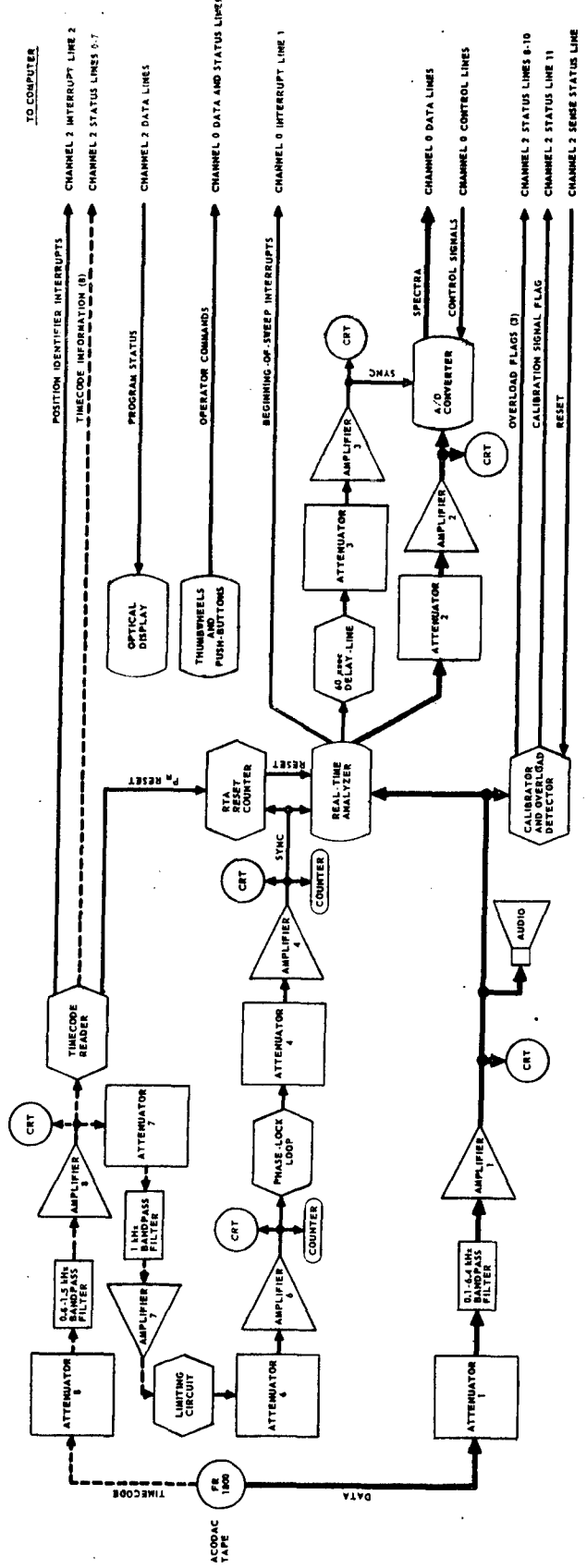

UNCLASSIFIED

197782

Figure B-1. (U) Analog Equipment Configuration for Analysis of ACODAC Data Via RTA

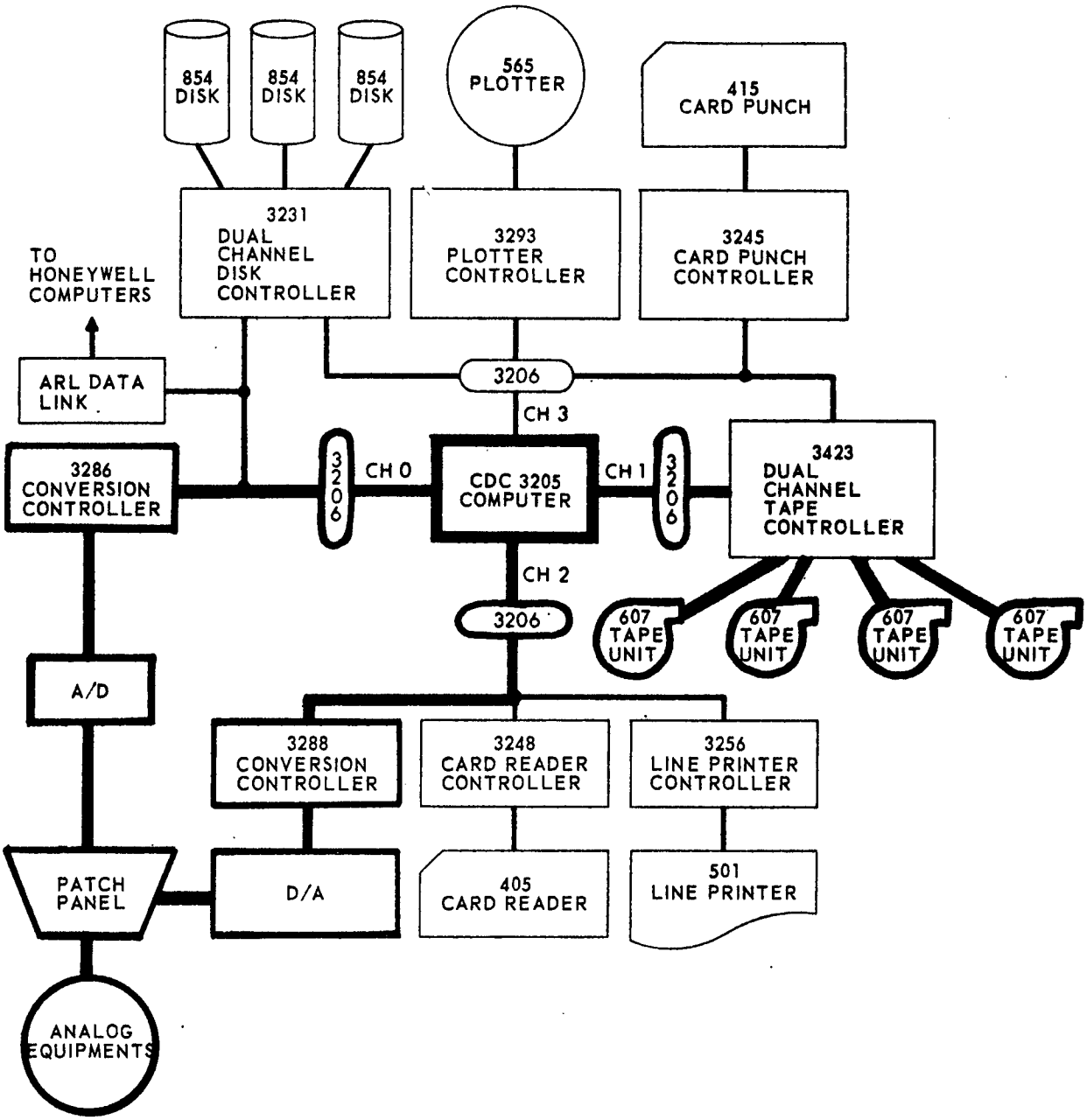

197783

UNCLASSIFIED

Figure B-2. (U) CDC Computer System at ARL

synchronization is also used by the RTA reset counter, which causes the real-time analyzer to input a single frequency sweep each time its memory is filled. These sweeps cover contiguous blocks of data. The RTA reset counter is, in turn, synchronized to the beginning of each ACODAC minute by means of the P_R position marker in the time code.

(U) With an effective sample rate of 900 Hz, the real-time analyzer will sweep from 0 to 300 Hz 12 times a second, each sweep covering 1-2/3 second of ACODAC data. During each sweep, the linear-step spectrum output of the analyzer is digitized and stored in the CDC 3200 computer. The data are also being constantly monitored by a hardware calibration and overload signal detector. Information regarding any such detections is also stored in the computer.

(U) To prevent distortion caused by ACODAC gain changes and amplifier switching transients, those sweeps generated during the first and last 5 seconds of each ACODAC minute are disregarded. The remaining 50 seconds of each minute are divided into five 10-second blocks. For each of the six sweeps generated during a 10-second block, the 500 spectral lines output by the real-time analyzer are floated, squared, and tested for distortion caused by a spectral output exceeding the maximum input amplitude range of the A/D converter (RTA). If the input range is exceeded, the process is aborted, and the operator is instructed to reduce the amplification of the spectral outputs before restarting the process at the place where the distortion began. Once this testing is completed, all six of the sweeps in each 10-second block are averaged, frequency-line-by-frequency-line; 1/3-octave bands are then formed by summing over the appropriate frequency lines. The data are then stored on digital tape in 10-second averages. The computer constantly monitors the time code data to ensure that synchronization is maintained between the data and the time code information.

B. (U) Calibration

(U) Each ACODAC data tape contains a header which consists of a sequence of externally supplied calibration signals at known levels followed by a sequence of internally generated calibration signals. The external calibration sequence consists of five frequencies (12.5, 25, 50, 100, and 200 Hz), each of which is supplied at four levels (−50, −40, −30, and −20 dB re 1 V_{rms}). For the lowest level, −50 dB re 1 V_{rms}, the ACODAC amplifiers are in the highest of their four gain states (40, 30, 20, and 10 dB), and stepped through the remaining states as the external signal level was increased. These external calibration signals are used to measure overall frequency response as a function of frequency and amplifier gain state.

(U) As the header signals are recorded before each ACODAC deployment, changes in the frequency response could occur because of changes in the system's environment. The internal calibration signals are used to supply this *in situ* correction. An internal calibration signal consists of two frequencies (50 to 200 Hz), supplied in parallel at four different levels. Once again, the amplifiers step through their gain states as the signal level is increased. An internal calibration sequence is generated every 6 hours; thus, four such signals occur during each 24-hour analysis period. The *in situ* correction is obtained by measuring the differences between the internal calibration sequence in the header and those occurring during the analysis period. These differences are corrected for the −0.27 dB change in the outputs of the calibration signal generator as measured by Texas Instruments during environmental testing.

(U) The absolute levels of the external calibration signals, the measured frequency responses, and the measured *in situ* corrections are then combined with the hydrophone sensitivities and a

bandwidth correction that normalizes each band to 1 Hz. The result is a set of calibration factors which are then applied to the data to yield noise intensities in dB/μPa/Hz$^{1/2}$.

C. (U) Display

(U) The calibrated 10-second averages are used to generate a histogram of noise intensity, standard plots of noise intensity versus time, and a tabulated version of noise intensity versus time.

D. (U) Processing Error Analysis

(U) The error bands for the noise intensity estimates are ±0.3 dB. This limit includes the effects of the playback recorder and the analysis system. The uncertainties in the ACODAC system and the tape duplication process are not being included [reference *ACODAC Processing Error Budget Analysis*, B-K Dynamics, Inc., TR-3186 (March 1974)].

(U) A cross check of the analysis system that includes the RTA was conducted during the analysis phase. The reference is a broadband (5 to 300 Hz) digitization and FFT processing system. The results from the reference system differ from the RTA system by approximately 0.1 dB.

II. (U) 24-HOUR RECORDS OF AMBIENT NOISE INTENSITY

(U) Figures B-3 through B-17 present 24-hour ambient noise levels, corresponding to various 1/3-octave frequency bands, obtained from the three ACODAC sites (A, C, and D). A comparison can be made of the noise levels at different depths for a given frequency band, day, and location. Thus, in Figure B-3, the ambient noise level in the 1/3-octave band centered about 12.6 Hz is shown for the hydrophone depths 749 m, 4,046 m, and 4,353 m. All noise intensities are expressed in dB/μPa/Hz$^{1/2}$.

III. (C) VARIATION OF AMBIENT NOISE INTENSITY WITH DEPTH (U)

(C) The ambient noise data, obtained at sites A and C, indicate (Figures B-18 through B-22) that the noise intensity, for a given frequency, was about 4 or 5 dB greater near the sound channel axis than it was at the critical depth. Furthermore, when the depth was increased to approximately 300 m below the critical depth (Figure B-23, from CHURCH ANCHOR Synopsis Report), an additional decrease of about 5 dB was observed in the ambient noise level.

(U) The variations of noise levels with frequency (as shown in Figures B-18 through B-22) are based on approximations of the average intensity of the noise in a given frequency band over a 24-hour period. These approximations are based on observations of the noise intensity, disregarding large variations caused, perhaps, by nearby shipping traffic. There is an error in the data of Figure B-21, in that the noise levels at the depth of 4,361 m are about 12 dB lower than expected.

(C) Data from site D are shown in Figure B-22 where, in contrast to Figures B-1 through B-4, it is difficult to draw any firm conclusions about the change in noise intensity with depth. It is interesting to note that all these depths shown in Figure B-22 are below the critical depth (approximately 2,840 m). If a conclusion can be made, it is that the variation of noise intensity with depth is not as great below the critical depth as it is when a transition is made from above the critical depth to below the critical depth.

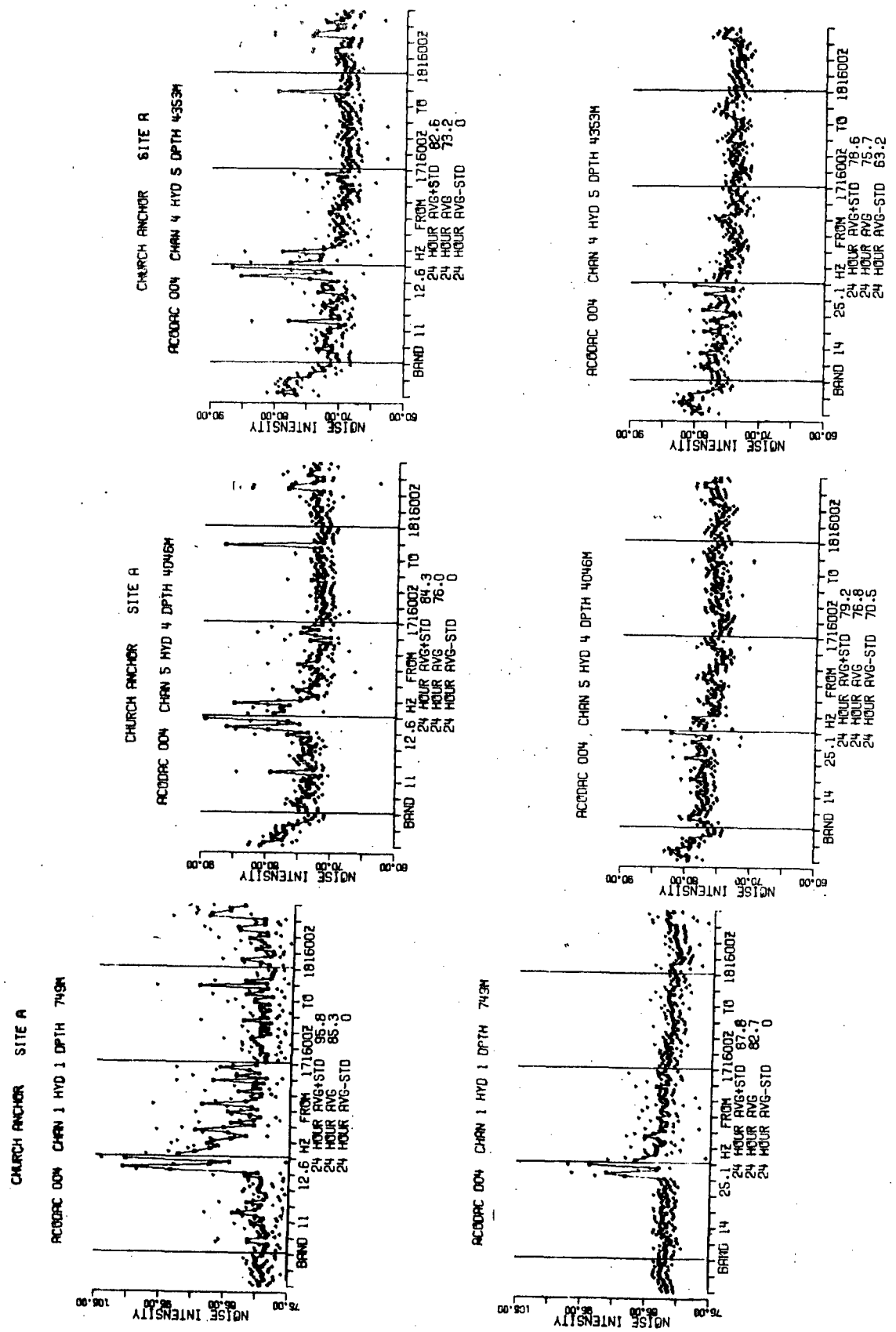

CONFIDENTIAL

Figure B-3. (C) Twenty-Four-Hour Noise Intensity Time Series at Site A, September 1973 (U)

197784

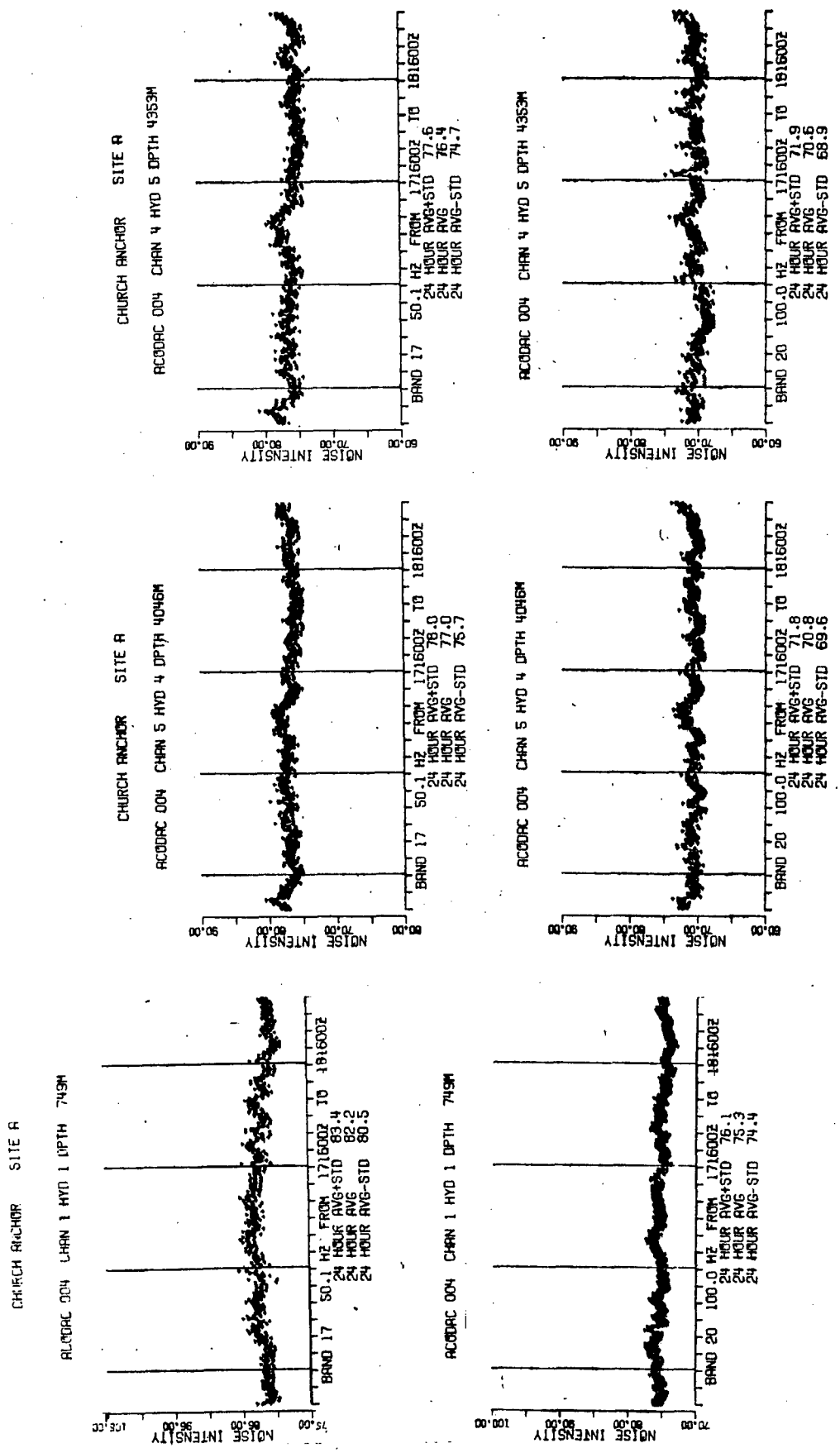

Figure B-4. (C) Twenty-Four-Hour Noise Intensity Time Series at Site A, September 1973 (U)

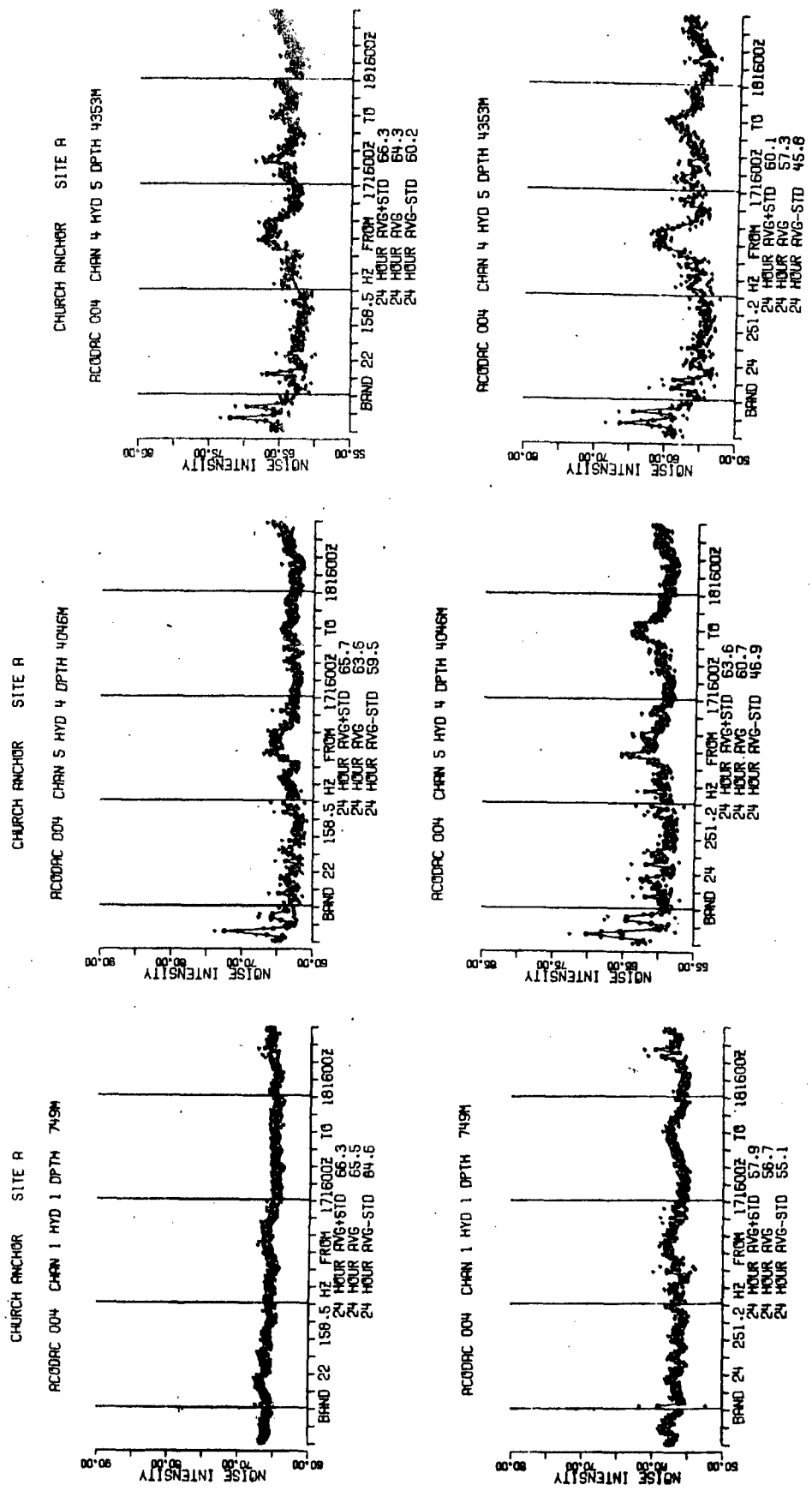

CONFIDENTIAL

197786

Figure B-5. (C) Twenty-Four-Hour Noise Intensity Time Series at Site A, September 1973 (U)

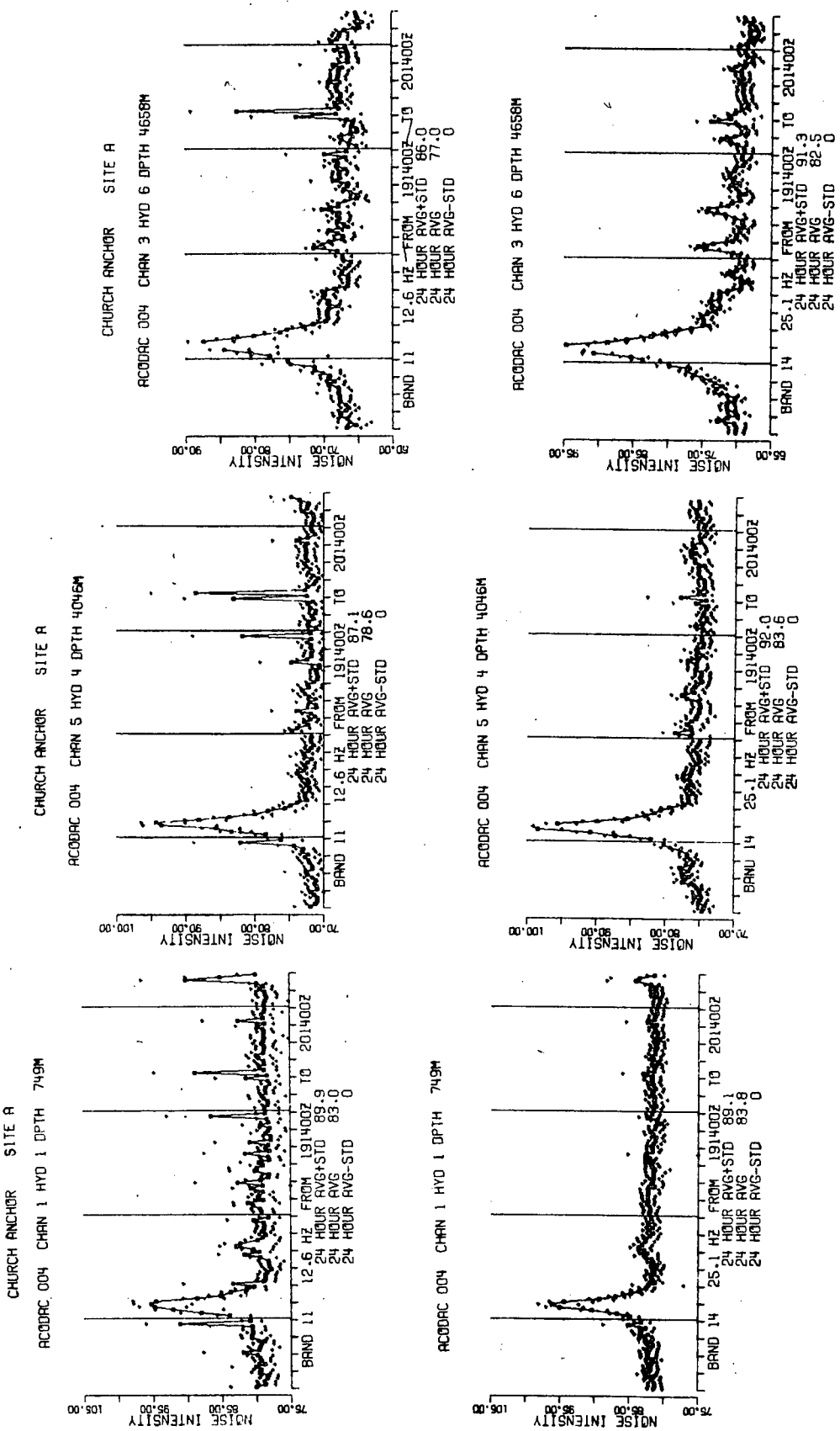

Figure B-6. (C) Twenty-Four-Hour Noise Intensity Time Series at Site A, September 1973 (U)

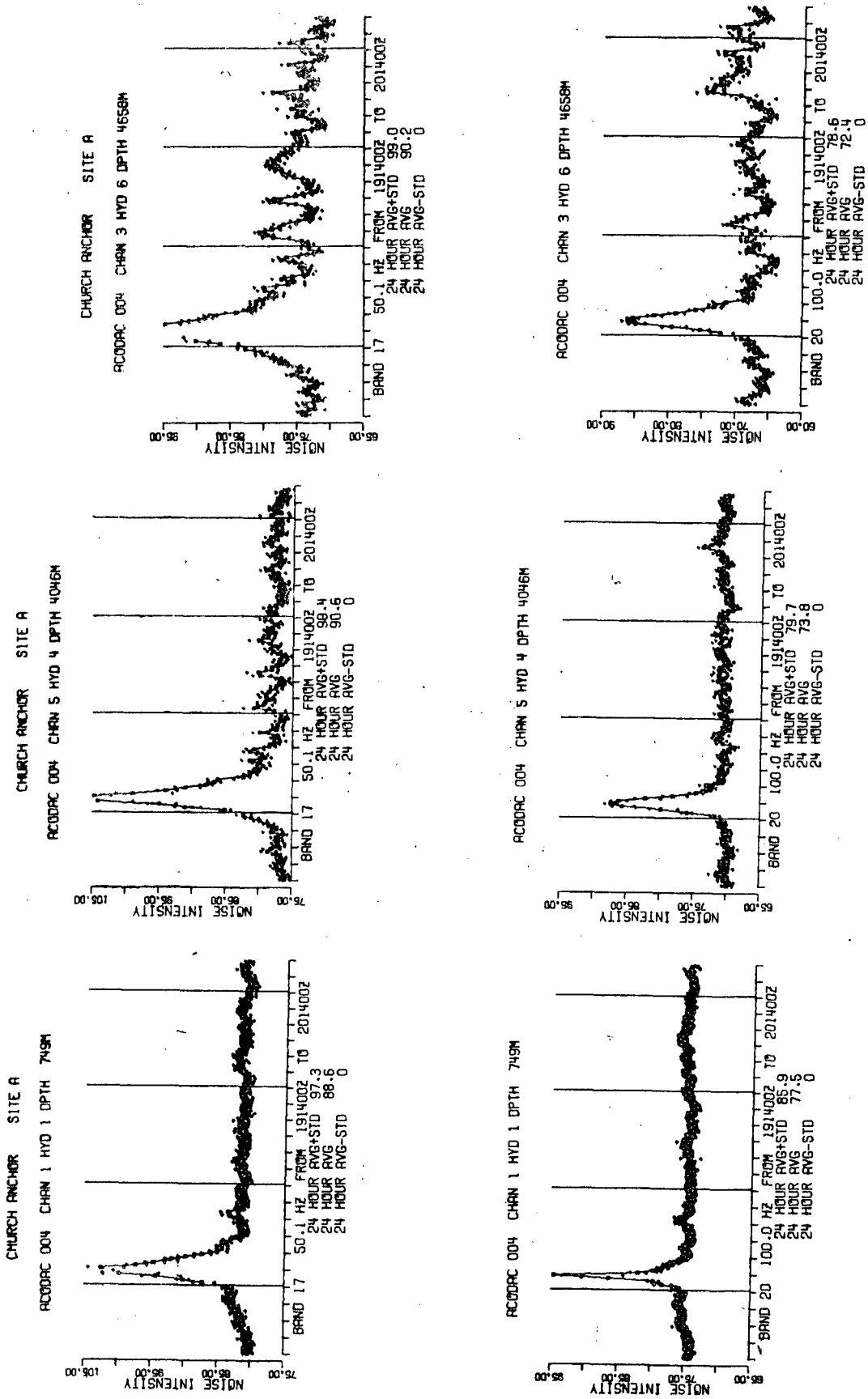

Figure B-7. (C) Twenty-Four-Hour Noise Intensity Time Series at Site A, September 1973 (U)

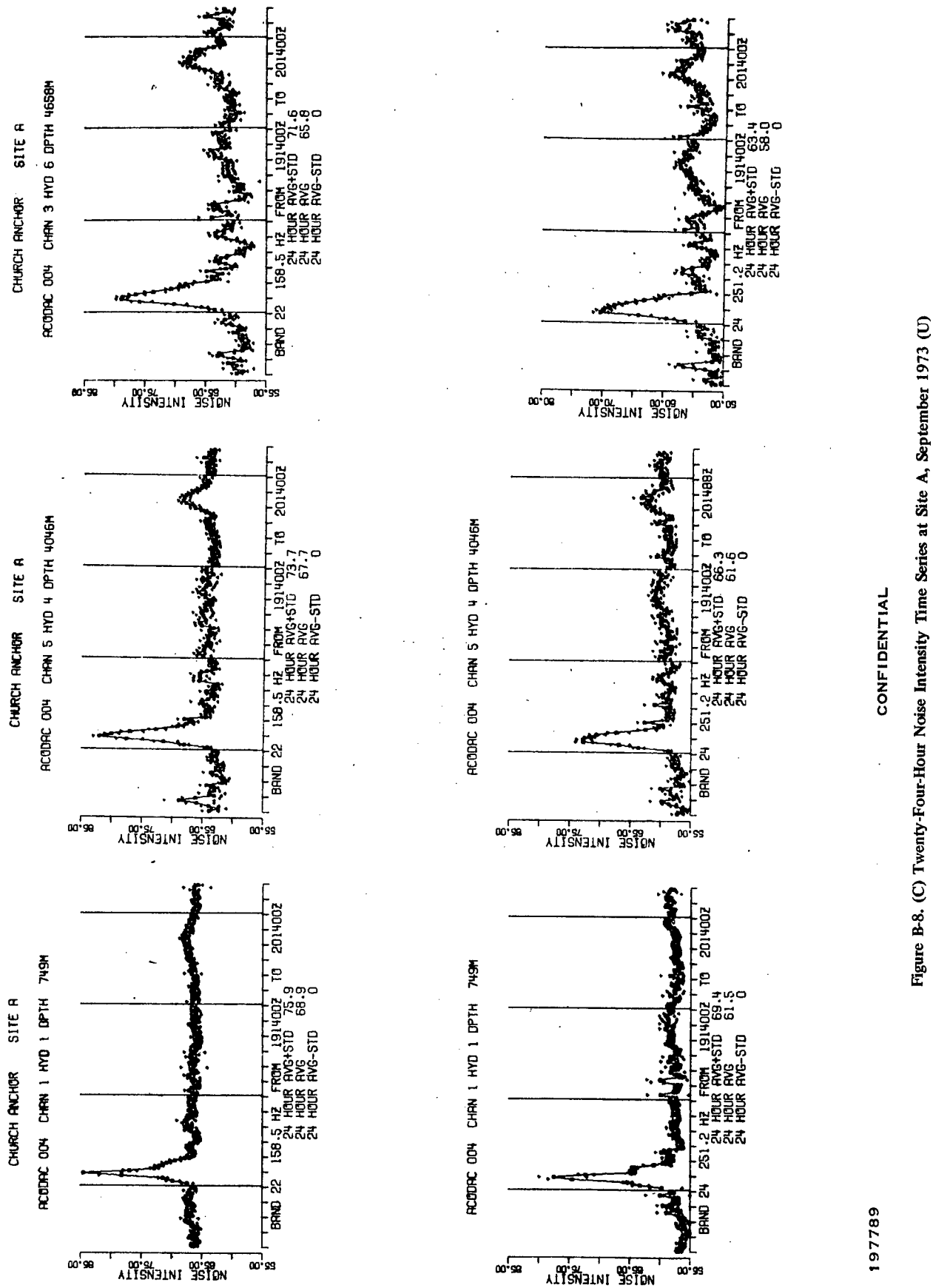

CONFIDENTIAL

197789

Figure B-8. (C) Twenty-Four-Hour Noise Intensity Time Series at Site A, September 1973 (U)

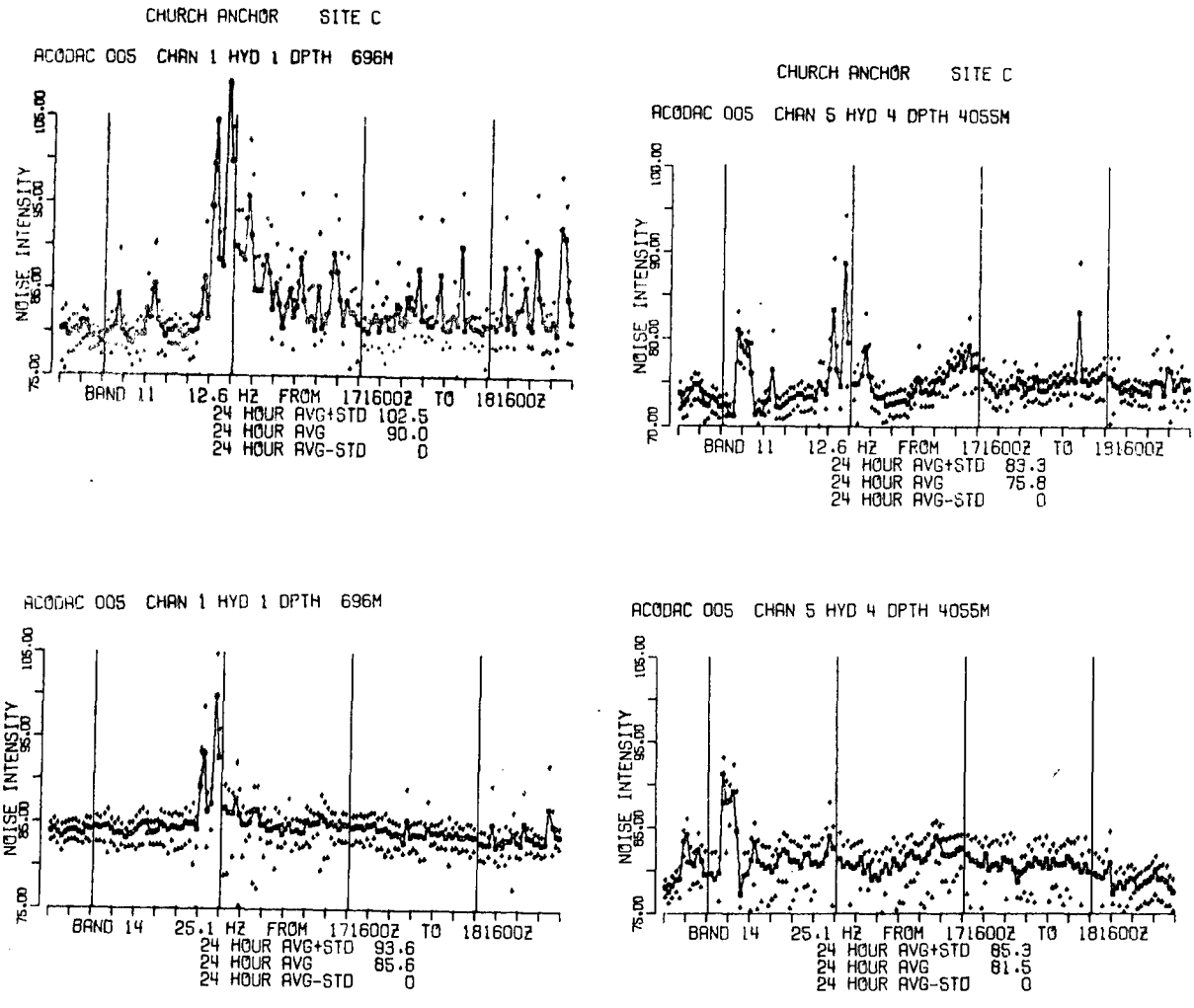

197790

CONFIDENTIAL

Figure B-9. (C) Twenty-Four-Hour Noise Intensity Time Series at Site C, September 1973 (U)

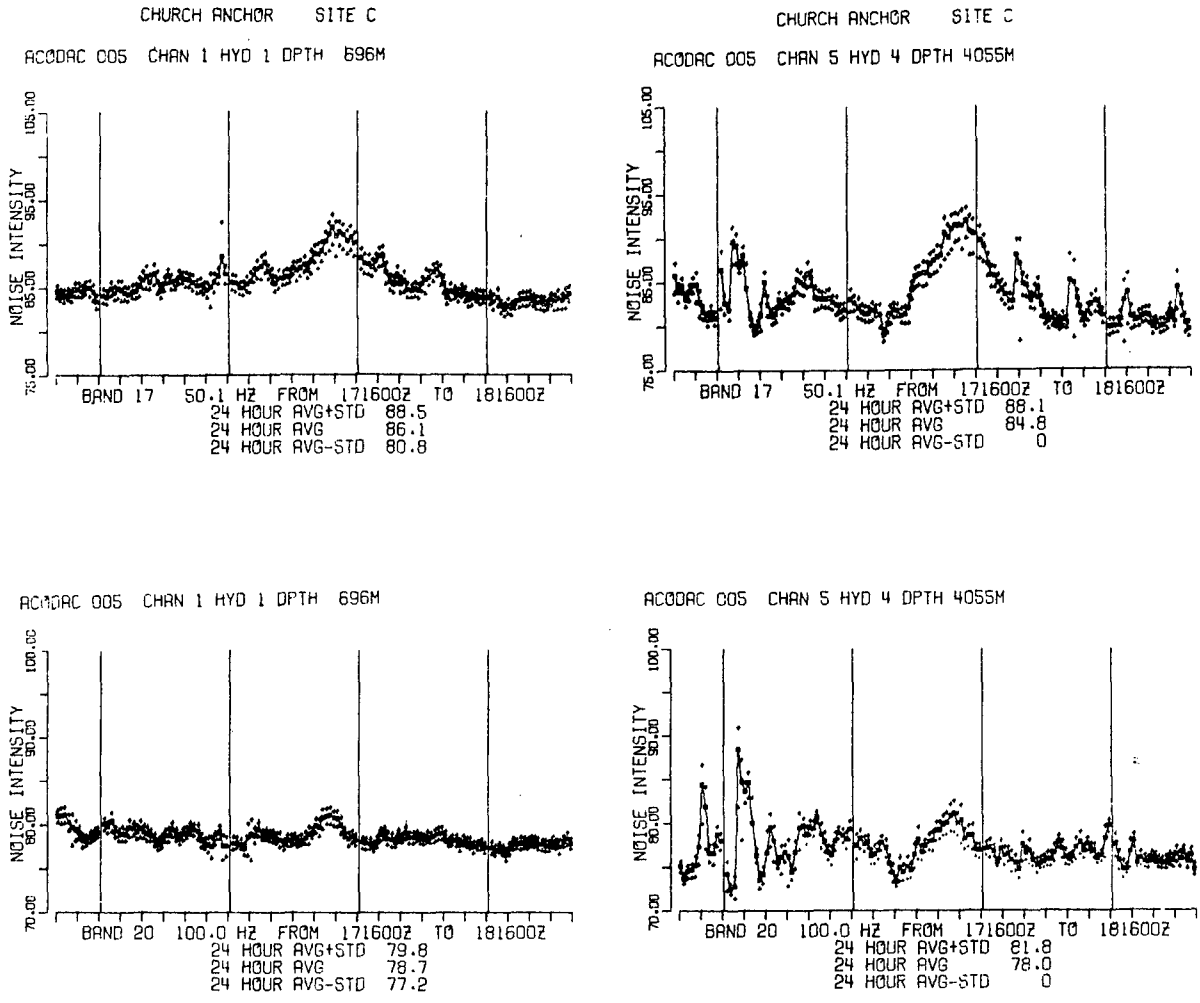

197791

CONFIDENTIAL

Figure B-10. (C) Twenty-Four-Hour Noise Intensity Time Series at Site C (U)

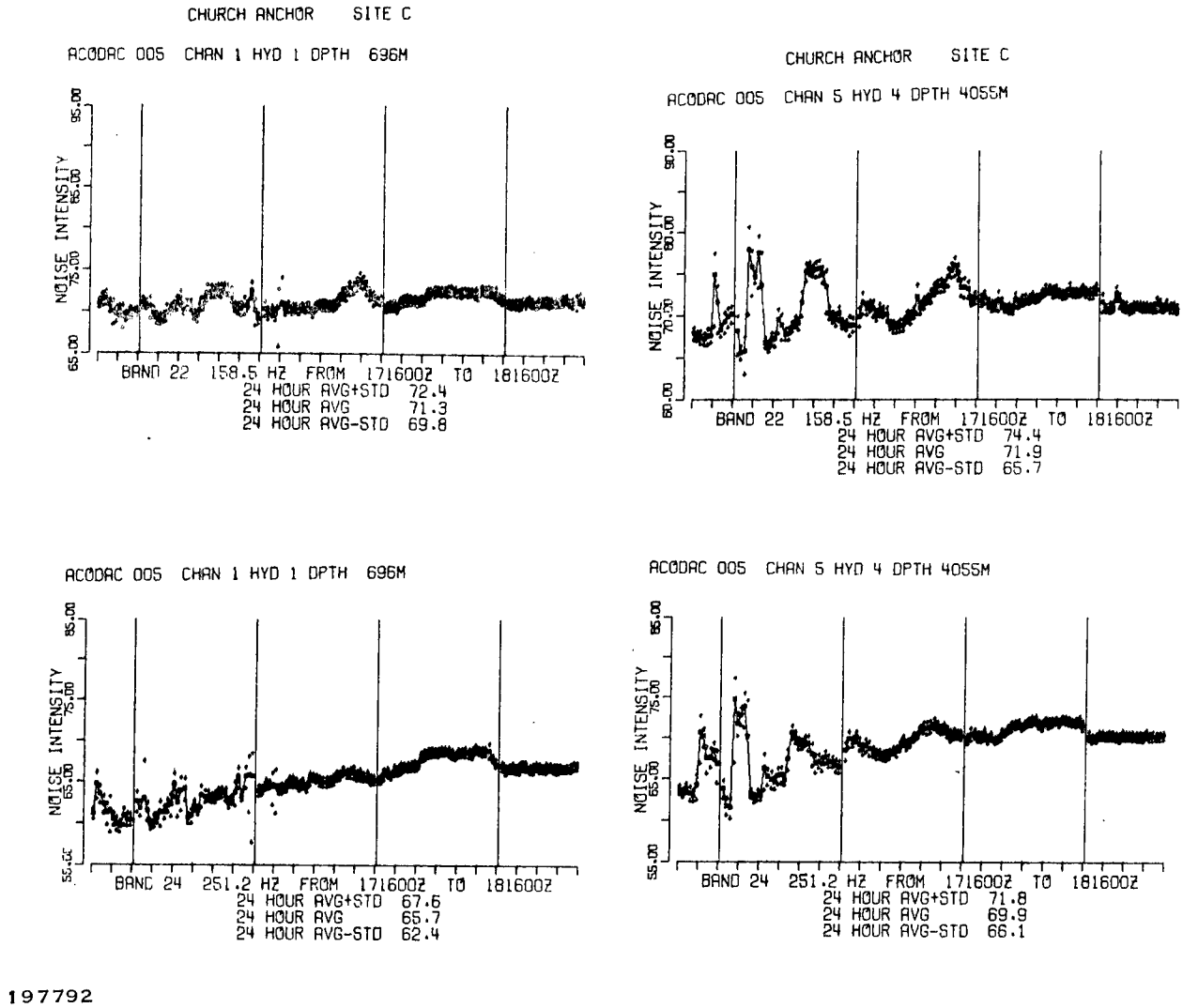

197792

CONFIDENTIAL

Figure B-11. (C) Twenty-Four-Hour Noise Intensity Time Series at Site C, September 1973 (U)

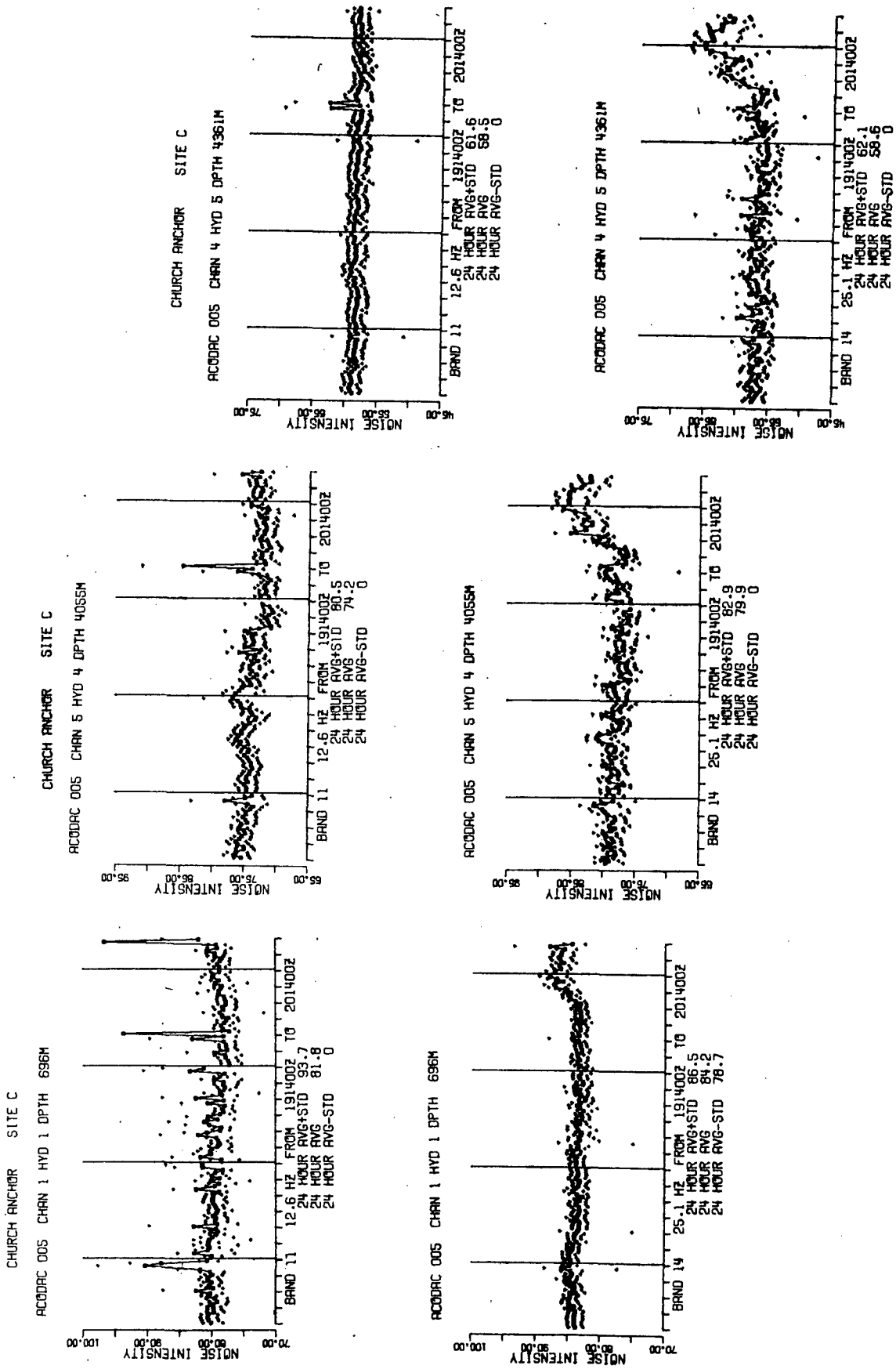

Figure B-12. (C) Twenty-Four-Hour Noise Intensity Time Series at Site C, September 1973 (U)

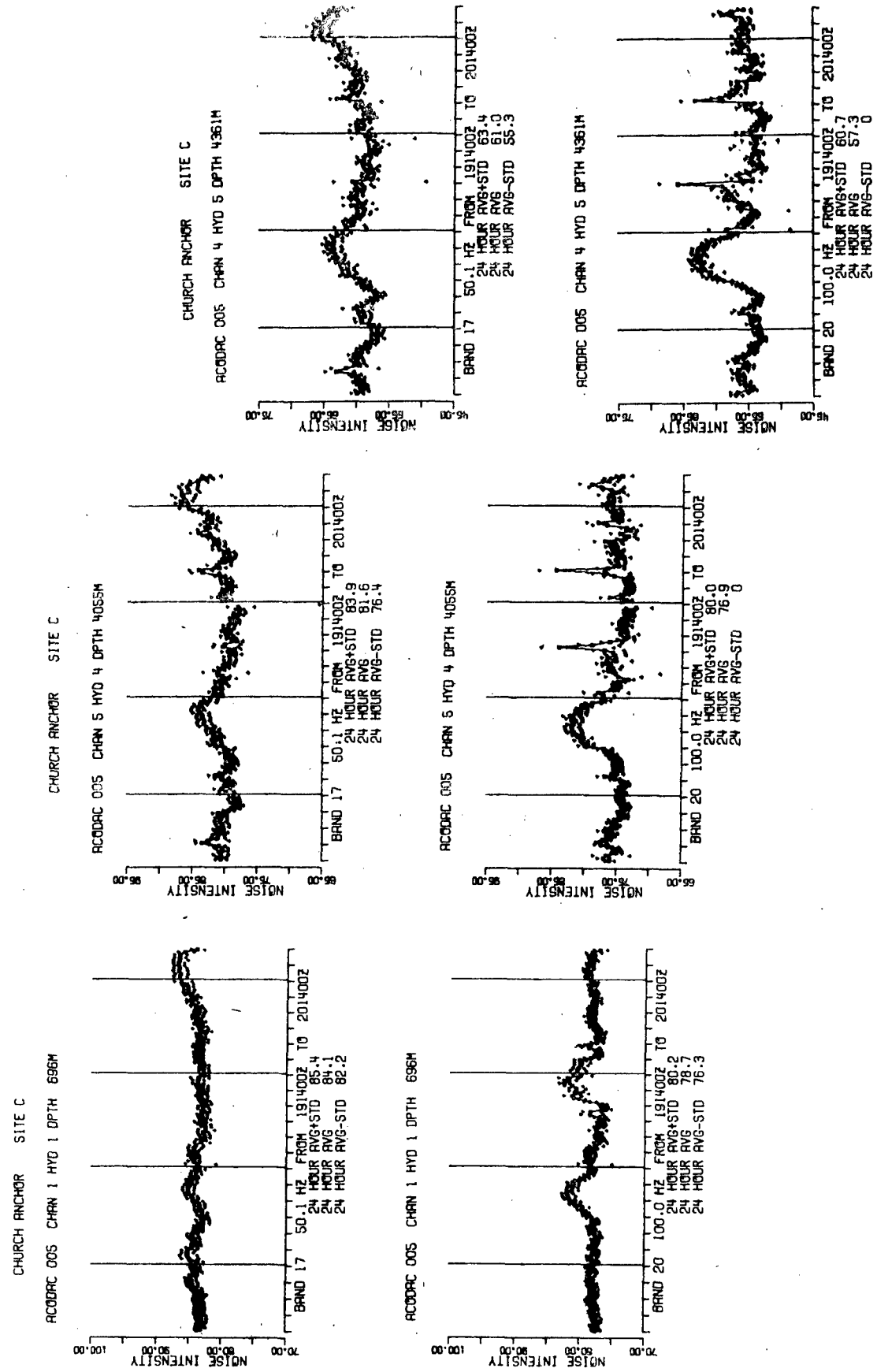

CONFIDENTIAL

Figure B-13. (C) Twenty-Four-Hour Noise Intensity Time Series at Site C, September 1973 (U)

197794

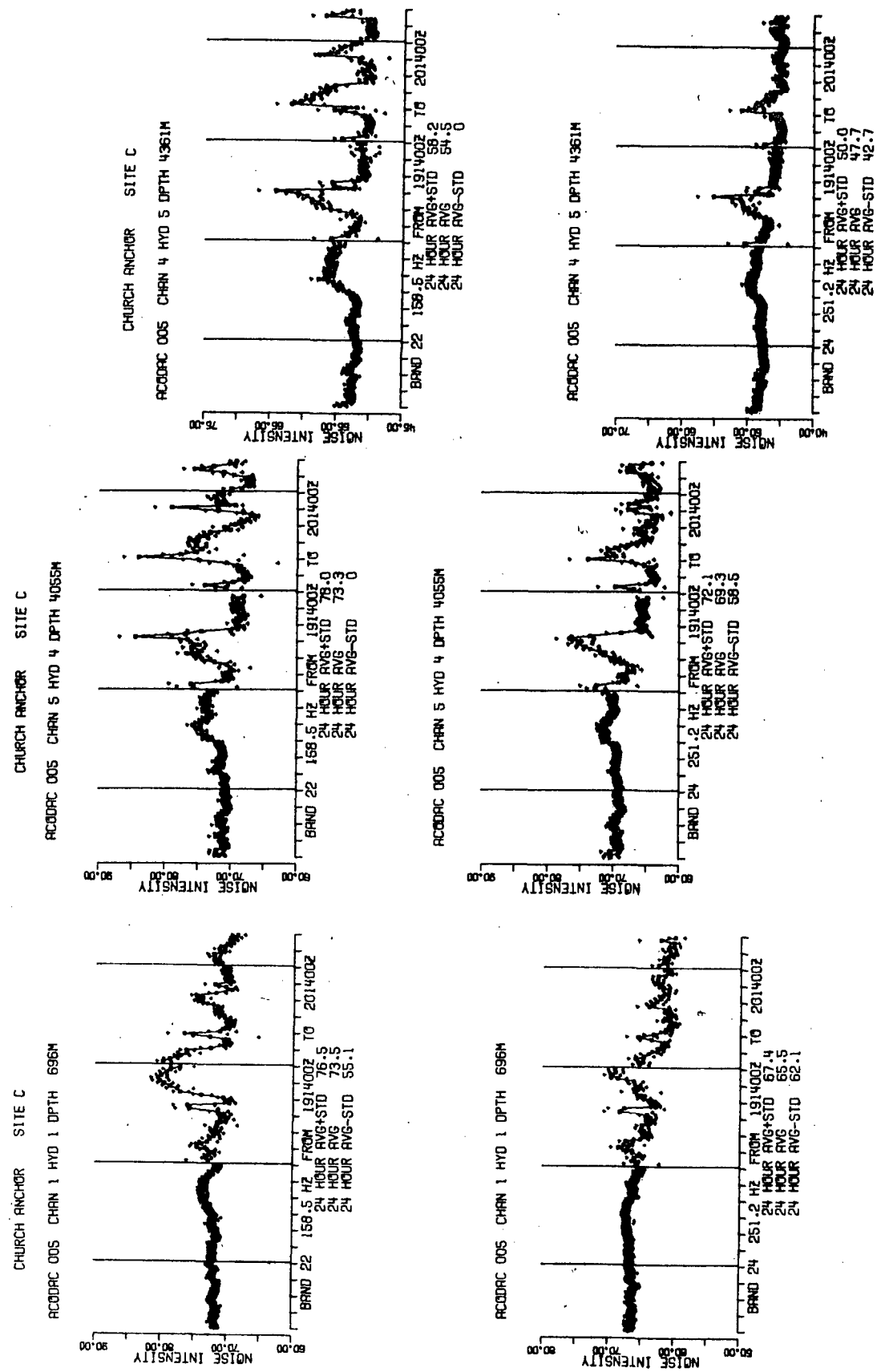

Figure B-14. (C) Twenty-Four-Hour Noise Intensity Time Series at Site C, September 1973 (U)

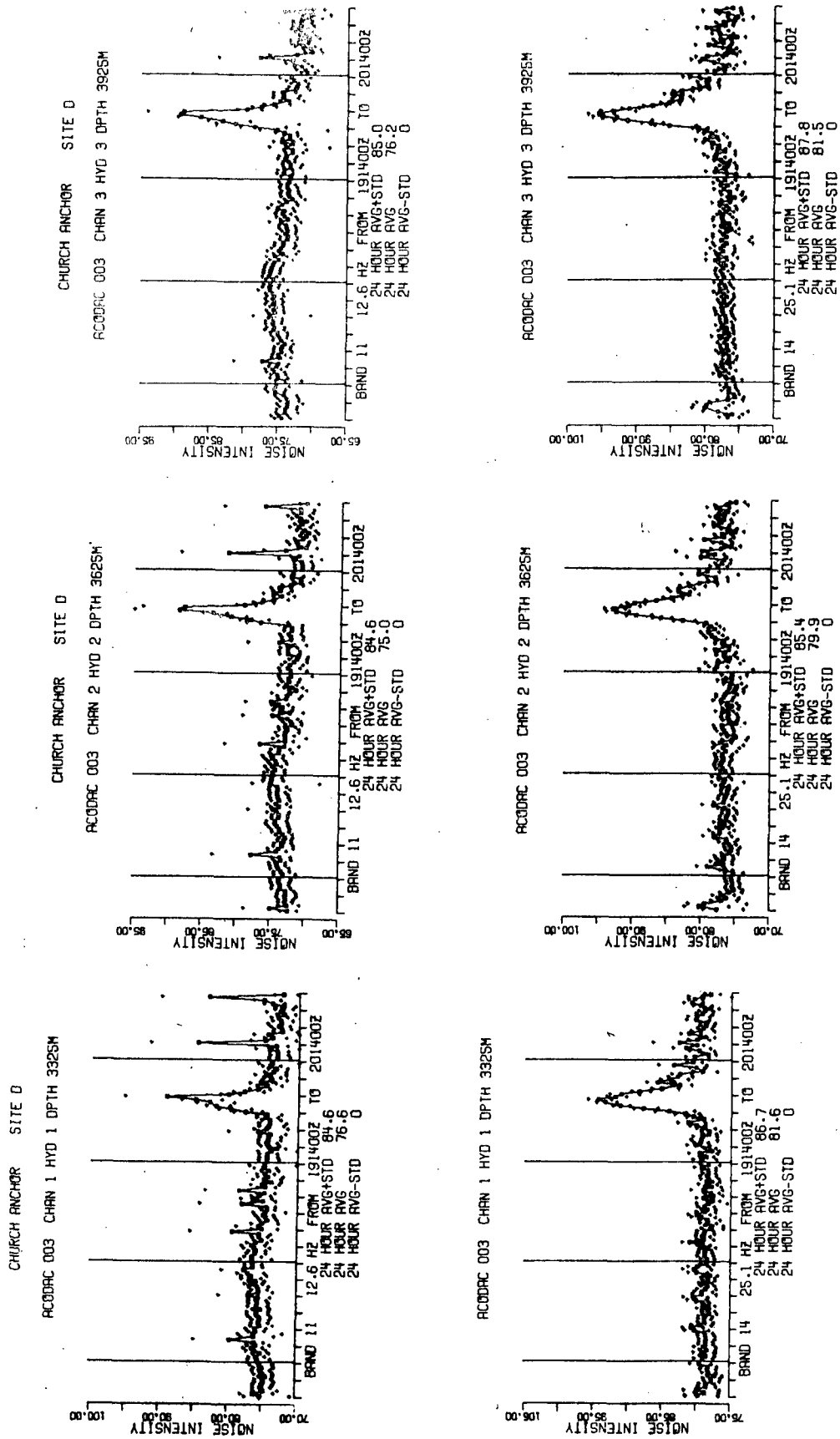

CONFIDENTIAL

197796

Figure B-15. (C) Twenty-Four-Hour Noise Intensity Time Series at Site D, September 1973 (U)

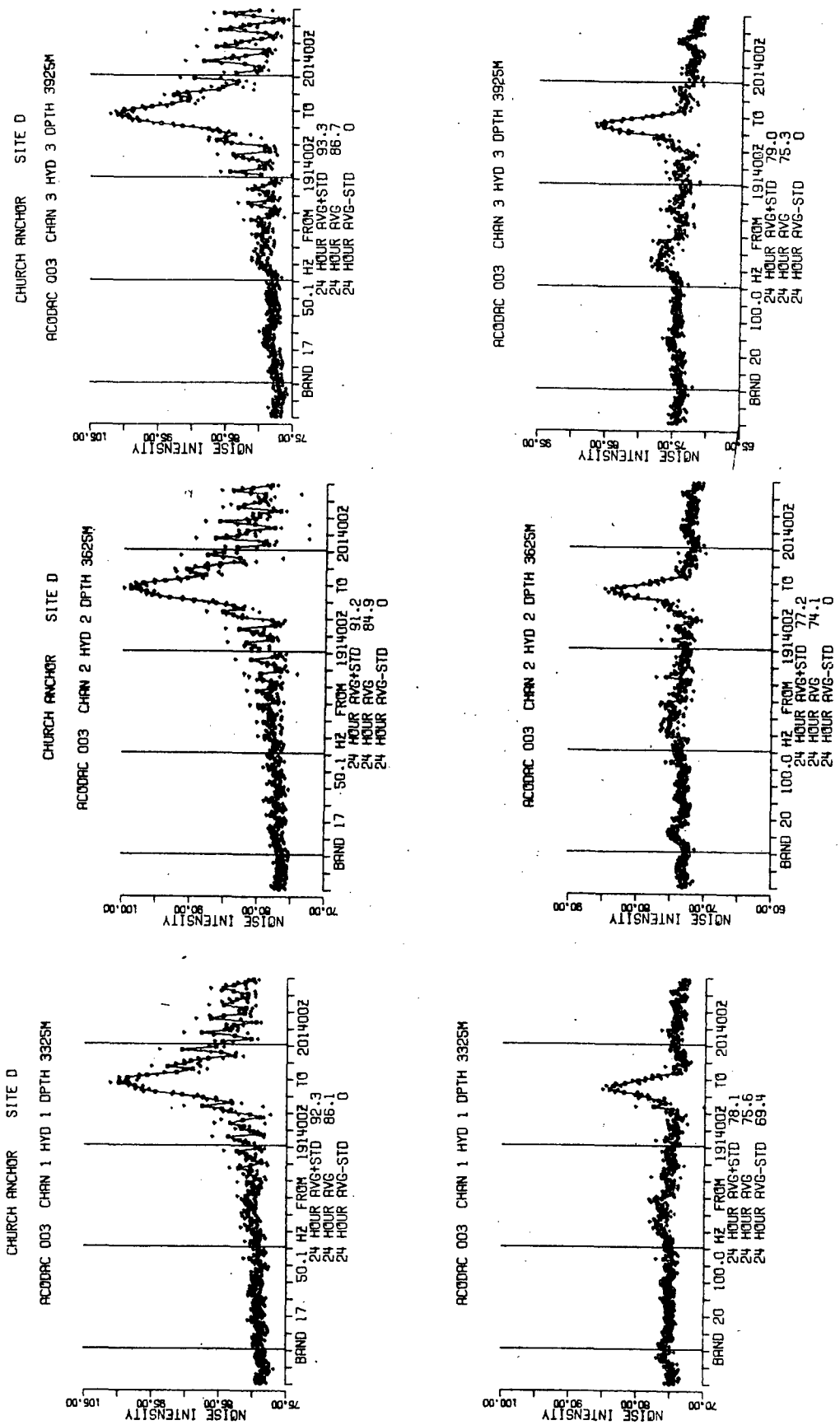

Figure B-16. (C) Twenty-Four-Hour Noise Intensity Time Series at Site D, September 1973 (U)

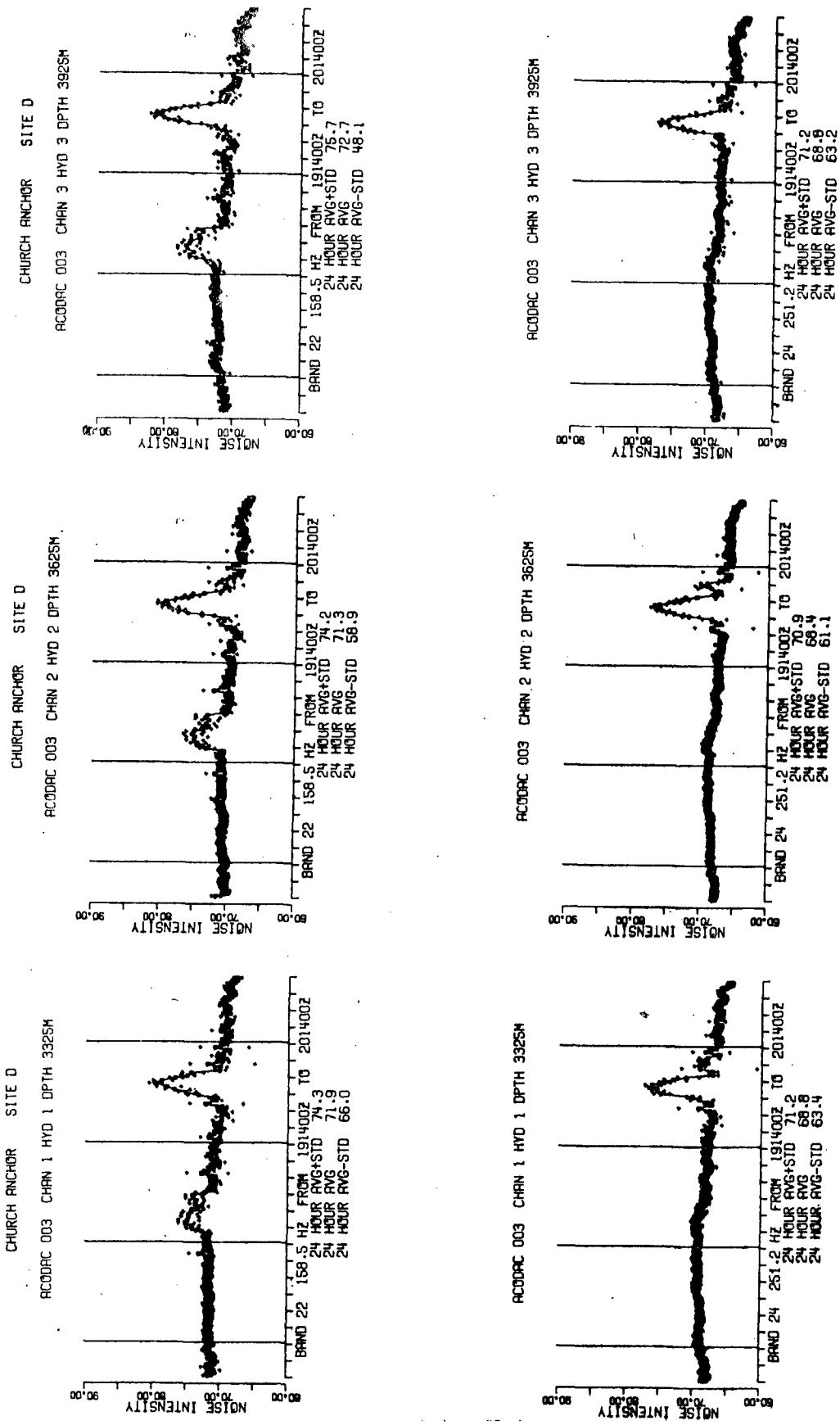

Figure B-17. (C) Twenty-Four-Hour Noise Intensity Time Series at Site D, September 1973 (U)

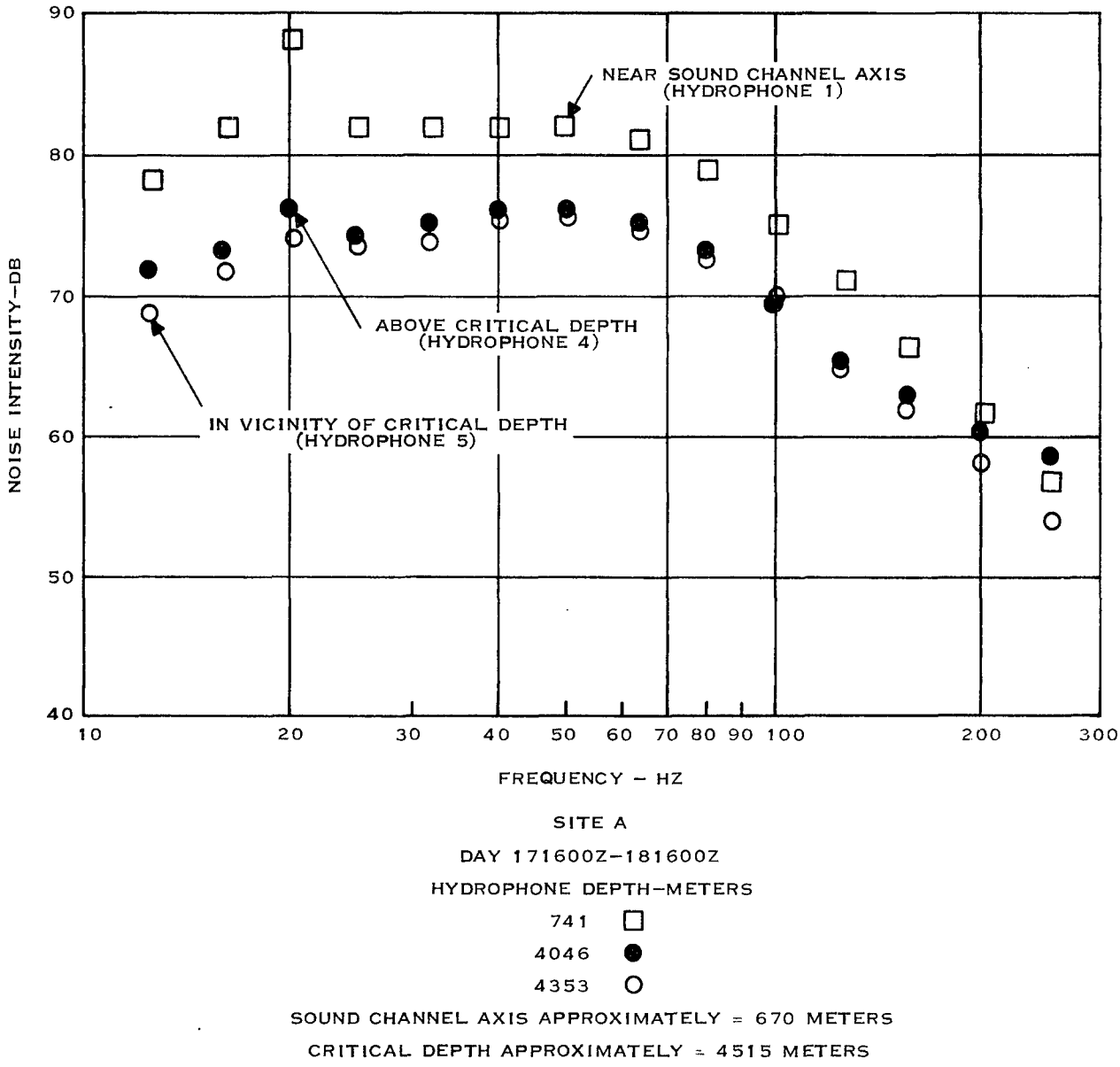

197799

CONFIDENTIAL

Figure B-18. (C) Variation of Noise Intensity With Frequency (U)

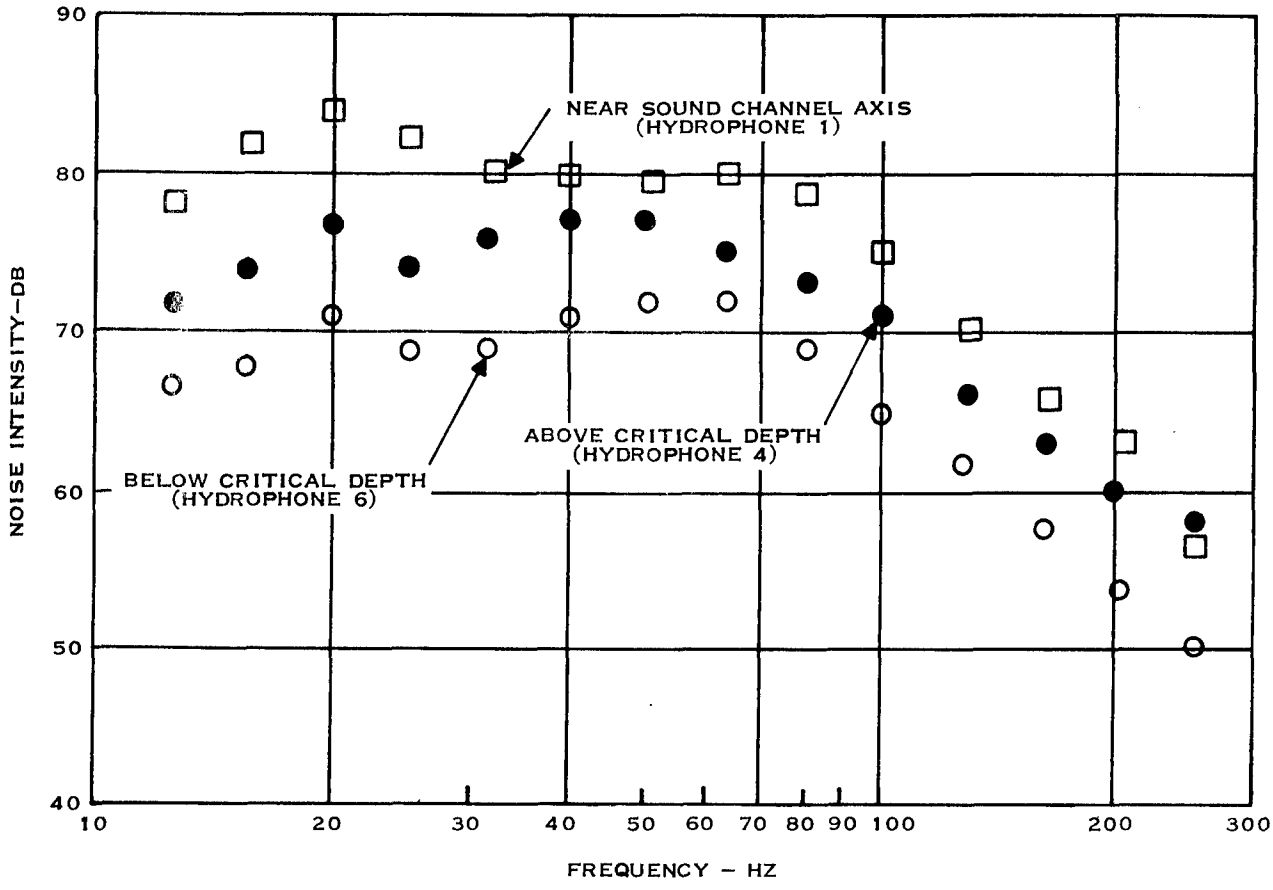

197800

CONFIDENTIAL

Figure B-19. (C) Variation of Noise Intensity With Frequency (U)

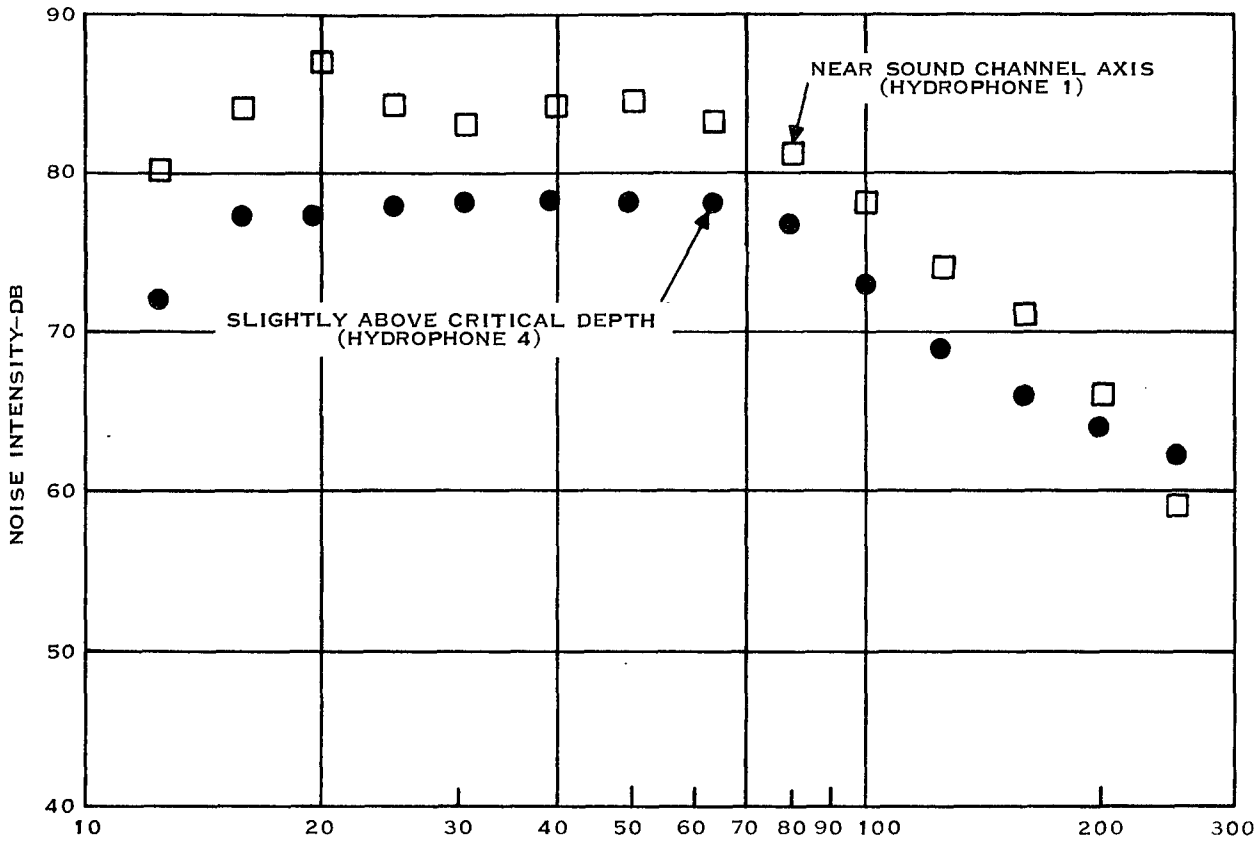

197801

CONFIDENTIAL

Figure B-20. (C) Variation of Noise Intensity With Frequency (U)

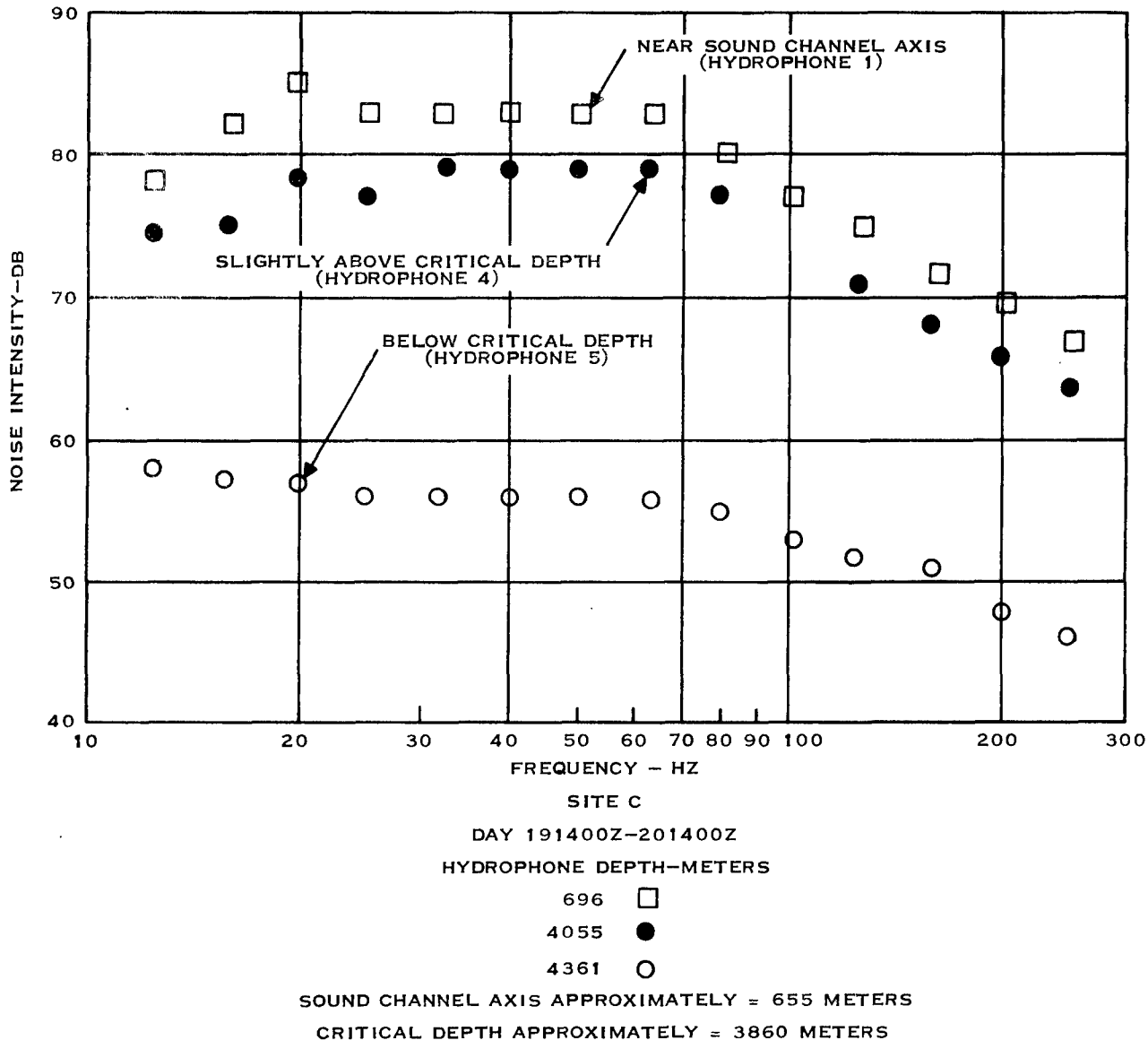

197802

CONFIDENTIAL

Figure B-21. (C) Variation of Noise Intensity With Frequency (U)

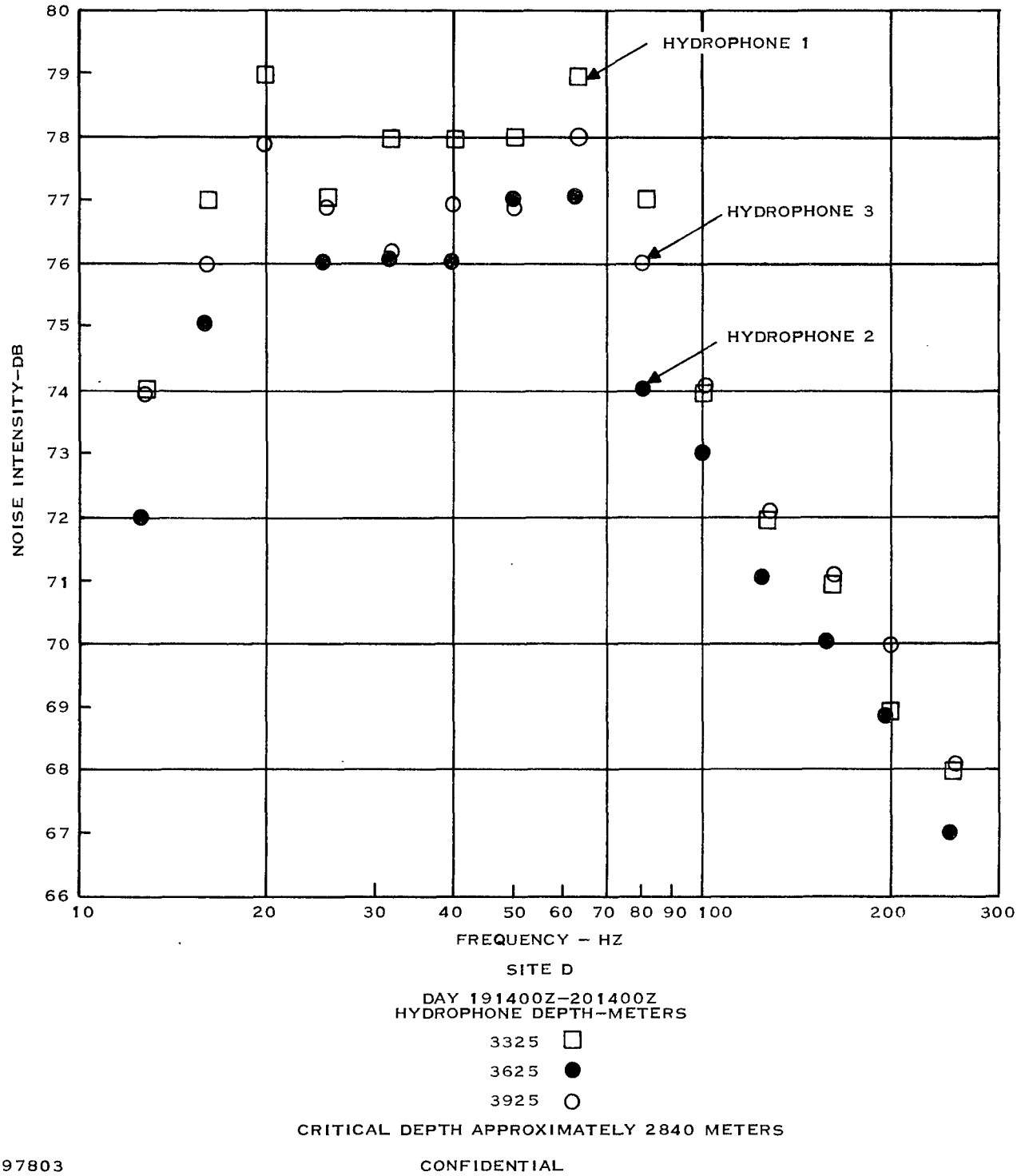

Figure B-22. (C) Variation of Noise Intensity With Frequency (U)

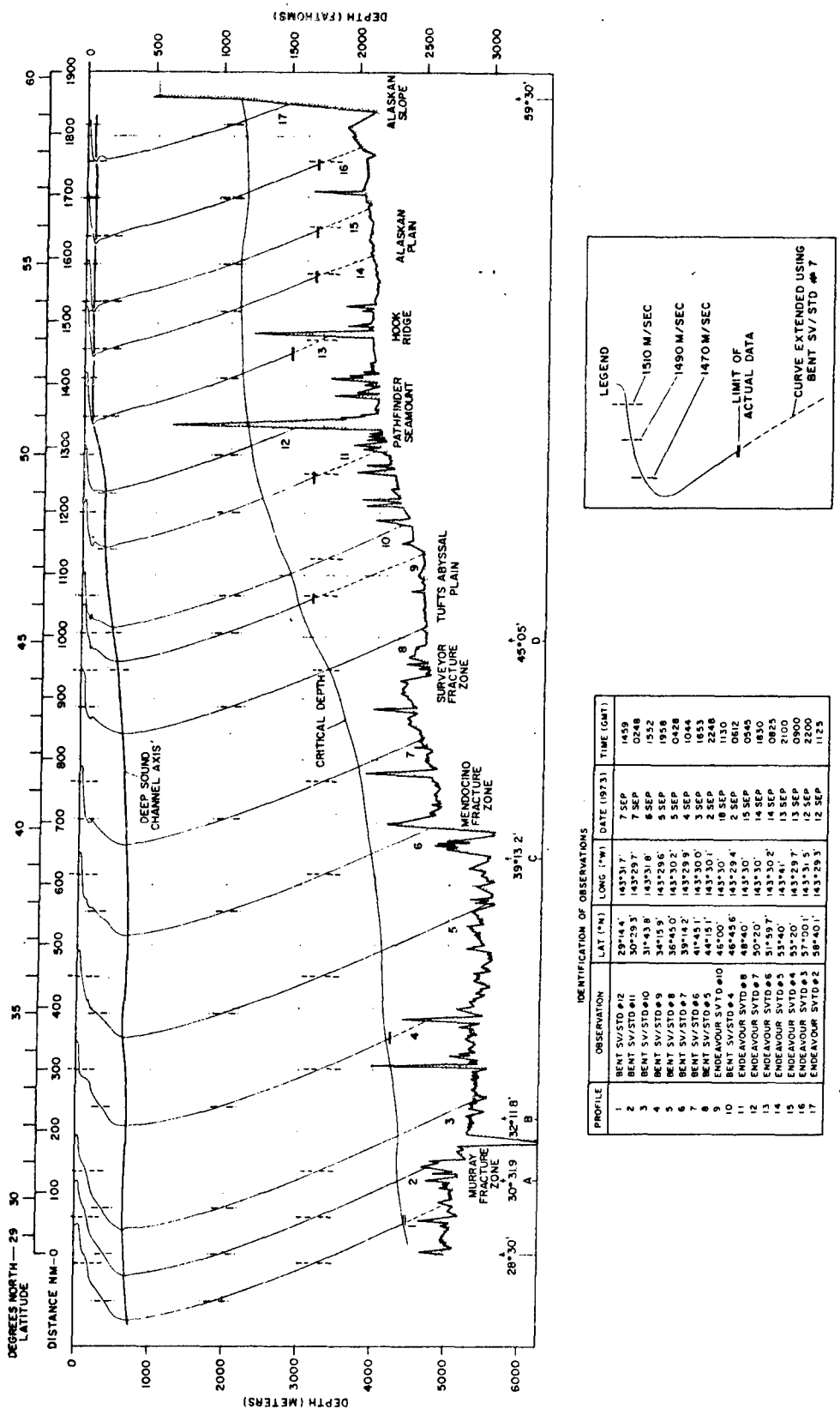

IDENTIFICATION OF OBSERVATIONS

PROFILE	OBSERVATION	LAT (°N)	LONG (°W)	DATE (1973)	TIME (GMT)
1	BENT SV/STD #12	29°14.4'	143°31.7'	7 SEP	1459
2	BENT SV/STD #11	30°29.3'	143°29.7'	7 SEP	0248
3	BENT SV/STD #10	31°43.8'	143°31.8'	8 SEP	1552
4	BENT SV/STD #9	34°15.9'	143°29.6'	5 SEP	1958
5	BENT SV/STD #8	36°45.0'	143°30.2'	5 SEP	0428
6	BENT SV/STD #7	39°14.2'	143°29.9'	4 SEP	1044
7	BENT SV/STD #6	41°45.1'	143°30.0'	3 SEP	1653
8	BENT SV/STD #5	44°15.1'	143°30.1'	2 SEP	2248
9	ENDEAVOUR SVTD #10	46°00'	143°30'	18 SEP	1130
10	BENT SV/STD #4	46°45.6'	143°29.4'	2 SEP	0612
11	ENDEAVOUR SVTD #8	48°40'	143°30'	15 SEP	0545
12	ENDEAVOUR SVTD #7	50°20'	143°30'	14 SEP	1830
13	ENDEAVOUR SVTD #6	51°59.7'	143°30.2'	14 SEP	0825
14	ENDEAVOUR SVTD #5	53°40'	143°41'	13 SEP	2100
15	ENDEAVOUR SVTD #4	55°20'	143°29.7'	13 SEP	0900
16	ENDEAVOUR SVTD #3	57°00.1'	143°31.5'	12 SEP	2200
17	ENDEAVOUR SVTD #2	58°40.1'	143°29.3'	12 SEP	1125

CONFIDENTIAL

197804

Figure B-23. (C) Sound Velocity Structure and Bathymetric Cross Section Along CHURCH ANCHOR Exercise Baseline (143°30'W) (U)

TABLE B-2. (C) APPROXIMATE NOISE INTENSITIES FOR TWO DAYS AND TWO SITES (A AND C) (U)

Frequency (Hz)	Day (171600Z to 181600Z)		Day (191400Z to 201400Z)	
	Site A	Site C	Site A	Site C
25.1	82	85	82	83
50.1	82	85	80	83
100.0	75	78	75	77
125.1	71	74	70	75
191.5	61	66	63	70

CONFIDENTIAL

IV. (C) VARIATION OF THE AMBIENT NOISE INTENSITY ALONG THE SOUND CHANNEL AXIS (U)

(C) Again referring to Figures B-18 through B-21, information on the noise intensity near the sound channel axis for different days and different sites is available. For example, Table B-2 indicates the intensities for selected frequencies. These data indicate that the noise level near the sound channel axis at site C is generally a few decibels greater than at site A.

V. (C) VARIATIONS OF THE AMBIENT NOISE INTENSITY WITH FREQUENCY (U)

(C) It is easy to see that the noise levels plotted in Figures B-18 through B-22 can be divided into two regions:

Region A: 10 Hz to 70 Hz. Here the ambient noise is relatively constant as the frequency varies.

Region B: 70 Hz to 250 Hz. In this region, the noise intensity decreases rapidly with increasing frequency. In Figure B-18, the decrease is about 12 to 15 dB per octave and Figure B-19 it is about 10 dB per octave. Similar decreases are seen in Figures B-20 and B-21. One other point of interest is that, below critical depth, the decrease in noise intensity with increasing frequency is not nearly so noticeable. This phenomenon is most clearly evident in Figure B-22, which shows a decrease of about 4 dB per octave.

VI. (C) GENERAL OBSERVATIONS (U)

(C) One of the more significant features of the ambient noise data is the nonstationarity as reflected in the rapid change in noise intensity that can occur over a period of only a few hours. As the depth increases, the relative nonstationarity likewise increases, perhaps because of a general decrease in the stationary component of the noise process. Nearby shipping traffic is likely the source of these nonstationarities. Some of these fluctuations in the intensity patterns have convergence zone characteristics, as can be seen in Figure B-16, for example.

(C) There is a general decrease in the noise level with depth with the most rapid decrease (considering the total change in depth) occurring as the transition across the critical depth is made. In this case, the noise decrease is about 5 dB.

(C) There is some variation along the sound channel axis (Table B-2) although the variation is much less than that observed with changes in depth.

(C) The data presented here indicate that there are no major changes in noise intensity level from day (171600Z to 181600Z) to day (191400Z to 201400Z). This conclusion is reached by comparing the intensities of these two days for the same hydrophones and sites (Figures B-18 through B-21). This applies, of course, only to the noise background, disregarding fluctuations from nearby shipping.

APPENDIX C

(C) OMNIDIRECTIONAL NOISE MEASUREMENTS FROM CFAV *ENDEAVOUR* (U)

I. (C) SYSTEM (U)

A. (C) MESA (U)

(C) During the CHURCH ANCHOR exercise, a single hydrophone of the MESA system was used for omnidirectional noise measurements at two anchor stations, 57°N and 46°N, on the prime exercise track, 143°30'W. The MESA system, shown in Figure C-1, was decoupled from the wave motion and cable strumming by a two-stage suspension system. The entire system was decoupled mechanically from the ship during a measurement period by paying out cables. During a measurement period (quiet period), all the ship's machinery was turned off, and batteries supplied power to the laboratory equipment.

B. (C) Processing System (U)

(C) The processing and analysis steps applied to the data are shown in Figure C-2. The ambient noise signals from the array hydrophones were amplified and stored on analog magnetic tape. The signals were then passed through an analog-to-digital converter (sample rate 2.5 kHz) and processed using an HP 2100A computer with a hard-wired fast Fourier transform box (5470A) into discrete 256-point spectra averaged over 1 minute. These spectra were recorded on digital magnetic tape and then applied to an XDS Sigma 7 computer where they were calibrated, further averaged, and processed into 1/3-octave bands.

II. (C) ERROR ANALYSIS (U)

A. (C) System Accuracy (U)

(C) The absolute system error was 0.7 dB. The hydrophones had an absolute calibration error of ±0.5 dB over the frequency band of interest and were the largest single contributors to the system error. The rest of the system made up the other ±0.2 dB of the absolute system error.

(C) Hydrophone self-noise levels fell off sharply with increasing frequency and were down at least 18 dB from the ambient noise levels at 20 Hz.

B. (C) System Performance (U)

(C) The system performed well both electrically and acoustically; however, physical problems encountered in handling the MESA system necessitated a change in the original measurement schedule. Table C-1 shows the schedule of quiet periods achieved, as well as the ship's position and the wind speed during each period.

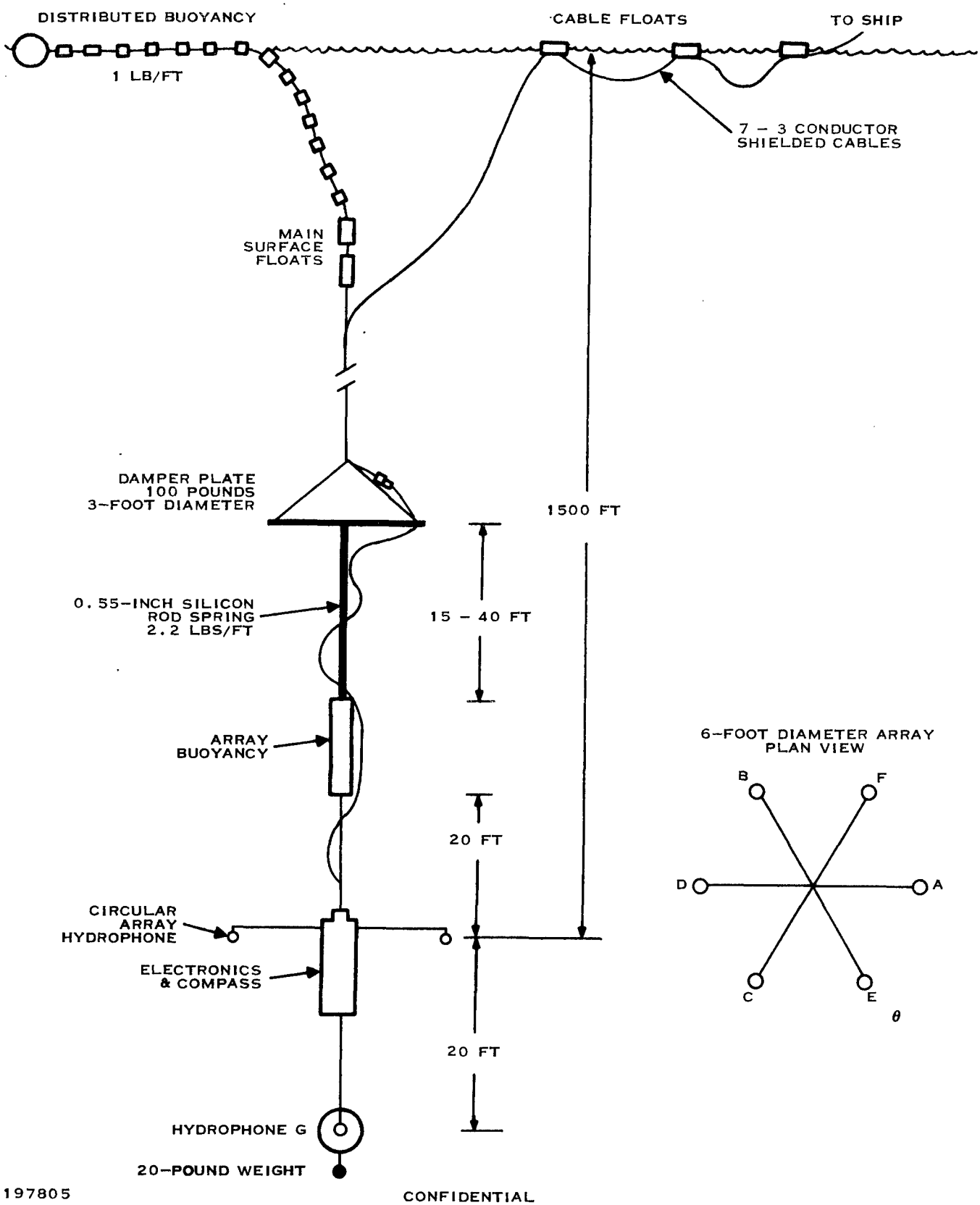

Figure C-1. (C) MESA System Configuration (U)

TABLE C-1. (C) SCHEDULE OF QUIET PERIODS (U)

Quiet Period Number	Ship Position	Time	Hydrophone Depth (meters)	Wind Speed (knots)
1	57°10.0'N 143°29.0'W	0400Z 10 Sept. 73	100	14
2	57°13.5'N 143°14.0'W	2315Z 10 Sept. 73	100	9
3	57°13.5'N 143°14.0'W	0210Z 11 Sept. 73	100	6
4	57°12.5'N 143°14.0'W	0445Z 11 Sept. 73	100	10
5	57°12.8'N 143°13.0'W	0800Z 11 Sept. 73	100	13
6	57°12.0'N 143°13.0'W	1145Z 11 Sept. 73	100	13
7	57°11.6'N 143°14.9'W	1950Z 11 Sept. 73	100	11
8	45°57.6'N 143°43.4'W	0810Z 19 Sept. 73	460	14
9	45°48.8'N 143°27.0'W	0230Z 20 Sept. 73	460	27
10	45°59.0'N 143°25.0'W	0515Z 21 Sept. 73	400	4
11	45°59.3'N 143°26.0'W	0915Z 21 Sept. 73	400	11
12	45°59.0'N 143°28.0'W	1540Z 21 Sept. 73	400	15
14	45°57.8'N 143°29.1'W	0410Z 22 Sept. 73	400	11
16	46°2.3'N 143°27.1'W	2310Z 22 Sept. 73	400	25

NOTE: (1) The time for each quiet period is rounded off to the first even fifth minute in each period.

(2) For quiet periods 3, 6, 8, 9, 10, 11, and 12, thirty minutes of noise data was available.

CONFIDENTIAL

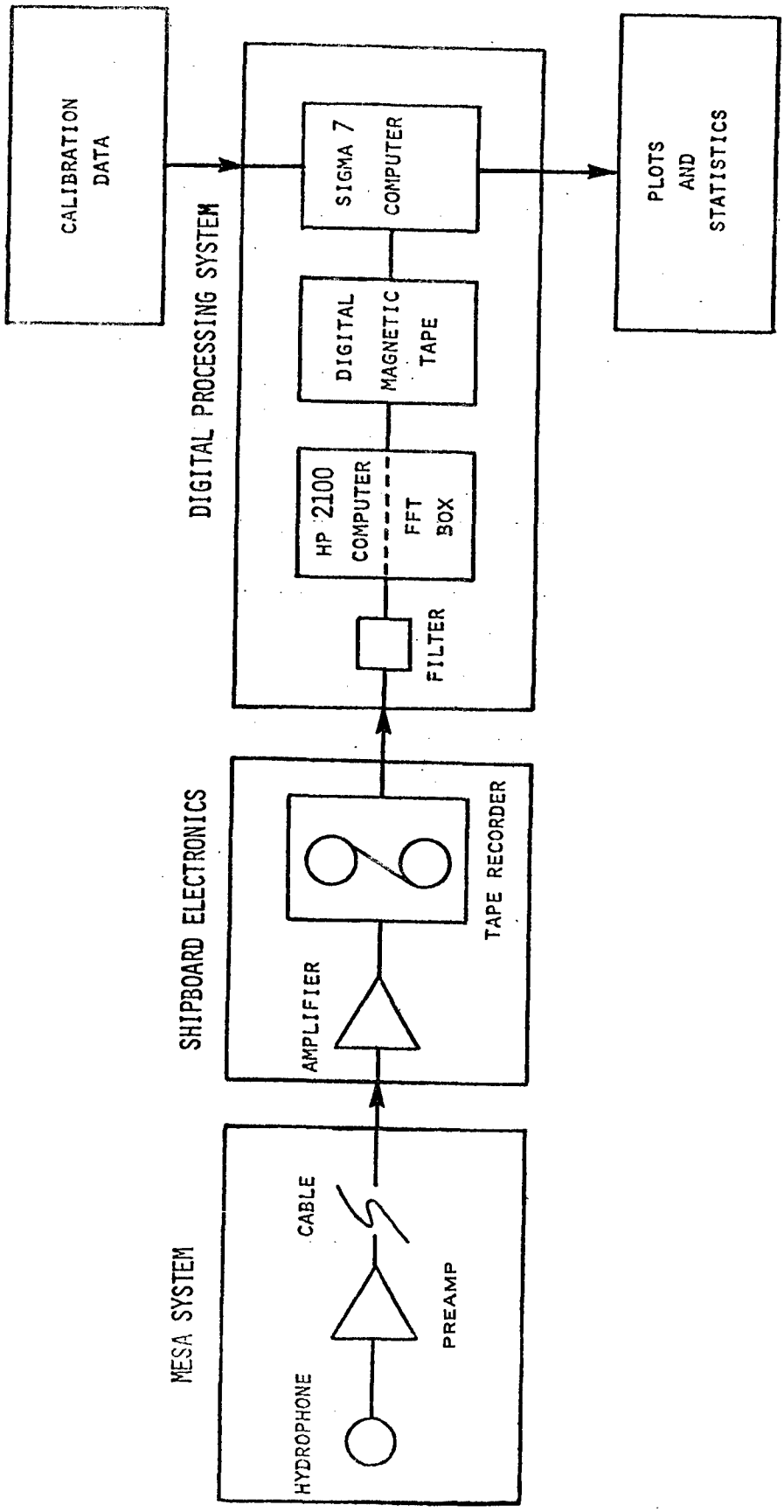

Figure C-2. (C) Block Diagram of the Data Collection and Analysis System (U)

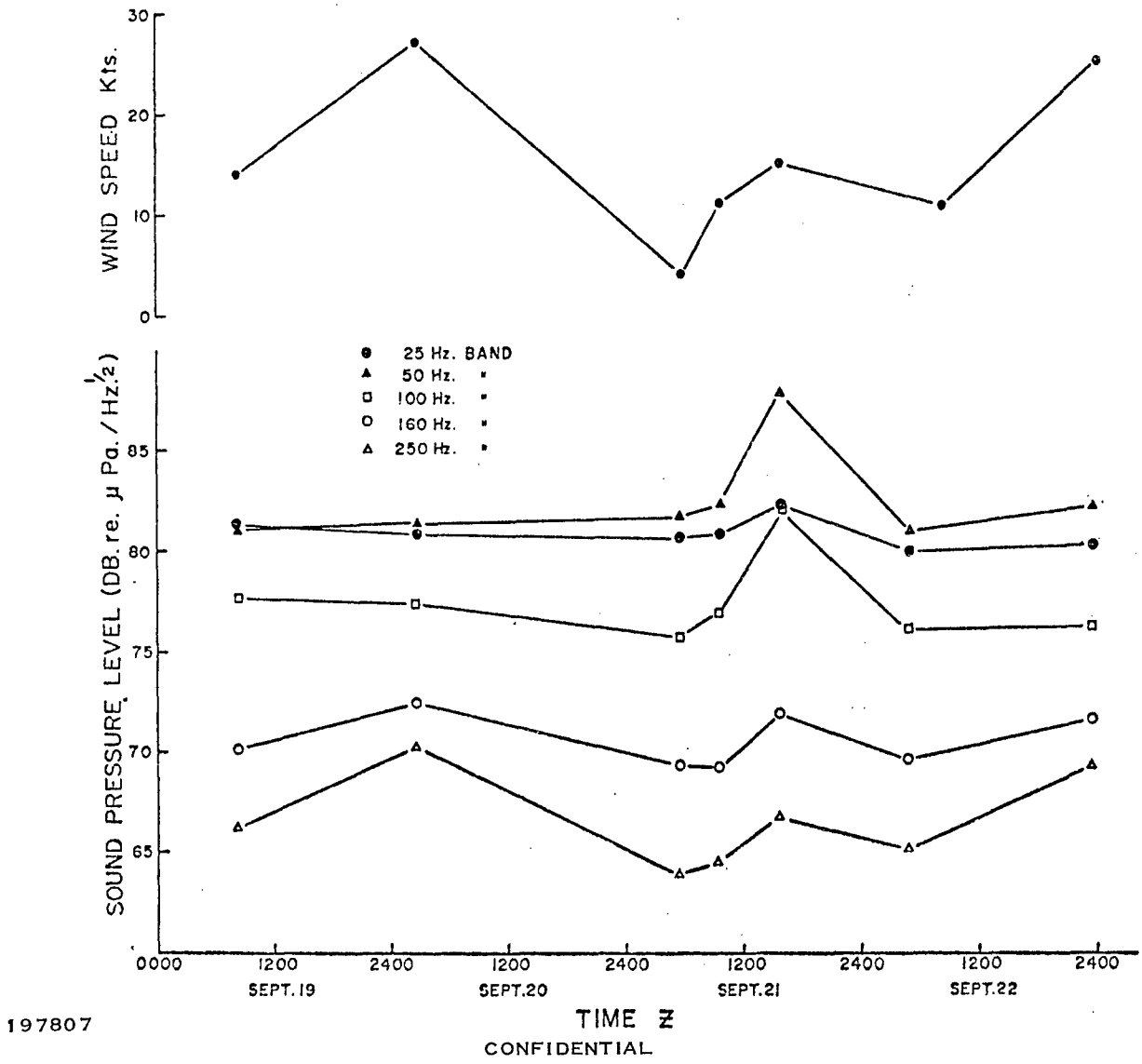

Figure C-3. (C) Ambient Sound Pressure Levels Averaged Over 15 Minutes In Five 1/3-Octave Bands Versus Time (Southern Station, 46°N, 143°30'W) (U)

III. (C) PRESENTATION OF REDUCED DATA (U)

A. (C) Ambient Sound Pressure Levels in 1/3-Octave Bands Versus Time (U)

(C) Plots of ambient sound pressure levels in the five 1/3-octave bands (25, 50, 100, 160, and 250 Hz) versus time for the southern (46°N) and northern (57°N) stations are shown in Figures C-3 and C-4, respectively.

(C) At the southern station, the levels measured in the 160- and 250-Hz bands had a direct dependence on wind speed. The increase in level that occurred at 1545Z September 21 was because of a nearby broadband source; however, no ship was evident in the area.

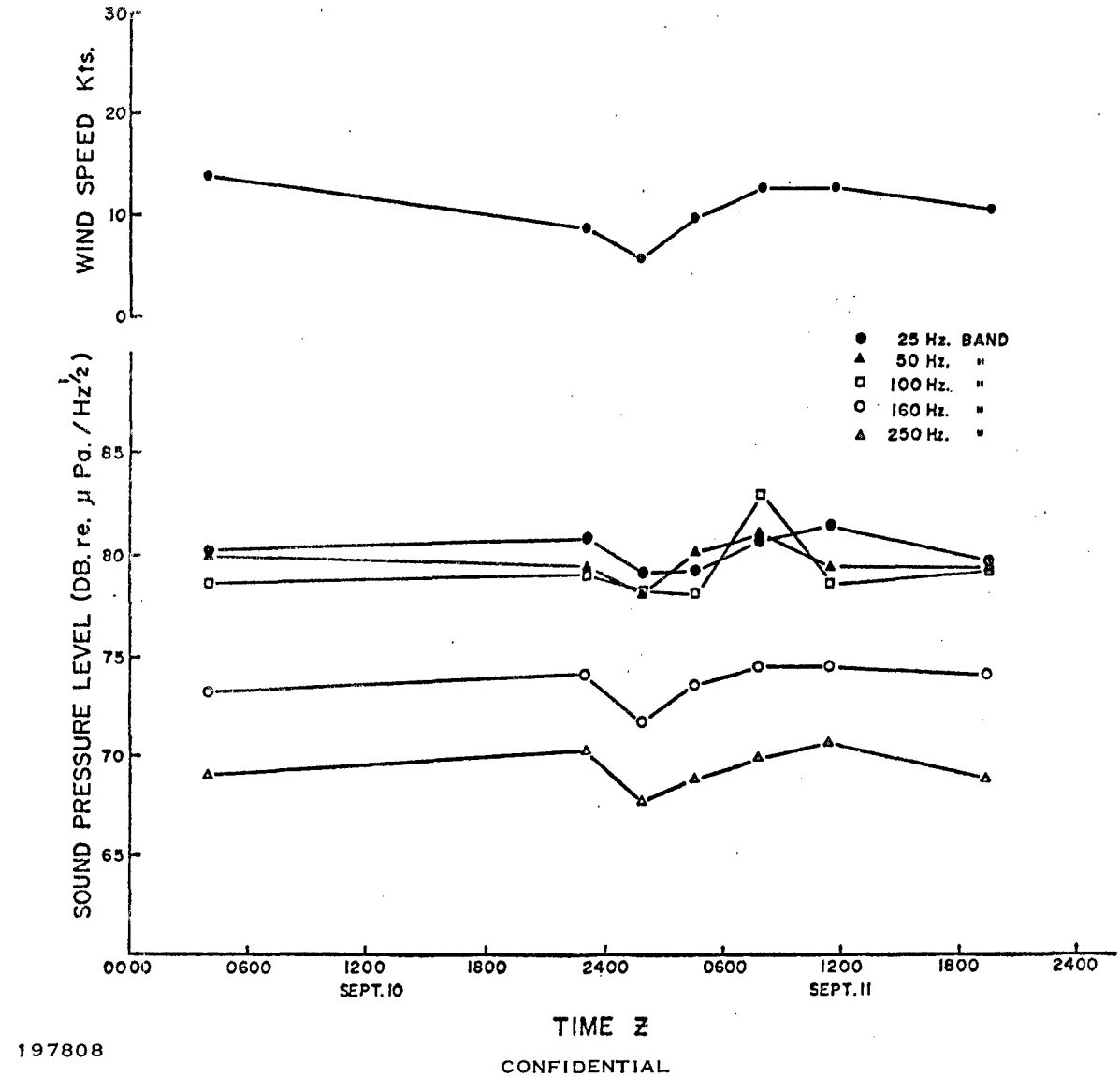

Figure C-4. (C) Ambient Sound Pressure Levels Averaged Over 15 Minutes In Five 1/3-Octave Bands Versus Time (Northern Station, 57°N, 143°30'W) (U)

(C) At the northern station, correlation between wind speed and noise levels was very weak, even in the 160- and 250-Hz bands. The increase in noise level in the 100-Hz band that occurred at 0800Z September 11 was caused by a passing ship.

B. (C) Narrowband Spectra (U)

(C) Plots of the spectra measured at the southern station and the northern station are shown in Figures C-5 and C-6, respectively.

(C) The increase in levels observed during quiet periods 12 and 5 was caused, respectively, by the presence of the broadband source and the presence of the passing ship mentioned earlier.

QUIET PERIOD No.	8	0810 Z	19 SEPT. 1973
	9	0230 Z	20 "
	10	0515 Z	21 "
	11	0915 Z	21 "
	12	1540 Z	21 "
	14	0410 Z	22 "
	16	2310 Z	22 "

ANALYSIS BANDWIDTH=4.883 HZ
AVERAGING TIME=15 MIN

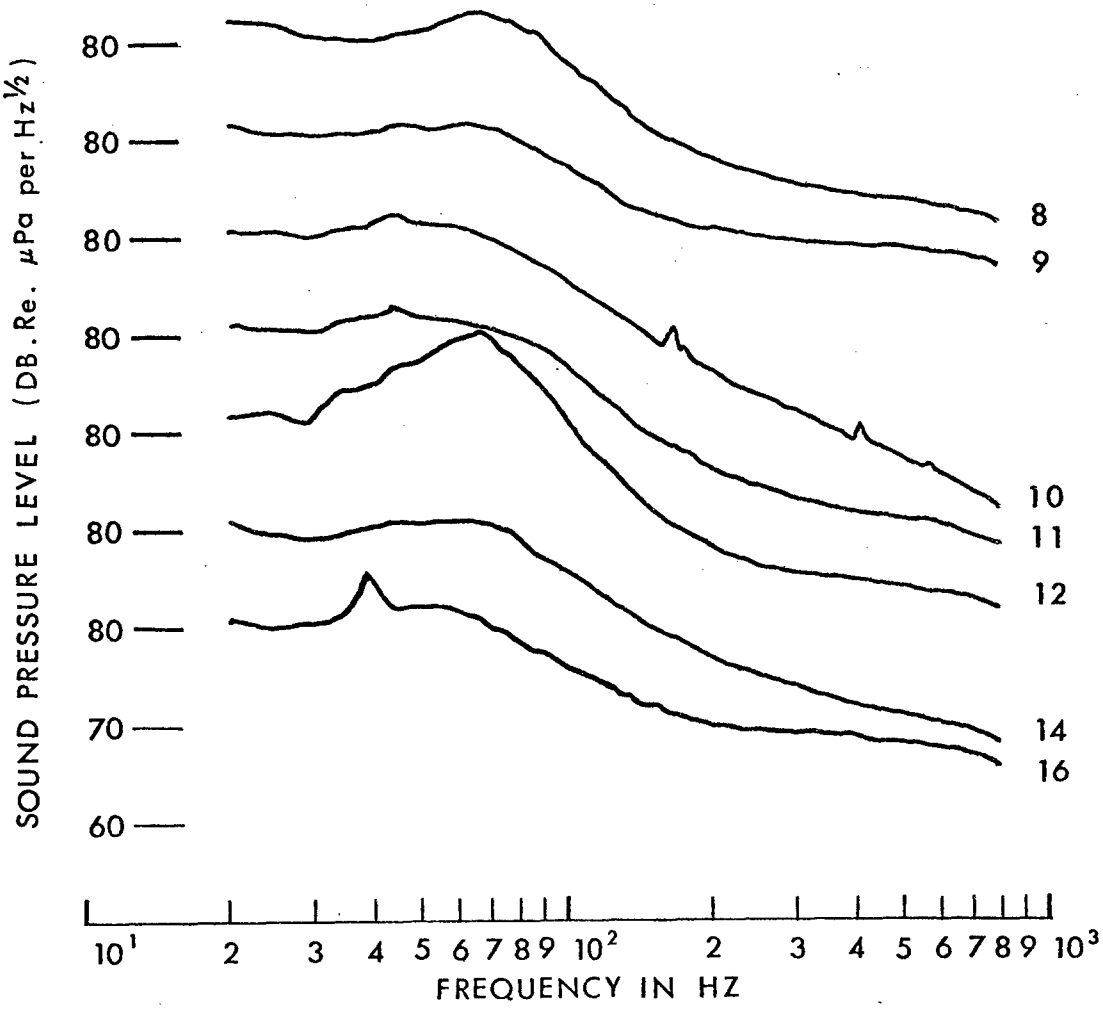

197809

CONFIDENTIAL

Figure C-5. (C) Representation of Ambient Noise Spectra for Quiet Periods 1–16 Excluding 13 and 15 (Southern Station) (U)

QUIET PERIOD No. 1	0400 Z	10 SEPT. 1973	
2	2315 Z	10	"
3	0210 Z	11	"
4	0445 Z	11	"
5	0800 Z	11	"
6	1145 Z	11	"
7	1950 Z	11	"

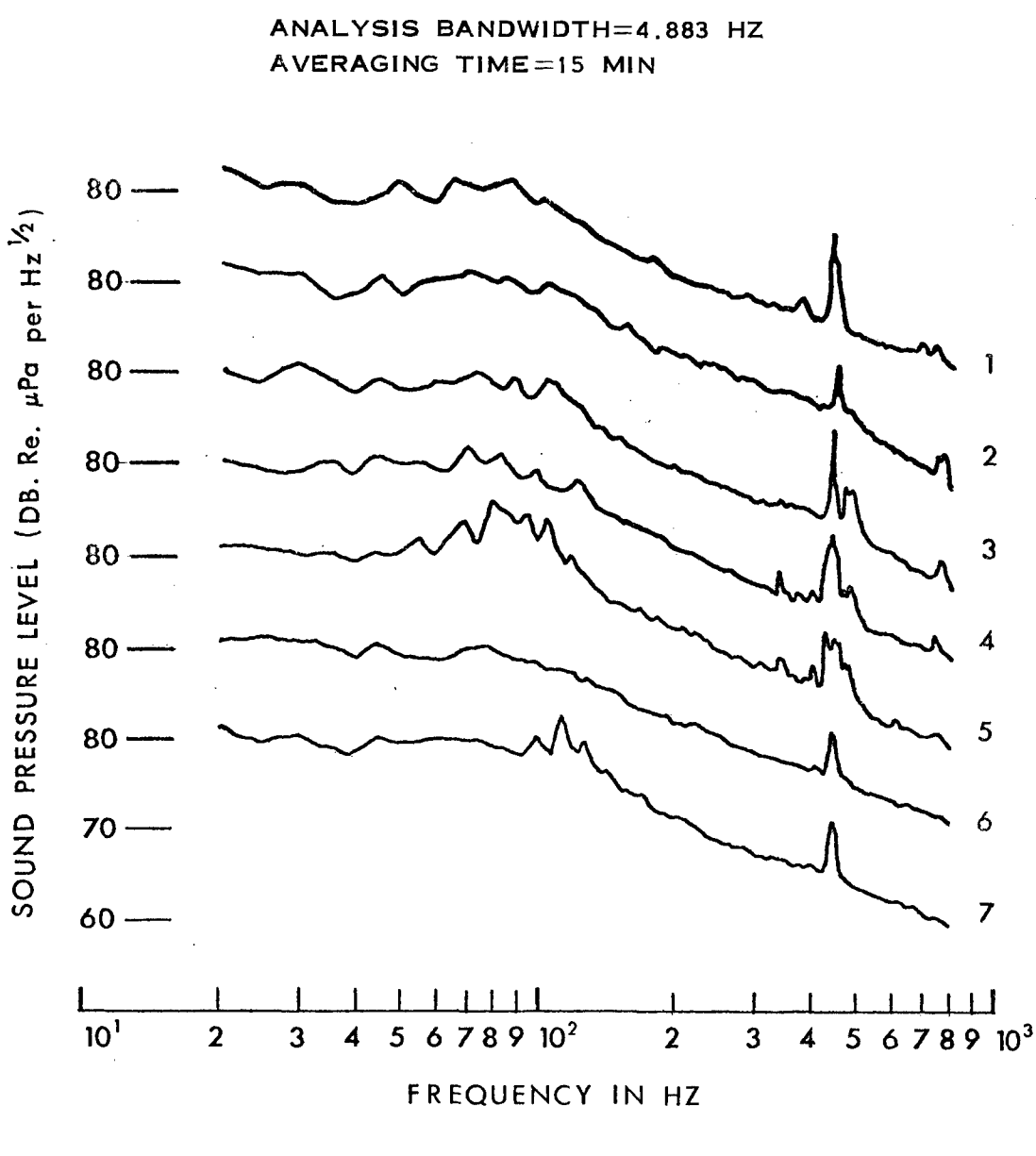

Figure C-6. (C) Representation of Ambient Noise Spectra for Quiet Periods 1–7 (Northern Station) (U)

(C) The line at 38 Hz that occurred during quiet period 16 was caused by the acoustic source towed by the M/V *Mediterranean Seal*. A very strong line at 440 Hz was present throughout the entire measurement period at the northern station.

IV. (C) ANALYSIS OF RESULTS (U)

A. (C) Variation of Noise Levels With Local Wind Speed (U)

(C) Plots of the ambient noise levels for the five 1/3-octave bands (25, 50, 100, 160, and 250 Hz) versus wind speed are shown in Figures C-7 and C-8.

(C) Noise levels measured in the lower frequency bands (25, 50, and 100 Hz) for both stations were attributed to noise generated by shipping, as there did not appear to be any dependence of the noise levels on wind speed.

(C) The noise levels measured in the higher frequency bands (160 and 250 Hz) were attributed to a combination of shipping and sea surface agitation (wind speed) at the southern station and to only shipping at the northern station. The noise levels appeared to have a direct dependence on wind speed at the southern station but did not fall off as sharply as one would expect for low wind speeds if sea surface agitation were the only mechanism contributing to the noise. Therefore, the noise levels measured were considered to be the result of shipping when the wind speed was low and a result of a combination of shipping and sea surface agitation when the wind speed was high. At the northern station, there did not appear to be any dependence of the noise levels on wind speed. Also, the noise levels were 3 to 4 dB higher than those measured at the southern station for equal wind speeds. Therefore, the dominant source of noise at the northern station was considered to be shipping.

B. (C) Comparison of Spectra Measured at Southern and Northern Stations (U)

(C) A plot comparing the spectrum recorded at the northern station with the spectrum recorded at the southern station for low wind speed conditions is shown in Figures C-9. This plot indicates the extent to which shipping noise influenced the ambient noise spectra at the two stations.

(C) The noise spectra attributed to shipping were of a different character at the two stations. The noise levels in the frequency range 30 to 70 Hz were 2 to 3 dB higher at the southern station than those at the northern station. However, above 90 Hz, the noise levels at the northern station were 3 to 4 dB higher than those at the southern station.

V. (C) SUMMARY (U)

(C) During the CHURCH ANCHOR exercise, the MESA system was used for omnidirectional noise measurements at two stations, 57°N and 46°N, on the exercise baseline 143°30'W.

(C) Noise levels measured in the 25-, 50-, and 100-Hz 1/3-octave bands were attributed to shipping. In the 160- and 250-Hz 1/3-octave bands, the noise levels were attributed to a combination of shipping and sea surface agitation (wind speed) at the southern station and to only shipping at the northern station.

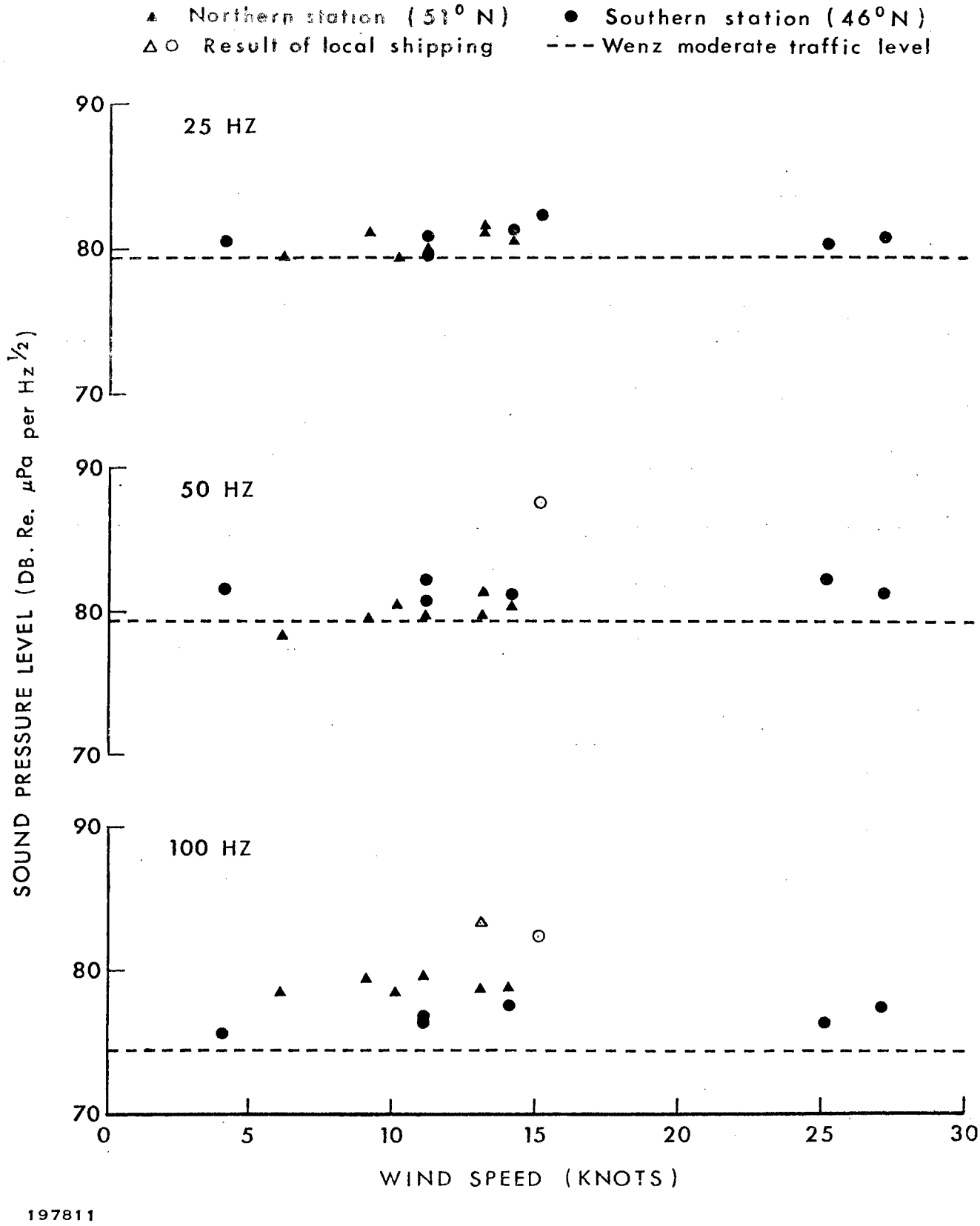

CONFIDENTIAL

Figure C-7. (C) Plots of Ambient Sound Pressure Levels Measured in the 1/3-Octave Bands Shown Versus Wind Speed (U)

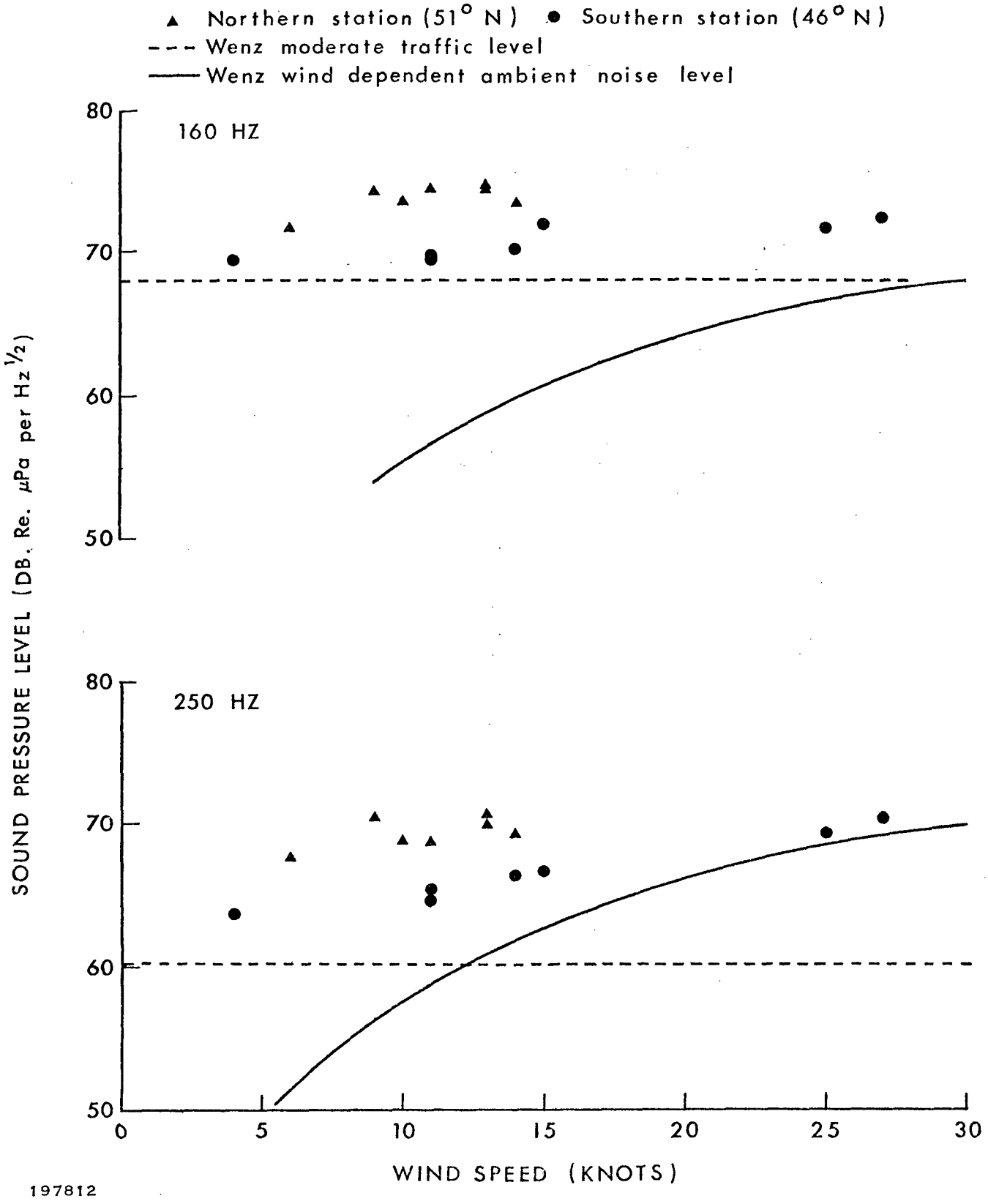

Figure C-8. (C) Plots of Ambient Sound Pressure Levels Measured in the 1/3-Octave Bands Shown Versus Wind Speed (U)

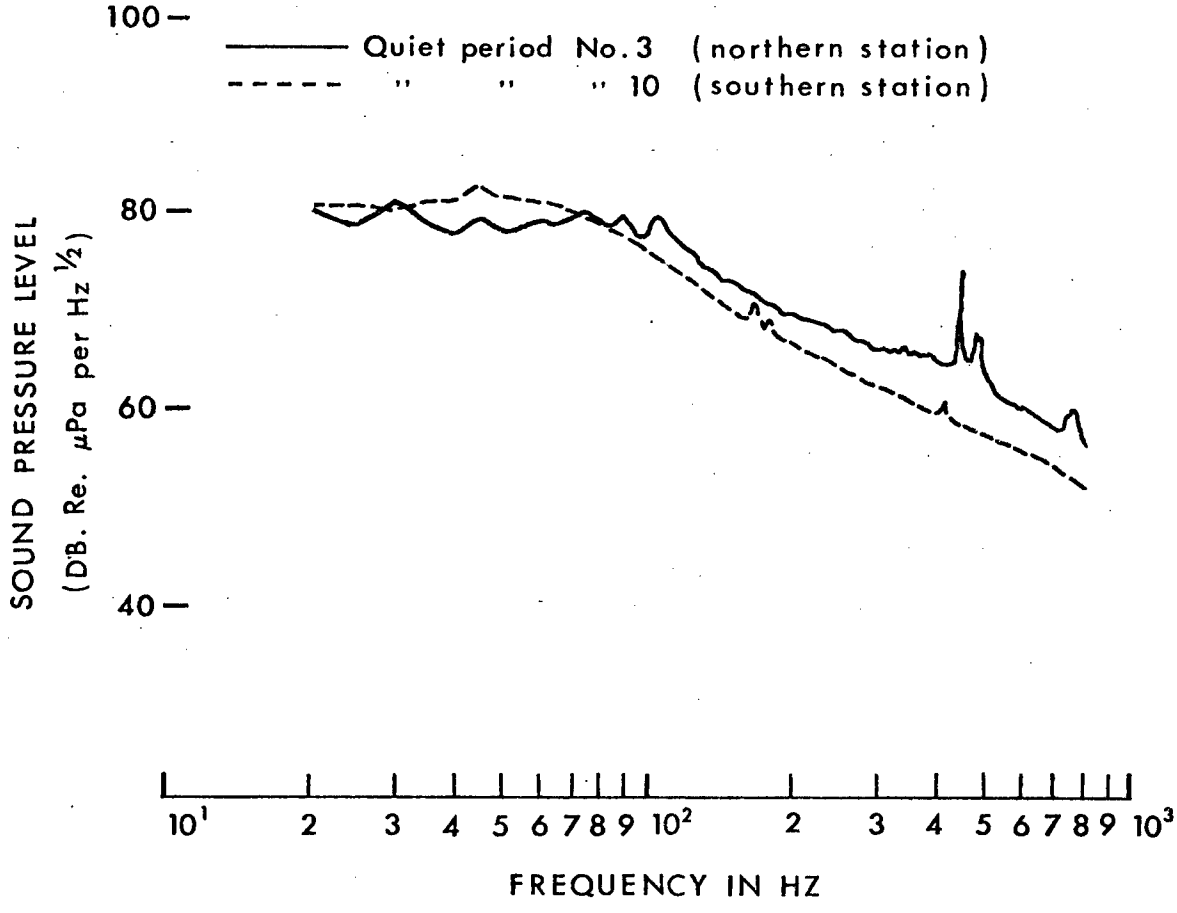

197813

CONFIDENTIAL

Figure C-9. (C) Plot Comparing the Spectrum Recorded at the Northern Station (57°N) With the Spectrum Recorded at the Southern Station (46°N) for Low Wind Speed Conditions (U)

(C) The noise spectra attributed to shipping were of different character at the two stations. The levels were higher in the frequency range (30- to 70 Hz) at the southern station and higher in the frequency range (above 90 Hz) at the northern station.

APPENDIX D

(C) AMBIENT NOISE MEASUREMENTS FROM R/P *FLIP* DURING THE CHURCH ANCHOR EXERCISE (U)

(U) This appendix represents an analysis by the Marine Physical Laboratory in the northeastern Pacific Ocean of ambient noise measurements made aboard the R/P *Flip*. These data were collected in September 1973 during the CHURCH ANCHOR exercise.[1] Some of the data obtained were presented and discussed previously in a synopsis[2] based on these data and on data gathered by other participants who were involved in the CHURCH ANCHOR exercise.

(U) The hydrophone system used in obtaining these data was deployed from the R/P *Flip* in two different configurations. During the first phase of the exercise, 20 hydrophones were deployed as a uniformly spaced, 20-element vertical array with a total aperture of 532 meters. Depth-dependence studies were made by sequentially positioning the array at six depths of chief interest distributed from near the sea floor to the sound channel axis as shown in Figure D-1. During the second phase, the hydrophones were deployed in five widely-spaced depth groups, as shown in Figure D-2, to allow simultaneous or near simultaneous sampling of the ambient noise throughout the water column.

I. (U) DATA PROCESSING SYSTEM

(U) Figure D-3 is a generalized block diagram of the acoustic data acquisition system, as used aboard R/P *Flip*. Each hydrophone module consists of a cage or support frame, the hydrophone, and the electronics package. The cage supports the hydrophone by an eight-point compliant suspension system to decouple cable motions from the lead zirconate pressure sensor. The individual hydrophone outputs are FM-multiplexed and telemetered to the onboard electronics where the signals are separated, demodulated, and made available to the processing units. The omnidirectional ambient noise data were low-pass-filtered, amplified, and processed by the PDP 11/20 computer system.

(U) Ambient noise information from four hydrophones was digitized simultaneously and fast Fourier transform (FFT) methods were used for performing on-line spectral analyses. Each of the four hydrophone outputs was sampled at a rate of 2.273 kHz over about 0.9 second to obtain 2,048 points for the FFT processor. The output was spectra with a 1.1-Hz constant-bandwidth resolution. Accumulations of 128 such individual spectra were averaged for each of the four sensors to obtain the final estimated noise spectrum levels, which were stored in digital format on DEC tape. The processing duty rate was about 67 percent; that is, it required about 3 minutes to sample, process, accumulate, and store the 2 minutes of data.

(U) Postexercise processing consisted of first reading the on-line processed digital data tape, entering individual hydrophone or channel calibration constants, and finally averaging the calibrated on-line spectral information from the appropriate 1.1-Hz bands to form one-third octave levels centered at 25, 50, 100, 150, and 250 Hz. These one-third octave levels, in decibels, were plotted versus time, or listed for subsequent plotting.

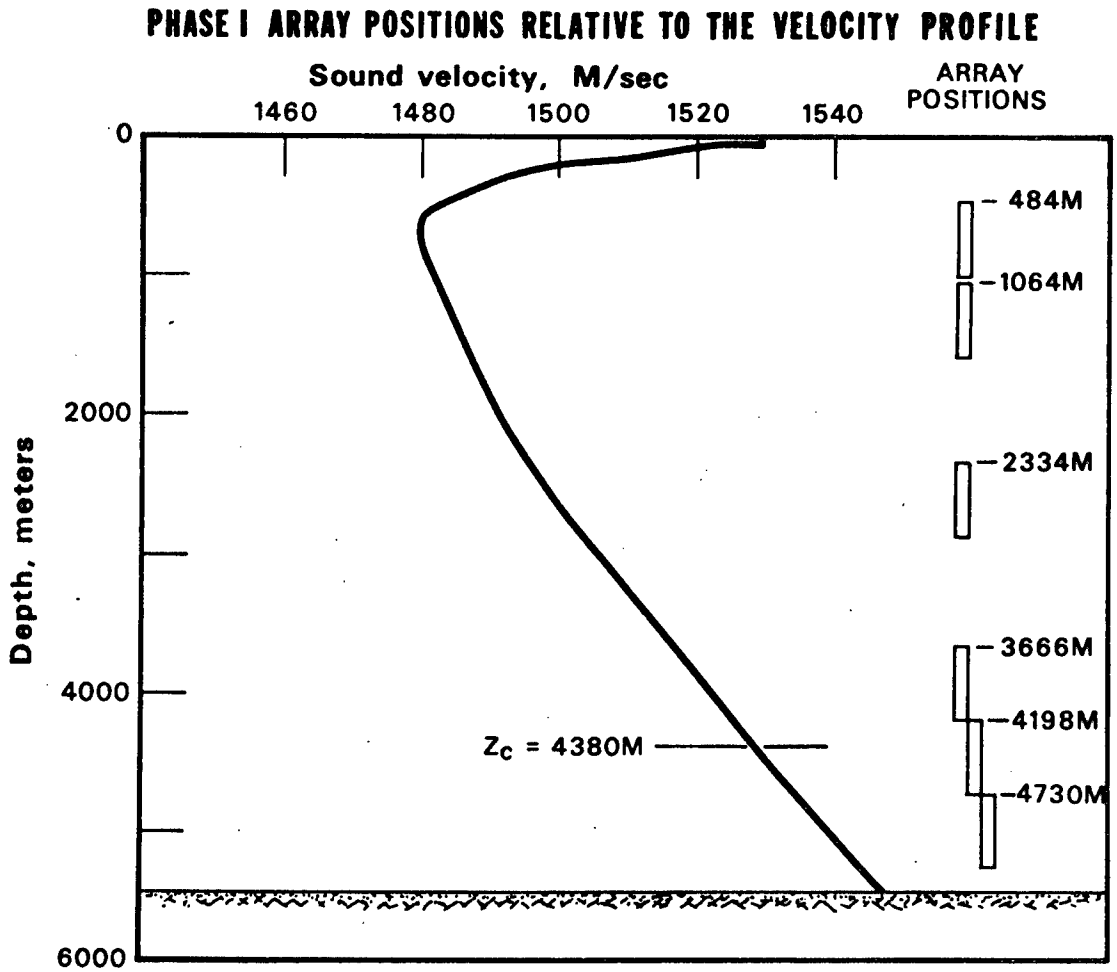

Figure D-1. (U) Phase I Array Positions Relative to the Velocity Profile

II. (U) ERROR ANALYSIS

(U) The accuracy of the ambient noise values derived from data taken aboard R/P *Flip* have been treated elsewhere.[3] Nonetheless, they are treated here, in summary, for completeness.

(U) The errors associated with the noise measurements have been divided into two categories: random errors to account for those that may change during the data-taking time interval and fixed bias errors to account for those that remain fixed in time for the system. In general, the random errors are believed to be small, amounting to a range of ±0.3 dB to ±0.5 dB, and perhaps even less, as the noise data are subject to both ensemble averaging over the 128 accumulations and frequency averaging to form the one-third octave values. The fixed-bias errors are attributed largely to the precision of the hydrophone sensitivity calibrations (±0.5 dB) and to differences

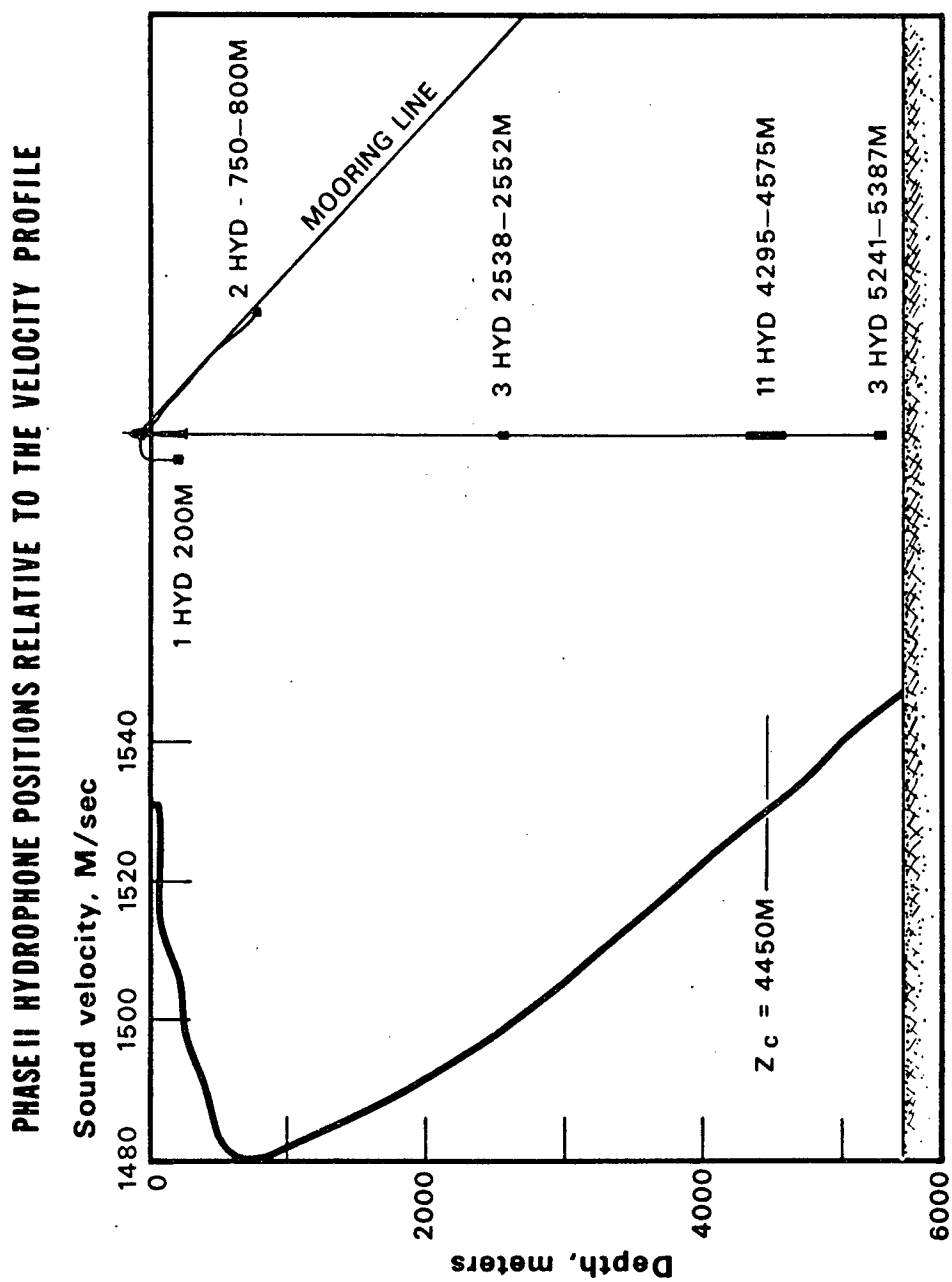

UNCLASSIFIED

197815

Figure D-2. (U) Phase II Hydrophone Positions Relative to the Velocity Profile

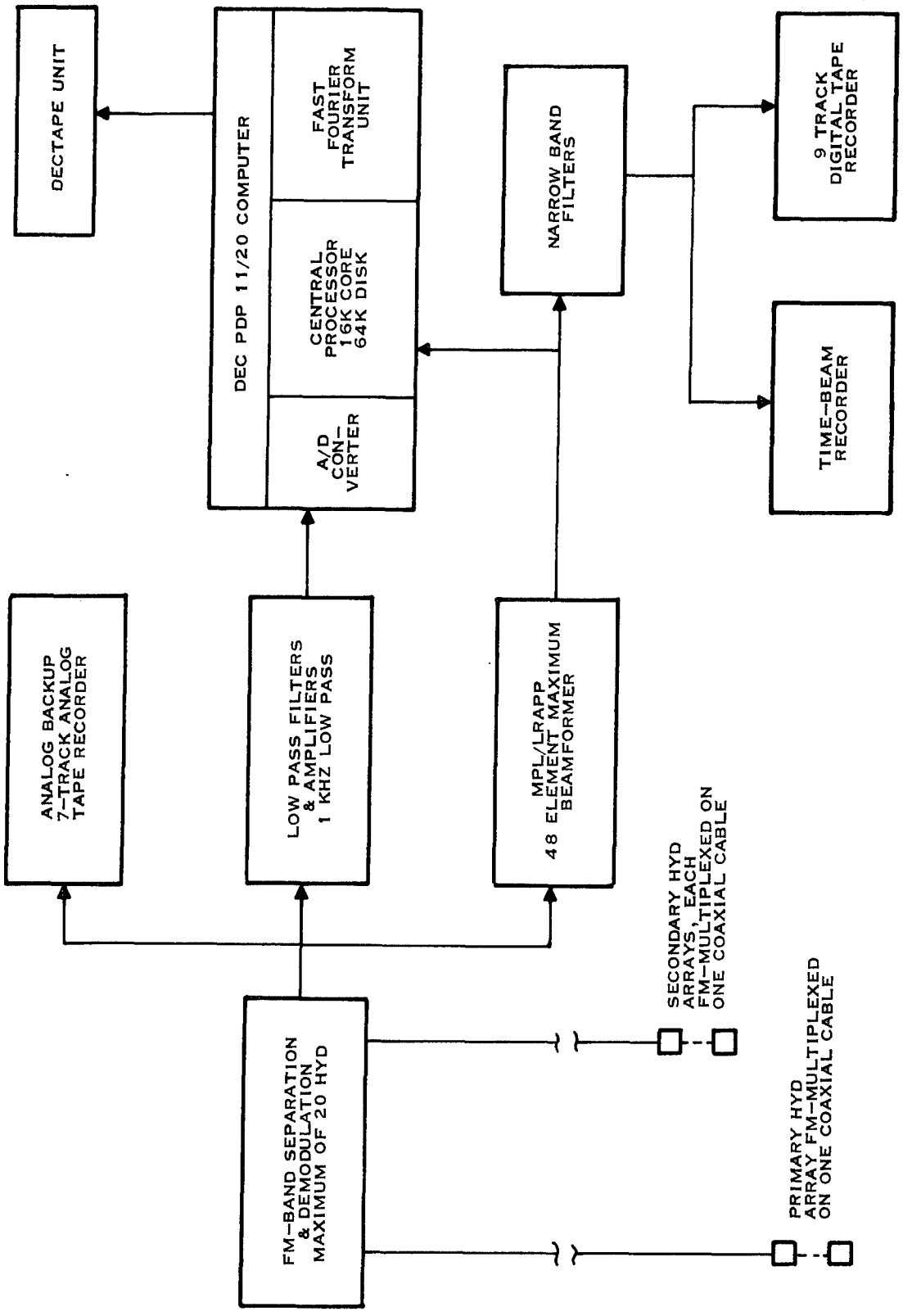

Figure D-3. (U) Block Diagram of Acoustic Data Acquisition System

between the pre-exercise and postexercise telemetry gain calibrations that varied over a maximum range of ±0.8 dB, with the majority occuring in the range of ±0.4 dB. Using the maximum errors associated with the telemetry, the total bias error for the acoustic noise data is estimated to be ±1.0 dB.

(U) Actual ambient noise data taken during the exercise at a depth intermediate between the axis and the bottom of the sound channel, a depth at which minimum depth dependence of noise is expected, have been examined for hydrophone-to-hydrophone differences. At 100 Hz, the 20 hydrophones yield a value of 0.8 dB for the standard deviation of the sound pressure level as determined from the levels measured at the individual sensors. While it is possible that part of the scatter in the values may indeed be true variations in the noise level over the 532-meter array, we can nevertheless interpret this ±0.8 dB as a maximum value for the relative differences between hydrophones. This value for scatter, as it is influenced by both the random and the bias error, is consistent with the analytical error analysis.

(U) Examination of the ambient noise spectra shows that there are discrete spectral lines associated with noise radiated from R/P *Flip* which have necessitated some adjustments or deletions of selected one-third octave analysis bands. The spectra for the hydrophone at 200 meters show a line near 23 Hz, thus contaminating the data for the one-third octave band centered at 25 Hz. These data have been deleted from the analysis. Spectra for all hydrophones, regardless of depth, exhibit a spectral line at about 174 Hz which is believed to be caused by an on-board salt-water pump and engine cooling system. One-third octave data at 150 Hz are therefore presented in lieu of data at 158.5 Hz which would have been contaminated by this particular 174-Hz line. For intersystem comparisons, it should be noted that the spectrum levels at 150 Hz will be slightly higher than the spectrum levels at 158.5 Hz as reported by others. For hydrophones within the sound channel, the spectral slope in this particular frequency region is typically −10-dB/octave, resulting in the 150-Hz levels being 0.8 dB higher than those at 158.5 Hz. For hydrophones below the sound channel, the slope is near −6-dB/octave, resulting in the 150-Hz levels being 0.5 dB too high.

III. (C) AMBIENT NOISE DATA (U)

(C) During the first phase of the array deployment three 24-hour periods were assigned for ambient noise. The depth-dependence studies were made by sequentially positioning the array at different depths and measuring ambient noise. Two depth cycles were taken during each 24-hour period with the exception of the first day, 2 September 1400Z to 3 September 1400Z, when only a partial cycle was completed. As all three days exhibit the same general effects, only data from the noise days 5 September 2000Z to 6 September 2000Z and 8 September 2200Z to 9 September 2200Z are presented and discussed.

(C) Figure D-4 shows the ship traffic as observed by radar from FLIP during the 5-6 September noise day. The array depth positions are numbered from one to six, with six being the deepest position. Note that there is a slight preference for ships to be nearby when the array was deep. The noise levels for selected one-third octave bands are given in Figure D-5. The radar observed ship traffic for 9 September is given by Figure D-6. For this day, although the traffic is less, there is a definite correlation between ship traffic and array depth; ships were nearby when the array was deep. The noise samples which were scheduled to start in 2200Z on 8 September were delayed about 3 hours to allow the noise from a passing freighter to subside. Figure D-7 gives the noise levels for the five one-third octave bands.

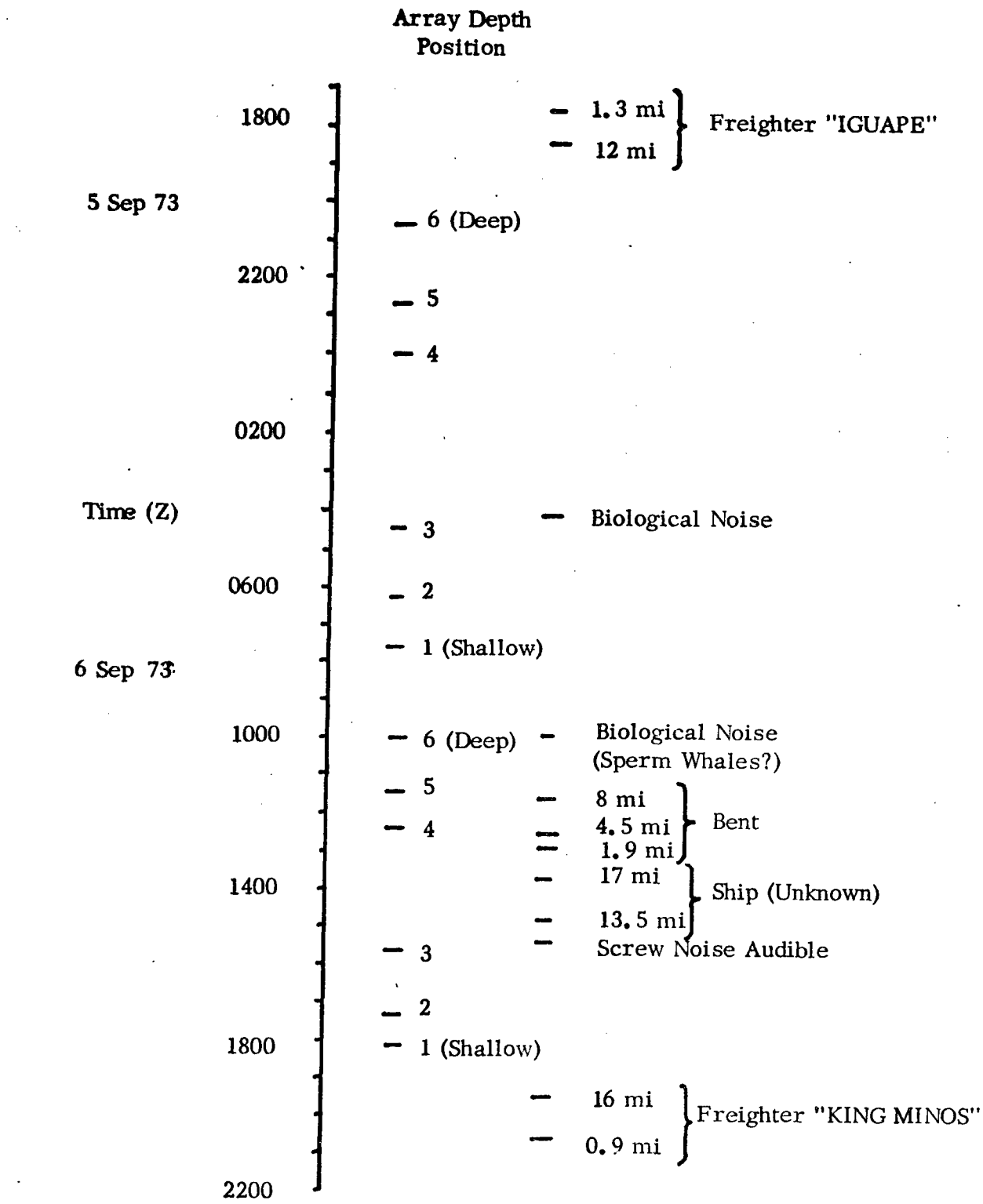

CONFIDENTIAL

Figure D-4. (C) Local Ship Traffic Near *Flip* During 5–6 September 1973 Noise Period (U)

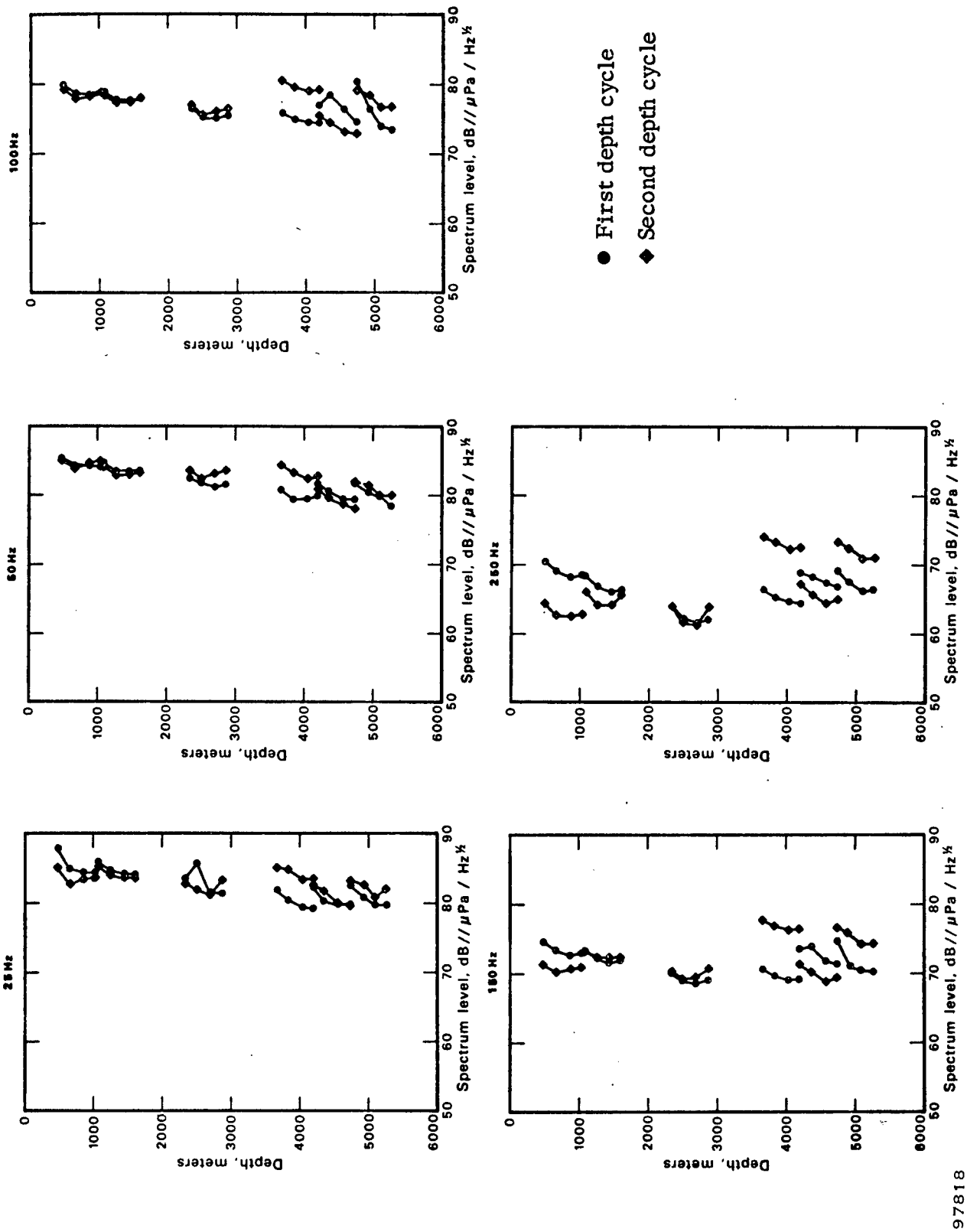

Figure D-5. (C) Ambient Noise Levels for Five One-Third Octave Bands During 5–6 September 1973 at Six Different Array Depths (U)

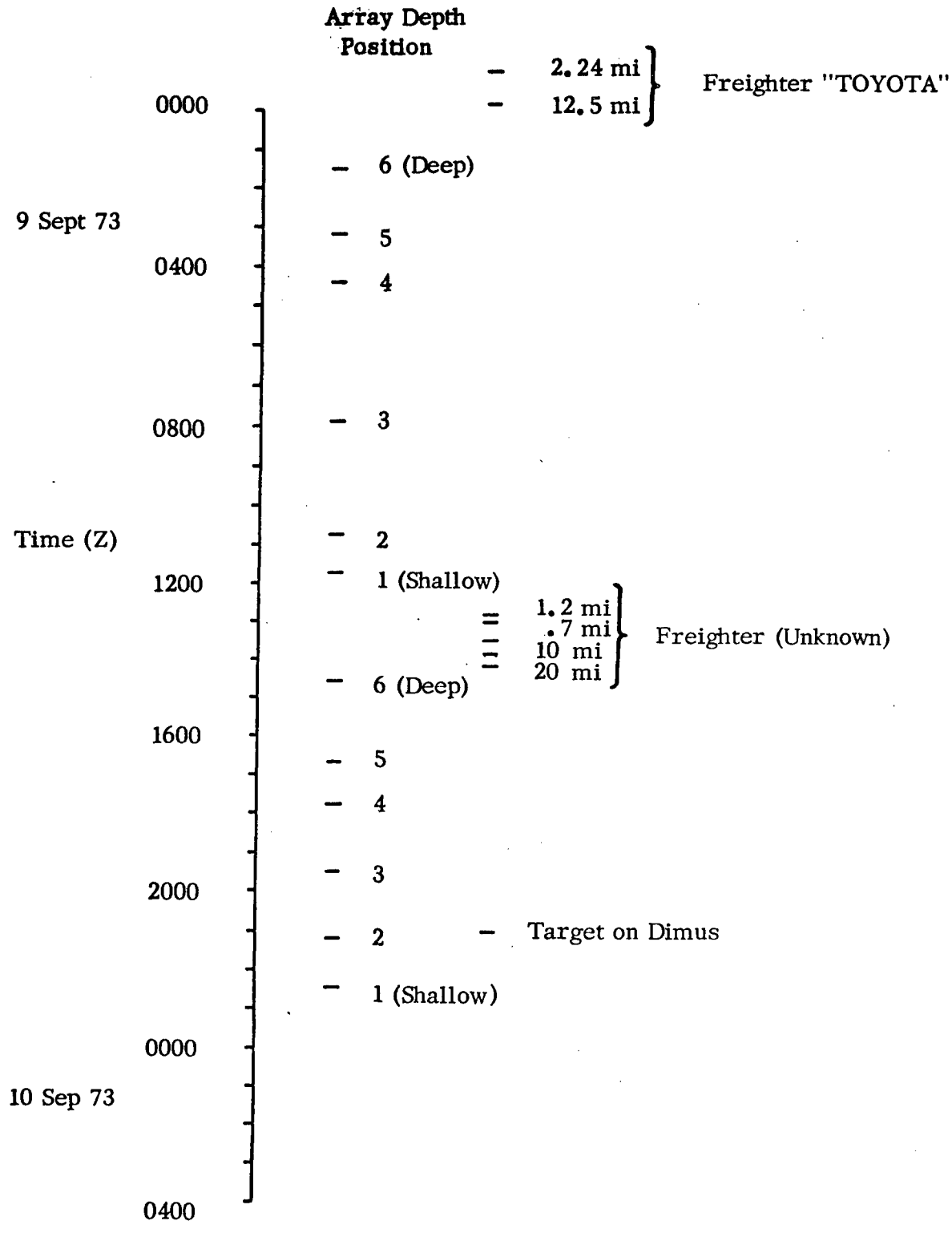

CONFIDENTIAL

Figure D-6. (C) Local Ship Traffic Near *Flip* During 8–9 September 1973 Noise Period (U)

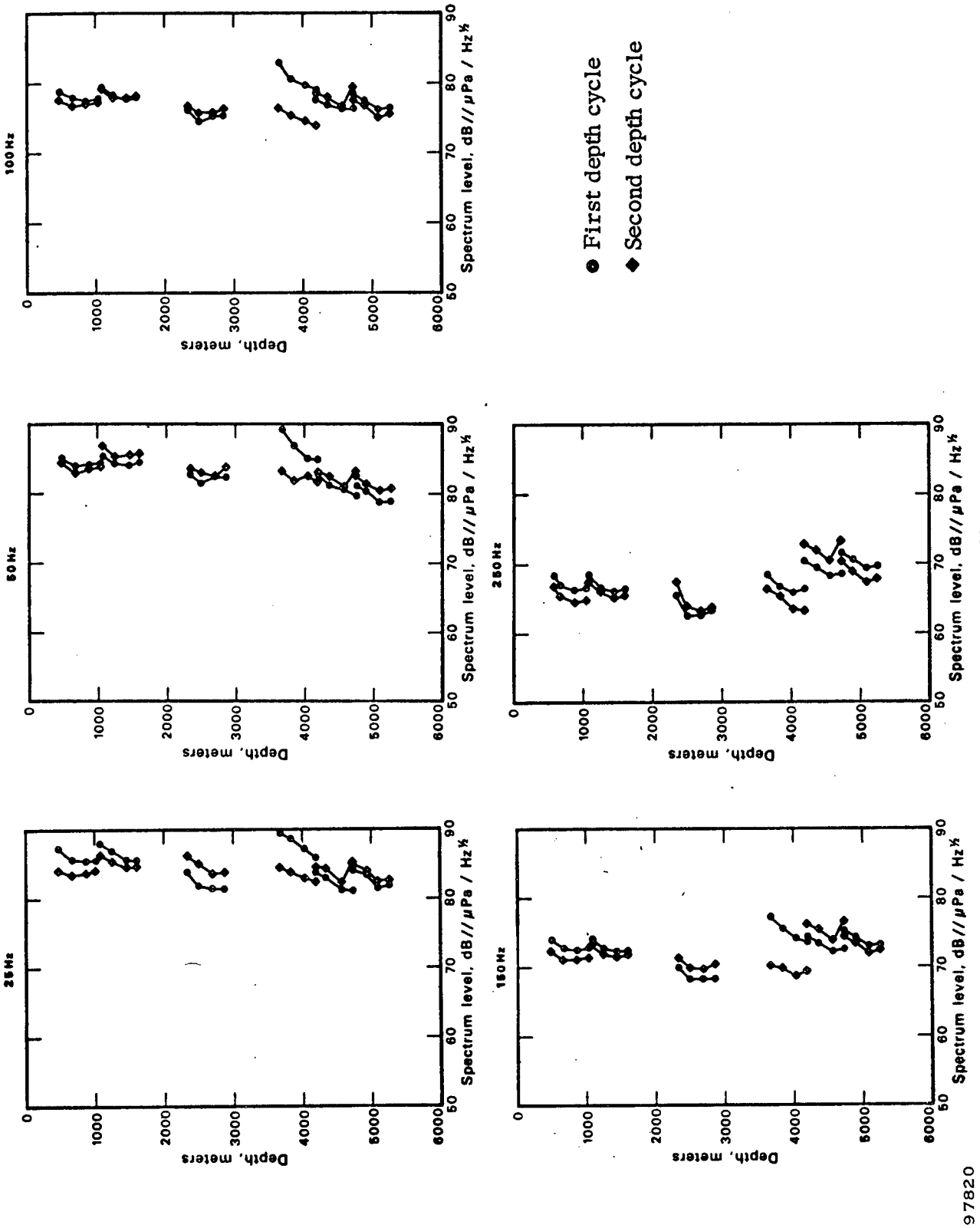

Figure D-7. (C) Ambient Noise Levels for Five One-Third Octave Bands During 9 September 1973 at Six Different Array Depths (U)

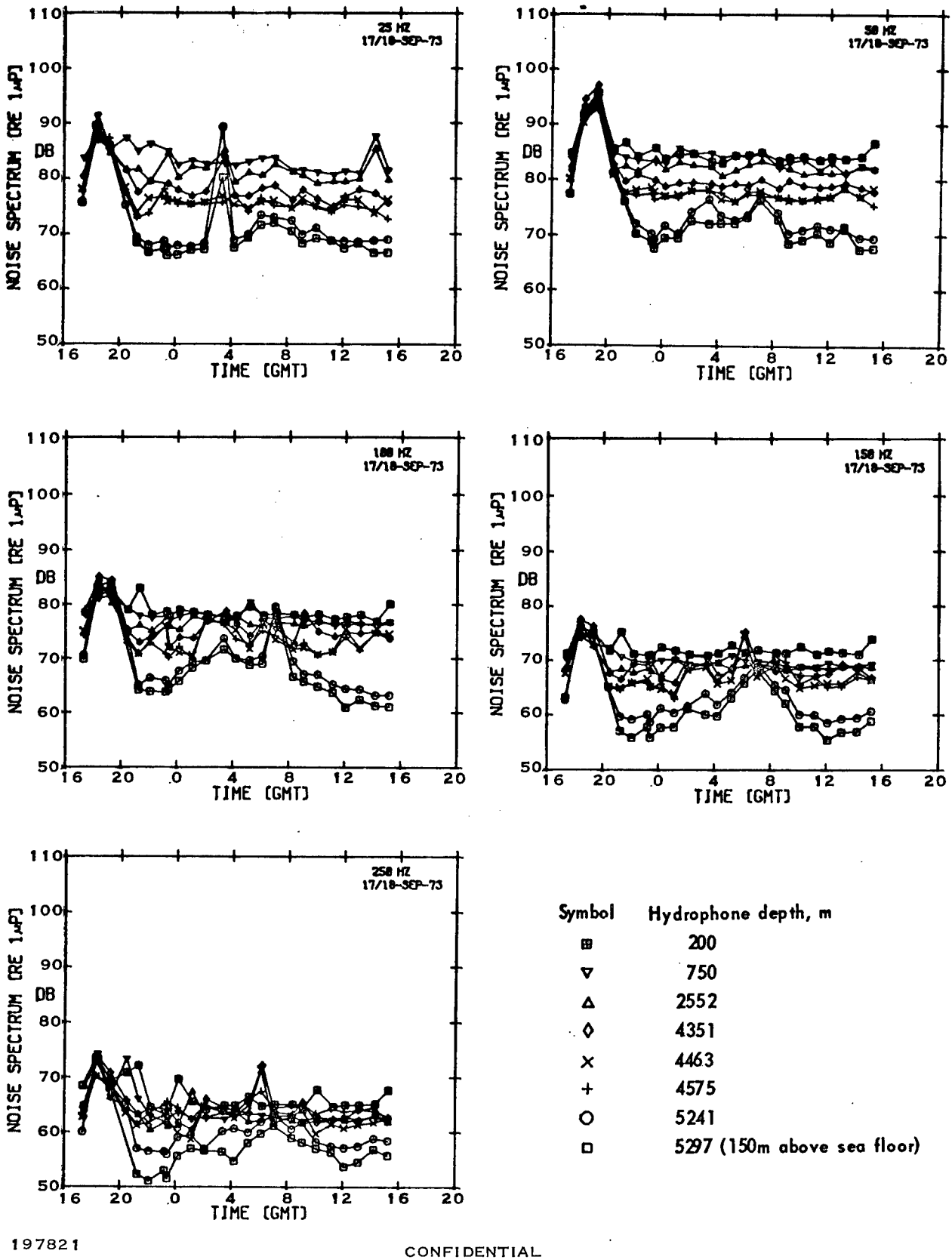

Figure D-8. (C) Ambient Noise Spectrum Levels for Five One-Third Octave Bands During 17–18 September 1973 as a Function of Time and Depth (U)

(C) All of the noise data taken during this first phase of the exercise suffer from the fact that spatial changes in the noise levels ascribed to depth cannot be separated from the temporal changes in the noise levels that resulted during the time required to change the depth of the array. This situation was particularly difficult for the noise days considered here, as shipping traffic was relatively high.

(C) During the second phase of the exercise, the hydrophones were deployed in five widely spaced depth groups to investigate, in particular, the depth dependence and the temporal variability of the omnidirectional ambient noise intensity. For two periods, each of about 24 hours, noise samples were taken approximately one time each hour.

(C) The ambient noise levels taken during the 17–18 September noise period for the five one-third octave bands are shown as a function of time for eight hydrophone depths in Figure D-8. The two prominent features of these data are the decrease in noise levels by as much as 10 to 15 dB with increasing depth for all the frequencies from 25 Hz to 250 Hz and the large changes in level with time. Perhaps the most prominent temporal change in level occurs between 1700Z and 2100Z 17 September with the passage of a Norwegian freighter, the *Jacara.* This ship approached within 0.9 nautical mile of R/P *Flip* at 1842Z. The effect of this ship on noise level varied with frequency and hydrophone depth but the total change in level was not only greater for the deeper hydrophones than for the shallow hydrophones but also persisted for a longer time period. Thus, the effect of a local ship, that is, one passing near the receiver, was far more prominent on the deeper hydrophones than on the shallow ones. Another major temporal change occurs between 0000Z and 1200Z on 18 September. Although no radar contacts were noted during this period, it is easily possible for ships to pass at a distance close enough to increase the noise level substantially yet be beyond radar contact range. It should be noted that this broad increase in level could have been caused by the passing of two ships, one with a closest point of approach occurring at about 0300Z and the other at 0700Z.

(C) The ambient noise data for the 19–20 September period are shown in Figure D-9. As in the previous noise period, the data exhibit both a substantial decrease in noise level with depth and a large variability in level with time. Radar contact with only one ship was made during this period. An unidentified ship traveling at 15 knots passed within 6 nautical miles of R/P *Flip* at 0605Z 20 September. Two additional apparent ship passings are also suggested by the acoustic data, one occurring during the early part of the noise sampling period at 1800Z or earlier on 19 September and the other near the end at about 1400Z 20 September. As in the previous noise period, the effects of nearby ships on the noise levels varied, depending upon the hydrophone depth, the frequency, and the ship-to-receiver range. In general, however, the deeper hydrophones exhibit a greater effect of passing ships mainly because the hydrophones themselves are in a quieter environment. This is clearly demonstrated by the 50-Hz data during the ship passage. All the hydrophones, regardless of depth, measure almost the same noise level at 0600Z.

IV. (C) ANALYSIS OF RESULTS (U)

(C) The temporal variations in the ambient noise levels observed during the last two noise periods are highly variable, with the changes being as great as 30 dB. These major changes are caused by ships passing within a few miles of the hydrophones, as confirmed by radar contacts. In addition, these temporal variations exhibit a depth dependency, with the hydrophones that are within 150 meters to 200 meters of the bottom having the most frequent and greatest changes in levels.

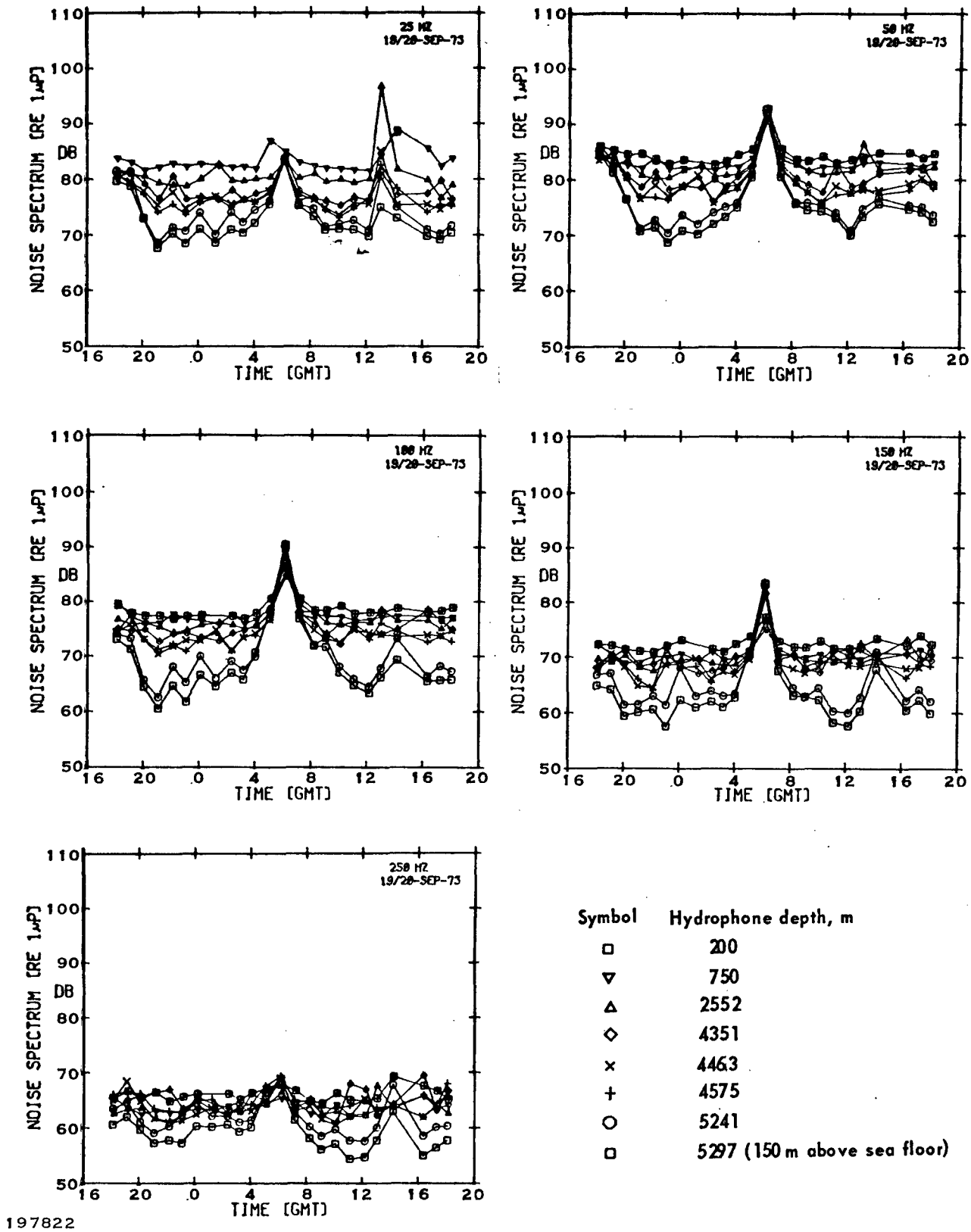

Figure D-9. (C) Ambient Noise Spectrum Levels for Five One-Third Octave Bands During 19–20 September 1973 as a Function of Time and Depth (U)

(C) The basic problem in ascertaining the noise versus depth relationship in how to handle this local shipping effect. Does one assume that the high noise levels from nearby ships are indeed part of the ambient noise field and include them in the analysis or should an attempt be made to eliminate their effects? The author believes that these effects should be eliminated from the noise versus depth analysis for the following reasons:

These local ship effects are very dependent upon local conditions and the data collection period. The measured noise levels could change significantly if the receiver was moved a short distance away from the major shipping traffic or if the data were taken over a slightly different time period.

Usually, in data analyses, simple or arithmetic averaging is used to determine a most likely value. Where distributions are normal, such averaging does tend to yield a most-likely-to-occur value. For distributions other than normal, particularly those that are single-sided, this is not the case. The effect of passing ships is to superimpose a high noise level on what may be regarded as a "baseline" ambient noise level. The result is, in general, a nonnormal distribution of noise level.

(C) Eliminating this local ship effect from the ambient noise becomes a problem of establishing this baseline or minimum noise level. For these data, this was accomplished by visually determining an "average minimum" baseline for the ambient noise for each frequency and for each hydrophone depth. The results of these determinations are shown in Figure D-10. These baseline ambient noise levels appear to be divided into two distinct depth groups on the basis of the noise gradient, that is the change in noise level with depth. One region is from the surface to near the bottom of the sound channel, and the other is in the region below the sound channel to the sea bottom. The boundary between the two regions appears to occur near 4,300 m, which is slightly above the 4,430-m critical depth as determined from sound velocity measurements. Table D-1 gives the vertical gradients for the ambient noise in the two regions. The gradients in the upper region show a consistent change with frequency. There are also differences in the gradients for the deeper region; however, those gradients are measured over a small depth interval where there is more scatter in the noise levels. The differences in the deep gradient may not be significant. The important point, however, is that the decrease in ambient noise with depth is five to ten times greater below the sound channel than it is within the channel itself.

TABLE D-1. (C) VERTICAL GRADIENTS OF BASELINE AMBIENT NOISE SPECTRUM LEVELS IN DECIBELS PER 1,000 METERS (U)

	Frequency				
	25 Hz	50 Hz	100 Hz	150 Hz	250 Hz
Surface to 4,300 m	−1.5	−1.2	−1.0	−0.6	0
4,300 m to sea bottom	−8	−8	−11	−9	−8

CONFIDENTIAL

(C) Figure D-11 shows the spectrum levels for seven of the eight hydrophones. For comparison, the idealized ambient noise spectra for deep water for different shipping densities, as reported by Swanson,[4] are given. The curve of average near shipping lanes compares favorably with the noise measurements made at shallow depths, whereas the deep hydrophone data agree with the idealized "quiet" curve.

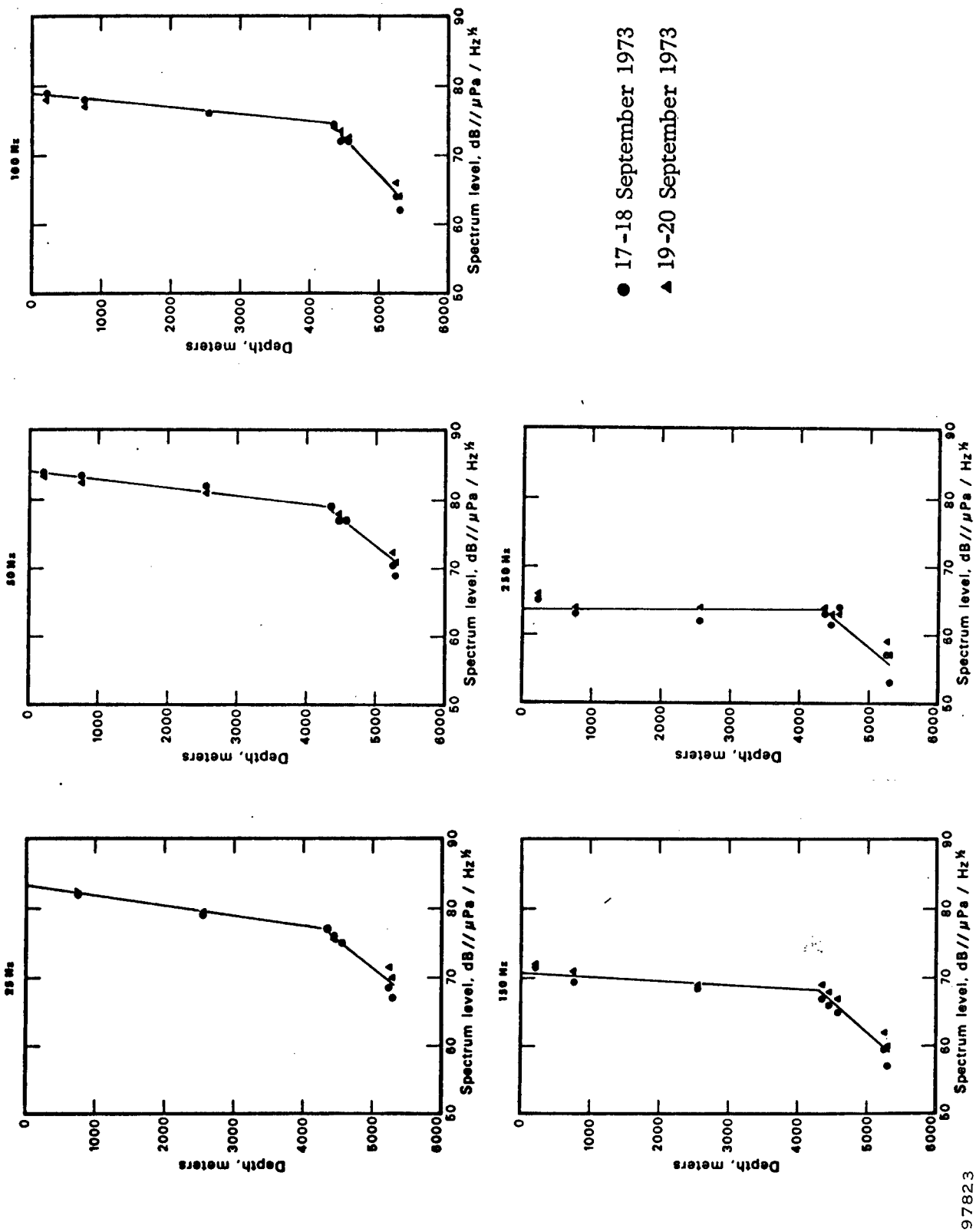

Figure D-10. (C) Variations of Deep-Ocean Ambient Noise Levels With Depth; Local Ship Effects Removed (U)

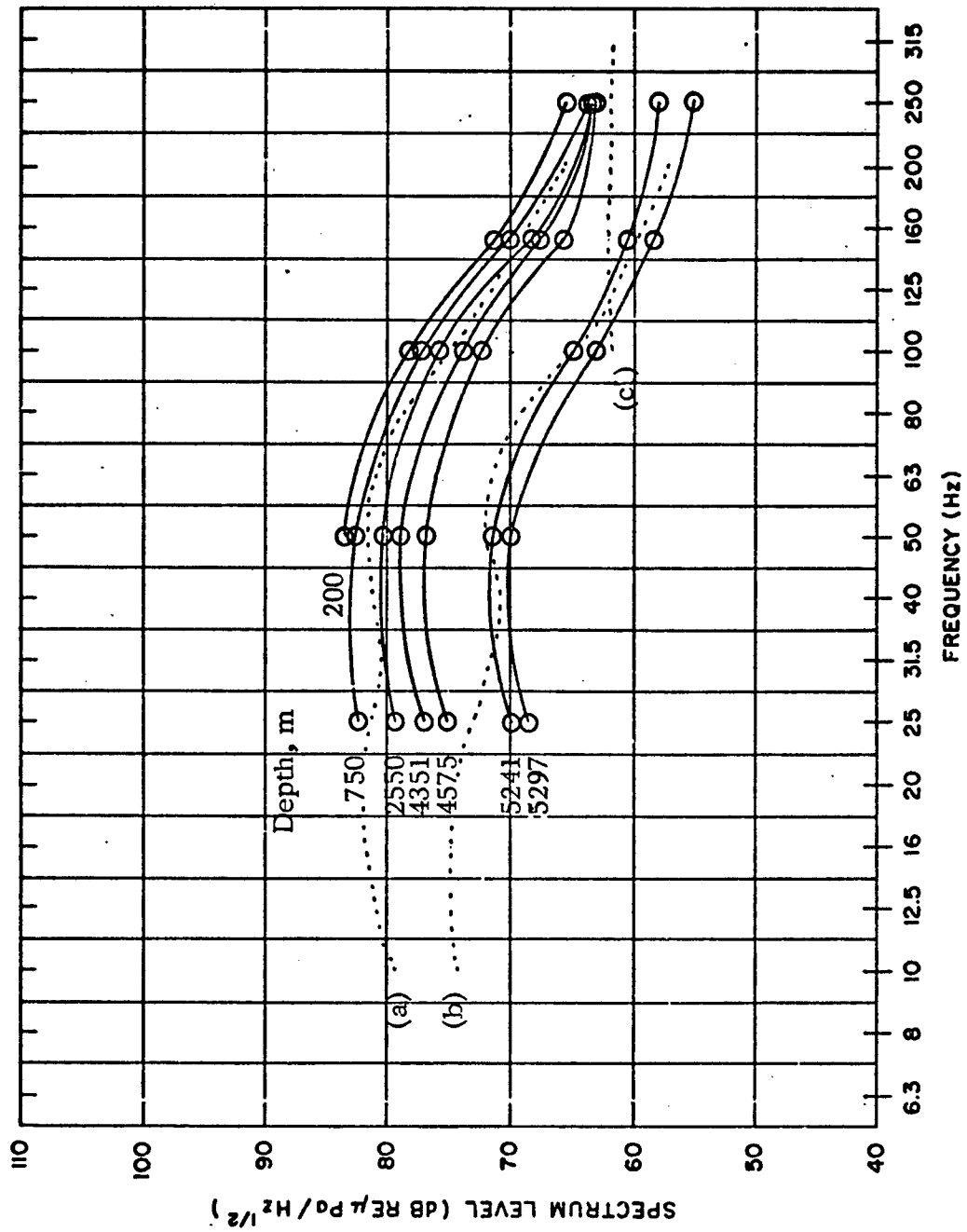

CONFIDENTIAL

Figure D-11. (C) Comparison of Observed Ambient Noise Spectra With Idealized Spectra as Reported by Swanson's Curves (a) Average Near Shipping Lanes, (b) Quiet, and (c) Sea State 2, Wind Speed 10 Knots (U)

197824

(U) REFERENCES

1. "CHURCH ANCHOR Exercise Plan (U)," Maury Center for Ocean Science, MC-011 (June 1973) (16 July Revision). CONFIDENTIAL

2. "CHURCH ANCHOR Data Analysis Plan (U)," Maury Center for Ocean Science, MC-001 (October 1973). Vol. 1 SECRET, Vol. 2 CONFIDENTIAL

3. R.J. Hecht, *Estimated Accuracy for Acoustic Data From R/P FLIP-CHURCH ANCHOR*, Underwater Systems, Inc. (March 8, 1974).

4. B.K. Swanson, "Oceanography for Long Range Sonar Systems," *Part 1 Introduction to Oceanography and Physics of Underwater Sound in the Sea*, U.S. Naval Oceanographic Office, SP-79 (February 1966).

APPENDIX E

(U) SOURCE OF 20-HZ PULSES

A distinctive noise source was observed in the data from sites A and C. These signals were of a repetitive nature and occurred near 20 Hz. Figure E-1 shows examples of these 20-Hz signals from the data at site C both as they appear on a lofargram and on a time plot of the waveform. As can be observed from this figure, these signals are relatively narrowband (10 to 15 Hz wide) and are repetitive in nature. The average period measured was 42.6 seconds and the pulses were paired. A first large-amplitude pair occurred, followed by a smaller pair about 23.4 seconds later. Each pulse duration was about 1 second. Although the source levels are not known, it appears that they are quite high since they are stronger than most of the lines generated by local shipping. The paired pulses that occurred about 2.7 seconds after each of the large and small pulses on the 4,055 m hydrophone and about 3.2 seconds on the 5,521 m hydrophone are believed to be surface reflections. Figure E-2 indicates the probable propagation path involved and would indicate that the source of the pulses is submerged. A surface reflection is indicated (unless a more complicated propagation path is theorized) rather than a bottom bounce, since the time difference of arrival between the main pulse and the reflected pulse is less for the shallow phone than for the deeper phone.

The 20-Hz pulses are believed to be of biological origin, probably the finback whale, species Balaenoptera Physalus, that may have been in the vicinity during the CHURCH ANCHOR tests. The major reasons for this conclusion are:

Finback whales are known to frequent this part of the ocean. They move generally at a rate of 1 to 4 knots, and sometimes as high as 8 knots. Their density is low, usually one to several hundred square miles, although several may be observed together.

The frequency, pulse period, pulse duration, and fading cycle characteristics all agree with data derived from known finback whale pulse signals. Several different sequences of pulses have been observed in the past. In one sequence, the pulses were constant-amplitude pulses and were repeated at approximately 12-second intervals. In a second observed sequence, the pulse interval ranged from 21 to 32 seconds. In yet a third sequence, the period was about 37 to 40 seconds, except that the pulses were paired. A first large-amplitude pulse occurred, followed about 22 seconds later by a smaller pulse. This last sequence, of course, closely resembles the pattern observed in the data from sites A and C.

The pulses do not appear to correlate with the track of any ship although it is believed that the whales may be stimulated to emit pulses by the presence of ships and by changes in the speed of a ship's engine. In addition, the presence of ships may also cause the whales to cease emission.

Figure E-3 shows the times and levels of 20-Hz pulses observed on the 4,659 m and 5,521 m phones from sites A and C, respectively. Lower level activity was observed at site D. As can be seen from Figure E-3, 20-Hz pulse trains were observed for periods of 24 hours or longer, except for short fading periods of an hour or so. In some of these periods, the pulses would fade

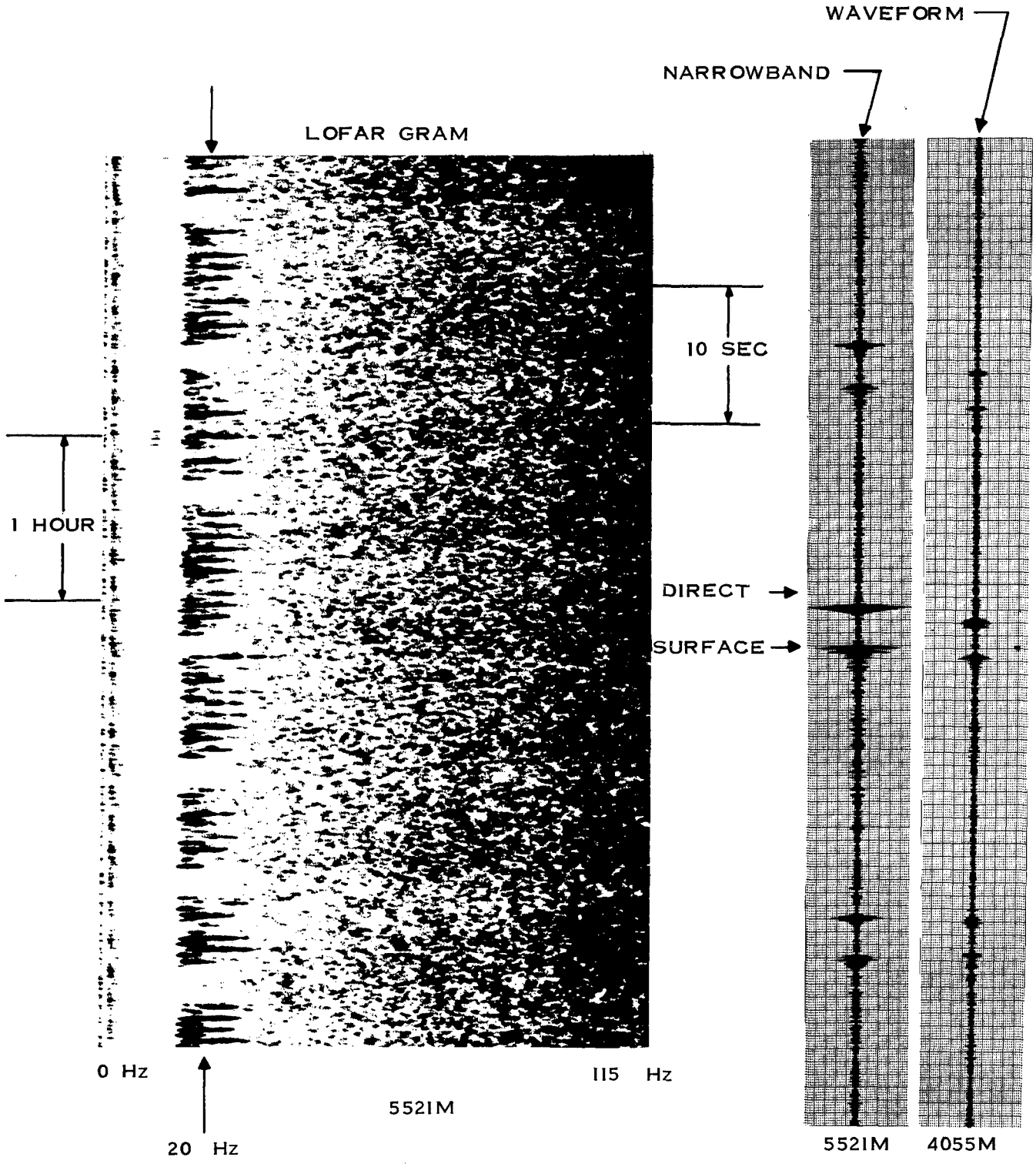

Figure E-1. (U) Example of 20-Hz Pulses at Site C

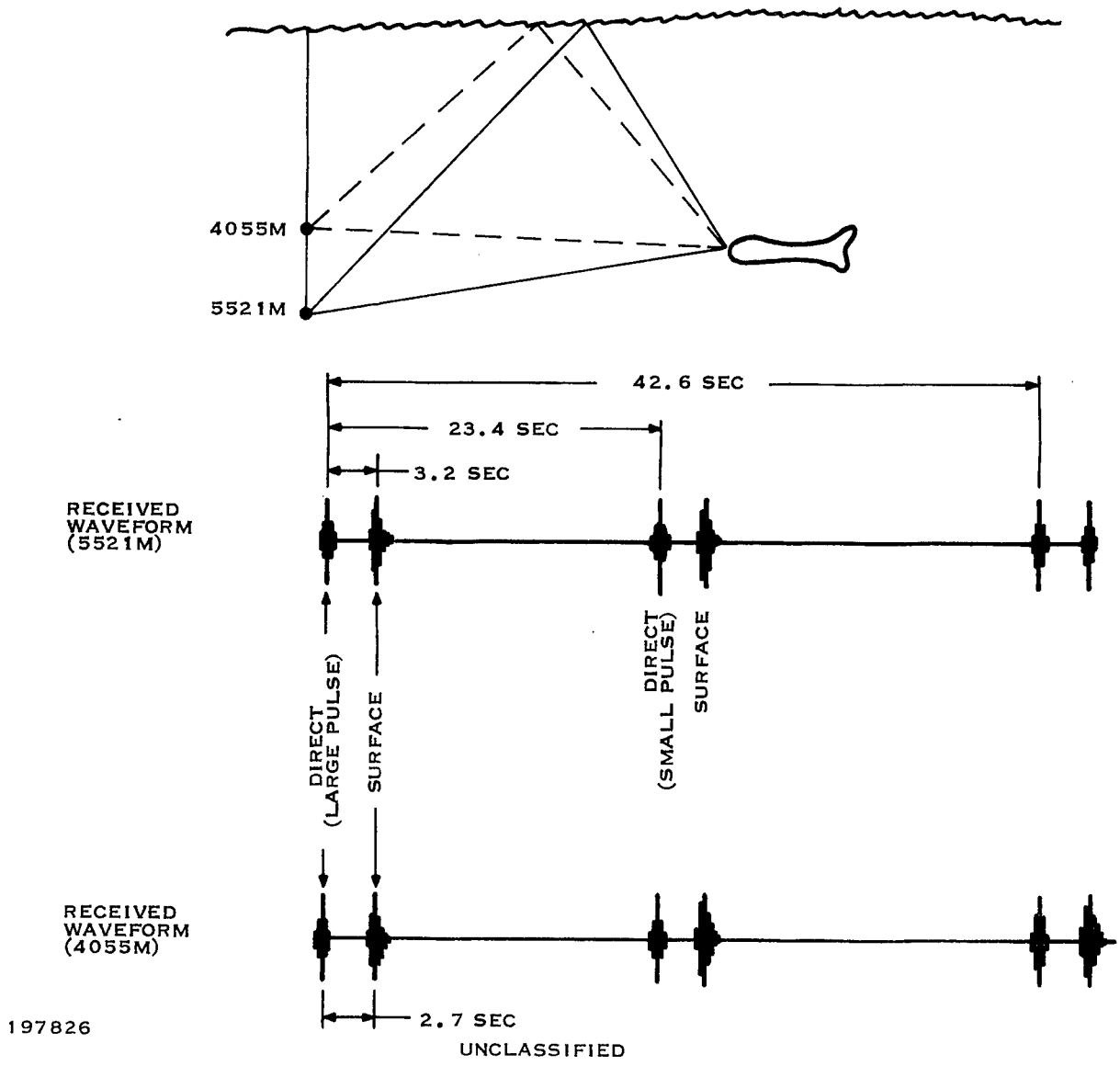

Figure E-2. (U) Probable Propagation Paths for 20-Hz Pulses at Site C

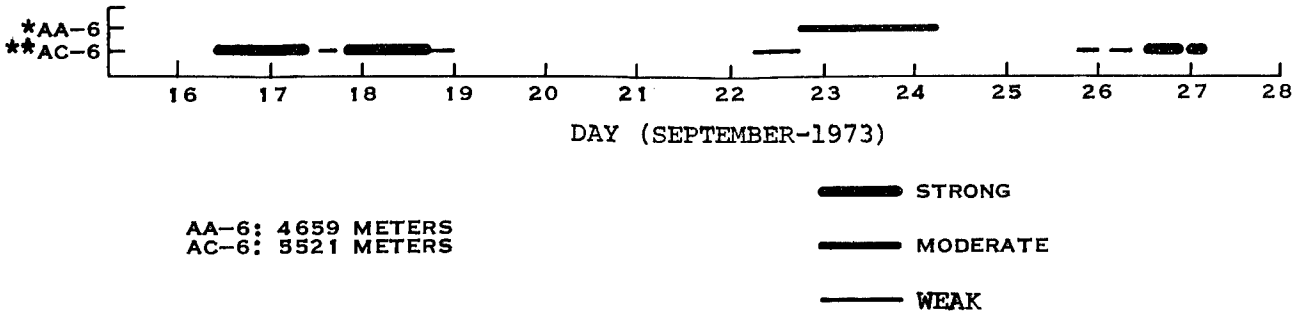

Figure E-3. (U) Occurrence of 20-Hz Pulses

out gradually while in others the pulses would stop abruptly. From analysis of the data, the pulses did not correlate or originate from any shipping in the data and appeared to originate at some depth. No attempt was made to estimate source range or depth.

APPENDIX F
(U) SHIP SIGNATURES

A summary of typical ship signatures identified from the lofargrams is discussed in the following section.

I. R/V *NORTH SEAL*

The primary mission of the R/V *North Seal* was to deploy, recycle, and retrieve three ACODACs in the exercise area. From the track charts, the ship was near site C between September 14 and 16, and site D around September 18. Significant evidence of the ship was observed in the lofargrams in the 10-day ACODAC plots during these time periods at these two sites.

Figure F-1 shows lofargrams of the R/V *North Seal* signature and the effects of multipath interference as it passed near site C at about 161400Z September. Note the blade lines which appear with a fundamental spacing of about 8 Hz. With four blades per screw, this gives a shaft speed of 120 rpm. Some shaft lines can be observed; but, with two shafts apparently turning at slightly different speeds, combined with some evidence of cavitation; a clean blade and shaft pattern is somewhat obscured.

Strong multipath interference effects were observed on most of the sensors with a closest point of approach occurring about 161400Z. The mirror frequency (spacing between lines in the interference pattern) decreased for the shallower depth phones. This is as it should be for radiated noise from a surface ship arriving by direct and bottom-bounce paths.

As can be observed from the lofargrams and the 10-day time-series plots shown later in this section, the effect of the R/V *North Seal* on ambient noise levels was more severe (by as much as 10 to 15 dB) at depths below the sound channel axis. Although the time periods during which the ambient level was significantly increased in one or more of the 1/3-octave bands were limited to a few hours (2 to 6 hours in most cases), relatively strong discrete lines were observed for much longer periods of time on lofargram.

II. M/V *MEDITERRANEAN SEAL*

The primary mission of the M/V *Mediterranean Seal* was the deployment of two hydro-acoustic sources at various depths, frequencies, and power levels. A secondary mission was collection of environmental data including XBT profiles and meteorologic data. From the track charts, the M/V *Mediterranean Seal* passed near site C between September 20 and 21. During this time, its radiated noise energy dominated several 1/3-octave bands and also produced strong multipath interference effects.

Figure F-2 shows the lofargrams of the signature of the M/V *Mediterranean Seal* at several phone depths as it passed through the first convergence zone. According to computer range readouts, the M/V *Mediterranean Seal* was approximately 30 miles from site C at this time. As can be seen from the lofargrams, the signature peaks at about 201200Z and falls off in strength on either side and is quite characteristic of convergence zone reception. Strong blade lines with a

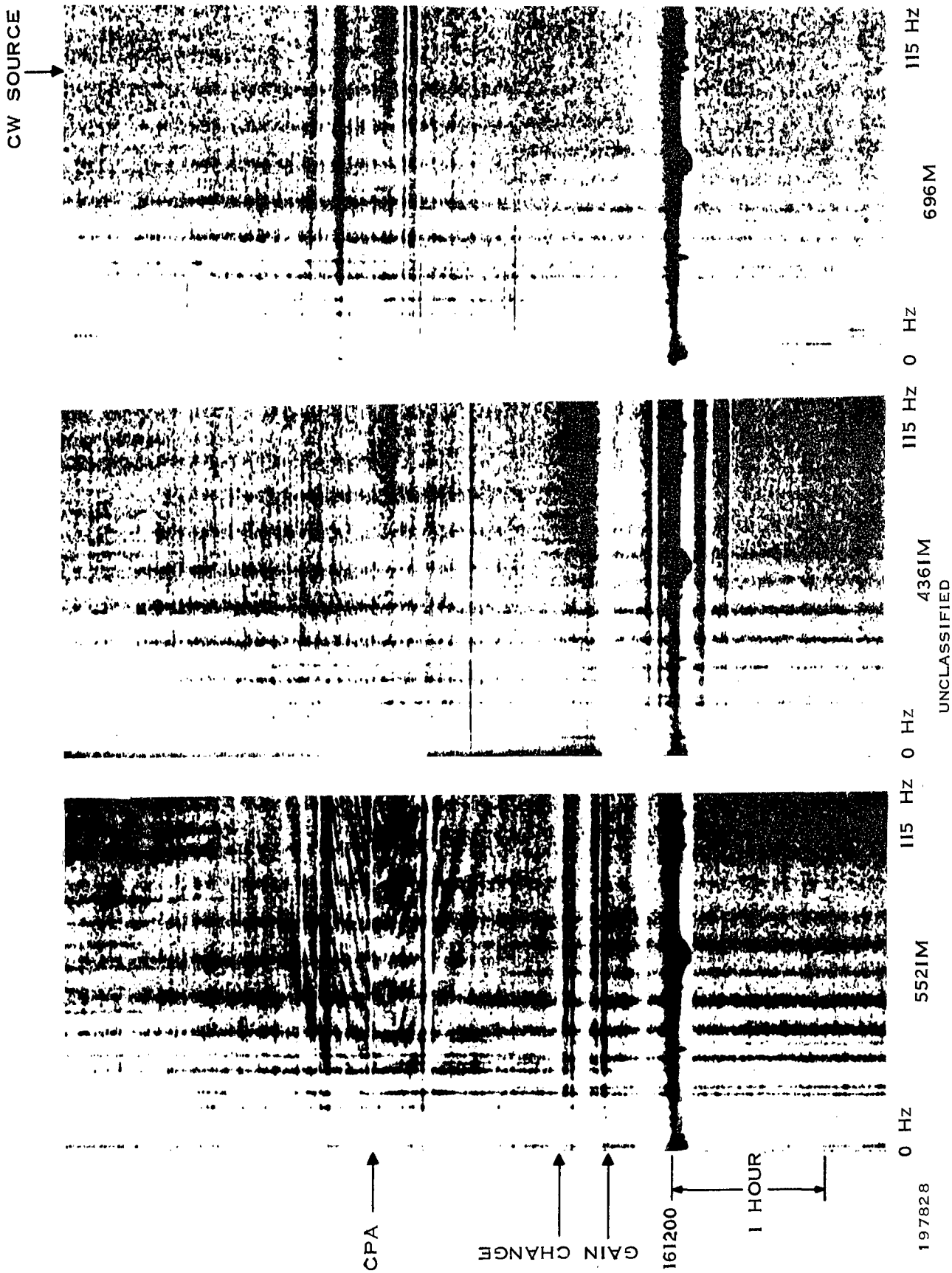

Figure F-1. (U) Lofargram Signature of R/V *North Seal* at Site C

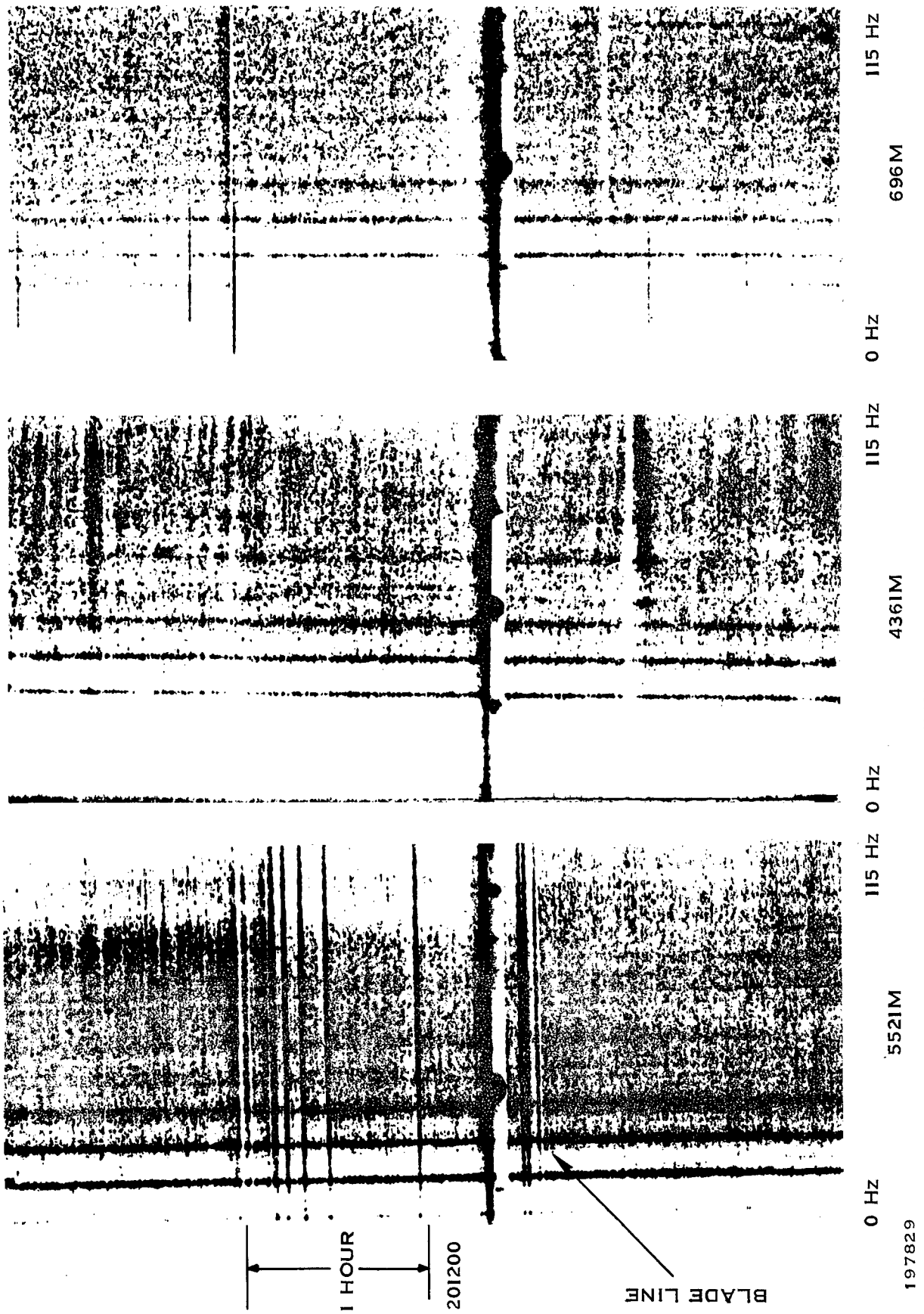

Figure F-2. (U) Lofargram Signature of M/V *Mediteranean Seal* at Site C

fundamental spacing of about 9 Hz are observed with slight evidence of three shaft lines between each blade line, which indicates a four-bladed prop. Some evidence of cavitation is noted by the diffusion of the blade lines. The effect of depth is quite apparent on these lofargrams, with the signature effects being much stronger for the deeper phones.

III. USNS *SILAS BENT*

The primary mission of the USNS *Silas Bent* included implantment and recovery of moored current meter arrays, deployment of SUS charges, and collection of general environmental information. From the track charts, the USNS *Silas Bent* passed fairly near all three sites between the 22nd and 26th of September. Evidence of significant changes in the ambient noise was observed at each of the sites (A, C, and D) when the ship was near each site.

IV. UNKNOWN SHIPPING

A relatively large number of ships of unidentified source are observed on the lofargrams and, to a lesser extent, on the 10-day time-series plots. In many instances, the signatures of unknown ships were observed on the lofargrams but did not pass near enough to a site to appreciably affect the noise levels in the 1/3-octave bands. Also, at times, signatures from more than one ship were observed on the lofargrams.

APPENDIX G

(U) DISTRIBUTION LIST FOR "CHURCH ANCHOR AMBIENT NOISE REPORT"

Chief of Naval Operations
ATTN: OP-951 1
OP-955F 1
OP-981H 1
Department of the Navy
Washington, D.C. 20350

Commander 2
Third Fleet
FPO, San Francisco, California 96610

Commander, Submarine Forces 1
U.S. Pacific Fleet
FPO, San Francisco, California 96610

Commander 1
Oceanographic Systems, Pacific
Box 1390
FPO, San Francisco, California 96610

Commander 1
Oceanographic Systems, Atlantic
Box 100
Norfolk, Virginia 23511

Commander 1
Naval Sea Systems Command
Department of the Navy
ATTN: PMS-302
Washington, D.C. 20360

Commander 1
Naval Air Systems Command
Department of the Navy
ATTN: NAIR-540
Washington, D.C. 20360

Project Manager 1
Antisubmarine Warfare Systems
Project
ATTN: ASW-11 1
ASW-111 1
Department of the Navy
Washington, D.C. 20360

Commander
Naval Electronic Systems Command
ATTN: PME-124 1
PME-124/TA 1
PME-124/20 1
PME-124/30 1
PME-124/40 1
PME-124/60 1
Department of the Navy
Washington, D.C. 20360

Commanding Officer 1
Naval Intelligence Support Center
4301 Suitland Road
Washington, D.C. 20390

Oceanographer of the Navy 1
Hoffman Building
200 Stoval Street
Alexandria, Virginia 22332

Chief of Naval Research
Department of the Navy
ATTN: Code 102-OS 1
Code 102-OSC 3
Code 431 1
Code 212 1
Code 486 1
Code AESD 2
Arlington, Virginia 22217

Commander 1
U.S. Naval Oceanographic Office
ATTN: Code 6130 2
Department of the Navy
Washington, D.C. 20373

Director
Center for Naval Analysis
ATTN: Capt. C. Woods 1
Arlington, Virginia

Commander
Naval Undersea Center
ATTN: Code 4007 2
San Diego, California 92132

Officer-in-Charge 1
New London Laboratory
Naval Underwater Systems Center
ATTN: Code TA 1
Code TA11 1
New London, Connecticut 06320

Director 1
Naval Research Laboratory
ATTN: Code 2627 1
Code 8101 1
Code 8160 1
Washington, D.C. 20390

Commander 1
Naval Surface Weapons Center
White Oak Laboratory
ATTN: Code 021 1
Silver Spring, Maryland 20910

Commanding Officer 1
Fleet Numerical Weather Central
Monterey, California 93940

Director 1
Strategic Systems Projects Office
(PM-1)
Naval Material Command (CM-3)
Jefferson Davis Highway
Arlington, Virginia 22209

Commander 1
Naval Ship Research and
Development Center
Bethesda, Maryland 20034

Commander 1
Naval Air Development Center
ATTN: Code 205 1
Warminster, Pennsylvania 18974

Defense Documentation Center 2
Cameron Station
Alexandria, Virginia 22314

Arthur D. Little, Inc.
ATTN: Dr. G. Raisbeck 1
15 Acorn Park
Cambridge, Massachusetts 02140

B-K Dynamics, Inc.
ATTN: Mr. A.E. Fadness 1
15825 Shady Grove Road
Rockville, Maryland 20850

Bell Telephone Laboratories
ATTN: Dr. G. Fox 1
1 Whippany Road
Whippany, New Jersey 07981

Bolt, Beranek & Newman, Inc.
ATTN: Mr. C. Burroughs 1
Suite 1001
1701 North Fort Meyer Drive
Arlington, Virginia 22209

Hawaii Institute of Geophysics
ATTN: Dr. G. Woollard 1
Mr. M. Odegard 1
2525 Correa Road
Honolulu, Hawaii 96722

Director 1
Marine Physical Laboratory
ATTN: Dr. G.B. Morris 1
Scripps Institution of Oceanography
San Diego, California 92152

Planning Systems, Inc.
ATTN: Dr. L.P. Solomon 1
7900 Westpark Drive, Suite 507
The Honeywell Center
McLean, Virginia 22101

TRW Systems Group
ATTN: Mr. C.C. Carter 1
Mr. R.T. Brown 1
7600 Coleshire Drive
McLean, Virginia 22101

Tetra Tech, Inc.
ATTN: Mr. C. Dabney 1
1911 Fort Meyer Drive
Arlington, Virginia 22209

Texas Instruments Incorporated
ATTN: Mr. A. Kirst 1
13500 North Central Expressway
Dallas, Texas 75222

Tracor, Inc.
Ocean Technology Division
ATTN: Mr. J. Gottwald 1
Dr. A.F. Wittenborn 1
1601 Research Boulevard
Rockville, Maryland 20850

Underwater Systems, Inc.
ATTN: Dr. M. Weinstein 1
8121 Georgia Avenue
Silver Spring, Maryland 20910

Woods Hole Oceanographic Institution
ATTN: Dr. E.E. Hays 1
Woods Hole, Massachusetts 02543

Undersea Research Corporation
ATTN: J.A. Hess 1
7777 Leesburg Pike, Suite 306
Falls Church, Virginia 22043

Xonics, Incorporated
ATTN: Mr. S. Kulek 1
6837 Hayvenhurst Avenue
Van Nuys, California 91406

University of Miami
ATTN: Dr. S.C. Daubin 1
School of Marine & Atmospheric Sciences
10 Rickenbacker Causeway
Miami, Florida 33149

University of Texas at Austin
Applied Research Laboratories
ATTN: Dr. L.D. Hampton 1
Mr. G.E. Ellis 1
P.O. Box 8029
10000 FM Road 1325
Austin, Texas 78712

DEPARTMENT OF THE NAVY
OFFICE OF NAVAL RESEARCH
875 NORTH RANDOLPH STREET
SUITE 1425
ARLINGTON VA 22203-1995

IN REPLY REFER TO:

5510/1
Ser 321OA/011/06
31 Jan 06

MEMORANDUM FOR DISTRIBUTION LIST

Subj: DECLASSIFICATION OF LONG RANGE ACOUSTIC PROPAGATION PROJECT (LRAPP) DOCUMENTS

Ref: (a) SECNAVINST 5510.36

Encl: (1) List of DECLASSIFIED LRAPP Documents

1. In accordance with reference (a), a declassification review has been conducted on a number of classified LRAPP documents.

2. The LRAPP documents listed in enclosure (1) have been downgraded to UNCLASSIFIED and have been approved for public release. These documents should be remarked as follows:

   Classification changed to UNCLASSIFIED by authority of the Chief of Naval Operations (N772) letter N772A/6U875630, 20 January 2006.

   DISTRIBUTION STATEMENT A: Approved for Public Release; Distribution is unlimited.

3. Questions may be directed to the undersigned on (703) 696-4619, DSN 426-4619.

BRIAN LINK
By direction

Subj: DECLASSIFICATION OF LONG RANGE ACOUSTIC PROPAGATION PROJECT (LRAPP) DOCUMENTS

DISTRIBUTION LIST:

NAVOCEANO (Code N121LC – Jaime Ratliff)
NRL Washington (Code 5596.3 – Mary Templeman)
PEO LMW Det San Diego (PMS 181)
DTIC-OCQ (Larry Downing)
ARL, U of Texas
Blue Sea Corporation (Dr.Roy Gaul)
ONR 32B (CAPT Paul Stewart)
ONR 321OA (Dr. Ellen Livingston)
APL, U of Washington
APL, Johns Hopkins University
ARL, Penn State University
MPL of Scripps Institution of Oceanography
WHOI
NAVSEA
NAVAIR
NUWC
SAIC

Declassified LRAPP Documents

Report Number	Personal Author	Title	Publication Source (Originator)	Pub. Date	Current Availability	Class.
TIRC1871976F	Hoffmann, J., et al.	CHURCH ANCHOR AMBIENT NOISE FINAL REPORT (U)	Texas Instruments, Inc.	750901	ADC070512; NS; AU; ND	C
Unavailable	Unavailable	SQUARE DEAL ANALYSIS EXECUTIVE SUMMARY (U)	University of Texas, Applied Research Laboratories	751001	AU	C
Unavailable	Unavailable	SQUARE DEAL ENVIRONMENTAL ACOUSTIC SUMMARY SEC. IV-SIGNAL PROPAGATION (U)	Xonics, Inc.	751101	AU	C
Unavailable	Unavailable	CHURCH ANCHOR CW PROPAGATION LOSS AND SIGNAL EXCESS REPORT (U) PRELIMINARY	Texas Instruments, Inc.	751201	AU	C
SAN-BBOP-76-U127. B38485	Unavailable	MSS CONFIGURED ACODAC SYSTEMS FINAL ENGINEERING REPORT (U)	Sanders Associates, Inc.	760115	ND	C
Unavailable	Unavailable	MSS CONFIGURED ACODAC SYSTEMS PRELIMINARY TEST REPORT-BEARING STAKE (U)	Sanders Associates, Inc.	761111	AU	C
ARL-TR-76-52	Watkins, S. L.	MOORED SURVEILLANCE SYSTEM FIELD VALIDATION TEST AMBIENT SOUNDFIELD AND PROPAGATION MEASUREMENTS FOR NEAR-BOTTOM SENSORS AT SITE A3 (U)	University of Texas, Applied Research Laboratories	761201	ND	C
Unavailable	Unavailable	REAL-WORLD MEASUREMENTS Of MSS ACODAC HYDROPHONE RESPONSE PATTERNS (U) PHASE REPORT - PRELIM DRAFT	Naval Air Development Center	761222	AU	C
XONICSTR109OSD	Morey, C. F.	EFFECT OF ARRAY TILT ON BEAM NOISE, SIGNAL-TO-NOISE RATIO, AND DETECTION OPPORTUNITY	Xonics, Inc.	770101	NS; ND	C
NRL-7996	Andriani, C. R., et al.	ACOUSTIC PROPAGATION IN THE LABRADOR SEA	Naval Research Laboratory	770308	ND	C
Unavailable	Gabrielson, T. B.	REAL-WORLD MEASUREMENTS Of MSS ACODAC HYDROPHONE RESPONSE PATTERNS	Naval Air Development Center	770601	ADC010980	C
NAVSO P970V27, NO. 3	Del Balzo, D. R.	TOWED ARRAY DYNAMICS AND ACOUSTIC IMPLICATIONS (U)	Office of Naval Research	770701	ND	C
WHOI-77-55	Baxter, L.	MSS-FVT ACODAC DATA ASSESSMENT AND AMBIENT NOISE THIRD OCTAVE DATA PROCESSING (U)	Woods Hole Oceanographic Institution	770801	AU; ND	C
Unavailable	Unavailable	LARGE APERTURE MARINE BASIC DATA ARRAY (LAMBDA) SYSTEM DESCRIPTION	Naval Ocean R&D Activity	770901	AU	C
Unavailable	Unavailable	CHURCH STROKE REVIEW (U)	University of Texas, Applied Research Laboratories	770912	AU	C
NOSCTR169	Yee, G. S.	BEARING STAKE EXERCISE PRELIMINARY RESULTS (U) RESEARCH AND DEVELOPMENT REPORT OF JAN-MAY 77	Naval Ocean Systems Center	771031	NS; AU; ND	C
LRAPPRC77020	Palumbo, J. X., et al.	LRAPP EXERCISE ACOUSTIC DATA INVENTORY DECEMBER 1977 (U)	Naval Ocean R&D Activity	771201	NS; ND	C